

**NASA TECHNICAL
REPORT**



NASA TR R-354

C.1

**LOAN COPY: RETURN
AFWL (DOGL)
KIRTLAND AFB, N.**

0068427



NASA TR R-354

**THE STABILITY AND PERFORMANCE
CHARACTERISTICS OF AN EARTH-ORIENTED
GIMBALED-REACTION-WHEEL-SCANNER
CLASS OF SPACECRAFT**

by H. Richard Freeman

*Goddard Space Flight Center
Greenbelt, Md. 20771*



0068427

1. Report No. NASA TR R-354		2. Government Accession No.		3. Recipient's Catalog No.	
4. Title and Subtitle The Stability and Performance Characteristics of an Earth-Oriented Gimbale-Reaction-Wheel-Scanner Class of Spacecraft				5. Report Date November 1970	
				6. Performing Organization Code	
7. Author(s) H. Richard Freeman				8. Performing Organization Report No. G-996	
9. Performing Organization Name and Address Goddard Space Flight Center Greenbelt, Maryland 20771				10. Work Unit No.	
				11. Contract or Grant No.	
12. Sponsoring Agency Name and Address National Aeronautics and Space Administration Washington, D.C. 20546				13. Type of Report and Period Covered Technical Report	
				14. Sponsoring Agency Code	
15. Supplementary Notes Submitted as a thesis in partial fulfillment of the requirements for the degree of Doctor of Philosophy in Electrical Engineering, University of Maryland, College Park, Maryland, May 1970.					
16. Abstract The performance characteristics of the general class of earth-oriented spacecraft controlled by a gimbale-reaction-wheel-scanner attitude-control system are presented. Stability thresholds are analytically determined for this general class of vehicle in terms of its six system parameters. System stability in the presence of periodically varying pitch-momentum bias is considered, and a technique is established for the analysis of the general linearized equation set when it contains periodically time-varying coefficients. A comprehensive numerical study is performed, and the study concludes with an attempt at the analytic determination of stability thresholds for a system with a variational pitch-momentum bias. Also considered is system performance in the presence of a realistic disturbance torque model. A factor-of-merit function is established, and a method is presented that allows a potential user the means of choosing a "best" set of system parameters from a large six-dimensional array of possible parameters. Finally, this report concerns itself with the validation of the results obtained using a linearized time-invariant equation set. The validation procedure makes use of linear and non-linear digital computer simulations and the Floquet stability criterion technique.					
17. Key Words Suggested by Author Attitude Control Gimbale Reaction Wheel Scanner Spacecraft Stability Stability and Performance				18. Distribution Statement Unclassified-Unlimited	
19. Security Classif. (of this report) Unclassified	20. Security Classif. (of this page) Unclassified		21. No. of Pages 221	22. Price* \$3.00	

SUMMARY

This report presents a study of the stability and the performance characteristics of the general class of earth-oriented spacecraft controlled by a gimbaledd-reaction-wheel-scanner (GRWS) attitude-control system. The desirability of establishing these properties is of practical interest because a gimbaledd-reaction-wheel-scanner offers the space industry a relatively simple and inexpensive self-contained three-axis attitude-control package.

The report begins with the analytic determination of the stability thresholds for this general class of vehicle in terms of its six system parameters. These thresholds separate parameter sets that correspond to stable systems from those that correspond to unstable systems.

As an aid to the development of the generalized stability thresholds, a modification to the familiar Hurwitz technique is presented. This modification was extended to characteristic polynomials of various orders.

The device that actively controls the vehicle pitch axis is a pitch reaction wheel whose associated momentum varies periodically in response to periodic pitch-axis disturbance torques. Because the pitch reaction wheel is also the source of pitch-momentum bias, the study of system stability in the presence of a periodically varying pitch-momentum bias was considered. As a result of this study, a technique is established for the analysis of the general linearized equation set when it contains periodically time-varying coefficients. Furthermore, certain general conclusions concerning this class of problem are drawn as a result of a comprehensive numerical study. This study concludes with an attempt at the analytic determination of stability thresholds for a system with a variational pitch-momentum bias.

The next area of work is the consideration of system performance in the presence of a realistic disturbance torque model. A factor-of-merit function is established, and a driven solar panel assembly is introduced into the spacecraft configuration. This function, along with a digital computer program, allows a potential user the means of choosing a "best" set of system parameters from a large six-dimensional array of possible parameters. The associated digital computer program offers the user the option of maximizing the perturbations resulting from his disturbance model to make his findings more meaningful.

The inclusion of the driven solar panels complicates the linearized equation set by the introduction of time-varying inertia terms. A technique is established for the analysis of the general linearized equation set when it contains periodically time-varying inertia terms and all other terms are time invariant.

Finally, the report concerns itself with the validation of the results obtained using a linearized time-invariant equation set. The validation procedure makes use of linear and nonlinear digital computer simulations and the Floquet stability criterion technique.

Numerical examples are presented to illustrate many of the topics discussed in this report.

CONTENTS

Chapter	Page
1. INTRODUCTION.	1
2. DEVELOPMENT OF THE SYSTEM EQUATIONS.	9
2-1. General Discussion	9
2-2. Active Pitch Loop	12
2-3. Dynamic Equations.	14
3. DEVELOPMENT OF THE LINEARIZED EQUATION SET.	31
3-1. General Discussion	31
3-2. Linearizing the General System Equation Set.	33
3-3. Linearizing the Scanner Error Equation.	36
3-4. Determination of the Rotor Equilibrium Speed	36
3-5. Resulting Linearized Equation Set	37
4. STABILITY	43
4-1. General Discussion	43
4-2. Asymptotic Stability of Linearized Equations	43
4-3. Definition of Characteristic Polynomials.	47
4-4. Development of Modified Hurwitz Criterion	52
4-5. Application of Modified Hurwitz Criterion	56
4-6. Extension of Modified Hurwitz Technique	66
5. THE STABILITY OF THE LINEARIZED EQUATION SET WITH TIME-VARYING COEFFICIENTS.	77
5-1. General Discussion	77
5-2. Development of Floquet Theory.	77
5-3. Deriving Physical Meaning From Floquet Theory	84
5-4. Application of Floquet Theory to Time Variations Caused by Momentum Bias.	87
5-5. Numerical Example	90
5-6. Summary of Results	103
5-7. An Attempt at a Generalized Floquet Approach.	112
6. PERFORMANCE.	121
6-1. General Discussion	121
6-2. Development of Error Transfer Functions	124
6-3. Factor-of-Merit Function	127
6-4. Formulation of the Weighted Performance Function	129
6-5. Digital Computer Optimization Program	136
7. SOLAR PANELS AND ASSOCIATED SPACECRAFT STABILITY	139
7-1. General Discussion	139
7-2. Equations of Motion With Inertia Variation.	139
7-3. Floquet Problem	144

Chapter	Page
8. VALIDATION OF THE USE OF A LINEARIZED TIME-INVARIANT EQUATION SET	149
8-1. General Discussion	149
8-2. Method of Validation	149
8-3. Numerical Examples	152
ACKNOWLEDGMENTS	159
Selected Bibliography	160
APPENDIX A. Development of Fully Expanded Expressions	161
APPENDIX B. Listing of Floquet Computer Programs for Variational Pitch-Momemtum Bias and Variational Inertia	171
APPENDIX C. Derivation of the Residual Magnetic Disturbance Torque Model	183
APPENDIX D. Listing of Optimization Computer Program	197
APPENDIX E. Development of State Matrix for Equation Set With Driven Solar Panels	207
APPENDIX F. Listing of Linear Digital Simulation Program	211
APPENDIX G. Listing of Nonlinear Digital Simulation Program	217

LIST OF FIGURES

Figure	Page
1.1. Definitions of the spacecraft orbit plane and the inertial and orbit reference coordinate systems. The plane of the paper defines the orbit plane. The orbit reference axes travel at orbit velocity about the earth	2
1.2. Spacecraft axes. The plane of orbit is the x, z plane. The orbit-velocity vector points into the paper. For earth-oriented spacecraft, $x = x_r$, $y = y_r$, and $z = z_r$	3
1.3. Pitch-momentum bias control augmentation	4
1.4. Control moment gyro attitude-control configuration	5
1.5. Gimbaled-reaction-wheel-scanner control configuration	6
2.1. Assumed configuration for gimbaled-reaction-wheel-scanner spacecraft.	10
2.2. Horizon scanner related axes, (a) view of the plane of the local vertical and scan cone axis, and (b) view looking down the scan cone axis	13
2.3. Active pitch control loop	14
4.1. Representation of a_0 and a_1 lines shown in the plot of ρ versus α	60
4.2. Representation of a_0 and a_1 lines for $(k - h) \leq 0$. The $a_0 = 0$ curves degenerate into the single upper branch VLW when $k = h$	63
4.3. Stability constraints for fifth-order polynomial.	68
4.4. Stability constraints for fourth-order polynomial, (a) D_3 versus a_3/a_1 , and (b) D_2 versus a_3/a_1	72
5.1. Approximation for momentum bias variations, (a) $H_b = H_0 + dH S (2\pi/\tau)t$, and (b) $\dot{H}_b = (2\pi/\tau)dH C (2\pi/\tau)t$	92
5.2. Time solutions for Cases 1 or 2. $dH = 0$, $I.C. = \dot{\psi} = 0.05^\circ/\text{sec}$, and all other system states are initially zero. Angles are in radians	101
5.3. Time solutions for Cases 3, 4, and 5. $I.C. = \dot{\psi} = 0.05^\circ/\text{sec}$, and all other system states are initially zero. $\omega_0 = 2.21\Omega_0$. Angles are in radians, variational H_b is in ft-lb-sec.	102
5.4. Time solutions illustrating frequency tracking characteristics. Each case is run for dH near the Floquet stability threshold. $I.C. = \dot{\psi} = 0.05^\circ/\text{sec}$, and all other system states are initially zero. Angles are in radians, variational H_b is in ft-lb-sec.	104
5.5. Time solutions illustrating nonperiodic instability. $I.C. = \dot{\psi} = 0.05^\circ/\text{sec}$, and all other system states are initially zero. $\omega_0 = 3.2\Omega_0$. For $dH = 0.55$ ft-lb-sec, $\lambda_{\max} = -0.581 \pm j0.808$, $ \lambda_{\max} = 0.9951$; for $dH = 0.6$ ft-lb-sec, $\lambda_{\max} = -0.596 \pm j0.822$, $ \lambda_{\max} = 1.015$. Angles are in radians, variational H_b is in ft-lb-sec	105
5.6. Floquet stability thresholds, dH versus $\omega_0/2$. dH is in ft-lb-sec and is the amplitude of a sinusoidal disturbance. ω_0 is in orbit rates (one orbit rate is 10^{-3} rad/sec) and is the frequency of the driven coefficient	106
5.7. Time solutions for parameter variation Case III (square-wave momentum variation). $I.C. = \dot{\psi} = 0.05^\circ/\text{sec}$, and all other system states are initially zero. $\omega_0 = 2.739\Omega_0$. For $dH = 0.025$ ft-lb-sec, $\lambda_{\max} = -0.9968$; for $dH = 0.075$ ft-lb-sec, $\lambda_{\max} = -1.017$. Angles are in radians, variational H_b is in ft-lb-sec	108

LIST OF FIGURES (Continued)

Figure	Page
5.8. Time solutions for parameter variation Case VI (square-wave momentum variation). <i>I.C.</i> = $\dot{\psi} = 0.05^\circ/\text{sec}$, and all other system states are initially zero. $\omega_0 = 2.266\Omega_0$. For $dH = 0.4 \text{ ft-lb-sec}$, $\lambda_{\max} = -0.9566$; for $dH = 0.5 \text{ ft-lb-sec}$, $\lambda_{\max} = -1.05$. Angles are in radians, variational H_b is in ft-lb-sec	109
5.9. Time solutions for parameter variation Case III (sine wave momentum variation). <i>I.C.</i> = $\dot{\psi} = 0.05^\circ/\text{sec}$, and all other system states are initially zero. $\omega_0 = 2.739\Omega_0$. Angles are in radians, variational H_b is in ft-lb-sec	110
5.10. Time solutions for parameter variation Case VI (sine wave momentum variation). <i>I.C.</i> = $\dot{\psi} = 0.05^\circ/\text{sec}$, and all other system states are initially zero. $\omega_0 = 2.266\Omega_0$. Angles are in radians, variational H_b is in ft-lb-sec	111
5.11. Fourier stability thresholds superimposed on Floquet stability thresholds, dH ver- sus $\omega_0/2$. dH is in ft-lb-sec and is the amplitude of a sinusoidal disturbance. ω_0 is in orbit rates (one orbit rate is 10^{-3} rad/sec) and is the frequency of the driven coefficient	120
6.1. Spacecraft magnetic moment in spherical coordinates	131
8.1. Time responses for optimum spacecraft for Example 1. <i>I.C.</i> = $\phi = \psi = 10^\circ$, and all other system states are initially zero. Angles are in degrees.	154
8.2. Time responses for optimum spacecraft for Example 2. <i>I.C.</i> = $\phi = \psi = 10^\circ$, and all other system states are initially zero. Angles are in degrees	157
C.1. Orientation of the ecliptic plane relative to the equatorial plane	184
C.2. Orientation of the orbit plane relative to the equatorial plane	184
C.3. Solar panel assembly, (a) view looking down panel hinge line, and (b) view normal to shaft and hinge line	187
C.4. Definition of sun angle	190
C.5. Definition of initial solar panel reference angle. <i>S</i> is not necessarily in the orbit plane	191
C.6. Definition of half umbra angle	192
C.7. Plot of incident sun energy versus orbit position	194

LIST OF TABLES

Table	<i>Page</i>
5.1 Parameter variation study	107
5.2 Fourier coefficients associated with simulation Case III.	116
8.1 Parameter array for use in optimization program	153
8.2 Results of optimization for Example 1	153
8.3 Results of variational momentum bias Floquet study Example 1	155
8.4 Results of optimization for Example 2	156
8.5 Results of variational inertia Floquet study Example 2	158
8.6 Results of variational momentum bias Floquet study Example 2	158

THE STABILITY AND PERFORMANCE CHARACTERISTICS OF AN EARTH-ORIENTED GIMBALED-REACTION-WHEEL-SCANNER CLASS OF SPACECRAFT*

by

H. Richard Freeman
Goddard Space Flight Center

CHAPTER I INTRODUCTION

Stabilization and control, as it pertains to unmanned earth-oriented satellites, covers the entire spectrum from fully active to fully passive control. When designing a control configuration for the purpose of fulfilling a specific mission, one must consider which class of control will best meet the mission requirements. The choices include fully active, semiactive, and fully passive attitude control.

Figure 1.1 defines the orbit plane as well as the inertial and orbit reference coordinate systems. The orientation of the orbit plane is assumed to be inertially fixed in space with respect to the sun; however, the center of the orbit plane rotates about the sun with the earth. As the spacecraft travels in the orbit plane, its velocity vector is defined to be the direction of its positive roll axis. Positive yaw is defined to be the earth-pointing vector referenced from the spacecraft. The spacecraft pitch axis is perpendicular to the orbit plane in such a direction that the roll, pitch, and yaw axes form a right-handed system. The spacecraft orbit-velocity vector is parallel with and directed opposite to the spacecraft pitch axis. This is illustrated by Figure 1.2.

In a fully active spacecraft control system, attitude and, possibly, rate errors are sensed in each of the three spacecraft axes. The sensors provide inputs to the control mechanisms that force the attitude and/or rate errors to zero, the spacecraft equilibrium state. These control mechanisms might include momentum storing reaction wheels and/or mass-expulsion-torquing systems. When momentum storage is accomplished by the use of reaction wheels, a means of momentum control must be available

*Submitted as a thesis in partial fulfillment of the requirements for the degree of Doctor of Philosophy in Electrical Engineering, University of Maryland, College Park, Maryland, May 1970.

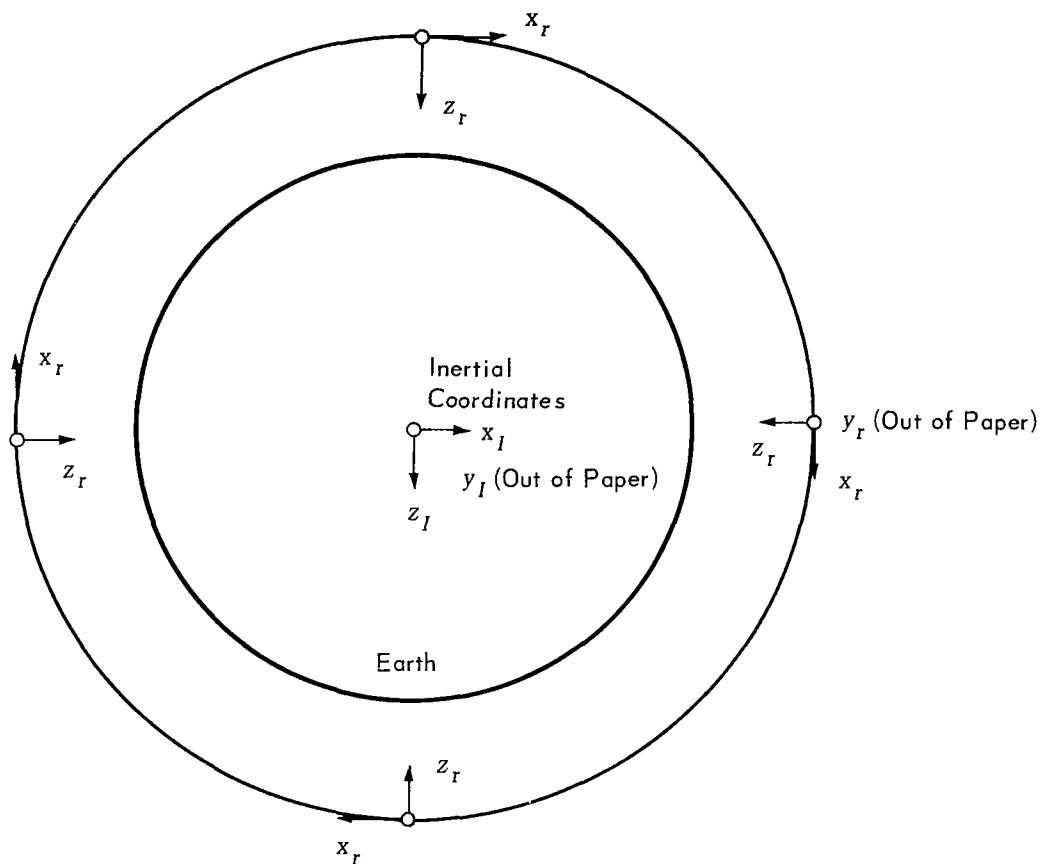


Figure 1.1—Definitions of the spacecraft orbit plane and the inertial and orbit reference coordinate systems. The plane of the paper defines the orbit plane. The orbit reference axes travel at orbit velocity about the earth.

to unload or to unwind the wheels. Unloading could be accomplished by the use of mass expulsion or through the use of the environmental torques such as gravity-gradient torques, magnetic torques, and so forth. It should be noted, however, that a favorable spacecraft inertia distribution is required to properly utilize gravity-gradient torquing.

A spacecraft with a fully active control system has an excellent performance potential. Its sensors can be designed to afford a high degree of pointing accuracy, and its control law can be established to give decreased sensitivity to internally as well as externally generated torque disturbances.

Spacecraft with a fully passive control system rely wholly on environmental torques for their means of control. The physical configuration is constrained, because for these spacecraft, a favorable inertia distribution must be presented with respect to their environment for earth stabilization to be

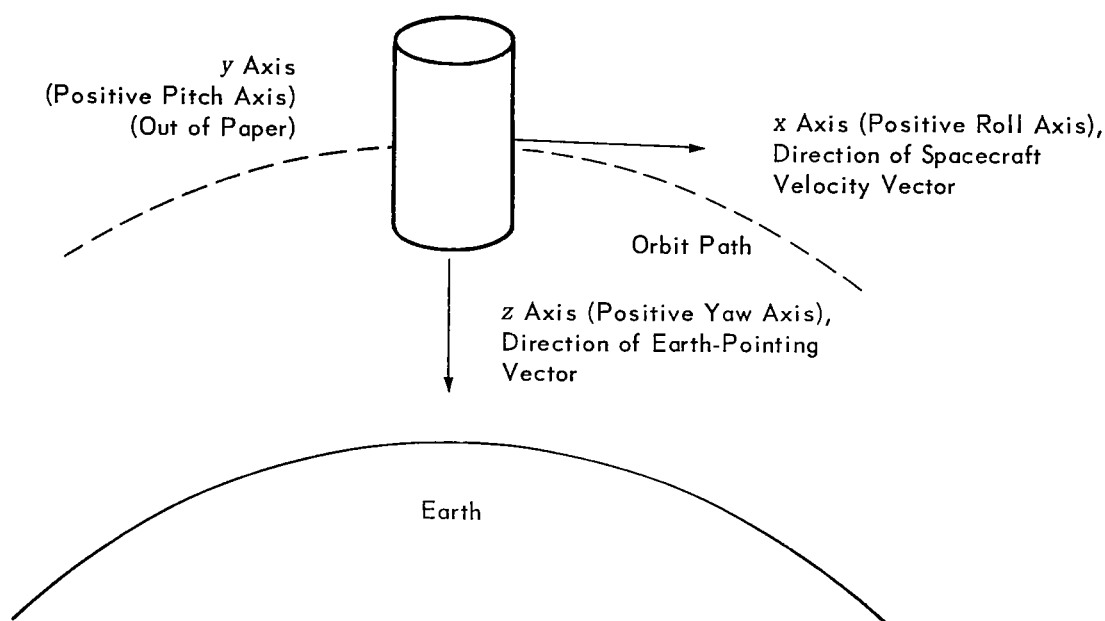
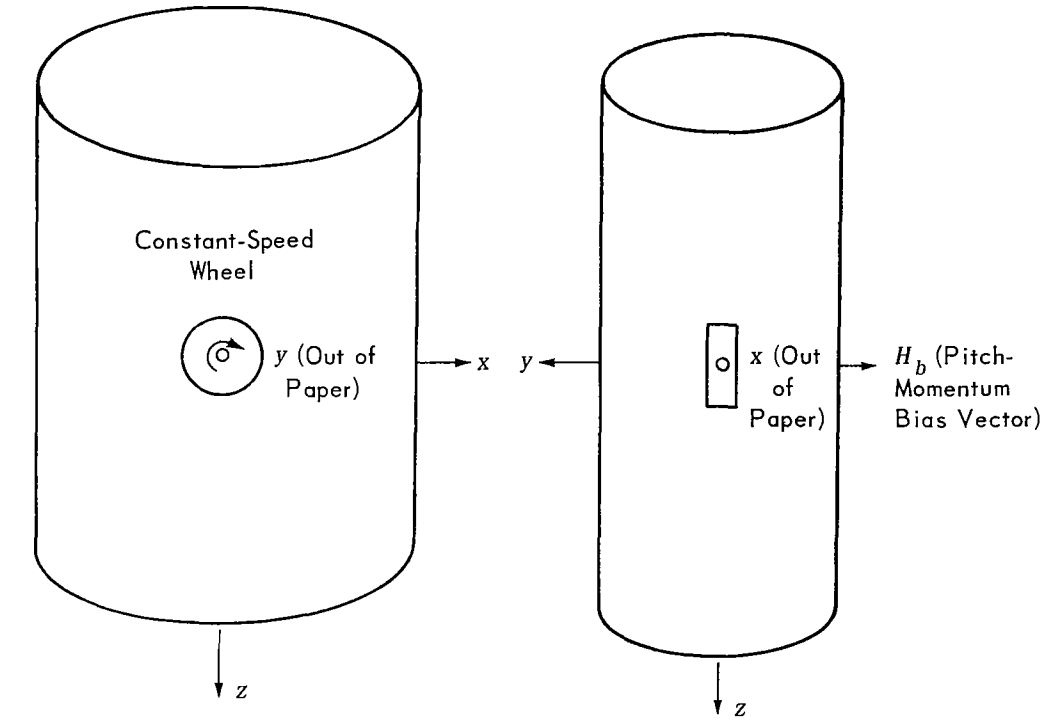


Figure 1.2—Spacecraft axes. The plane of orbit is the x, z plane. The orbit-velocity vector points into the paper. For earth-oriented spacecraft, $x = x_r$, $y = y_r$, and $z = z_r$.

achieved. If the spacecraft moments of inertia are properly chosen, the gravitational torques exerted upon the vehicle cause the spacecraft to align itself in a desired earth-pointing orientation. Neither onboard error sensing nor actively mechanized torquing systems are required. However, in considering the advantages of the implied simplifications, one must also consider the problems of inertia augmentation, passive dampers, the reduction in pointing accuracies, and the increased sensitivity to internally and externally generated torque disturbances.

An obvious compromise between the two types of systems already discussed is a semiactive (or semipassive) attitude-control system. A variety of semiactive configurations might be cited as examples of this type of control. For instance, Figure 1.3 illustrates the use of a constant-speed pitch reaction wheel to afford pitch-momentum bias to an otherwise fully passive gravity-gradient spacecraft. This additional momentum vector normal to the orbit plane increases the spacecraft pointing accuracy by augmenting the environmental torques acting upon the fully passive vehicle with gyroscopic torques caused by the presence of the pitch-momentum bias.

The gyroscopic effect of this constant-speed wheel has a rate-seeking property. Gyroscopic torques will always act to align the rotor spin vector with the angular rate vector of the spacecraft. If



$$I_x \dot{\omega}_x + (I_z - I_y) \omega_y \omega_z = T_{gx} + H_b \omega_z$$

$$I_y \dot{\omega}_y + (I_x - I_z) \omega_x \omega_z = T_{gy} - \dot{H}_b$$

$$I_z \dot{\omega}_z + (I_y - I_x) \omega_x \omega_y = T_{gz} - H_b \omega_x$$

Figure 1.3—Pitch-momentum bias control augmentation.

one recalls that the spacecraft rotates about its pitch axis once each orbit, affording the spacecraft a constant pitch rate, the usefulness of this pitch-momentum bias should become apparent.

A slightly more complex example might be one in which a control-moment gyro* is used to generate the pitch-momentum bias as shown in Figure 1.4. This is desirable because, in addition to the pitch-momentum bias, the control-moment gyro affords system damping as a result of the relative motion between its fluid-immersed gyro rotor and that of the main body to which the rotor is gimbaled. For a single-axis gyro system, the gimbal axis must lie in the roll-yaw plane so that the rotor spin axis lies nominally along the spacecraft pitch axis.

*A control-moment gyro is one that exerts control torques on the spacecraft, as opposed to one that is used to sense attitude errors.

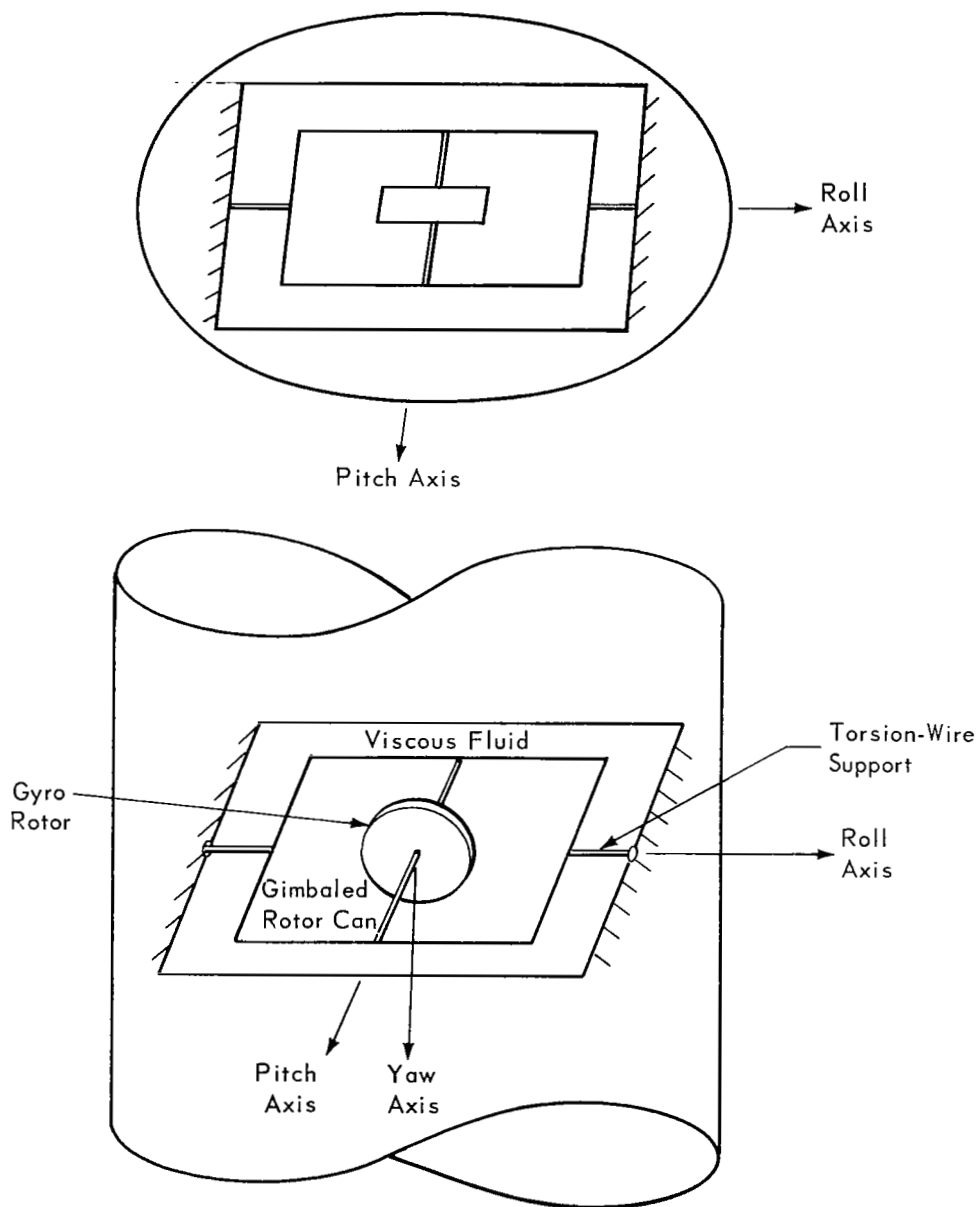
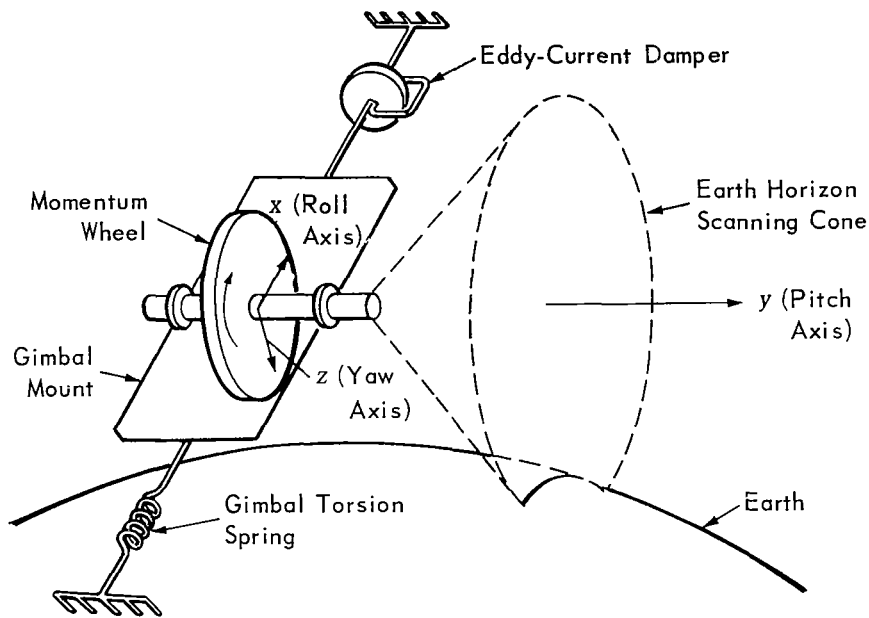


Figure 1.4—Control-moment gyro attitude-control configuration.

A third and more complex example constitutes the subject of this dissertation. In the spacecraft shown in Figure 1.5, the roll and yaw axes are passively controlled and the pitch axis is actively controlled. The active portion of the control system allows a high degree of pointing accuracy in pitch as well as a decrease in sensitivity to internally generated momentum disturbances that might be produced



	Sensing	Torquing	Damping	Wheel momentum removal
Pitch	Horizon scanning	Momentum wheel	Electronic compensation	Gravity-gradient
Roll Yaw	Passive	Gravity-gradient and gyroscopic	Eddy-current damper and gimbal motion	

Figure 1.5—Gimbaled-reaction-wheel-scanner control configuration.

along this controlled axis. Such disturbances might, for example, be produced by a large in-flight tape recorder or by actively driven solar panels. The passive portion of the control system offers the advantage of the simplicity inherent in a fully passive system, and the associated critical constraints of inertia distribution that plague a fully passive system are somewhat relaxed. The spacecraft is designed so that a single reaction wheel, when properly oriented, provides a pitch-momentum bias that tightens the passive control of the roll-yaw axes. This reaction wheel is gimballed to the spacecraft in its roll-yaw plane by means of a torsion wire spring and an eddy-current damper. The gimbal, whose axis is located at an arbitrary angle in the roll-yaw plane, provides both roll and yaw damping as a result of spacecraft roll-yaw coupling. Gravity-gradient torques provide the mechanism necessary to unload the reaction wheel when it deviates from its bias speed as a result of spacecraft pitch perturbations.

Pitch control is implemented by actively controlling the reaction wheel about its bias speed. The control error signal is derived from a conical infrared horizon scanner whose rotating optical prism is physically mounted on the reaction wheel rotor. Because all functions are packaged into one unit, the controller is called a gimbaledd-reaction-wheel-scanner (GRWS) attitude-control system.

The purpose of this dissertation is to study the stability and performance characteristics of earth-oriented spacecraft that are controlled by a gimbaledd-reaction-wheel-scanner. Establishing these properties is of practical interest because a gimbaledd-reaction-wheel-scanner offers the space industry a relatively simple, inexpensive, and self-contained three-axis attitude-control package. To date, only sketchy attempts to analyze this class of artificial satellites have been made, and these analyses have dealt mainly with a very special combination of spacecraft parameters (Reference 1).

The dissertation discusses in Chapters 3 and 4 the analytical determination, in terms of the six system parameters, of the stability thresholds for the general class of spacecraft controlled by a gimbaledd-reaction-wheel-scanner. These thresholds separate parameter sets that correspond to stable systems from those that correspond to unstable systems. Because the equation set that mathematically describes the system is highly coupled and extremely nonlinear, it was necessary to derive the stability thresholds from a set of equations that were linearized about the desired spacecraft equilibrium position.

As an aid to the development of the generalized stability thresholds, a modification of the familiar Hurwitz technique is presented. Chapter 4 concludes with the extension of this modified technique to polynomials of various orders.

The device that actively controls the vehicle pitch axis is the pitch reaction wheel, the associated momentum of which varies periodically in response to pitch-axis disturbance torques. Because the pitch reaction wheel is also the source of the pitch-momentum bias, the second major area of work, described in Chapter 5, was a study of system stability in the presence of a periodically varying pitch-momentum bias. As a result of this study, a technique was established that facilitated the analysis of the general, linearized equation set when it contained periodically time-varying coefficients. It also proved possible, as a result of a comprehensive numerical study, to reach certain general conclusions concerning this class of problem. Chapter 5 concludes with an attempt to determine analytically stability thresholds for a system having a periodically varying pitch-momentum bias.

The third major area of work was the consideration of system performance in the presence of a realistic disturbance torque model. In Chapter 6, a factor-of-merit function was established and a driven solar panel assembly was introduced into the spacecraft configuration. This function along with a digital computer program allows a potential user the means of choosing an optimum set of system parameters from a large, six-dimensional array of possible parameters. The associated digital computer program offers the user the option of maximizing the perturbations resulting from his disturbance model to make his findings more meaningful.

The inclusion of the driven solar panels complicates the linearized equation set by the introduction of time-varying inertia terms. A technique is established in Chapter 7 that allows the analysis of the general, linearized equation set when it contains periodically time-varying inertia terms, and all other terms are time invariant.

The final chapter of this dissertation concerns the validation of the results in Chapters 4 and 6, obtained through the use of a linearized time-invariant equation set. The validation procedure makes use of linear and nonlinear digital computer simulations, as well as the Floquet stability criterion technique. Chapter 8 concludes with a numerical example that illustrates many of the topics discussed in this dissertation.

CHAPTER 2

DEVELOPMENT OF THE SYSTEM EQUATIONS

2.1 General Discussion

The spacecraft configuration that has been chosen for study is shown in Figure 2.1. This skewed unsymmetric configuration was studied in order not to prejudge any conclusions that might have seemed obvious had certain symmetries been assumed. Shown in the figure are the main spacecraft body (body number 1), the gimbal and wheel combination (body number 2), and the wheel rotor alone (body number 3).

We define the axes sets

$$\hat{X}_I \equiv \begin{bmatrix} x_I \\ y_I \\ z_I \end{bmatrix} = \text{inertial set of axes}$$

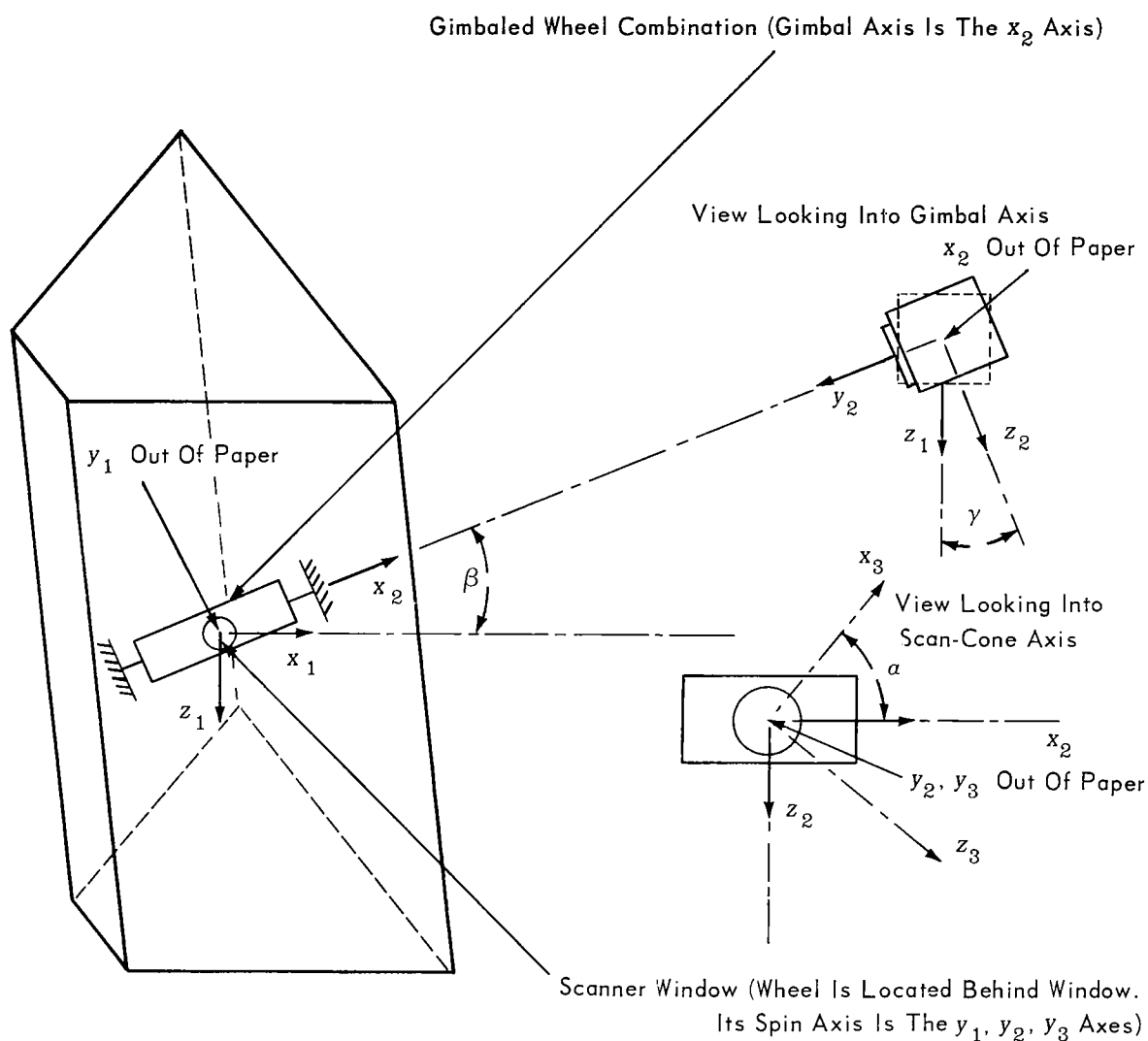
and

$$\hat{X}_r \equiv \begin{bmatrix} x_r \\ y_r \\ z_r \end{bmatrix} = \text{orbit reference set of axes.}$$

The inertial axes are fixed in the orbit plane and have a fixed orientation with respect to the sun. The orbit reference axes travel at orbit velocity about the center of the earth. They describe the desired orientation of the coordinates of an earth-oriented spacecraft. The plane containing both x_I and z_I , or both x_r and z_r , is defined as the orbit plane.

We also define the specific axes

$$\hat{X}_1 \equiv \begin{bmatrix} x_1 \\ y_1 \\ z_1 \end{bmatrix} = \text{controlled axes of main body} = \begin{bmatrix} \text{spacecraft roll axis} \\ \text{spacecraft pitch axis} \\ \text{spacecraft yaw axis} \end{bmatrix},$$



- β Is Angle Of Gimbal Axis
- γ Is Gimbal Angle
- α Is Wheel Rotor Angle
- y_1 Is Spacecraft Pitch Axis (Perpendicular To Orbit Plane)
- z_1 Is Spacecraft Yaw Axis (Earth-Pointing Vector)
- x_1 Is Spacecraft Roll Axis (Velocity Vector)
- Ω_0 Is Orbit Rate

Figure 2.1—Assumed configuration for the gimbaled-reaction-wheel-scanner spacecraft.

$$\tilde{X}_2 \equiv \begin{bmatrix} x_2 \\ y_2 \\ z_2 \end{bmatrix} \equiv \text{principal axes of gimbal and wheel combination,}$$

and

$$\tilde{X}_3 \equiv \begin{bmatrix} x_3 \\ y_3 \\ z_3 \end{bmatrix} \equiv \text{principal axes of wheel rotor alone,}$$

and the inertia tensors

$$\Phi_1 \equiv \begin{bmatrix} I_1(11) & -I_1(12) & -I_1(13) \\ -I_1(21) & I_1(22) & -I_1(23) \\ -I_1(31) & -I_1(32) & I_1(33) \end{bmatrix} \equiv \text{inertia tensor of main body,}$$

$$\Phi_2 \equiv \begin{bmatrix} I_2(11) & 0 & 0 \\ 0 & I_2(22) & 0 \\ 0 & 0 & I_2(33) \end{bmatrix} \equiv \text{inertia tensor of gimbal alone,} \quad \left\{ \begin{array}{l} \text{It was assumed that} \\ \text{the products of inertia} \\ \text{equal zero.} \end{array} \right.$$

and

$$\Phi_3 \equiv \begin{bmatrix} I_3(11) & 0 & 0 \\ 0 & I_3(22) & 0 \\ 0 & 0 & I_3(33) \end{bmatrix} \equiv \text{inertia tensor of wheel rotor alone} \cdot \left\{ \begin{array}{l} \text{It was assumed that} \\ \text{the products of inertia} \\ \text{equal zero and that} \\ I_3(11) = I_3(33). \end{array} \right.$$

The reaction wheel scanner is gimballed to the spacecraft by means of a torsion wire spring and an eddy-current viscous damper. The gimbal axis is mounted on the spacecraft at a positive rotation β from the positive roll axis in the roll-yaw plane.

The gimbaling parameters are

gimbal angle = γ ,

torsion wire spring constant = k_g ,

and

viscous damping coefficient = B_g .

It is assumed that the centers of mass of the three bodies are coincident and that they are located at the origins of \tilde{X}_1 , \tilde{X}_2 , and \tilde{X}_3 .

2.2 Active Pitch Loop

Attitude error sensing for the actively controlled pitch loop is provided by the conical infrared horizon scanner portion of the gimbaled-reaction-wheel-scanner. The apex of the scan cone is the origin of the \tilde{X}_3 coordinate system [which is defined as the (x_3, y_3, z_3) coordinate system] with the scan axis in the direction of the positive y_3 axis. The scanning motion results from the rotation of an optical prism which is attached to the reaction wheel rotor. Control logic maintains a minimum wheel speed to ensure proper functioning of the scanner. A portion of the scan cone normally intercepts the earth while the remainder of this cone scans through cold space. The higher earth temperature relative to that of space results in an earth pulse which is processed electronically to provide spacecraft attitude information.

If the rotation angle β and the gimbal angle γ , as defined in Figure 2.1, were both equal to zero, the scanner output would be a simple function of the spacecraft pitch attitude. But in general, these angles are not zero, and the scanner output must be defined as a complex function of spacecraft pitch angle θ , spacecraft roll angle ϕ , and gimbal angle γ .

The orbit reference coordinate z_r defines the local vertical, and the positive y_2 axis defines the scan cone axis.

The scanner error is defined equal to the angle β when the z_2 axis lies in the $z_r y_2$ plane. A positive scanner error θ_s is defined as a positive rotation of the spacecraft about the positive y_2 axis. The minimum angle between the positive z_2 axis and $z_r y_2$ plane has the magnitude $(\theta_s + \beta)$.

In order to derive an expression that relates θ_s to θ , ϕ , and γ , reference is made to Figure 2.2a and 2.2b.

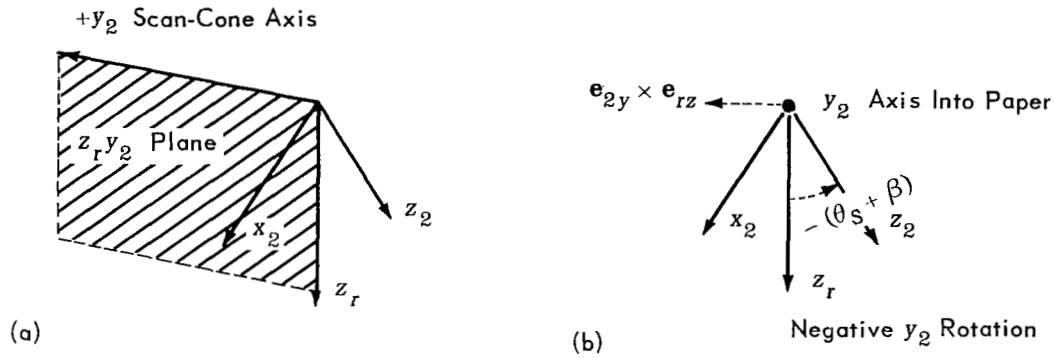


Figure 2.2—Horizon scanner related axes; (a) view of the plane of the local vertical and scan cone axis, and (b) view looking down the scan cone axis.

We define \mathbf{e}_{2x} , \mathbf{e}_{2y} , and \mathbf{e}_{2z} as unit vectors whose directions are parallel to \mathbf{x}_2 , \mathbf{y}_2 , and \mathbf{z}_2 , respectively. Similarly, \mathbf{e}_{rx} , \mathbf{e}_{ry} , and \mathbf{e}_{rz} are unit vectors having the same directions as \mathbf{x}_r , \mathbf{y}_r , and \mathbf{z}_r , respectively.

The vector cross product $\mathbf{e}_{2y} \times \mathbf{e}_{rz}$ defines a vector normal to the $z_r y_2$ plane as shown in Figure 2.2b. If this vector is normalized and the result dotted into \mathbf{e}_{2z} , the resulting dot product is the cosine of the angle between $\mathbf{e}_{2y} \times \mathbf{e}_{rz}$ and \mathbf{e}_{2z} :

$$\frac{\mathbf{e}_{2y} \times \mathbf{e}_{rz}}{|\mathbf{e}_{2y} \times \mathbf{e}_{rz}|} \cdot \mathbf{e}_{2z} = \cos [90 - (\theta_s + \beta)] = \sin (\theta_s + \beta).$$

The resulting expression relating θ_s with ϕ , θ , and γ may be written

$$\tan (\theta_s + \beta) = \frac{\sin (\theta + \beta) \cos \phi}{\cos (\theta + \beta) \cos \phi \cos \gamma - \sin \phi \sin \gamma}. \quad (2.1)$$

The block diagram shown in Figure 2.3 defines the active pitch control loop.

T_w is the torque applied to the reaction wheel rotor, $-T_w$ is the resultant reaction torque applied to the spacecraft, ϵ is the error signal at the output of the lead compensation network, and θ_s is the scanner signal output. (Note that wheel torque acts to reduce θ_s and not necessarily θ .) The equations that describe this control loop are

$$\epsilon = [T_1 \dot{\theta}_s + \theta_s - T_2 \dot{\epsilon}], \quad (2.2)$$

$$p = \epsilon - (H_w - H_b)C_t,$$

$$p = T_1 \dot{\theta}_s + \theta_s - T_2 \dot{\epsilon} - (H_w - H_b)C_t,$$

and

$$T_w = k_T [T_1 \dot{\theta}_s + \theta_s - T_2 \dot{\epsilon} - (H_w - H_b)C_t] - H_w B_f. \quad (2.3)$$

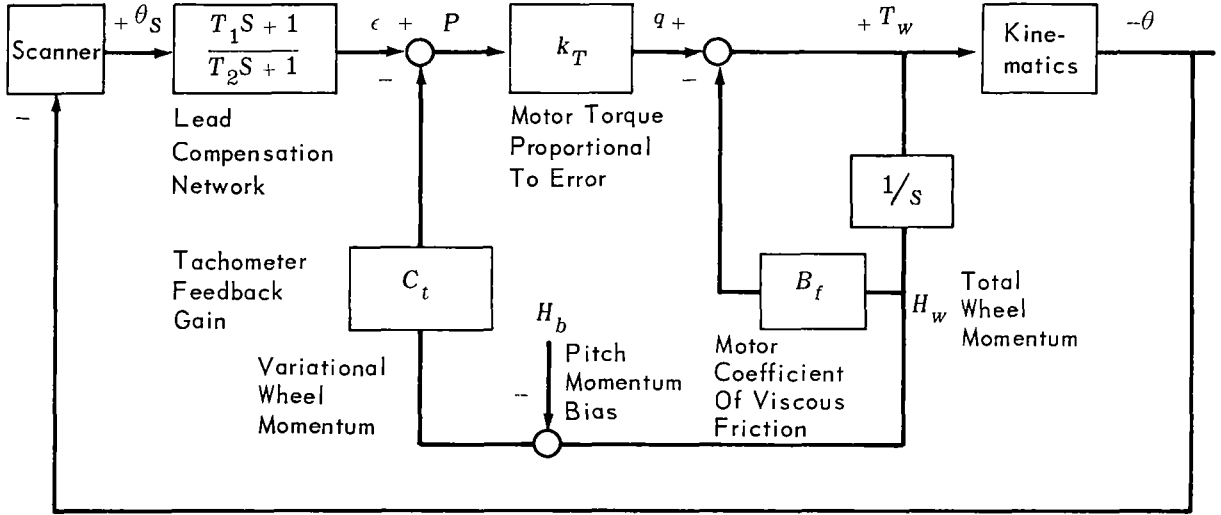


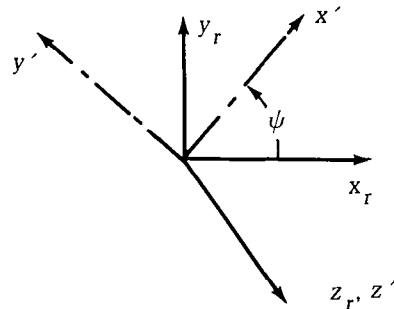
Figure 2.3—Active pitch control loop.

2.3 Dynamic Equations

An Euler rotational sequence of yaw, roll, and pitch has been chosen in order to relate the orbit reference axes $\tilde{\tilde{X}}_r$ to the spacecraft main body axes $\tilde{\tilde{X}}_1$. In order to simplify the notation throughout the development of equations, $\sin(\text{angle})$ will be written S (angle) and $\cos(\text{angle})$ will be written C (angle). The coordinate transformation from $\tilde{\tilde{X}}_r$ to $\tilde{\tilde{X}}_1$ follows.

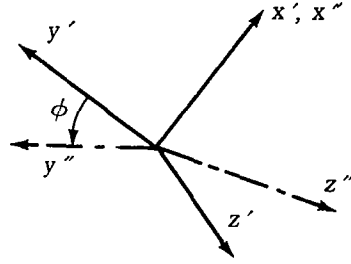
1) Yaw rotation

$$\begin{bmatrix} x' \\ y' \\ z' \end{bmatrix} = \begin{bmatrix} C\psi & S\psi & 0 \\ -S\psi & C\psi & 0 \\ 0 & 0 & 1 \end{bmatrix} \begin{bmatrix} x_r \\ y_r \\ z_r \end{bmatrix}.$$



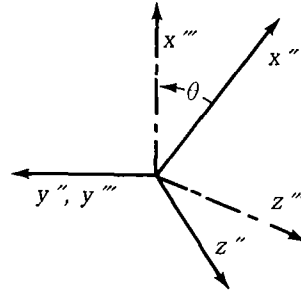
2) Roll rotation

$$\begin{bmatrix} x'' \\ y'' \\ z'' \end{bmatrix} = \begin{bmatrix} 1 & 0 & 0 \\ 0 & C\phi & S\phi \\ 0 & -S\phi & C\phi \end{bmatrix} \begin{bmatrix} x' \\ y' \\ z' \end{bmatrix}.$$



3) Pitch rotation

$$\begin{bmatrix} x''' \\ y''' \\ z''' \end{bmatrix} = \begin{bmatrix} C\theta & 0 & -S\theta \\ 0 & 1 & 0 \\ S\theta & 0 & C\theta \end{bmatrix} \begin{bmatrix} x'' \\ y'' \\ z'' \end{bmatrix} \equiv \begin{bmatrix} x_1 \\ y_1 \\ z_1 \end{bmatrix}.$$



The total transformation matrix is the product of the 3 rotational transformations. Thus,

$$\begin{bmatrix} x_1 \\ y_1 \\ z_1 \end{bmatrix} = \begin{bmatrix} C\theta & 0 & -S\theta \\ 0 & 1 & 0 \\ S\theta & 0 & C\theta \end{bmatrix} \begin{bmatrix} 1 & 0 & 0 \\ 0 & C\phi & S\phi \\ 0 & -S\phi & C\phi \end{bmatrix} \begin{bmatrix} C\psi & S\psi & 0 \\ -S\psi & C\psi & 0 \\ 0 & 0 & 1 \end{bmatrix} \begin{bmatrix} x_r \\ y_r \\ z_r \end{bmatrix}.$$

or

$$\begin{bmatrix} x_1 \\ y_1 \\ z_1 \end{bmatrix} = \begin{bmatrix} C\theta C\psi - S\theta S\phi S\psi & C\theta S\psi + S\theta S\phi C\psi & -S\theta C\phi \\ -C\phi S\psi & C\phi C\psi & S\phi \\ S\theta C\psi + C\theta S\phi S\psi & S\theta S\psi - C\theta S\phi C\psi & C\theta C\phi \end{bmatrix} \begin{bmatrix} x_r \\ y_r \\ z_r \end{bmatrix}.$$

The A_{1r} transformation matrix defines the matrix that transforms from $\bar{\bar{X}}_r$ into $\bar{\bar{X}}_1$ coordinates

$$\bar{\bar{X}}_1 = A_{1r} \bar{\bar{X}}_r.$$

The notation used to expand the A_{1r} matrix into its elementary form is

$$A_{1r} = \begin{bmatrix} a_{1r}(11) & a_{1r}(12) & a_{1r}(13) \\ a_{1r}(21) & a_{1r}(22) & a_{1r}(23) \\ a_{1r}(31) & a_{1r}(32) & a_{1r}(33) \end{bmatrix}.$$

The A_{21} transformation matrix that defines the coordinate transformation from the axes of the main body of the spacecraft $\tilde{\tilde{X}}_1$ to the gimbaled wheel axes $\tilde{\tilde{X}}_2$ follows in two steps. Thus,

$$\begin{bmatrix} x'_2 \\ y'_2 \\ z'_2 \end{bmatrix} = \begin{bmatrix} C\beta & 0 & -S\beta \\ 0 & 1 & 0 \\ S\beta & 0 & C\beta \end{bmatrix} \begin{bmatrix} x_1 \\ y_1 \\ z_1 \end{bmatrix},$$

followed by

$$\begin{bmatrix} x_2 \\ y_2 \\ z_2 \end{bmatrix} = \begin{bmatrix} 1 & 0 & 0 \\ 0 & C\gamma & S\gamma \\ 0 & -S\gamma & C\gamma \end{bmatrix} \begin{bmatrix} x'_2 \\ y'_2 \\ z'_2 \end{bmatrix},$$

or

$$\tilde{\tilde{X}}_2 = A_{21} \tilde{\tilde{X}}_1.$$

Note that $\tilde{\tilde{X}}_1 = A_{21}^{-1} \tilde{\tilde{X}}_2 = A_{12} \tilde{\tilde{X}}_2$.

The transformation from the gimbaled wheel axes $\tilde{\tilde{X}}_2$ to the wheel rotor axes $\tilde{\tilde{X}}_3$ is

$$\begin{bmatrix} x_3 \\ y_3 \\ z_3 \end{bmatrix} = \begin{bmatrix} C\alpha & 0 & -S\alpha \\ 0 & 1 & 0 \\ S\alpha & 0 & C\alpha \end{bmatrix} \begin{bmatrix} x_2 \\ y_2 \\ z_2 \end{bmatrix},$$

or

$$\tilde{\tilde{X}}_3 = A_{32} \tilde{\tilde{X}}_2.$$

Note that $\tilde{\tilde{X}}_2 = A_{32}^{-1} \tilde{\tilde{X}}_3 = A_{23} \tilde{\tilde{X}}_3$.

Since the transformations described throughout this development are orthogonal, $A_{ij}^{-1} = A_{ij}^T$.

Next, the kinematic relationships are developed for bodies 1, 2, and 3. We define

$$\bar{\omega}_1 \equiv \begin{bmatrix} \omega_{1x} \\ \omega_{1y} \\ \omega_{1z} \end{bmatrix} = \begin{bmatrix} \omega_{1x\psi} + \omega_{1x\phi} + \omega_{1x\theta} \\ \omega_{1y\psi} + \omega_{1y\phi} + \omega_{1y\theta} \\ \omega_{1z\psi} + \omega_{1z\phi} + \omega_{1z\theta} \end{bmatrix},$$

where ω_{1ij} is the i th component of angular velocity resulting from a j th angular rotation of body 1 ($i = x, y, z; j = \phi, \theta, \psi$).

1) Yaw rotation

$$\bar{\omega}_{1\psi} = A_{1r} \begin{bmatrix} 0 \\ 0 \\ \dot{\psi} \end{bmatrix} = \begin{bmatrix} -\dot{\psi} S \theta C \phi \\ \dot{\psi} S \phi \\ \dot{\psi} C \theta C \phi \end{bmatrix} = \begin{bmatrix} \omega_{1x\psi} \\ \omega_{1y\psi} \\ \omega_{1z\psi} \end{bmatrix}.$$

2) Roll rotation

$$\bar{\omega}_{1\phi} = A_{1x'} \begin{bmatrix} \dot{\phi} \\ 0 \\ 0 \end{bmatrix} = \begin{bmatrix} C \theta & S \theta S \phi & S \theta C \phi \\ 0 & C \phi & S \phi \\ S \theta & -C \theta S \phi & S \theta C \phi \end{bmatrix} \begin{bmatrix} \dot{\phi} \\ 0 \\ 0 \end{bmatrix} = \begin{bmatrix} \omega_{1x\phi} \\ \omega_{1y\phi} \\ \omega_{1z\phi} \end{bmatrix}.$$

or

$$\bar{\omega}_{1\phi} = \begin{bmatrix} \dot{\phi} C \theta \\ 0 \\ \dot{\phi} S \theta \end{bmatrix}.$$

3) Pitch rotation

$$\bar{\omega}_{1\theta} = A_{1x''} \begin{bmatrix} 0 \\ \dot{\theta} \\ 0 \end{bmatrix} = \begin{bmatrix} 0 \\ \dot{\theta} \\ 0 \end{bmatrix} = \begin{bmatrix} \omega_{1x\theta} \\ \omega_{1y\theta} \\ \omega_{1z\theta} \end{bmatrix}.$$

The resulting total angular velocity of body 1, referenced to the orbit reference axes and in terms of Euler angles and Euler angle rates, is

$$\bar{\omega}_1 = \begin{bmatrix} \omega_{1x} \\ \omega_{1y} \\ \omega_{1z} \end{bmatrix} = \begin{bmatrix} -\dot{\psi}S\theta C\phi + \dot{\phi}C\theta \\ \dot{\psi}S\phi + \dot{\theta} \\ \dot{\psi}C\theta C\phi + \dot{\phi}S\theta \end{bmatrix}.$$

But the spacecraft travels with an orbital velocity $-\Omega_0 \mathbf{e}_{Iy}$ (i.e., with a velocity of magnitude Ω_0 whose direction corresponds to the negative pitch inertial axis), therefore

$$\bar{\omega}_{1I} = \bar{\omega}_{1r} + A_{1r} \begin{bmatrix} 0 \\ -\Omega_0 \\ 0 \end{bmatrix},$$

and

$$\bar{\omega}_{1I} = \bar{\omega}_{1r} - \Omega_0 \begin{bmatrix} C\theta S\psi + S\theta S\phi C\psi \\ C\phi C\psi \\ S\theta S\psi - C\theta S\phi C\psi \end{bmatrix},$$

where $\bar{\omega}_{1I}$ is referenced to the inertial frame and $\bar{\omega}_{1r}$ is referenced to the orbit reference frame. From this point, all angular rates $\bar{\omega}_k$ are referenced to the inertial frame ($k = 1, 2, 3$).

$$\bar{\omega}_1 = \begin{bmatrix} \omega_{1x} \\ \omega_{1y} \\ \omega_{1z} \end{bmatrix} = \begin{bmatrix} -\dot{\psi}S\theta C\phi + \dot{\phi}C\theta - \Omega_0(C\theta S\psi + S\theta S\phi C\psi) \\ \dot{\psi}S\phi + \dot{\theta} - \Omega_0(C\phi C\psi) \\ \dot{\psi}C\theta C\phi + \dot{\phi}S\theta - \Omega_0(S\theta S\psi - C\theta S\phi C\psi) \end{bmatrix}.$$

The total angular velocity of body 2 can be written as $\bar{\omega}_2 = \bar{\omega}_1$ (transformed to the body 2 coordinate set) plus the angular rate of the gimbal. Note that the gimbal is only free to move about its x axis.

$$\bar{\omega}_2 = A_{21} \bar{\omega}_1 + \begin{bmatrix} \dot{\gamma} \\ 0 \\ 0 \end{bmatrix}.$$

The total angular velocity of body 3 can be written as $\bar{\omega}_3 = \bar{\omega}_2$ (transformed to body 3 coordinates) plus the angular rate of the wheel rotor.

$$\bar{\omega}_3 = A_{32}\bar{\omega}_2 + \begin{bmatrix} 0 \\ \dot{\alpha} \\ 0 \end{bmatrix} = A_{31}\bar{\omega}_1 + A_{32} \begin{bmatrix} \dot{\gamma} \\ 0 \\ 0 \end{bmatrix} + \begin{bmatrix} 0 \\ \dot{\alpha} \\ 0 \end{bmatrix}.$$

The system dynamics are developed by writing one vector equation for each of the three bodies considered.

Extended reference is made throughout the subsequent text to Goldstein (Reference 2). When Newtonian mechanics are applied to a rotating body, the following relationships become important. If we define \mathbf{G} as an arbitrary vector quantity, then

$$\begin{array}{ccccc} d\mathbf{G} & = & d\mathbf{G} & + & d\mathbf{G} \\ \text{(as observed in} & & \text{(as observed in} & & \text{(as observed in} \\ \text{body coordinates)} & & \text{space coordinates)} & & \text{rotating coordinates)} \end{array};$$

but

$$\begin{array}{cc} d\mathbf{G} & = \mathbf{G} \times d\Omega, \\ \text{(in rotating coordinates)} & \end{array}$$

where $d\Omega$ is the rate of rotation. Therefore

$$\begin{array}{ccccc} \dot{\mathbf{G}} & = & \dot{\mathbf{G}} & + & \omega \times \mathbf{G}, \\ \text{(as observed in} & & \text{(as observed in} & & \\ \text{space coordinates)} & & \text{body coordinates)} & & \end{array}$$

where ω is the angular rate of change of \mathbf{G} . Finally, the three vector equations that result from applying Newton's second law to the three bodies chosen are the following:

$$\mathbf{T}_1 = \dot{\mathbf{H}}_1 + \bar{\omega}_1 \times \mathbf{H}_1,$$

$$\mathbf{T}_2 = \dot{\mathbf{H}}_2 + \bar{\omega}_2 \times \mathbf{H}_2, \tag{2.4}$$

and

$$\mathbf{T}_3 = \dot{\mathbf{H}}_3 + \bar{\omega}_3 \times \mathbf{H}_3,$$

where \mathbf{T}_k is the total torque applied to body k ($k = 1, 2, 3$), \mathbf{H}_k is the total momentum of body k , and $\bar{\omega}_k$ is the total angular velocity of body k .

The components of the vector torque \mathbf{T}_k include gravity-gradient torques, control torques (both reaction wheel and gimbal spring damper), disturbance torques, and constraint torques.

Expanding the left-hand side of each of the vector equations, we obtain

$$\mathbf{T}_k = \mathbf{T}_{k1} + \mathbf{T}_{k2} + \mathbf{T}_{k3} + \mathbf{T}_{k4}, \quad (2.5)$$

where \mathbf{T}_{k1} is the total gravity-gradient torque acting upon the k th body, \mathbf{T}_{k2} is the total control torque acting upon the k th body, \mathbf{T}_{k3} is the total disturbance torque acting upon the k th body, and \mathbf{T}_{k4} is the total constraint torque acting upon the k th body.

Detailing the vector equation for the reaction wheel rotor, we obtain

$$\mathbf{T}_3 = \dot{\mathbf{H}}_3 + \bar{\omega}_3 \times \mathbf{H}_3,$$

where $\mathbf{H}_3 = \Phi_3 \bar{\omega}_3$.

After expanding,

$$\begin{bmatrix} T_{3x} \\ T_{3y} \\ T_{3z} \end{bmatrix} = \begin{bmatrix} \dot{H}_{3x} + \omega_{3y}H_{3z} - \omega_{3z}H_{3y} \\ \dot{H}_{3y} + \omega_{3z}H_{3x} - \omega_{3x}H_{3z} \\ \dot{H}_{3z} + \omega_{3x}H_{3y} - \omega_{3y}H_{3x} \end{bmatrix}.$$

Detailing the vector equation for the gimbal and wheel combination, we obtain

$$\mathbf{T}_2 = \dot{\mathbf{H}}_2 + \bar{\omega}_2 \times \mathbf{H}_2,$$

where \mathbf{H}_2 is the momentum of the gimbal alone plus that of the wheel rotor transformed into body 2 coordinates:

$$\mathbf{H}_2 = \Phi_2 \bar{\omega}_2 + A_{23} \mathbf{H}_3.$$

After expanding,

$$\begin{bmatrix} T_{2x} \\ T_{2y} \\ T_{2z} \end{bmatrix} = \begin{bmatrix} \dot{H}_{2x} + \omega_{2y}H_{2z} - \omega_{2z}H_{2y} \\ \dot{H}_{2y} + \omega_{2z}H_{2x} - \omega_{2x}H_{2z} \\ \dot{H}_{2z} + \omega_{2x}H_{2y} - \omega_{2y}H_{2x} \end{bmatrix}.$$

Finally, detailing the vector equation for the main body alone, we obtain

$$\mathbf{T}_1 = \dot{\mathbf{H}}_1 + \bar{\omega}_1 \times \mathbf{H}_1,$$

where $\mathbf{H}_1 = \Phi_1 \bar{\omega}_1$.

After expanding,

$$\begin{bmatrix} T_{1x} \\ T_{1y} \\ T_{1z} \end{bmatrix} = \begin{bmatrix} \dot{H}_{1x} + \omega_{1y}H_{1z} - \omega_{1z}H_{1y} \\ \dot{H}_{1y} + \omega_{1z}H_{1x} - \omega_{1x}H_{1z} \\ \dot{H}_{1z} + \omega_{1x}H_{1y} - \omega_{1y}H_{1x} \end{bmatrix}.$$

Detailing the left-hand side of each of the vector equations, we recall that \mathbf{T}_k , the torque acting upon each of the three bodies, is composed of four components.

$$\mathbf{T}_k = \underbrace{\mathbf{T}_{k1}}_{\text{(gravity gradient)}} + \underbrace{\mathbf{T}_{k2}}_{\text{(control)}} + \underbrace{\mathbf{T}_{k3}}_{\text{(disturbance)}} + \underbrace{\mathbf{T}_{k4}}_{\text{(constraint)}}.$$

Each of these components will be developed separately.

For the determination of \mathbf{T}_{k1} , Sabroff (Reference 3) showed that the gravity-gradient torque acting upon an arbitrary rigid body may be defined as follows.

Assume that $\tilde{\tilde{X}}_k$ represents the body axes of the k th body and that these axes are located at the center of mass of the body. Relate the body axes $\tilde{\tilde{X}}_k$ to the orbit reference axes $\tilde{\tilde{X}}_r$ by the coordinate transformation

$$\tilde{\tilde{X}}_k = A_{kr} \tilde{\tilde{X}}_r,$$

where

$$\tilde{\tilde{X}}_k = \begin{bmatrix} x_k \\ y_k \\ z_k \end{bmatrix},$$

$$\tilde{\tilde{X}}_r = \begin{bmatrix} x_r \\ y_r \\ z_r \end{bmatrix}.$$

and

$$A_{kr} = \begin{bmatrix} a_{kr}(11) & a_{kr}(12) & a_{kr}(13) \\ a_{kr}(21) & a_{kr}(22) & a_{kr}(23) \\ a_{kr}(31) & a_{kr}(32) & a_{kr}(33) \end{bmatrix}.$$

If the inertia tensor for the k th body is defined as

$$I_k = \begin{bmatrix} I'_k(11) & -I'_k(12) & -I'_k(13) \\ -I'_k(21) & I'_k(22) & -I'_k(23) \\ -I'_k(31) & -I'_k(32) & I'_k(33) \end{bmatrix},$$

then the gravity-gradient torque vector acting upon the k th body is described by the following expression:

$$\mathbf{T}_{k1} = 3\Omega_0^2 \begin{bmatrix} \left\{ \left[I'_k(33) - I'_k(22) \right] a_{kr}(23) a_{kr}(33) + I'_k(12) a_{kr}(13) a_{kr}(33) \right. \\ \left. - I'_k(13) a_{kr}(13) a_{kr}(23) - I'_k(23) \left[a_{kr}^2(23) - a_{kr}^2(33) \right] \right\} \\ \left\{ \left[I'_k(11) - I'_k(33) \right] a_{kr}(13) a_{kr}(33) + I'_k(13) \left[a_{kr}^2(13) - a_{kr}^2(33) \right] \right. \\ \left. + I'_k(23) a_{kr}(13) a_{kr}(23) - I'_k(12) a_{kr}(23) a_{kr}(33) \right\} \\ \left\{ \left[I'_k(22) - I'_k(11) \right] a_{kr}(13) a_{kr}(23) + I'_k(12) \left[a_{kr}^2(23) - a_{kr}^2(13) \right] \right. \\ \left. + I'_k(13) a_{kr}(23) a_{kr}(33) - I'_k(23) a_{kr}(13) a_{kr}(33) \right\} \end{bmatrix}.$$

From this generalized relationship, it is possible to detail the gravity-gradient torques acting upon each of the three bodies under consideration. The inertia tensors used in the evaluation of these gravity-gradient torques are

$$I_1 = \Phi_1,$$

$$I_2 = [\Phi_2] + A_{32}[\Phi_3]A_{32}^T,$$

and

$$I_3 = \Phi_3.$$

where I_2 is the sum of Φ_2 , the inertia tensor of the gimbal, and Φ_3 , the inertia tensor of the wheel rotor, transformed to the gimbal coordinates.

The control torques \mathbf{T}_{k2} were defined to include both the torques resulting from the presence of the actively controlled reaction wheel and those resulting from the gimbal spring damper.

Detailing the control torques acting upon each of the three bodies, the following relationships are found to exist.

$$\mathbf{T}_{32} = \begin{bmatrix} 0 \\ T_w \\ 0 \end{bmatrix},$$

where T_w is the torque applied to the wheel rotor minus the frictional torque.

$$\mathbf{T}_{22} = \begin{bmatrix} -k_g\gamma - B_g\dot{\gamma} \\ 0 \\ 0 \end{bmatrix}.$$

Since body 2 represents the combined wheel and rotor, the rotor torque T_w does not appear in \mathbf{T}_{22} either as a direct torque or as a reaction torque.

The reaction torque of the spring damper transformed to body 1 coordinates \mathbf{T}_{12} is

$$\mathbf{T}_{12} = A_{12} \begin{bmatrix} k_g\gamma + B_g\dot{\gamma} \\ 0 \\ 0 \end{bmatrix}.$$

For the purpose of detailing the disturbance torques, it was assumed that all disturbance torques are generated in the orbit reference set of axes and are defined as \mathbf{T}_d in this set of axes. Under these assumptions, the following relationships are found to exist.

$$\mathbf{T}_{33} = A_{3r}\mathbf{T}_d,$$

$$\mathbf{T}_{23} = A_{2r}\mathbf{T}_d,$$

and

$$\mathbf{T}_{13} = A_{1r}\mathbf{T}_d.$$

Finally it is necessary to detail the constraint torques acting upon each of the three bodies.

When the constraint torques act upon the wheel rotor alone, the rotor is free to rotate about its spin axis, y_3 , and is constrained about its x_3 and z_3 axes. Therefore,

$$\mathbf{T}_{34} = \begin{bmatrix} T_{34x} \\ 0 \\ T_{34z} \end{bmatrix}.$$

When the constraint torques act upon the gimbaled wheel combination, the gimbal is free to rotate about its x_2 axis and is constrained about its y_2 and z_2 axes. Therefore,

$$\mathbf{T}_{24} = \begin{bmatrix} 0 \\ T_{24y} \\ T_{24z} \end{bmatrix}.$$

The constraint torques acting upon the main body alone are the reaction from the body 2 constraint torques transformed to the body 1 set of coordinates. Therefore,

$$\mathbf{T}_{14} = A_{12} \begin{bmatrix} 0 \\ -T_{24y} \\ -T_{24z} \end{bmatrix}.$$

At this point the three vector equations are completely determined. Although these vector equations allow us to write nine separate equations, clearly not all of them are independent. The set of independent equations are those nondegenerate equations that remain after the constraint torques are substituted into the three vector equations. Detailing, we see that

$$\begin{bmatrix} T_{34x} \\ 0 \\ T_{34z} \end{bmatrix} = \begin{bmatrix} \dot{H}_{3x} + \omega_{3y}H_{3z} - \omega_{3z}H_{3y} \\ \dot{H}_{3y} + \omega_{3z}H_{3x} - \omega_{3x}H_{3z} \\ \dot{H}_{3z} + \omega_{3x}H_{3y} - \omega_{3y}H_{3x} \end{bmatrix} - \mathbf{T}_{31} - \mathbf{T}_{32} - \mathbf{T}_{33},$$

$$\begin{bmatrix} 0 \\ T_{24y} \\ T_{24z} \end{bmatrix} = \begin{bmatrix} \dot{H}_{2x} + \omega_{2y}H_{2z} - \omega_{2z}H_{2y} \\ \dot{H}_{2y} + \omega_{2z}H_{2x} - \omega_{2x}H_{2z} \\ \dot{H}_{2z} + \omega_{2x}H_{2y} - \omega_{2y}H_{2x} \end{bmatrix} - \mathbf{T}_{21} - \mathbf{T}_{22} - \mathbf{T}_{23},$$

and

$$A_{12} \begin{bmatrix} 0 \\ -T_{24y} \\ -T_{24z} \end{bmatrix} = \begin{bmatrix} \dot{H}_{1x} + \omega_{1y}H_{1z} - \omega_{1z}H_{1y} \\ \dot{H}_{1y} + \omega_{1z}H_{1x} - \omega_{1x}H_{1z} \\ \dot{H}_{1z} + \omega_{1x}H_{1y} - \omega_{1y}H_{1x} \end{bmatrix} - \mathbf{T}_{11} - \mathbf{T}_{12} - \mathbf{T}_{13}.$$

The resulting nondegenerate equations are

$$\dot{H}_{3y} + \omega_{3z}H_{3x} - \omega_{3x}H_{3z} = T_{31y} + T_{32y} + T_{33y},$$

$$\dot{H}_{2x} + \omega_{2y}H_{2z} - \omega_{2z}H_{2y} = T_{21x} + T_{22x} + T_{23x},$$

and

(2.6)

$$\left. \begin{array}{l} \dot{H}_{1x} + \omega_{1y}H_{1z} - \omega_{1z}H_{1y} \\ \dot{H}_{1y} + \omega_{1z}H_{1x} - \omega_{1x}H_{1z} \\ \dot{H}_{1z} + \omega_{1x}H_{1y} - \omega_{1y}H_{1x} \end{array} \right\} = \mathbf{T}_{11} + \mathbf{T}_{12} + \mathbf{T}_{13} + A_{12} \begin{bmatrix} 0 \\ -T_{24y} \\ -T_{24z} \end{bmatrix}.$$

These equations are functions of the variables and the derivatives of the variables listed below. Clearly, the fully expanded equations will be extremely nonlinear and lengthy; however, they do constitute a valid complete set of equations for the generalized spacecraft configuration under study. The variables are ϕ , the spacecraft roll angle, θ , the spacecraft pitch angle, ψ , the spacecraft yaw angle, γ , the gimbal angle, $\dot{\alpha}$, the wheel rotor angular velocity, and ϵ , the electrical signal out of the lead network in the active pitch loop.

The sixth equation required is Equation (2.2), the electrical error equation,

$$\epsilon = [T_1 \dot{\theta}_s + \theta_s - T_2 \dot{\epsilon}].$$

Note that β and H_b also appear in the final set of equations, but these are system parameters and not variables. We define

$$\omega_{1x} \equiv \omega_{11}$$

$$\omega_{1y} \equiv \omega_{12}$$

$$\omega_{1z} \equiv \omega_{13}$$

$$\Sigma \equiv \sum_{i=1}^3$$

Appendix A contains a detailed development of the dynamical and kinematic equations. Expansion of the left-hand side of Equations (2.4) results in the following expressions:

$$\begin{aligned} T_{3y} = I_3(22) \left\{ \Sigma \dot{a}_{31}(2i)\omega_{1i} + \Sigma a_{31}(2i)\dot{\omega}_{1i} + \dot{a}_{32}(21)\dot{\gamma} + a_{32}(21)\ddot{\gamma} + \ddot{\alpha} \right\} \\ + \left(I_3(11) - I_3(33) \right) \omega_{3x}\omega_{3z}. \end{aligned} \quad (2.7)$$

Note that when the rotor is assumed symmetric, the last term vanishes because

$$I_3(11) = I_3(33).$$

$$\begin{aligned} T_{2x} = I_2(11) \left[\Sigma \dot{a}_{21}(1i)\omega_{1i} + \Sigma a_{21}(1i)\dot{\omega}_{1i} + \ddot{\gamma} \right] + \dot{a}_{23}(11)I_3(11) \left[a_{32}(11)\dot{\gamma} + \Sigma a_{31}(1i)\omega_{1i} \right] \\ + \dot{a}_{23}(12)I_3(22) \left[\dot{a} + a_{32}(21)\dot{\gamma} + \Sigma a_{31}(2i)\omega_{1i} \right] + \dot{a}_{23}(13)I_3(33) \left[a_{32}(31)\dot{\gamma} + \Sigma a_{31}(3i)\omega_{1i} \right] \\ + a_{23}(11)I_3(11) \left[\dot{a}_{32}(11)\dot{\gamma} + a_{32}(11)\ddot{\gamma} + \Sigma \dot{a}_{31}(1i)\omega_{1i} + \Sigma a_{31}(1i)\dot{\omega}_{1i} \right] \\ + a_{23}(12)I_3(22) \left[\ddot{\alpha} + \dot{a}_{32}(21)\dot{\gamma} + a_{32}(21)\ddot{\gamma} + \Sigma \dot{a}_{31}(2i)\omega_{1i} + \Sigma a_{31}(2i)\dot{\omega}_{1i} \right] \\ + a_{23}(13)I_3(33) \left[\dot{a}_{32}(31)\dot{\gamma} + a_{32}(31)\ddot{\gamma} + \Sigma \dot{a}_{31}(3i)\omega_{1i} + \Sigma a_{31}(3i)\dot{\omega}_{1i} \right] \\ + \left\{ \Sigma a_{21}(2i)\omega_{1i} \right\} \left\{ I_2(33) \left[\Sigma a_{21}(3i)\omega_{1i} \right] + a_{23}(31)I_3(11) \left[a_{32}(11)\dot{\gamma} + \Sigma a_{31}(1i)\omega_{1i} \right] \right. \\ + a_{23}(32)I_3(22) \left[\dot{a} + a_{32}(21)\dot{\gamma} + \Sigma a_{31}(2i)\omega_{1i} \right] + a_{23}(33)I_3(33) \left[a_{32}(31)\dot{\gamma} + \Sigma a_{31}(3i)\omega_{1i} \right] \Big\} \\ - \left\{ \Sigma a_{21}(3i)\omega_{1i} \right\} \left\{ I_2(22) \left[\Sigma a_{21}(2i)\omega_{1i} \right] + a_{23}(21)I_3(11) \left[a_{32}(11)\dot{\gamma} + \Sigma a_{31}(1i)\omega_{1i} \right] \right. \\ + a_{23}(22)I_3(22) \left[\dot{a} + a_{32}(21)\dot{\gamma} + \Sigma a_{31}(2i)\omega_{1i} \right] + a_{23}(23)I_3(33) \left[a_{32}(31)\dot{\gamma} + \Sigma a_{31}(3i)\omega_{1i} \right] \Big\}, \end{aligned} \quad (2.8)$$

$$T_{1x} = I_1(11)\dot{\omega}_{1x} - I_1(12)\dot{\omega}_{1y} - I_1(13)\dot{\omega}_{1z} + \omega_{1y}\omega_{1z}[I_1(33) - I_1(22)] \\ - \omega_{1y}[I_1(31)\omega_{1x} + I_1(32)\omega_{1y}] + \omega_{1z}[I_1(21)\omega_{1x} + I_1(23)\omega_{1y}], \quad (2.9)$$

$$T_{1y} = -I_1(21)\dot{\omega}_{1x} + I_1(22)\dot{\omega}_{1y} - I_1(23)\dot{\omega}_{1z} + \omega_{1z}\omega_{1x}[I_1(11) - I_1(33)] \\ - \omega_{1z}[I_1(12)\omega_{1y} + I_1(13)\omega_{1z}] + \omega_{1x}[I_1(31)\omega_{1x} + I_1(32)\omega_{1y}], \quad (2.10)$$

and

$$T_{1z} = -I_1(31)\dot{\omega}_{1x} - I_1(32)\dot{\omega}_{1y} + I_1(33)\dot{\omega}_{1z} + \omega_{1x}\omega_{1y}[I_1(22) - I_1(11)] \\ - \omega_{1x}[I_1(21)\omega_{1x} + I_1(23)\omega_{1z}] + \omega_{1y}[I_1(12)\omega_{1y} + I_1(13)\omega_{1z}]. \quad (2.11)$$

Expansion of the right-hand side of Equations (2.4) yields

$$T_{3y} = T_w = k_T[T_1\dot{\theta}_s + \theta_s - T_2\dot{\epsilon} - (H_w - H_b)C_t] - H_w B_f, \quad (2.12)$$

$$T_{2x} = 3\Omega_0^2[I_2(33) + I_3(11) - I_2(22) - I_3(22)]a_{2r}(23)a_{2r}(33) - k_g\gamma - B_g\dot{\gamma}, \quad (2.13)$$

$$T_{1x} = 3\Omega_0^2\{[I_1(33) - I_1(22)]a_{1r}(23)a_{1r}(33) + I_1(12)a_{1r}(13)a_{1r}(33) - I_1(13)a_{1r}(13)a_{1r}(23) \\ - I_1(23)[a_{1r}^2(23) - a_{1r}^2(33)]\} + a_{12}(11)(k_g\gamma + B_g\dot{\gamma}) - a_{12}(12)T_{24y} - a_{12}(13)T_{24z}, \quad (2.14)$$

$$T_{1y} = 3\Omega_0^2\{[I_1(11) - I_1(33)]a_{1r}(13)a_{1r}(33) + I_1(13)[a_{1r}^2(13) - a_{1r}^2(33)] + I_1(23)a_{1r}(13)a_{1r}(23) \\ - I_1(12)a_{1r}(23)a_{1r}(33)\} + a_{12}(21)(k_g\gamma + B_g\dot{\gamma}) - a_{12}(22)T_{24y} - a_{12}(23)T_{24z}, \quad (2.15)$$

and

$$T_{1z} = 3\Omega_0^2\{[I_1(22) - I_1(11)]a_{1r}(13)a_{1r}(23) + I_1(12)[a_{1r}^2(23) - a_{1r}^2(13)] + I_1(13)a_{1r}(23)a_{1r}(33) \\ - I_1(23)a_{1r}(13)a_{1r}(33)\} + a_{12}(31)(k_g\gamma + B_g\dot{\gamma}) - a_{12}(32)T_{24y} - a_{12}(33)T_{24z}. \quad (2.16)$$

In order to detail the five nondegenerate equations of motion, it is necessary to define

$$\begin{bmatrix} \omega_{1x} \\ \omega_{1y} \\ \omega_{1z} \end{bmatrix} = \begin{bmatrix} -\dot{\psi}S\theta C\phi + \dot{\phi}C\theta - \Omega_0(C\theta S\psi + S\theta S\phi C\psi) \\ \dot{\psi}S\phi + \dot{\theta} - \Omega_0(C\phi C\psi) \\ \dot{\psi}C\theta C\phi + \dot{\phi}S\theta - \Omega_0(S\theta S\psi - C\theta S\phi C\psi) \end{bmatrix}, \quad (2.17)$$

$$\begin{bmatrix} \dot{\omega}_{1x} \\ \dot{\omega}_{1y} \\ \dot{\omega}_{1z} \end{bmatrix} = \begin{bmatrix} -\ddot{\psi}S\theta C\phi + \ddot{\phi}C\theta + \dot{\theta}(\Omega_0 S\theta - \Omega_0 C\theta S\phi C\psi) + \dot{\phi}(-\Omega_0 S\theta C\phi C\psi) \\ \quad + \dot{\psi}(\Omega_0 S\theta S\psi - \Omega_0 C\theta C\psi) - \dot{\psi}\dot{\theta}C\theta C\phi + \dot{\psi}\dot{\phi}S\theta S\phi - \dot{\phi}\dot{\theta}S\theta \\ \ddot{\psi}S\phi + \ddot{\theta} + \dot{\phi}\Omega_0 S\phi C\psi + \dot{\psi}\Omega_0 C\phi S\psi + \dot{\phi}\dot{\psi}C\phi \\ \ddot{\psi}C\theta C\phi + \ddot{\phi}S\theta + \dot{\theta}(-\Omega_0 C\theta S\psi - \Omega_0 S\theta S\phi C\psi) + \dot{\phi}(\Omega_0 C\theta C\phi C\psi) \\ \quad + \dot{\psi}(-\Omega_0 S\theta C\psi - \Omega_0 C\theta S\phi S\psi) + \dot{\phi}\dot{\theta}C\theta - \dot{\psi}\dot{\theta}S\theta S\phi - \dot{\psi}\dot{\phi}C\theta S\phi \end{bmatrix}, \quad (2.18)$$

and

$$A_{1r} = \begin{bmatrix} C\theta C\psi - S\theta S\phi S\psi & C\theta S\psi + S\theta S\phi C\psi & -S\theta C\phi \\ -C\phi S\psi & C\phi C\psi & S\phi \\ S\theta C\psi + C\theta S\phi S\psi & S\theta S\psi - C\theta S\phi C\psi & C\theta C\phi \end{bmatrix}. \quad (2.19)$$

Because all transformations are orthogonal,

$$a_{pg}(ij) = a_{gp}(ji),$$

and only A_{pg} or A_{gp} will be given.

$$A_{21} = \begin{bmatrix} C\beta & 0 & -S\beta \\ S\beta S\gamma & C\gamma & C\beta S\gamma \\ S\beta C\gamma & -S\gamma & C\beta C\gamma \end{bmatrix},$$

$$\dot{A}_{21} = \begin{bmatrix} 0 & 0 & 0 \\ \dot{\gamma}C\gamma S\beta & -\dot{\gamma}S\gamma & \dot{\gamma}C\gamma C\beta \\ -\dot{\gamma}S\gamma S\beta & -\dot{\gamma}C\gamma & -\dot{\gamma}S\gamma C\beta \end{bmatrix},$$

$$A_{23} = \begin{bmatrix} Ca & 0 & Sa \\ 0 & 1 & 0 \\ -Sa & 0 & Ca \end{bmatrix},$$

$$\dot{A}_{23} = \begin{bmatrix} -\dot{a}Sa & 0 & \dot{a}Ca \\ 0 & 0 & 0 \\ -\dot{a}Ca & 0 & -\dot{a}Sa \end{bmatrix},$$

$$A_{31} = \begin{bmatrix} CaC\beta - SaS\beta C\gamma & SaS\gamma & -CaS\beta - SaC\beta C\gamma \\ S\beta S\gamma & C\gamma & C\beta S\gamma \\ SaC\beta + CaS\beta C\gamma & -CaS\gamma & -SaS\beta + CaC\beta C\gamma \end{bmatrix},$$

and

$$\dot{A}_{31} = \begin{bmatrix} -\dot{a}C\beta Sa + \dot{\gamma}S\gamma SaS\beta - \dot{a}CaS\beta C\gamma & \dot{a}CaS\gamma + \dot{\gamma}C\gamma Sa & \dot{a}SaS\beta - \dot{a}CaC\beta C\gamma + \dot{\gamma}SaC\beta S\gamma \\ \dot{\gamma}C\gamma S\beta & -\dot{\gamma}S\gamma & \dot{\gamma}C\beta C\gamma \\ \dot{a}CaC\beta - \dot{a}SaS\beta C\gamma - \dot{\gamma}S\gamma CaS\beta & -\dot{\gamma}C\gamma Ca + \dot{a}SaS\gamma & -\dot{a}CaS\beta - \dot{\gamma}CaC\beta S\gamma - \dot{a}SaC\beta C\gamma \end{bmatrix}.$$

(Recall that β is a constant.)

The equation set for this complex eleventh-order system is now completely defined. However, these equations would be prohibitive even to write down, and linearization must be performed before the discussion can be continued.

CHAPTER 3

DEVELOPMENT OF THE LINEARIZED EQUATION SET

3.1 General Discussion

In general, any n th-order system can be represented by the vector equation

$$\dot{\mathbf{X}} = \mathbf{f}(\mathbf{X}) ,$$

where

$$\dot{\mathbf{X}} = \begin{bmatrix} \dot{x}_1 \\ \dot{x}_2 \\ \vdots \\ \dot{x}_n \end{bmatrix}$$

and

$$\mathbf{X} = \begin{bmatrix} x_1 \\ x_2 \\ \vdots \\ x_n \end{bmatrix} ,$$

where x_1, x_2, \dots, x_n are the various system states. Also,

$$\mathbf{f}(\mathbf{X}) = \begin{bmatrix} f_1(\mathbf{X}) \\ f_2(\mathbf{X}) \\ \vdots \\ f_n(\mathbf{X}) \end{bmatrix} ,$$

where $f_i(\mathbf{X})$ is some function, linear or nonlinear, of the system state variables.

This vector equation can be rewritten as shown below.

$$\dot{\mathbf{X}} = \mathbf{A}\mathbf{X} + \mathbf{G}(\mathbf{X}),$$

where

$$\mathbf{X} = \begin{bmatrix} x_1 \\ x_2 \\ \vdots \\ x_n \end{bmatrix} = \text{state variables},$$

$$\mathbf{A} = \begin{bmatrix} \frac{\partial f_1}{\partial x_1} & \frac{\partial f_1}{\partial x_2} & \cdots & \\ \frac{\partial f_2}{\partial x_1} & & & \\ \vdots & & & \\ & & \cdots & \frac{\partial f_n}{\partial x_n} \end{bmatrix},$$

and

$$\mathbf{G}(\mathbf{X}) = \begin{bmatrix} G_1(\mathbf{X}) \\ G_2(\mathbf{X}) \\ \vdots \\ G_n(\mathbf{X}) \end{bmatrix}.$$

Expanding the vector equation as shown makes it possible to represent all of the linear first-order terms by $\mathbf{A}\mathbf{X}$ while $\mathbf{G}(\mathbf{X})$ represents all of the other terms. Since by definition, $\mathbf{G}(\mathbf{X}_0)$ is zero, then in order to investigate stability in the neighborhood about which the system was linearized, it is only necessary to investigate the stability of the system of equations $\dot{\mathbf{X}} = \mathbf{A}\mathbf{X}$.

Clearly the system represented by these equations is asymptotically stable within some neighborhood of \mathbf{X}_0 if and only if all of the eigenvalues of \mathbf{A} have negative real parts. Conversely, the system is unstable if any of its eigenvalues have a real part which is positive or equal to zero.

Because the A matrix was fabricated by the technique of linearization, any conclusions reached concerning either stability and/or system performance must be verified. Clearly, these conclusions will be accurate for some limited variation of the state variables about \mathbf{X}_0 , their equilibrium state. However, whether or not this limited range of variation is sufficiently large to be of practical importance remains to be determined.

Aside from the necessary verification suggested above, situations that are expected to give rise to large deviations of any one state variable must be considered separately. Chapters 5 and 7 discuss in detail problems of this nature.

3.2 Linearizing the General System Equation Set

A gimballed-reaction-wheel-scanner-type spacecraft would fulfill conveniently the mission requirements placed upon a meteorological or observatory class of spacecraft. This class of vehicle is expected to maintain a single orientation in space, and its meteorological sensing devices are fixed to the main spacecraft body.

For the ease of locating sensors and experimental packages, it is of practical interest to define the equilibrium state vector as follows:

$$\mathbf{X}_0 = \begin{bmatrix} \theta \\ \phi \\ \psi \\ \dot{\theta} \\ \dot{\phi} \\ \dot{\psi} \\ \gamma \\ \dot{\gamma} \\ \epsilon \\ \dot{\epsilon} \\ \dot{\alpha} \end{bmatrix} = \begin{bmatrix} 0 \\ 0 \\ 0 \\ 0 \\ 0 \\ 0 \\ 0 \\ 0 \\ 0 \\ 0 \\ \dot{\alpha}_0 \end{bmatrix}. \quad (3.1)$$

Only the wheel rotor speed has a nonzero equilibrium condition, and this equilibrium speed can be found from the expression defining rotor torque T_w .

In order to linearize the five nondegenerate equations presented at the end of Chapter 2, each must be expanded into a Taylor series expansion about the system equilibrium. All terms of second order or higher are discarded.

The Taylor expansion for a function of n state variables, (x_1, x_2, \dots, x_n) , can be written

$$f(x_1 \dots x_n) = f(x_1 \dots x_n) \Big|_{\mathbf{X}_0} + (x_1 - x_{10}) \frac{\partial f(x_1 \dots x_n)}{\partial x_1} \Big|_{\mathbf{X}_0} + \dots + (x_n - x_{n0}) \frac{\partial f(x_1 \dots x_n)}{\partial x_n} \Big|_{\mathbf{X}_0}.$$

When the expression $f(x_1 \dots x_n)$ is sufficiently complicated, it is convenient to break up this expression and to write

$$f(x_1 \dots x_n) = f_1(x_1 \dots x_n) \dots f_m(x_1 \dots x_n)$$

or, in closed form,

$$f(x_1 \dots x_n) = \prod_{i=1}^m f_i(x_1 \dots x_n).$$

It is then possible, and probably more simple, to expand each of the $f_i(x_1 \dots x_n)$ into a Taylor series separately and finally multiply the resulting expressions together. The two results will be identical as long as terms of second and higher order are discarded.

It is possible to completely define the five nondegenerate equations of motion in terms of the linearized expressions for $\bar{\omega}_1$, $\bar{\dot{\omega}}_1$, and the coordinate transformation matrices, in view of this simplification. Detailing, we obtain

$$\begin{bmatrix} \omega_{1x} \\ \omega_{1y} \\ \omega_{1z} \end{bmatrix} = \begin{bmatrix} \dot{\phi} - \Omega_0 \psi \\ \dot{\theta} - \Omega_0 \\ \dot{\psi} + \Omega_0 \phi \end{bmatrix}, \quad (3.2)$$

$$\begin{bmatrix} \dot{\omega}_{1x} \\ \dot{\omega}_{1y} \\ \dot{\omega}_{1z} \end{bmatrix} = \begin{bmatrix} \ddot{\phi} - \Omega_0 \dot{\psi} \\ \ddot{\theta} \\ \ddot{\psi} + \Omega_0 \dot{\phi} \end{bmatrix}, \quad (3.3)$$

and

$$A_{1r} = \begin{bmatrix} 1 & \psi & -\theta \\ -\psi & 1 & \phi \\ \theta & -\phi & 1 \end{bmatrix}. \quad (3.4)$$

Because all transformations are orthogonal, it was assumed that the linearized transformation matrices are related by $A_{pg}^{-1} = A_{gp}^T$ while their elements are related by $a_{pg}(ij) = a_{gp}(ji)$. For this reason, only A_{pg} or A_{gp} will be written, as was done with the nonlinear coordinate transformations.

$$A_{21} = \begin{bmatrix} C\beta & 0 & -S\beta \\ \gamma S\beta & 1 & \gamma C\beta \\ S\beta & -\gamma & C\beta \end{bmatrix},$$

$$\dot{A}_{21} = \begin{bmatrix} 0 & 0 & 0 \\ \dot{\gamma} S\beta & 0 & \dot{\gamma} C\beta \\ 0 & \dot{\gamma} & 0 \end{bmatrix},$$

$$A_{23} = \begin{bmatrix} C\alpha & 0 & S\alpha \\ 0 & 1 & 0 \\ -S\alpha & 0 & C\alpha \end{bmatrix},$$

$$\dot{A}_{23} = \begin{bmatrix} -\dot{\alpha} S\alpha & 0 & \dot{\alpha} C\alpha \\ 0 & 0 & 0 \\ -\dot{\alpha} C\alpha & 0 & -\dot{\alpha} S\alpha \end{bmatrix},$$

$$A_{31} = \begin{bmatrix} C\alpha C\beta - S\alpha S\beta & \gamma S\alpha & -S\beta C\alpha - S\alpha C\beta \\ \gamma S\beta & 1 & \gamma C\beta \\ S\alpha C\beta + C\alpha S\beta & -\gamma C\alpha & -S\alpha S\beta + C\alpha C\beta \end{bmatrix},$$

and

$$\dot{A}_{31} = \begin{bmatrix} -\dot{\alpha}CaS\beta - \dot{\alpha}SaC\beta & \dot{\gamma}Sa + \gamma\dot{\alpha}Ca & \dot{\alpha}SaS\beta - \dot{\alpha}C\beta Ca \\ \dot{\gamma}S\beta & 0 & \dot{\gamma}C\beta \\ -\dot{\alpha}S\beta Sa + \dot{\alpha}C\beta Ca & -\dot{\gamma}Ca + \gamma\dot{\alpha}Sa & -\dot{\alpha}SaC\beta - \dot{\alpha}S\beta Ca \end{bmatrix}.$$

Note that α is not a state variable and cannot be linearized out.

3.3 Linearizing the Scanner Error Equation

The scanner equation was developed in Section (2.2) and can be written as

$$\tan(\theta_s + \beta) = \frac{\sin(\theta + \beta) \cos \phi}{\cos(\theta + \beta) \cos \phi \cos \gamma - \sin \phi \sin \gamma}.$$

Taking the arc tangent and linearizing, we obtain

$$(\theta_s + \beta) = \tan^{-1} [f(\theta\phi\gamma)] \Big|_0 + \frac{\partial \tan^{-1} [f(\theta\phi\gamma)]}{\partial \theta} \Big|_0 \theta + \frac{\partial \tan^{-1} [f(\theta\phi\gamma)]}{\partial \phi} \Big|_0 \phi + \frac{\partial \tan^{-1} [f(\theta\phi\gamma)]}{\partial \gamma} \Big|_0 \gamma.$$

Evaluation of this expression gives rise to the simple result

$$\theta_s + \beta = \theta + \beta$$

or

$$\theta_s = \theta.$$

(3.5)

3.4 Determination of Rotor Equilibrium Speed

The useful wheel torque was derived in Section (2.2) and can be written as

$$T_w = k_T [T_1 \dot{\theta}_s + \theta_s - T_2 \dot{\epsilon} - C_t \dot{I}_3(22) + C_t H_b] - B_f \dot{I}_3(22).$$

Solving for the equilibrium momentum, we obtain

$$\dot{\alpha} [k_T C_t I_3(22) + B_f I_3(22)] = C_t k_T H_b,$$

or

$$\dot{\alpha} I_3(22) = \frac{C_t k_T}{C_t k_T + B_f} H_b = \text{equilibrium momentum},$$

where \dot{a} in this expression is the actual wheel speed. Linearizing about a small variational wheel speed, we obtain

$$T_w = k_T \left[T_1 \dot{\theta}_s + \theta_s - T_2 \dot{\epsilon} - C_t \left(\dot{a} I_3(22) + \frac{C_t}{C_t k_T + B_f} H_b \right) + C_t H_b \right] - B_f \left[\dot{a} I_3(22) + \frac{C_t k_T}{C_t k_T + B_f} H_b \right],$$

where \dot{a} in this expression is the variational wheel speed. Finally, eliminating the bias momentum, we see that

$$T_w = k_T [T_1 \dot{\theta}_s + \theta_s - T_2 \dot{\epsilon} - C_t \dot{a} I_3(22)] - B_f \dot{a} I_3(22), \quad (3.6)$$

where \dot{a} is variation wheel speed.

3.5 Resulting Linearized Equations

After much algebraic manipulation, the linearized set of equations of motion can be written as shown on the following pages.

Recall that H_b is the pitch-momentum bias and is considered constant. Its derivative, $\dot{H}_b = \dot{a} I_3(22)$, is carried in these equations for its use in Chapter 5.

T_{3y} :

$$I_3(22) \ddot{\theta} + I_3(22) \ddot{a} = T_w = k_T T_1 \dot{\theta} \cdot [k_T C_t I_3(22) + B_f I_3(22)] \dot{a} - k_T T_2 \dot{\epsilon} + k_T \theta. \quad (3.7)$$

T_{2x} :

$$\begin{aligned} & [C\beta I_2(11) + C\beta I_3(11)] \ddot{\phi} + [-S\beta I_2(11) - S\beta I_3(11)] \ddot{\psi} + [I_2(11) + I_3(11)] \ddot{\gamma} \\ & + \{2\Omega_0 S\beta [I_2(22) - I_2(33)]\} \dot{\theta} + [S\beta \Omega_0 I_3(22) - S\beta \Omega_0 I_2(11) - 2S\beta \Omega_0 I_3(11) - H_b S\beta] \dot{\phi} \\ & + \{I_3(22) C\beta \Omega_0 - I_2(11) C\beta \Omega_0 - 2I_3(11) \Omega_0 C\beta - [I_2(33) - I_2(22)] C\beta \Omega_0 - C\beta H_b\} \dot{\psi} \\ & + B_g \dot{\gamma} + \{I_3(22) C\beta \Omega_0^2 - I_3(11) \Omega_0^2 C\beta - [I_2(33) - I_2(22)] C\beta \Omega_0^2 - 3C\beta \Omega_0^2 [I_2(33) \\ & + I_3(33) - I_2(22) - I_3(22)] - C\beta \Omega_0 H_b\} \phi + [I_3(11) \Omega_0^2 S\beta - I_3(22) S\beta \Omega_0^2 + H_b S\beta \Omega_0] \psi \\ & + \{I_3(22) \Omega_0^2 + k_g - [I_2(33) - I_2(22)] \Omega_0^2 - I_3(11) \Omega_0^2 - H_b \Omega_0 - 3\Omega_0^2 C^2 \beta [I_2(33) \\ & + I_3(33) - I_2(22) - I_3(22)]\} \gamma = -[I_2(33) - I_2(22)] S\beta \Omega_0^2. \end{aligned} \quad (3.8)$$

T_{1x} :

$$\begin{aligned}
& I_1(12)\ddot{\theta} - \{I_1(11) + S^2\beta[I_2(33) + I_3(11)]\}\ddot{\phi} + \{I_1(13) - S\beta C\beta[I_3(11) + I_2(33)]\}\ddot{\psi} \\
& + [-2\Omega_0 I_1(32)]\dot{\theta} + \{\Omega_0 I_1(13) - \Omega_0 I_1(31) - \Omega_0 S\beta C\beta[I_2(33) - I_3(22) - I_2(22) + I_2(11) \\
& + 2I_3(11)] - S\beta C\beta H_b\}\dot{\phi} + \{\Omega_0 I_1(11) + \Omega_0 I_1(33) - \Omega_0 I_1(22) + \Omega_0 S^2\beta[I_2(33) - I_3(22) \\
& - I_2(22) + I_2(11) + 2I_3(11)] + S^2\beta H_b\}\dot{\psi} + \{C\beta B_g - S\beta H_b - \Omega_0 S\beta[I_2(33) - I_3(22) \\
& - I_2(22) + I_2(11) + I_3(11)]\}\dot{\gamma} + [-3\Omega_0^2 I_1(12)]\theta + \{3\Omega_0^2[I_1(33) - I_1(22)] - \Omega_0^2[I_1(22) \\
& - I_1(33)] - S^2\beta\Omega_0^2[I_3(22) + I_2(22) - I_2(11) - I_3(11)] + S^2\beta\Omega_0 H_b - 3\Omega_0^2 S^2\beta[I_2(22) \\
& + I_3(22) - I_2(11) - I_3(11)]\}\phi + \{\Omega_0^2 I_1(31) - \Omega_0^2 S\beta C\beta[I_3(22) + I_2(22) - I_2(11) \\
& - I_3(11)] + \Omega_0 S\beta C\beta H_b\}\psi + \{-S\beta\ddot{a}I_3(22) + C\beta k_g - S\beta 3\Omega_0^2 S\beta C\beta[I_2(11) - I_2(33)] \\
& - 3\Omega_0^2 S^2\beta C\beta[I_2(22) + I_3(22) - I_2(11) - I_3(11)]\}\gamma = -[3\Omega_0^2 I_1(23) + I_1(32)\Omega_0^2]. \quad (3.9)
\end{aligned}$$

T_{1y} :

$$\begin{aligned}
& -[I_2(22) + I_3(22) + I_1(22)]\ddot{\theta} - I_1(21)\ddot{\phi} + I_1(23)\ddot{\psi} - I_3(22)\ddot{\alpha} + \{\Omega_0[I_1(23) + I_1(32)]\}\dot{\phi} \\
& - \{\Omega_0[I_1(12) + I_1(21)]\}\dot{\psi} + \{3\Omega_0^2[I_1(33) - I_1(11)] - (S^2\beta - C^2\beta)[-I_2(11) + I_2(33)]3\Omega_0^2\}\theta \\
& + [-3\Omega_0^2 I_1(12) - \Omega_0^2 I_1(12)]\phi - \Omega_0^2 I_1(32)\psi = 3\Omega_0^2\{[-I_2(33) + I_2(11)]S\beta C\beta + I_1(13)\}. \quad (3.10)
\end{aligned}$$

T_{1z} :

$$\begin{aligned}
& I_1(32)\ddot{\theta} + \{I_1(31) - S\beta C\beta[I_2(33) + I_3(11)]\}\ddot{\phi} + \{-I_1(33) - C^2\beta[I_3(11) + I_2(33)]\}\ddot{\psi} \\
& + [2\Omega_0 I_1(12)]\dot{\theta} + \{-\Omega_0 I_1(33) + \Omega_0[I_1(22) - I_1(11)] - C^2\beta\Omega_0[I_2(33) - I_3(22) + I_2(11) \\
& - I_2(22) + 2I_3(11)] - C^2\beta H_b\}\dot{\phi} + \{\Omega_0 I_1(13) + \Omega_0 S\beta C\beta[I_2(33) - I_3(22) - I_2(22) \\
& + I_2(11) + 2I_3(11)] + S\beta C\beta H_b - \Omega_0 I_1(31)\}\dot{\psi} + \{-S\beta B_g - C\beta H_b - C\beta\Omega_0[I_2(33) \\
& - I_3(22) - I_2(22) + I_2(11) + I_3(11)]\}\dot{\gamma} + [3\Omega_0^2 I_1(23)]\theta + \{3\Omega_0^2 I_1(13) - \Omega_0^2 C\beta S\beta[I_3(22) \\
& + I_2(22) - I_2(11) - I_3(11)] + S\beta C\beta H_b\Omega_0 - 3\Omega_0^2 S\beta C\beta[I_2(22) + I_3(22) - I_2(11) - I_3(11)] \\
& + \Omega_0^2 I_1(13)\}\phi + \{-C^2\beta\Omega_0^2[I_3(22) + I_2(22) - I_2(11) - I_3(11)] + \Omega_0 C^2\beta H_b - \Omega_0^2[I_1(22) \\
& - I_1(11)]\}\psi + \{-C\beta\ddot{a}I_3(22) - k_g S\beta - C\beta(3\Omega_0^2\{S\beta C\beta[I_2(11) - I_2(33)]\}) \\
& - 3\Omega_0^2 S\beta C^2\beta[I_2(22) + I_3(22) - I_2(11) - I_3(11)]\}\gamma = I_1(12)\Omega_0^2. \tag{3.11}
\end{aligned}$$

The required sixth equation is Equation (2.2),

$$T_2\dot{\epsilon} + \epsilon - T_1\dot{\theta}_s - \theta_s = 0.$$

The equilibrium state vector has previously been defined as

$$\mathbf{x}_0 = \begin{bmatrix} \theta \\ \phi \\ \psi \\ \dot{\theta} \\ \dot{\phi} \\ \dot{\psi} \\ \gamma \\ \dot{\gamma} \\ \epsilon \\ \dot{\epsilon} \\ \dot{a} \end{bmatrix} = \begin{bmatrix} 0 \\ 0 \\ 0 \\ 0 \\ 0 \\ 0 \\ 0 \\ 0 \\ 0 \\ 0 \\ \dot{a}_0 \end{bmatrix}.$$

Observation of the right-hand side of the linearized set of equations, however, shows that if \mathbf{X}_0 is to represent an equilibrium state for the system, certain constraints must be placed upon the physical configurations of bodies 1, 2, and 3. In particular, the gimbal alone must have spherical symmetry so that $I_2(11) = I_2(22) = I_2(33)$. Also, the product of inertia terms associated with the main body must be zero.

Although certain very specific combinations of body 1 cross-product inertia terms and gimbal inertia terms give rise to the desired equilibrium, these are of no practical interest.

As a result of the physical constraints placed upon bodies 1, 2, and 3, the set of linearized equations have been rewritten and presented in their final form on the following pages.

Recall that β is the gimbal axis angle as shown in Figure 2.1 and is constant. H_b is the pitch-momentum bias and represents the bias wheel momentum about which the pitch wheel is actively controlled. The \dot{a} term that appears in the linearized equations is the variational wheel speed about this bias. Finally, the state variables ϵ and $\dot{\epsilon}$ are error signals associated with the active pitch loop and appear because of the lead network in that loop.

T_{3y} :

$$I_3(22)\ddot{\theta} + I_3(22)\ddot{a} = T_w = k_T T_1 \dot{\theta} - I_3(22)(k_T C_t + B_t)\dot{a} - k_T T_2 \dot{\epsilon} + k_T \theta. \quad (3.12)$$

T_{2x} :

$$\begin{aligned} & C\beta[I_2(11) + I_3(11)]\ddot{\phi} - S\beta[I_2(11) + I_3(11)]\ddot{\psi} + [I_2(11) + I_3(11)]\ddot{\gamma} + \{S\beta\Omega_0[I_3(22) \\ & - I_2(11) - 2I_3(11)] - H_b S\beta\}\dot{\phi} + \{C\beta\Omega_0[I_3(22) - I_2(11) - 2I_3(11)] - C\beta H_b\}\dot{\psi} + B_g \dot{\gamma} \\ & + \{4C\beta\Omega_0^2[I_3(22) - I_3(11)] - C\beta\Omega_0 H_b\}\phi + \{\Omega_0^2 S\beta[I_3(11) - I_3(22)] + H_b S\beta\Omega_0\}\psi \\ & + \left(\Omega_0^2\{I_3(22) - I_3(11) + 3C^2\beta[I_3(22) - I_3(33)]\} + k_g - H_b\Omega_0\right)\gamma = 0. \end{aligned} \quad (3.13)$$

T_{1x} :

$$\begin{aligned}
& -\{I_1(11) + S^2\beta[I_2(33) + I_3(11)]\}\ddot{\phi} - S\beta C\beta[I_3(11) + I_2(33)]\ddot{\psi} + \{-S\beta C\beta H_b \\
& - \Omega_0 S\beta C\beta[I_2(11) + 2I_3(11) - I_3(22)]\}\dot{\phi} + \{\Omega_0[I_1(11) + I_1(33) - I_1(22)] \\
& + \Omega_0 S^2\beta[I_2(11) + 2I_3(11) - I_3(22)] + S^2\beta H_b\}\dot{\psi} + \{\Omega_0 S\beta[I_3(22) - I_2(11) - I_3(11)] \\
& - S\beta H_b + C\beta B_g\}\dot{\gamma} + \{4\Omega_0^2[I_1(33) - I_1(22)] - 4S^2\beta\Omega_0^2[I_3(22) - I_3(11)] + S^2\beta\Omega_0 H_b\}\phi \\
& + \{\Omega_0 S\beta C\beta[-\Omega_0 I_3(22) + \Omega_0 I_3(11) + H_b]\}\psi + \{3\Omega_0^2 S^2\beta C\beta[I_3(11) - I_3(22)] + C\beta k_g \\
& - S\beta\ddot{a}I_3(22)\}\gamma = 0.
\end{aligned} \tag{3.14}$$

T_{1y} :

$$-\{I_2(22) + I_3(22) + I_1(22)\}\ddot{\theta} - I_3(22)\ddot{a} + \{3\Omega_0^2[I_1(33) - I_1(11)]\}\theta = 0. \tag{3.15}$$

T_{1z} :

$$\begin{aligned}
& -S\beta C\beta[I_2(33) + I_3(11)]\ddot{\phi} + \{-I_1(33) - C^2\beta[I_3(11) + I_2(33)]\}\ddot{\psi} + \{-\Omega_0 I_1(33) + \Omega_0[I_1(22) \\
& - I_1(11)] - C^2\beta\Omega_0[I_3(22) + I_2(11) + 2I_3(11)] - C^2\beta H_b\}\dot{\phi} + \{\Omega_0 S\beta C\beta[I_2(11) \\
& + 2I_3(11) - I_3(22)] + S\beta C\beta H_b\}\dot{\psi} + \{C\beta\Omega_0[I_3(22) - I_2(11) - I_3(11)] - C\beta H_b - S\beta B_g\}\dot{\gamma} \\
& + \{4\Omega_0^2 C\beta S\beta[I_3(11) - I_3(22)] + S\beta C\beta H_b\Omega_0\}\phi + \{-C^2\beta\Omega_0^2[I_3(22) - I_3(11)] \\
& + \Omega_0 C^2\beta H_b - \Omega_0^2[I_1(22) - I_1(11)]\}\psi + \{-k_g S\beta - 3C^2\beta S\beta\Omega_0^2[I_3(22) - I_3(11)] \\
& - C\beta\ddot{a}I_3(22)\}\gamma = 0.
\end{aligned} \tag{3.16}$$

Error Equation (2.2):

$$T_2\dot{\epsilon} + \epsilon - T_1\dot{\theta}_s - \theta_s = 0.$$

The terms $\ddot{a}I_3(22) = \dot{H}_b$ have been included for use in Chapter 5.

CHAPTER 4

STABILITY

4.1 General Discussion

In order to investigate system stability it would appear that one must deal with a complex eleventh-order system of six equations. However, one immediate observation that can be made from the linearized equation set is that the six equations decoupled into two sets of three, one of fifth order and the other of sixth order. The T_{1x} , T_{1z} , and T_{2x} equations are functions of ϕ , ψ , and γ , while the equations for T_{3y} , T_{1y} , and ϵ are functions of θ , $\dot{\alpha}$, and ϵ .

The fact that the equation set decouples requires that the variations of the system variables as well as variations in the pitch-momentum bias H_b be small. In practice, however, H_b variations are often large, and the coupling that results must not be overlooked when arriving at the requirements for total system stability. This topic is considered in detail in Chapter 5.

The fact that the six equations can be decoupled could have been anticipated, as gyroscopic terms always contain the products ω_i , ω_j , where ($i = 1, 2, 3$; $j = 1, 2, 3$; $i \neq j$). As only first-order terms have been retained, only the gyroscopic coupling terms that involve ω_y have been kept because ω_y alone contains a constant term (i.e., $\omega_{1y} = \dot{\theta} - \Omega_0$, where Ω_0 is constant). Clearly, gyroscopic terms that appear in the pitch equations are not functions of ω_y , whereas those that appear in the roll and yaw equations are. For this reason, roll is coupled to yaw, but neither roll nor yaw is coupled to pitch.

It is of interest to determine the stability thresholds for the generalized class of spacecraft whose attitude is controlled by means of a gimbaled-reaction-wheel-scanner. A threshold of stability separates those spacecraft configurations which are stable from those that are unstable.

4.2 Asymptotic Stability of Linearized Equations

A common technique used to determine the asymptotic stability of a linear set of equations is the examination of the real part of the characteristic roots of those equations. A set of equations is

asymptotically stable if and only if all of its characteristic roots have negative real parts. The equations are unstable if any root has a real part which is positive or equal to zero.

Any set of linear equations can be written in the form

$$\dot{\mathbf{X}} = \mathbf{A}\mathbf{X},$$

where

$$\mathbf{X} = \begin{bmatrix} X_1 \\ X_2 \\ \vdots \\ X_n \end{bmatrix}.$$

When the system matrix A is time invariant, one can represent the homogeneous portion of the set of first-order equations in Laplace transform notation,

$$s\mathbf{X}(s) = \mathbf{A}\mathbf{X}(s).$$

The initial conditions have been assumed to be absent because the steady-state aspects of linear system performance are fully determined in their absence. This expression can be written

$$[A - sI] \mathbf{X}(s) = 0,$$

where s is the Laplace operator and I is the identity matrix. If the solution to this equation is to be nontrivial, the familiar eigenvalue problem results:

$$|A - sI| = 0.$$

Evaluation of the determinant results in the system characteristic polynomial, and the resulting values of s are the eigenvalues or the system characteristic values.

For the specific problem under study, it is possible to write the characteristic equation as the product of two polynomials, one of fifth order and the other of sixth order, because the system equations can be decoupled. It would indeed be a tedious task if one were to attempt to determine the roots of the characteristic polynomials. Fortunately, however, the Hurwitz criterion (Reference 4) affords both the necessary and sufficient conditions required to assure that all characteristic values have negative real parts without, in fact, having to solve for the actual characteristic roots.

Define the characteristic polynomial to be of the form

$$a_n s^n + a_{n-1} s^{n-1} + \dots + a_1 s + a_0 = 0.$$

Hurwitz states that two conditions must be satisfied in order to ensure that all zeros of the characteristic polynomial have negative real parts.

- I) All of the polynomial coefficients must be of the same sign, none being zero.
- II) Each member of the sequence of Hurwitz determinants D_1, D_2, \dots, D_{n-1} , defined below, must be positive.

$$D_1 = a_1 > 0,$$

$$D_2 = \begin{vmatrix} a_1 & a_0 \\ a_3 & a_2 \end{vmatrix} > 0,$$

and

$$D_3 = \begin{vmatrix} a_1 & a_0 & 0 \\ a_3 & a_2 & a_1 \\ a_5 & a_4 & a_3 \end{vmatrix} > 0.$$

The following diagram may serve as a memory aid in constructing the various Hurwitz determinants.

$$\begin{array}{l} D_1 \quad \begin{vmatrix} a_1 & a_0 \end{vmatrix} \quad 0 \quad 0 \quad 0 \\ D_2 \quad \begin{vmatrix} a_3 & a_2 & a_1 & a_0 \end{vmatrix} \quad 0 \\ D_3 \quad \begin{vmatrix} a_5 & a_4 & a_3 & a_2 & a_1 \end{vmatrix} \\ D_4 \quad \begin{vmatrix} a_7 & a_6 & a_5 & a_4 & a_3 \end{vmatrix} \end{array}$$

The determinants are formed as illustrated by forming determinants of successively larger numbers of rows and columns starting from the upper left corner of the array shown. Any coefficient absent from a particular characteristic equation is replaced by zero.

Consideration of the sixth-order characteristic polynomial requires the evaluation of D_1 through D_5 ; and consideration of the fifth-order polynomial, D_1 through D_4 .

It is possible to solve for the coefficients of the two characteristic polynomials by algebraically manipulating the linearized Equations (3.12) through (3.16) and (2.2). That is,

$$\left[\begin{array}{c} T_{3y} \left\{ \begin{array}{c} \dot{\theta}, \theta \\ \dot{\epsilon}, \epsilon \end{array} \right\} \\ T_{1y} \left\{ \begin{array}{c} \dot{\epsilon}, \epsilon \\ \dot{a} \end{array} \right\} \\ \text{Error equation} \end{array} \right] \rightarrow b_5 s^5 + b_4 s^4 + \dots + b_1 s + b_0 = 0$$

and

$$\left[\begin{array}{c} T_{2x} \left\{ \begin{array}{c} \dot{\psi}, \psi \\ \dot{\phi}, \phi \end{array} \right\} \\ T_{1x} \left\{ \begin{array}{c} \dot{\phi}, \phi \\ \dot{\gamma}, \gamma \end{array} \right\} \\ T_{1z} \left\{ \begin{array}{c} \dot{\gamma}, \gamma \end{array} \right\} \end{array} \right] \rightarrow a_6 s^6 + a_5 s^5 + \dots + a_1 s + a_0 = 0.$$

The sequence of Hurwitz determinants that are of interest are

$$D_1 = a_1 > 0,$$

$$D_2 = a_1 a_2 - a_0 a_3 > 0,$$

•

$$D_3 = a_3 D_2 - a_1 (a_1 a_4 - a_5 a_0),$$

$$D_4 = a_4 D_3 - a_2 a_5 D_2 + a_1 a_6 D_2 + a_0 a_5 (a_1 a_4 - a_5 a_0),$$

and

$$D_5 = a_5 D_4 - a_6 a_3 D_3 + a_6 a_1 a_5 D_2 - a_6^2 a_1^3.$$

It is often convenient to define D_3 and D_4 in terms of an intermediate quantity E_2 .

$$D_3 = a_3 D_2 - a_1 E_2,$$

$$D_4 = a_4 D_3 - a_2 a_5 D_2 + a_1 a_6 D_2 + a_0 a_5 E_2,$$

where

$$E_2 = a_1 a_4 - a_5 a_0$$

4.3 Definition of Characteristic Polynomials

Before continuing with a detailed development, the following definitions will be made in order to simplify the notation that follows.

Recalling that Φ_2 has spherical symmetry,

$$I_2(11) = I_2(22) = I_2(33),$$

and that the rotor is symmetric about its spin axis,

$$I_3(11) = I_3(33),$$

we define

$$I(22) = I_1(22) + I_2(22),$$

$$I_T(22) = I(22) + I_3(22),$$

$$D = k_T C_t + B_f,$$

$$K_{gg} = 3\Omega_0^2[I_1(11) - I_1(33)],$$

and

$$I_{23} = I_2(ii) + I_3(kk),$$

where $i = 1, 2$, or 3 , while $k = 1$ or 3 , and

$$I_{11} = I_1(11), \quad I_{12} = I_1(22), \quad \text{and} \quad I_{13} = I_1(33).$$

Also,

$$\rho_A = \Omega_0[I_3(33) - I_3(22) + I_2(11) + I_3(33)],$$

$$\rho_B = \Omega_0[I_3(22) - I_{23}],$$

$$\rho_C = 4\Omega_0^2[I_3(11) - I_3(22)],$$

$$\rho_D = \Omega_0^2[I_3(11) - I_3(22)],$$

and

$$\rho_E = 3\Omega_0^2[I_3(11) - I_3(22)].$$

The coefficients of the roll, yaw, and gimbal related characteristic polynomials are listed below.

$$\begin{aligned} a_0 = & S^2\beta\left\{-[\Omega_0^2H_b^2 + (\rho_D + \rho_C)\Omega_0H_b + \rho_C\rho_D]\Omega_0^2(I_{12} - I_{11})\right\} \\ & + C^2\beta\left\{4\Omega_0^2(I_{13} - I_{12})[\Omega_0H_b\rho_E + \rho_D\rho_E + \Omega_0^2H_b^2 + \rho_D^2 + 2\Omega_0H_b\rho_D - \rho_E\Omega_0^2(I_{12} - I_{11})]\right\} \\ & + 4\Omega_0^4(I_{13} - I_{12})(I_{12} - I_{11})(k_g - \Omega_0H_b - \rho_D) - k_g[\Omega_0^2H_b^2 + (\rho_D + \rho_C)\Omega_0H_b + \rho_D\rho_C] \\ & + k_g\Omega_0^2[(I_{12} - I_{11})(\Omega_0H_b + \rho_C) - 4(I_{13} - I_{12})(\Omega_0H_b + \rho_D)]. \end{aligned}$$

$$\begin{aligned} a_1 = & S\beta C\beta\left\{\Omega_0^2(\rho_B - H_b)[4(\Omega_0H_b + \rho_D)(I_{13} - I_{12}) + (\Omega_0H_b + \rho_C)(I_{12} - I_{11})]\right. \\ & + (\Omega_0H_b^2 + \rho_DH_b + \rho_AH_b\Omega_0 + \rho_D\rho_A)\Omega_0^2[4(I_{13} - I_{12}) + (I_{12} - I_{11})] \\ & + \Omega_0(I_{11} + I_{13} - I_{12})[\rho_D(\rho_D - \rho_C) + \Omega_0H_b(\rho_D - \rho_C)] \\ & + \rho_E\Omega_0[\Omega_0(H_b + \rho_A)(I_{12} - I_{11}) - (\Omega_0H_b + \rho_D)(I_{12} - I_{13} - I_{11})]\left.\right\} \\ & + B_g\left\{\Omega_0^2[(\Omega_0H_b + \rho_C)(I_{12} - I_{11}) - 4(\Omega_0H_b + \rho_D)(I_{13} - I_{12})]\right. \\ & \left.- [\Omega_0^2H_b^2 + (\rho_D + \rho_C)\Omega_0H_b + \rho_C\rho_D] + 4\Omega_0^4(I_{12} - I_{11})(I_{13} - I_{12})\right\}. \end{aligned}$$

$$\begin{aligned} a_2 = & S^2\beta\left\{(\rho_B - H_b)[(H_b + \rho_A)\Omega_0^2(I_{12} - I_{11}) - (\Omega_0H_b + \rho_D)\Omega_0(I_{12} - I_{13} - I_{11})]\right. \\ & + \Omega_0^2(I_{12} - I_{11})I_{23}(2\Omega_0H_b + \rho_C + \rho_D) - I_{13}[\Omega_0^2H_b^2 + (\rho_D + \rho_C)\Omega_0H_b + \rho_C\rho_D]\left.\right\} \\ & + C^2\beta\left\{\Omega_0(I_{12} - I_{13} - I_{11})[(\Omega_0H_b + \rho_C)(H_b - \rho_B) - \rho_E(H_b + \rho_A) + \Omega_0\rho_E(I_{12} - I_{13} - I_{11})]\right. \\ & - (\Omega_0H_b + \rho_D)\rho_EI_{11} - 4\rho_E\Omega_0^2(I_{13} - I_{12})(I_{23} + I_{13}) - (H_b + \rho_A)(\rho_B - H_b)4\Omega_0^2(I_{13} - I_{12}) \\ & - 8I_{23}\Omega_0^2(I_{13} - I_{12})(\Omega_0H_b + \rho_D) - I_{11}(\Omega_0^2H_b^2 + \rho_D^2 + 2\Omega_0H_b\rho_D) + \Omega_0^2(I_{12} - I_{11})I_{11}\rho_E\left.\right\} \\ & + \left\{I_{23}k_g(2\Omega_0H_b + \rho_C + \rho_D) - (H_b^2 + \rho_A^2 + 2H_b\rho_A)k_g + 4I_{23}\Omega_0^2(I_{13} - I_{12})\Omega_0^2(I_{12} - I_{11})\right. \\ & + (\Omega_0H_b + \rho_D - k_g)I_{11}\Omega_0^2(I_{12} - I_{11}) - I_{23}k_g\Omega_0^2(I_{12} - I_{11}) - 4I_{13}\Omega_0^2(I_{13} - I_{12})(\Omega_0H_b \\ & + \rho_D - k_g) + 4k_gI_{23}\Omega_0^2(I_{13} - I_{12}) + \Omega_0^2(I_{12} - I_{13} - I_{11})^2(\Omega_0H_b + \rho_D - k_g) \\ & \left. + (\Omega_0H_b + \rho_D)k_gI_{11} + (H_b + \rho_A)\Omega_0(I_{12} - I_{13} - I_{11})(2k_g - \Omega_0H_b - \rho_D) + (\Omega_0H_b + \rho_C)I_{13}k_g\right\}. \end{aligned}$$

$$\begin{aligned}
a_3 = & S\beta C\beta \left[I_{13}(\rho_E H_b + \rho_E \rho_A + \rho_D \rho_A + \Omega_0 H_b \rho_A + \rho_D H_b) - \Omega_0 I_{23}(I_{11} + I_{13} - I_{12})(\rho_E + \rho_D - \rho_C) \right. \\
& - I_{11}(\rho_D \rho_A + H_b \Omega_0 \rho_A + \rho_D H_b) + \rho_B(I_{13} - I_{11})\Omega_0 H_b + (H_b + \rho_A)\Omega_0^2 I_{23}[4(I_{12} - I_{13}) \\
& - (I_{12} - I_{11})] + (\rho_B - H_b)\{-\rho_D I_{11} + I_{13}\rho_C - I_{23}\Omega_0^2[4(I_{13} - I_{12}) + (I_{12} - I_{11})]\} \\
& + B_g[I_{11}\Omega_0 H_b + I_{11}\rho_D + I_{13}\Omega_0 H_b + I_{13}\rho_C - \Omega_0^2(I_{11} + I_{13} - I_{12})^2 \\
& - 2(H_b + \rho_A)\Omega_0(I_{11} + I_{13} - I_{12}) - (H_b^2 + \rho_A^2 + 2H_b \rho_A) + I_{23}(2\Omega_0 H_b + \rho_C + \rho_D) \\
& \left. + \Omega_0^2\{I_{13} + I_{23}\} 4(I_{13} - I_{12}) - (I_{11} + I_{23})(I_{12} - I_{11})\} \right].
\end{aligned}$$

$$\begin{aligned}
a_4 = & S^2\beta[(\rho_B - H_b)I_{13}(H_b + \rho_A) + I_{13}I_{23}(2\Omega_0 H_b + \rho_C + \rho_D) - I_{23}^2\Omega_0^2(I_{12} - I_{11})] \\
& + C^2\beta[(\rho_B - H_b)I_{11}(H_b + \rho_A) + I_{11}I_{23}(2\Omega_0 H_b + 2\rho_D) + I_{23}^2 4\Omega_0^2(I_{13} - I_{12}) \\
& + \rho_E I_{11}(I_{13} + I_{23})] + I_{23}[4\Omega_0^2 I_{13}(I_{13} - I_{12}) - \Omega_0^2 I_{11}(I_{12} - I_{11}) - I_{23}k_g - I_{13}k_g \\
& + \Omega_0^2(I_{11} + I_{13} - I_{12})(I_{12} - I_{13} - I_{11}) + \rho_B \Omega_0(I_{12} - I_{13} - I_{11}) + \Omega_0 \rho_A(I_{12} - I_{13} - I_{11}) \\
& - I_{11}k_g] - k_g I_{13}I_{11} + I_{11}I_{13}\Omega_0 H_b.
\end{aligned}$$

$$a_5 = S\beta C\beta[\Omega_0 I_{23}I_3(33)(I_{11} - I_{13})] - B_g[I_{23}(I_{23} + I_{13} + I_{11}) + I_{11}I_{13}].$$

$$a_6 = I_{23}[I_{13}I_{11} + I_{23}(I_{11}C^2\beta + I_{13}S^2\beta)].$$

To make the stability problem manageable, certain approximations were made at this point of the development. Nominal values and an associated dynamic range of 100 to 1 were chosen for each of the system parameters. Those terms more than three orders of magnitude below any other terms included in any polynomial coefficient were dropped. In determining which terms should be dropped, the full dynamic range of each parameter was considered. In this manner, very little generality has been lost and with the exception of certain terms in the a_5 and a_6 coefficients, the terms that were found to be negligible were all of those terms containing the inertia I_{23} and/or the terms ρ_A through ρ_E . The I_{23} terms were not dropped from a_5 or a_6 at this point in the development.

The coefficients resulting from this simplification are listed below.

$$\begin{aligned}
a_0 = & C^2\beta\{\Omega_0^4 H_b^2[(I_{11} - I_{12}) + 4(I_{12} - I_{13})]\} + (I_{11} - I_{12})\{\Omega_0^4[4(I_{12} - I_{13})(\Omega_0 H_b - k_g) - H_b^2]\} \\
& + [(I_{11} - I_{12}) - 4(I_{12} - I_{13})]\Omega_0^3 k_g H_b + k_g \Omega_0^2 H_b^2.
\end{aligned}$$

$$a_1 = B_g \Omega_0^2 \left\{ \Omega_0 (I_{11} - I_{12}) [H_b - 4\Omega_0 (I_{12} - I_{13})] - 4(I_{12} - I_{13}) \Omega_0 H_b + H_b^2 \right\}.$$

$$a_2 = C^2 \beta \left\{ H_b^2 \Omega_0^2 [2(I_{11} - I_{13}) + 3(I_{12} - I_{13})] \right\} + \Omega_0^2 (\Omega_0 H_b - k_g) [I_{11} (I_{11} - I_{12}) - 4I_{13} (I_{12} - I_{13}) \\ - (I_{12} - I_{13} - I_{11})^2] + H_b^2 [k_g - \Omega_0^2 (I_{11} - I_{12} - I_{13})] + \Omega_0 k_g H_b [(I_{11} - I_{12}) - (I_{12} - I_{13})].$$

$$a_3 = B_g \left\{ \Omega_0^2 [-I_{11} (I_{11} - I_{12}) + 4I_{13} (I_{12} - I_{13}) + (I_{12} - I_{13} - I_{11})^2] + (I_{11} + I_{13} - 2I_{12}) \Omega_0 H_b + H_b^2 \right\}.$$

$$a_4 = C^2 \beta [H_b^2 (I_{11} - I_{13})] + I_{13} [H_b^2 + I_{11} (k_g - \Omega_0 H_b)].$$

$$a_5 = B_g [I_{11} I_{13} + I_{23} (I_{11} + I_{13})].$$

$$a_6 = C^2 \beta [I_{23}^2 (I_{11} - I_{13})] + I_{23} (I_{13} I_{11} + I_{23} I_{13}).$$

Proceeding in this same manner with the development of the Hurwitz D_2 , D_3 , D_4 , and D_5 , it was found that those elements of the D 's that contain the parameter I_{23} were at least two orders of magnitude smaller than any of the other elements. It was therefore concluded that it was valid to set the remaining I_{23} terms as well as the entire coefficient a_6 equal to zero.

Further discussion of this characteristic equation is left for Section (4.5).

The coefficients associated with the rotor, error, and pitch equation related characteristic polynomial are listed below.

$$b_0 = 0,$$

$$b_1 = k_{gg} D,$$

$$b_2 = (T_2 D + 1) k_{gg} + k_T,$$

$$b_3 = T_2 k_{gg} + k_T T_1 + [I_3(22) + I(22)] D,$$

$$b_4 = T_2 [I_3(22) + I(22)] D + I(22),$$

and

$$b_5 = T_2 I(22).$$

The fact that the wheel rotor equation represents a rate loop rather than a position loop is exemplified by the fact that $b_0 = 0$. Therefore, for stability, it is necessary only to deal with the fourth-order characteristic equation

$$b'_4 s^4 + \dots + b'_1 s + b'_0 = 0,$$

where $b'_i = b_{i+1}$ for $i = 0, 1, 2, 3$.

The nature of these coefficients, together with the physical requirement that the inertias, D , T_1 , T_2 , $(T_1 - T_2)$, and k_T are all individually positive quantities, cause this characteristic equation to be one which is relatively straightforward to handle. In fact, the only condition posed by the requirement that all the polynomial coefficients have the same sign, is that

$$I_{11} \geq I_{13}.$$

Expansion of the Hurwitz determinants yields

$$D_2 = k_{gg} \left\{ T_2^2 (k_{gg} D) + T_2 (D T_1 k_T + k_T + k_{gg}) + [T_1 k_T + I_3(22) D] \right\} + k_T [k_T T_1 + I_T(22) D],$$

and

$$\begin{aligned} D_3 = I(22) \left\{ (k_{gg} k_T T_2 D + k_{gg} k_T + k_T^2) (T_1 - T_2) + k_T T_2 D^2 [I(22) + 2I_3(22)] \right. \\ \left. + [k_{gg} k_T T_1 T_2 D + I_3(22) k_{gg} D] (1 + T_2 D) + k_T^2 T_1 T_2 D + [I_3(22) + I(22)] k_T D \right\} \\ + I_3(22) \left\{ D k_{gg} T_2 [(T_2 k_{gg} + k_T T_1) (1 + T_2 D) + k_T T_2 + I_3(22) D] + D k_T T_2 [T_1 k_T + D I_3(22)] \right\}. \end{aligned}$$

Clearly, both D_2 and D_3 are always positive because of the physical constraints stated earlier, and no further conclusions can be drawn from this characteristic polynomial.

In comparison with the example above, the complexity associated with the application of the Hurwitz criterion to the roll, yaw, and gimbal related characteristic polynomial is by far a different matter.

In general, aside from those unusual cases in which the coefficients and associated Hurwitz determinants result in simple expressions, application of these criteria is limited to numerical problems that seek to establish whether or not a particular set of parameters gives rise to a stable system configuration, or those in which a single system parameter is adjusted until stability is achieved. Therefore, in order to determine algebraically the stability thresholds for the generalized gimbaled-reaction-

wheel-scanner class of spacecraft, it was necessary to develop a somewhat modified Hurwitz criterion. The following section deals with a detailed discussion of this modification.

4.4 Development of Modified Hurwitz Criterion

Recall that the application of the classical Hurwitz criterion to a fifth-order characteristic polynomial would require, for asymptotic stability,

$$a_i > 0 \text{ for } i = 0, \dots, 5,$$

and

$$D_k > 0 \text{ for } k = 2, \dots, 4.$$

It would indeed be a horrendous, if not impossible, task to demonstrate that these nine algebraic quantities are simultaneously greater than zero. Clearly, however, at a threshold of stability, at least one of these quantities must pass through zero.

With this point in mind, it is possible to show that before either D_2 and/or D_3 can go to zero, D_4 must already have gone negative. This means that if any of the D 's are to establish the stability threshold, then that D must in fact be D_4 . Furthermore, if any coefficient goes to zero, then at least one of the determinants will already be negative except when either a_0 or a_5 go to zero first. But in this problem, $a_5 = I_{11}I_{13}B_g \neq 0$, so that as far as the coefficients are concerned, we must only concern ourselves with the possibility of $a_0 = 0$ first.

In summary, the results of this modified technique show that at most three situations need be considered in order to define the stability thresholds for a general algebraic fifth-order system.

(I) Set $a_0 = 0$. Demonstrate that on the $a_0 = 0$ line,

$$a_i \geq 0 \text{ for } i = 1, \dots, 5$$

and

$$D_4 \geq 0.$$

Set $a_0 > 0$. Demonstrate that within the $a_0 > 0$ region,

$$a_i > 0 \text{ for } i = 1, \dots, 5$$

and

$$D_4 > 0.$$

The complete set of thresholds has been established if these conditions are satisfied. If not, it is necessary to proceed to Step (II).

(II) Set $D_4 = 0$. Demonstrate that on the $D_4 = 0$ line,

$$a_i \geq 0 \text{ for } i = 0, \dots, 5.$$

Set $D_4 > 0$. Demonstrate that within the $D_4 > 0$ region,

$$a_i > 0 \text{ for } i = 0, \dots, 5.$$

Similarly, if these conditions are satisfied, the complete set of thresholds have been established. If it is not possible to satisfy either condition (I) or (II), then it is necessary to proceed to Step (III).

(III) Demonstrate that a piecewise combination of (I) and (II) can be satisfied.

Proof: When the sequence of determinants is the limiting factor in the determination of stability thresholds for a particular set of system parameters, it is convenient to set equal to zero that D_i which first approaches zero. Having done this, it is possible to express the other determinants, taking into account the constraints imposed by the fact that one of the D_i 's is identically equal to zero.

Recall that

$$D_2 = a_1 a_2 - a_0 a_3 > 0,$$

$$D_3 = a_3(a_1 a_2 - a_0 a_3) - a_1(a_4 a_5 - a_0 a_5) > 0,$$

and

$$D_4 = a_4 D_3 - a_2 a_5 D_2 + a_0 a_5(a_1 a_4 - a_0 a_5) > 0.$$

Assume that $a_i > 0$ for $i = 0, 1, \dots, 5$.

A) Let $D_2 = \epsilon$, $\epsilon > 0$ but arbitrarily close to zero.

Select system parameters such that

$$D_2 = a_2 a_1 - a_0 a_3 = \epsilon$$

and

$$D_4 = a_4 [a_3 D_2 - a_1(a_4 a_5 - a_0 a_5)] - a_2 a_5 D_2 + a_0 a_5(a_1 a_4 - a_0 a_5) \stackrel{?}{>} 0.$$

Substituting with $\epsilon \rightarrow 0$,

$$D_4 = -a_1 a_4 (a_1 a_4 - a_5 a_0) + a_0 a_5 (a_1 a_4 - a_0 a_5) \stackrel{?}{>} 0$$

and

$$D_4 = -(a_1 a_4 - a_5 a_0)^2,$$

which is clearly negative.

B) Let $D_3 = \epsilon$, with $\epsilon \rightarrow 0$.

Select parameters such that

$$D_3 = a_3 D_2 - a_1 (a_1 a_4 - a_5 a_0) = 0,$$

or

$$(a_1 a_4 - a_5 a_0) = \left(\frac{a_3}{a_1} \right) D_2;$$

but

$$D_4 = -a_2 a_5 D_2 + a_0 a_5 (a_1 a_4 - a_0 a_5) \stackrel{?}{>} 0,$$

that is

$$D_4 = -a_2 a_5 D_2 + a_0 a_5 \frac{a_3}{a_1} D_2 \stackrel{?}{>} 0:$$

and

$$a_1 D_4 = -a_5 D_2^2,$$

which is clearly a negative quantity.

C) Let $D_2 = D_3 = \epsilon$, with $\epsilon \rightarrow 0$.

For this trivial case, $D_4 = 0$ as well.

Therefore, if a Hurwitz determinant is the limiting factor in the determination of stability thresholds, it is necessary to consider only that for $D_4 = 0$, $a_i \geq 0$ for $i = 0, \dots, 5$; and within the region where $D_4 > 0$, $a_i > 0$ for $i = 0, \dots, 5$.

Similarly if a stability threshold is crossed because one of the a_i 's approaches zero first, it is possible to set that a_i equal to zero and to evaluate the D_i 's accordingly.

A) Let $a_0 = 0$, $a_i > 0$ for $i = 1, \dots, 5$.

$$D_2 = a_2 a_1 > 0,$$

$$D_3 = a_1(a_3 a_2 - a_1 a_4) > 0,$$

and

$$D_4 = a_1 [a_4(a_3 a_2 - a_1 a_4) - a_2(a_2 a_5)] > 0.$$

Note that $D_3 > 0$ is implied by and is a weaker condition than $D_4 > 0$.

B) Let $a_1 = 0$, $a_i > 0$ for $i = 0, 2, 3, 4, 5$.

$$D_2 = -a_0 a_3 < 0.$$

C) Let $a_2 = 0$, $a_i > 0$ for $i = 0, 1, 3, 4, 5$.

$$D_2 = -a_0 a_3 < 0.$$

D) Let $a_3 = 0$, $a_i > 0$ for $i = 0, 1, 2, 4, 5$.

$$D_2 = a_2 a_1 > 0,$$

$$D_3 = -a_1(a_1 a_4 - a_5 a_0),$$

and

$$a_1 D_4 = -\frac{D_3^2}{a_1} - D_2^2 a_5 < 0.$$

E) Let $a_4 = 0$, $a_i > 0$ for $i = 0, 1, 2, 3, 5$.

$$D_2 = a_2 a_1 - a_0 a_3 > 0,$$

$$D_3 = a_3 D_2 + a_1 a_5 a_0 > 0,$$

and

$$D_4 = -a_2 a_5 D_2 - a_0^2 a_5^2 < 0 \text{ for } D_2 > 0.$$

F) $a_5 = I_{11} I_{13} B_g \neq 0$.

Therefore, if a characteristic polynomial coefficient going to zero is the limiting factor in the determination of a stability threshold, it is necessary to consider only the following.

For $a_0 = 0$,

$$a_i \geq 0 \text{ for } i = 1, \dots, 5 \text{ and } D_4 \geq 0;$$

and within the region where $a_0 > 0$,

$$a_i > 0 \text{ for } i = 1, \dots, 5 \text{ and } D_4 > 0.$$

No other useful cases are found by letting combinations of the a_i 's go to zero simultaneously.

4.5 Application of Modified Hurwitz Criterion

Conveniently, it was possible to establish that the gimballed-reaction-wheel-scanner class of spacecraft falls into Category (I). As a result, it was possible to express the stability thresholds for a complex system in relatively simple terms. In fact, this method of presentation made it possible to give physical meaning to these thresholds as well as to indicate the type of instability encountered once a threshold was crossed.

The details of this example are presented below.

It is convenient to express the coefficients of the characteristic equation under study as

$$A_0 = (k_g - \Omega_0 H_b) [\Omega_0^2 (I_{12} - I_{11}) - \Omega_0 H_b] [4\Omega_0^2 (I_{12} - I_{13}) - \Omega_0 H_b] - \Omega_0^2 H_b^2 S^2 \beta [4\Omega_0^2 (I_{12} - I_{13}) - \Omega_0 H_b] \\ - \Omega_0^2 H_b^2 C^2 \beta [\Omega_0^2 (I_{12} - I_{11}) - \Omega_0 H_b],$$

$$\frac{A_1}{B_g} = [\Omega_0^2 (I_{12} - I_{11}) - \Omega_0 H_b] [4\Omega_0^2 (I_{12} - I_{13}) - \Omega_0 H_b],$$

$$A_2 = \Omega_0^2 (k_g - \Omega_0 H_b) [I_{11} (-I_{12} + 2I_{13}) + (I_{12} + 3I_{13})(I_{12} - I_{13})] + k_g [\Omega_0 H_b (I_{11} - 2I_{12} + I_{13}) + H_b^2] \\ + \Omega_0^2 H_b^2 C^2 \beta [I_{11} + 4(I_{12} - I_{13})] + \Omega_0^2 H_b^2 S^2 \beta [I_{12} - I_{11} + I_{13}],$$

$$\frac{A_3}{B_g} = \Omega_0^2 [I_{11} (-I_{12} + 2I_{13}) + (I_{12} + 3I_{13})(I_{12} - I_{13})] + \Omega_0 H_b (I_{11} - 2I_{12} + I_{13}) + H_b^2,$$

$$A_4 = (k_g - \Omega_0 H_b) I_{11} I_{13} + H_b^2 (I_{11} C^2 \beta + I_{13} S^2 \beta),$$

and

$$\frac{A_5}{B_g} = I_{11} I_{13}.$$

A normalized set of equations results when the following substitutions are made into the equation set shown above.

$$I_{11} = \alpha I_3,$$

$$I_{12} = \rho I_3,$$

$$I_{13} = I_3,$$

$$H_b = h \Omega_0 I_3,$$

$$k_g = k \Omega_0^2 I_3,$$

$$A_{2n} = a_{2n} \Omega_0^{6-2n} I_{13}^3, \quad n = 0, 1, 2,$$

and

$$\frac{A_{1+2n}}{B_g} = a_{1+2n} \Omega_0^{4-2n} I_{13}^2, \quad n = 0, 1, 2.$$

The resulting normalized equations are:

$$a_0 = (k - h)(-\alpha + \rho - h)(4\rho - 4 - h) - h^2 C^2 \beta(-\alpha + \rho - h) - h^2 S^2 \beta(4\rho - 4 - h), \quad (4.1)$$

$$a_1 = (-\alpha + \rho - h)(4\rho - 4 - h), \quad (4.2)$$

$$a_2 = (k - h)(a_3) + h^2 C^2 \beta(2\alpha + 2\rho - 3 + h) + h^2 S^2 \beta(-\rho + h + 2), \quad (4.3)$$

$$a_3 = \alpha(-\rho + 2 + h) + \rho^2 + 2(1 - h)\rho - 3 + h + h^2 = (-\alpha + \rho - h)(\rho - 2 - h) + (4\rho - 4 - h) + 1, \quad (4.4)$$

$$a_4 = \alpha(k - h) + h^2(\alpha C^2 \beta + S^2 \beta), \quad (4.5)$$

and

$$a_5 = \alpha. \quad (4.6)$$

The expanded Hurwitz determinants can be detailed in terms of the normalized coefficients. The resulting expressions are

$$\frac{D_2}{h^2} = (-a + \rho - h) C^2 \beta [a(7\rho - 6 - h) + 9(\rho - 1)^2] + (4\rho - 4 - h) S^2 \beta (4\rho - 3 - h), \quad (4.7)$$

$$\frac{E_2}{h^2} = (-a + \rho - h) C^2 \beta [a(4\rho - 3 - h)] + (4\rho - 4 - h) S^2 \beta (\rho - h), \quad (4.8)$$

$$\begin{aligned} \frac{D_3}{h^2} = & (-a + \rho - h) C^2 \beta [a^2(9\rho^2 - 8\rho - h) + 9a(1 - \rho)^2(-\rho + 2 + h) + 9(1 - \rho)^2(a_3)] \\ & + (4\rho - 4 - h) S^2 \beta [a(7\rho - 6 - h) + 9(\rho - 1)^2], \end{aligned} \quad (4.9)$$

and

$$\begin{aligned} \frac{D_4}{h^4} = & 9(\rho - 1)^2 [a(-a + \rho - h)^3 C^4 \beta + (-a + \rho - h) S^2 \beta C^2 \beta (a_3) \\ & + (4\rho - 4 - h) S^4 \beta]. \end{aligned} \quad (4.10)$$

Recall that E_2 was defined in Section (4.2) as

$$E_2 = a_1 a_4 - a_5 a_0.$$

With the coefficients and the Hurwitz determinants now completely defined, it is possible to analytically demonstrate that the characteristic polynomial under study falls into category (I) of the modified Hurwitz criterion presented in the previous section. An analytic proof follows.

The expression $a_0 = 0$ is a single-valued function of α .

Solving for $d\rho/d\alpha$ on the $a_0 = 0$ line, we find

$$\frac{d\rho}{d\alpha} = \frac{(k - h)(4\rho - 4 - h) - h^2 C^2 \beta}{(k - h)[(-a + \rho - h)4 + (4\rho - 4 - h)] - h^2 C^2 \beta - 4h^2 S^2 \beta}.$$

From Equation (4.1), when $a_0 = 0$,

$$(-a + \rho - h) = \frac{h^2 S^2 \beta (4\rho - 4 - h)}{(k - h)(4\rho - 4 - h) - h^2 C^2 \beta}.$$

Substituting, we obtain

$$\frac{d\rho}{d\alpha} = \frac{[(k-h)(4\rho-4-h) - h^2C^2\beta]^2}{[(k-h)(4\rho-4-h) - h^2C^2\beta]^2 + 4h^4S^2\beta C^2\beta}.$$

From this expression,

$$1 \geq \frac{d\rho}{d\alpha} \geq 0.$$

The second form of $d\rho/d\alpha$ shows that $a_0 = 0$ has two branches, one having a horizontal asymptote FG^* for which $d\rho/d\alpha = 0$, and one having a 45° asymptote JK for which $d\rho/d\alpha = 1$. For $d\rho/d\alpha = 0$,

$$(k-h)(4\rho-4-h) - h^2C^2\beta = 0,$$

or

$$(4\rho-4-h) = \frac{h^2C^2\beta}{(k-h)},$$

and for $d\rho/d\alpha = 1$,

$$4(-\alpha + \rho - h) = \frac{4h^2S^2\beta}{(k-h)}.$$

Figure 4.1 is a representation of these curves along with the $a_1 = 0$ lines, MN and QR .

For Case I, consider the conditions $(k-h) > 0$ and $\beta \neq 0^\circ, 90^\circ, \rho \neq 1$.

In this case, the horizontal asymptote of a_0 is above the horizontal $a_1 = 0$ line MN , and the 45° a_0 asymptote is to the left of the 45° $a_1 = 0$ line QR .

The lower branch of the $a_0 = 0$ curve TU passes through the intersection of the two $a_1 = 0$ lines, and both a_0 and a_1 are simultaneously zero at the point of intersection:

$$(\alpha, \rho) = \left(1 - \frac{3h}{4}, 1 + \frac{h}{4}\right).$$

This $a_0 = 0$ branch lies entirely above the two $a_1 = 0$ line segments QL and LN .

In order to determine the positive regions of a_0 , consider the expression

$$\frac{\partial a_0}{\partial \rho} = h^2 \frac{4C^2\beta(-\alpha + \rho - h)^2 + S^2\beta(4\rho - 4 - h)^2}{(-\alpha + \rho - h)(4\rho - 4 - h)}.$$

*Lettered references to line segments refer to those shown in Figure 4.1 for Case I, and to those shown in Figure 4.2 for Case II.

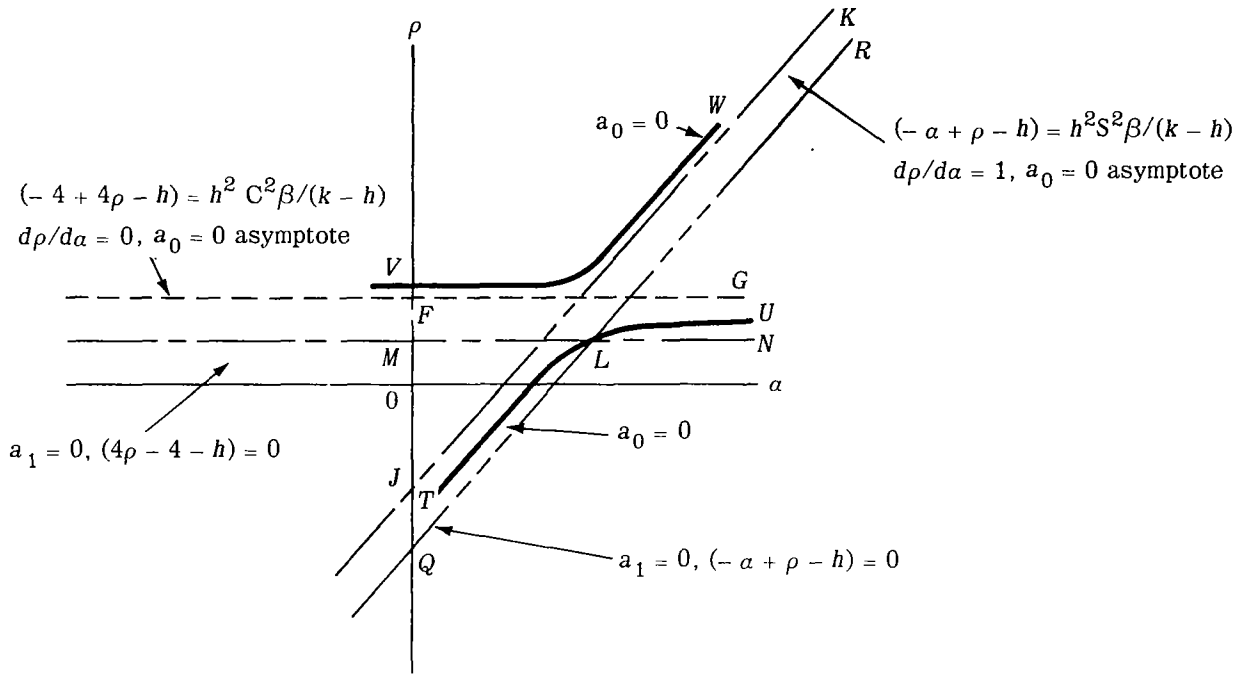


Figure 4.1—Representation of a_0 and a_1 lines shown in the plot of ρ versus α .

This expression is positive everywhere on the upper $a_0 = 0$ branch (curve VW) and negative everywhere on the lower $a_0 = 0$ branch (curve TU). These facts are sufficient to show that $a_0 > 0$ everywhere above the upper and below the lower branches of the $a_0 = 0$ curves.

(a) Consider the upper branch of $a_0 = 0$

$$a_3 = 1 + (-\alpha + \rho - h)(\rho - 2 - h) + (4\rho - 4 - h).$$

On the horizontal $a_1 = 0$ line,

$$a_3 = 1 + (-\alpha + \rho - h)(\rho - 2 - h) = \alpha \left(1 + \frac{3h}{4}\right) + \left(\frac{3h}{4}\right)^2,$$

while

$$\frac{\partial a_3}{\partial \alpha} = 1 + \frac{3h}{4}.$$

At $\alpha = 0$,

$$a_3 = \left(\frac{3h}{4}\right)^2$$

which is always greater than zero. At the intersection of the two $a_1 = 0$ lines (point L).

$$\alpha = 1 - \frac{3h}{4},$$

and $a_3 = 1$, which is clearly greater than zero.

Since $\partial a_3 / \partial \alpha$ is constant for any particular value of h regardless of its polarity, and since $a_3 > 0$ at both $\alpha = 0$ and $\alpha = 1 - (3h/4)$, $a_3 > 0$ at all points on the line segment where $0 \leq \alpha \leq 1 - (3h/4)$. Negative α has no physical meaning. On the $45^\circ a_1 = 0$ line QR ,

$$a_3 = 1 + (4\rho - 4 - h).$$

Therefore, on and above MN , the horizontal $a_1 = 0$ line $(4\rho - 4 - h) = 0$, $a_3 \geq 1$ and a_3 is clearly greater than zero.

$$\frac{\partial a_3}{\partial \rho} = (-\alpha + \rho - h) + (\rho - 2 - h) + 4 = \alpha + 2 + 2(-\alpha + \rho - h).$$

This slope is positive everywhere for positive α and to the left of the $45^\circ a_1 = 0$ line. Since a_3 is positive or zero on the $a_1 = 0$ boundaries MLR and increases as ρ increases, then $a_3 \geq 0$ everywhere in the upper $a_1 \geq 0$ region bounded by MLR and $a_3 > 0$ everywhere in the upper $a_0 \geq 0$ region, that region bounded by the curve VW .

From Equation (4.10), it is clear that $D_4 > 0$ everywhere in the upper $a_1 > 0$ region above MLR , since both $(-\alpha + \rho - h) > 0$ and $(4\rho - 4 - h) > 0$ in this region.

It follows, therefore, that excluding the cases for which $h = 0$ and $\rho = 1$, D_4 is greater than zero everywhere in the upper $a_0 \geq 0$ region on and above curve VW .

Because α must be a positive number, $I_{11} = \alpha I_3$, both a_4 and a_5 are greater than zero everywhere in the region of interest.

All that remains to be shown for Case I(a) is that $a_2 > 0$ in the upper $a_0 \geq 0$ region. For this condition, an indirect demonstration is easier than a direct one.

$$\frac{E_2}{h^2} = (-\alpha + \rho - h)C^2\beta[\alpha(4\rho - 4 - h + 1) + (4\rho - 4 - h)S^2\beta(\rho - h)].$$

Each of the terms that make up E_2/h^2 are either equal to or greater than zero on or above the horizontal, and on or to the left of the $45^\circ a_1 = 0$ lines. That is, on and above MN , $(4\rho - 4 - h) \geq 0$; on and to the

left of QR , $(-\alpha + \rho - h) \geq 0$; and on and to the left of QR , $(\rho - h) \geq \alpha$. Therefore, $E_2 \geq 0$ on and above MLR , and $E_2 > 0$ above the upper $a_0 = 0$ boundary defined by curve VW . Recalling that the determinant

$$D_4 = \frac{E_2 D_3 - a_5 D_2^2}{a_1},$$

and rewriting it, we see that

$$D_4 = \frac{(a_3 D_2 - a_1 E_2) E_2 - D_2^2 a_5}{a_1}.$$

Finally, regrouping terms gives

$$a_1 D_4 = a_3 D_2 E_2 - (a_1 E_2^2 + a_5 D_2^2).$$

However, because

$$D_2 = a_2 a_1 - a_0 a_3,$$

and because it has already been demonstrated that D_4 , E_2 , a_0 , a_1 , a_3 , and a_5 are all greater than zero in this region, it follows that a_2 must also be positive.

(b) Next, consider the lower branch of $a_0 = 0$.

Because this branch passes through the intersection of the two $a_1 = 0$ lines and remains above the line segments QL and LN , the region between these line segments and the $a_0 = 0$ lower branch, defined by the curve TU , is excluded from the region of stability because $a_1 < 0$ in this region. The region below the $a_1 = 0$ lines bounded by QLN will be excluded by demonstrating that either D_4 or a_3 are negative in this region.

$$\frac{D_4}{h^4[9(\rho - 1)^2]} = \alpha(-\alpha + \rho - h)^3 C^4 \beta + (-\alpha + \rho - h) S^2 \beta C^2 \beta(a_3) + (4\rho - 4 - h) S^4 \beta,$$

and in this lower region both $(-\alpha + \rho - h)$ and $(4\rho - 4 - h)$ are always negative. Because only odd powers of these terms appear, all of the components of D_4 must be negative unless a_3 itself is negative. In either case, either $D_4 < 0$ and/or $a_3 < 0$, and the entire region below the lower branch of $a_0 = 0$ is excluded from the region of stability.

In summary, for the case of $(k - h) > 0$, the only region that was found to be stable was that region bounded at the bottom by the upper $a_0 = 0$ branch.

For Case II, consider the conditions $(k - h) \leq 0$ and $\beta \neq 0^\circ, 90^\circ; \rho \neq 1$.

When $k = h$, the $a_0 = 0$ curves degenerate into a single line because a_0 is no longer quadratic in ρ . The upper section of this line curves up and goes to infinity while the lower section becomes a straight line heading toward minus infinity parallel to the α axis. This line passes through the intersection of the two $a_1 = 0$ lines as shown in Figure 4.2 and has the slope defined by

$$\frac{d\rho}{d\alpha} = \frac{1}{4 \tan^2 \beta + 1}.$$

From this expression, it is clear that for $1 \geq d\rho/d\alpha \geq 0$, a_0 is less than zero above and to the left of the $a_0 = 0$ curve, and is greater than zero below and to the right of it. But neither a_1 nor D_4 nor a_3 contains the factor $(k - h)$, so that this lower region bounded by the $a_0 = 0$ curve is excluded for the same reason that it was when $(k - h)$ was greater than zero. One can recall that at least one of these quantities was shown to be negative at all points below the Case I lower branch of the $a_0 = 0$ line. (In Case I, it was the lower branch $a_0 = 0$ curve that passed through the intersection of the $a_1 = 0$ lines.)

For $(k - h) < 0$, the horizontal $a_0 = 0$ asymptote lies below MN (Figure 4.2), and the 45° $a_0 = 0$ asymptote lies to the right of QR , as is shown in the figure.

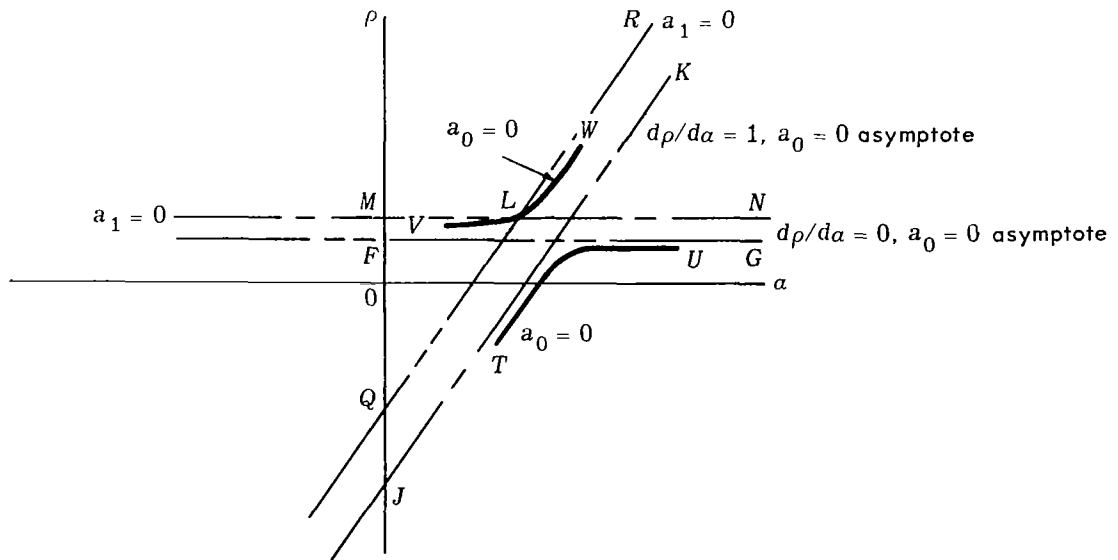


Figure 4.2—Representation of a_0 and a_1 lines for $(k - h) \leq 0$. The $a_0 = 0$ curves degenerate into the single upper branch VLW when $k = h$.

For this case, it is the upper $a_0 = 0$ branch (curve VW) that passes through the intersection of the two $a_1 = 0$ lines. Further, this branch remains entirely below the $a_1 = 0$ boundary MLR . On the $a_0 = 0$ curves,

$$\frac{\partial a_0}{\partial \rho} = \frac{4h^2 C^2 \beta}{4\rho - 4 - h} + \frac{h^2 S^2 \beta}{-\alpha + \rho - h}.$$

However, since this is always negative on the upper $a_0 = 0$ branch and positive on the lower $a_0 = 0$ branch TU , the only region for which a_0 is greater than zero is that between the two $a_0 = 0$ branches. Clearly, this region is excluded because at least one of a_1 , D_4 , or a_3 have been shown to be negative in this region. It may therefore be concluded that no stable region exists when $(k - h) \leq 0$.

In summary, with the exception of those cases for which $\beta = 0^\circ$, $\beta = 90^\circ$, or $\rho = 1$, the stability threshold for this complex system is completely defined by the upper $a_0 = 0$ curve VW ($k > h$). Specifically, on and above this $a_0 = 0$ curve, it has been shown that $a_i > 0$ ($i = 1, \dots, 5$) and $D_4 > 0$. The mode of instability encountered at the threshold stated above is a loss of null reference. When $a_0 = 0$, one root of the characteristic equation is equal to zero. If the remaining fourth-order characteristic polynomial were examined for its stability properties, one finds that it is stable both on the thresholds and within the regions under discussion.

Consider the special case of $\beta = 0^\circ$. In this case, the curved $a_0 = 0$ boundaries degenerate into its asymptotes. The horizontal line, $(k - h)(4\rho - 4 - h) - h^2 = 0$, is always above the $a_1 = 0$ line, $(4\rho - 4 - h) = 0$, for $(k - h) > 0$. On this boundary, a_0 alone is equal to zero with all other quantities of interest positive as before. However, the 45° asymptote, $(-\alpha + \rho - h) = 0$, now coincides with the 45° $a_1 = 0$ line and along this line, a_1 and a_0 become zero simultaneously. As a result, all of the D_i 's and E_2 are simultaneously zero and the characteristic equation has two roots of $s = 0$ along this line. The stability properties of the remaining third-order characteristic polynomial were studied, and it was found that the D_2 Hurwitz determinant associated with the third-order equation is zero. This condition implies that the system will have an undamped oscillation in addition to two roots equal to zero on this particular stability threshold.

Next, consider the special case of $\beta = 90^\circ$. Once again, $a_0 = 0$ degenerates into its two asymptotes. In this case, the 45° line, $(k - h)(-\alpha + \rho - h) - h^2 = 0$, is to the left of the $a_1 = 0$ line, $(-\alpha + \rho - h) = 0$, for $(k - h) > 0$. It is the horizontal line that now coincides with the $a_1 = 0$ line, $(4\rho - 4 - h) = 0$, and on this line, a_1 and a_0 are simultaneously zero. Accordingly, the characteristic equation

exhibits two $s = 0$ roots along this line. The D_2 Hurwitz determinant associated with the remaining cubic equation was examined in this case, and it was found to be greater than zero. This fact implies that the remainder of the system roots, along the segment in question, have negative real parts.

Finally, consider the singular line $\rho = 1$. Independent of all of the coefficients of the characteristic polynomial and all of the other determinants, $D_4 = 0$ for $\rho = 1$. This fact implies that if any portion of the $\rho = 1$ line lies within a region that has otherwise been found to be stable, the system would exhibit a sustained oscillation if ρ were set equal to one.

For $h > 0$, the $a_1 = 0$ line lies above the $\rho = 1$ line, so that only negative values of h are of interest when considering this special case. There will be a segment of the $\rho = 1$ line above the upper branch of the $a_0 = 0$ curve when

$$(k - h) > h^2 \left(\frac{C^2 \beta}{-h} + \frac{S^2 \beta}{1 - h} \right).$$

In order to give physical meaning to this singularity in D_4 , it is informative to evaluate the various coefficients when $\rho = 1$.

$$a_0 = (k - h)(-a + 1 - h)(-h) - h^2 C^2 \beta (-a + 1 - h) - h^2 S^2 \beta (-h),$$

$$a_1 = (-a + 1 - h)(-h),$$

$$a_2 = (k - h)[a(1 + h) - h + h^2] + h^2 C^2 \beta (2a - 1 + h) + h^2 S^2 \beta (1 + h),$$

$$a_3 = a(1 + h) - h + h^2,$$

$$a_4 = a(k - h) + h^2(a C^2 \beta + S^2 \beta),$$

and

$$a_5 = a.$$

It can easily be seen that $a_2 = a_4 + a_0$ and $a_3 = a_1 + a_5$. Substituting for a_3 and a_2 , the characteristic polynomial can be written as

$$a_0 + a_1 s + (a_4 + a_0) s^2 + (a_1 + a_5) s^3 + a_4 s^4 + a_5 s^5 = 0.$$

But this can be factored and rewritten as

$$(s^2 + 1)(a_0 + a_1 s + a_4 s^2 + a_5 s^3) = 0.$$

This presentation of the fifth-order characteristic equation clearly illustrates the term giving rise to the sustained oscillation mentioned earlier. Since orbit frequency Ω_0 was normalized out of the coefficients, it is clear that the sustained oscillation will occur at orbit rate.

Examination of the derived thresholds makes possible a very simple physical explanation of the stability threshold asymptotes $(4\rho - 4 - h) = 0$ and $(-a + \rho - h) = 0$. These terms, as will be demonstrated, simply represent the restoring torques for the roll axis, yaw axis, and gimbal equations.

Roll:

Gyroscopic torque	$\propto I_2 - I_3 \propto \rho - 1$
Gravity-gradient torque	$\propto 3(I_2 - I_3) \propto 3(\rho - 1)$
Momentum bias	$\propto -h$
<hr/> Total restoring torque	<hr/> $\propto 4\rho - 4 - h$

Yaw:

Gyroscopic torque	$\propto I_2 - I_1 \propto \rho - a$
Gravity-gradient torque	none
Momentum bias	$\propto -h$
<hr/> Total restoring torque	<hr/> $\propto \rho - a - h$

Gimbal:

Total restoring torque	$\propto k - h$
------------------------	-----------------

Stability requires that the three restoring torques be simultaneously positive.

4.6 Extension of Modified Hurwitz Technique

It was found to be an interesting academic exercise to extend the modification of the Hurwitz criterion and to consider characteristic polynomials of various orders.

(I) Consider the fifth-order equation

$$a_0 + a_1 s + \dots + a_5 s^5 = 0.$$

For this polynomial, the necessary and sufficient conditions for all roots to have negative real parts are

$$a_i > 0 \text{ for } i = 0, \dots, 5,$$

$$D_2 = a_1 a_2 - a_0 a_3 > 0,$$

$$D_3 = a_3(a_1 a_2 - a_0 a_3) - a_1(a_1 a_4 - a_5 a_0) > 0,$$

and

$$D_4 = a_4 D_3 - a_2 a_5 D_2 + a_0 a_5(a_1 a_4 - a_0 a_5) > 0.$$

But $D_2 \rightarrow 0$ first requires that

$$D_4 = -(a_1 a_4 - a_5 a_0)^2 < 0$$

and $D_3 \rightarrow 0$ first requires that

$$a_1 D_4 = -a_5 D_2^2 < 0.$$

Therefore, for $a_i > 0$ for $i = 0, \dots, 5$, D_4 must approach zero first.

$$D_4 = a_4 D_3 - a_2 a_5 D_2 + a_0 a_5(a_1 a_4 - a_0 a_5) \geq 0,$$

and from the expression for D_3 , we obtain

$$(a_1 a_4 - a_5 a_0) = \frac{a_3 D_2 - D_3}{a_1}.$$

Substituting in the expression for D_4 , we obtain

$$a_1 D_4 = -\frac{1}{a_1} D_3^2 + \frac{a_3}{a_1} D_2 D_3 - a_5 D_2^2 \geq 0.$$

Solving for the zeros of D_4 with $a_1 > 0$, we obtain

$$D_3 = \frac{D_2}{2} \left(a_3 \mp \sqrt{a_3^2 - 4a_1a_5} \right).$$

The quantity a_1D_4 can be plotted against D_3 , and a typical curve is shown in Figure 4.3 as curve B. Also shown in this figure are the two limiting curves, marked A and C. Curve A represents the parabola for which

$$\left(\frac{a_3}{a_1} \right)^2 = 4 \left(\frac{a_5}{a_1} \right)$$

or

$$D_3 = \frac{a_3D_2}{2}$$

while curve C represents the parabola for which

$$4 \frac{a_5}{a_1} \ll \left(\frac{a_3}{a_1} \right)^2.$$

Curve C represents the uppermost permissible curve, because, if the system is to be stable, neither a_5 nor a_1 may be negative.

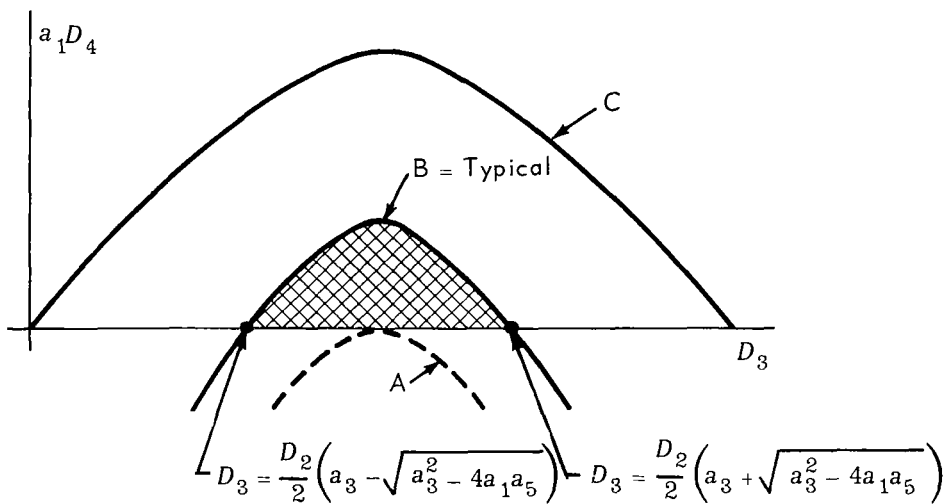


Figure 4.3—Stability constraints for fifth-order polynomial.

As a result, the shaded region under the parabola and above the D_3 axis represents the stable region and the parabola itself represents transitional stability. For stability, D_3 must take a value defined by

$$\frac{D_2}{2} \left(a_3 + \sqrt{a_3^2 - 4a_1a_5} \right) > D_3 > \frac{D_2}{2} \left(a_3 - \sqrt{a_3^2 - 4a_1a_5} \right).$$

The fact that D_3 must be real for any physical system adds the constraint that

$$\frac{a_3}{a_1} > 4 \frac{a_5}{a_3}.$$

Next, consider the special case for which

$$\frac{a_3}{a_1} = 4 \frac{a_5}{a_3}.$$

For this case, it is possible to find only a transitionally stable point, this point being defined by

$$D_3 = \frac{a_3}{2} D_2.$$

Finally, consider the special transitional case for which

$$D_4 = D_3 = D_2 = 0.$$

Let $D_4 = 0$ and $D_2 \rightarrow 0$. D_3 is then given by

$$D_3 = -a_1(a_1a_4 - a_5a_0).$$

But

$$D_4 = a_4[-a_1(a_1a_4 - a_5a_0)] + a_0a_5(a_1a_4 - a_0a_5) = 0,$$

or

$$D_4 = -(a_1a_4 - a_5a_0)^2 = 0,$$

and therefore

$$D_3 = 0.$$

Next let $D_4 = 0$ and $D_3 \rightarrow 0$. D_2 is then obtained from

$$D_3 = a_3 D_2 - a_1(a_1 a_4 - a_5 a_0) = 0,$$

or

$$(a_1 a_4 - a_5 a_0) = \frac{a_3 D_2}{a_1}.$$

But

$$D_4 = -a_2 a_5 D_2 + a_0 a_5 \frac{a_3}{a_1} D_2 = 0,$$

or

$$a_1 D_4 = -a_5 D_2^2 = 0,$$

and, therefore,

$$D_2 = 0.$$

Since

$$D_2 = a_2 a_1 - a_0 a_3 = 0$$

and

$$D_3 = -a_1(a_1 a_4 - a_5 a_0) = 0,$$

and if there is to be a transitional case for $D_4 = D_3 = D_2 = 0$, the following ratios must hold:

$$\frac{a_1}{a_0} = \frac{a_5}{a_4} = \frac{a_3}{a_2}.$$

(II) When this modification was applied to a fourth-order equation, a similar set of results were obtained. Consider the polynomial

$$a_0 + a_1 s + \cdots + a_4 s^4 = 0.$$

The necessary and sufficient conditions for all roots to have negative real parts are

$$a_i > 0 \text{ for } i = 0, \cdots, 4,$$

$$D_2 = a_1 a_2 - a_0 a_3 > 0,$$

and

$$D_3 = a_3(a_1 a_2 - a_0 a_3) - a_1^2 a_4 > 0.$$

But $D_2 \rightarrow 0$ first requires that

$$D_3 = -a_1^2 a_4 < 0,$$

and therefore, for $a_i > 0$ for $i = 0, \dots, 4$, D_3 must approach zero first.

$$D_3 = a_3(a_1 a_2 - a_0 a_3) - a_1^2 a_4 \geq 0,$$

or

$$D_3 = \left[\frac{a_3}{a_1} \left(a_2 - a_0 \frac{a_3}{a_1} \right) - a_4 \right] \geq 0,$$

that is,

$$D_3 = -a_0 \left(\frac{a_3}{a_1} \right)^2 + a_2 \left(\frac{a_3}{a_1} \right) - a_4 \geq 0.$$

Solving for the zeros of D_3 , we obtain

$$\frac{a_3}{a_1} = \frac{1}{2a_0} \left(a_2 \mp \sqrt{a_2^2 - 4a_0 a_4} \right).$$

A plot of D_3 versus a_3/a_1 is shown in Figure 4.4(a), and a plot of D_2 versus a_3/a_1 is shown in Figure 4.4(b). For stability, a_3/a_1 must take a value defined by

$$\frac{1}{2a_0} \left(a_2 + \sqrt{a_2^2 - 4a_0 a_4} \right) > \frac{a_3}{a_1} > \frac{1}{2a_0} \left(a_2 - \sqrt{a_2^2 - 4a_0 a_4} \right).$$

In addition, since a_3/a_1 must be real for any physical system, there exists an additional constraint that $a_2^2 > 4a_0 a_4$.

Consider the special case shown in Figure 4.4(a) for which $a_2^2 = 4a_0 a_4$. For this case, only a transitionally stable point can be found. This point is defined by

$$\frac{a_3}{a_1} = \frac{a_2}{2a_0}.$$

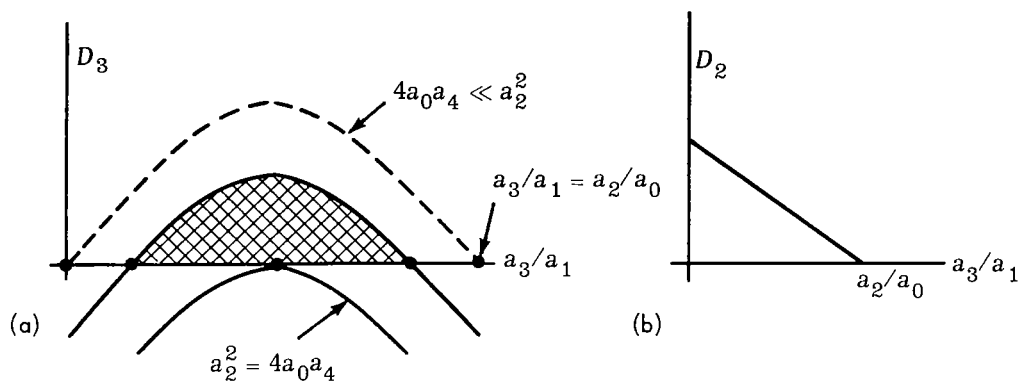


Figure 4.4—Stability constraints for fourth-order polynomial, (a) D_3 versus a_3/a_1 and (b) D_2 versus a_3/a_1 .

(III) Finally, consider the sixth-order characteristic equation

$$a_0 + a_1s + \dots + a_6s^6 = 0.$$

The necessary and sufficient conditions for all roots to have negative real parts are

$$a_i > 0 \text{ for } i = 0, \dots, 6,$$

$$D_2 = a_1a_2 - a_0a_3 > 0,$$

$$D_3 = a_3D_2 - a_1(a_1a_4 - a_5a_0) > 0,$$

$$D_4 = a_4D_3 - a_2a_5D_2 + a_1a_6D_2 + a_0a_5(a_1a_4 - a_5a_0) > 0,$$

and

$$D_5 = a_5D_4 - a_6a_3D_3 + a_6a_1a_5D_2 - a_6^2a_1^3 > 0.$$

But $D_2 \rightarrow 0$ first requires that

$$D_3 = -a_1(a_1a_4 - a_5a_0),$$

$$D_4 = -a_4a_1(a_1a_4 - a_5a_0) + a_0a_5(a_1a_4 - a_5a_0),$$

and

$$D_4 = -(a_1a_4 - a_5a_0)^2 < 0.$$

$D_3 \rightarrow 0$ first requires that

$$D_3 = a_3 D_2 - a_1(a_1 a_4 - a_5 a_0) = 0,$$

then

$$(a_1 a_4 - a_5 a_0) = \frac{a_3 D_2}{a_1}$$

and

$$D_4 = -a_2 a_5 D_2 + a_1 a_6 D_2 + a_0 a_5 \frac{D_2 a_3}{a_1}.$$

Manipulating, we obtain

$$a_1 D_4 = D_2(a_1^2 a_6 - a_5 D_2).$$

But

$$D_5 = a_5 D_4 + a_1 a_6 (a_5 D_2 - a_6 a_1^2),$$

so by substitution, we obtain

$$D_5 = a_5 D_4 + a_6 a_1 \left(-\frac{a_1 D_4}{D_2} \right),$$

or

$$D_2 D_5 = D_4 (a_5 D_2 - a_1^2 a_6),$$

and

$$D_2 D_5 = -a_1 \frac{D_4^2}{D_2},$$

and therefore

$$D_5 = -a_1 \frac{D_4^2}{D_2^2} < 0.$$

$D_4 \rightarrow 0$ first requires that

$$D_4 = a_4 D_3 - a_2 a_5 D_2 + a_1 a_6 D_2 + a_0 a_5 (a_1 a_4 - a_5 a_0) = 0.$$

But

$$(a_1 a_4 - a_5 a_0) = \frac{-D_3 + a_3 D_2}{a_1},$$

so by substitution, we obtain

$$a_1 D_4 = D_3(a_1 a_4 - a_5 a_0) + D_2(-a_2 a_5 a_1 + a_1^2 a_6 + a_0 a_5 a_3) = 0.$$

But

$$\left[a_1^2 a_6 + a_5(a_0 a_3 - a_2 a_1) \right] = a_1^2 a_6 + a_5(-D_2) ,$$

and therefore

$$D_2(a_5 D_2 - a_1^2 a_6) = D_3(a_1 a_4 - a_5 a_0) ,$$

and

$$D_5 = -a_6 a_3 D_3 + a_6 a_1(a_5 D_2 - a_6 a_1^2) .$$

Substituting, we obtain

$$D_5 = -a_6 a_3 D_3 + a_1 a_6 D_3 \frac{(a_1 a_4 - a_5 a_0)}{D_2} ,$$

or

$$D_2 D_5 = -a_6 a_3 D_3 D_2 + a_1 a_6 D_3 \left(\frac{-D_3 + a_3 D_2}{a_1} \right) .$$

Finally as

$$D_2 D_5 = -a_6 D_3^2 < 0 ,$$

then

$$D_5 < 0 ,$$

for $D_2 > 0$. It follows that, for $a_i > 0$ for $i = 0, \dots, 6$ and for $D_2 > 0$, D_5 must approach zero first.

$$D_5 = a_5 D_4 - a_6 a_3 D_3 + a_6 a_1 a_5 D_2 - a_6^2 a_1^3 \geq 0 ,$$

after substitution for D_4 ,

$$D_5 = a_5 \left[a_4 D_3 - a_2 a_5 D_2 + a_1 a_6 D_2 + a_0 a_5(a_1 a_4 - a_5 a_0) \right] - a_6 a_3 D_3 + a_6 a_1 a_5 D_2 - a_6^2 a_1^3 \geq 0 ;$$

after rearranging terms,

$$D_5 = -a_5^2 D_2^2 + a_5 D_3 \left(\frac{a_3 D_2 - D_3}{a_1} \right) + 2a_1^2 a_6 a_5 D_2 - a_6 a_3 a_1 D_3 - a_6^2 a_1^4 ;$$

and, after multiplication,

$$a_1 D_5 = -a_5^2 a_1 D_2^2 + (a_5 a_3 D_3 + 2a_1^3 a_6 a_5) D_2 + [(-a_1^2 a_6 a_3 - a_5 D_3) D_3 - a_6^2 a_1^5],$$

or

$$a_1 D_5 = -a_5 D_3^2 + (-a_1^2 a_6 a_3 + a_5 a_3 D_2) D_3 + (-a_5^2 a_1 D_2^2 + 2a_1^3 a_6 a_5 D_2 - a_6^2 a_1^5).$$

Once again, one can solve for the zeros of the quadratic equation $a_1 D_5$ in terms of the coefficients of either D_3 or D_2 . As was true in the cases of the fourth and fifth-order characteristic polynomials, one can write the stability conditions in terms of these roots. For simplicity, we may write

$$a_1 D_5 = a D_2^2 + b D_2 + c$$

or

$$a_1 D_5 = a' D_3^2 + b' D_3 + c'.$$

Then for stability, either

$$\frac{b + \sqrt{b^2 - 4ac}}{2a} > D_2 > \frac{b - \sqrt{b^2 - 4ac}}{2a} ; D_2 > 0$$

or

$$\frac{b' + \sqrt{b'^2 - 4a'c'}}{2a'} > D_3 > \frac{b' - \sqrt{b'^2 - 4a'c'}}{2a'} ; D_3 > 0$$

must hold.

The constraint imposed by the fact that D_2 or D_3 must be real is $b^2 > 4ac$ or $b'^2 > 4a'c'$.

For the special case where $b^2 = 4ac$, as before, stability requires that

$$D_2 = \frac{b}{2a}.$$

In summary, it appears that there exists at least a similarity in the method of modification of the Hurwitz criterion for the fourth-, fifth-, and sixth-order characteristic polynomials. The manner in which these modifications can be put to practical advantage is not at all obvious and is beyond the scope of this dissertation. It was felt, however, that the modifications themselves were of sufficient interest to present them at this point.

CHAPTER 5

THE STABILITY OF THE LINEARIZED EQUATION SET WITH TIME-VARYING COEFFICIENTS

5.1 General Discussion

This chapter discusses in detail certain aspects of the analysis of coupled linear equations with periodically varying coefficients.

The set of linearized equations discussed up to this point included as part of their coefficient terms the term H_b , which had been defined earlier as the pitch-momentum bias and, until now, had been constant. This bias results from the pitch reaction wheel momentum, and in practice, the instantaneous momentum of this actively controlled wheel varies sinusoidally, or at least periodically, about some average H_0 in response to certain orbital disturbance torques that act upon the spacecraft.

Because the active pitch loop responds to this periodic torque disturbance, the stability of a gimbaled-reaction-wheel-scanner class of spacecraft in the presence of a large periodically varying pitch momentum bias becomes an issue of considerable importance.

A theorem commonly used in the analysis of variational equations with time periodic coefficients is credited to Floquet (Reference 5).

5.2 Development of Floquet Theory

Let $\dot{\mathbf{X}} = A(t) \mathbf{X}$ be a system of first-order linear differential equations

where

$$\mathbf{X} = (x_1, \dots, x_n); \quad -\infty < t < \infty$$

and $A(t)$ denotes an $n \times n$ matrix whose elements are continuous periodic functions of period τ such that $A(t + \tau) = A(t)$.

Floquet asserts that a typical component of the solution vector for this system of first-order linear differential equations takes the form

$$x_k = \sum_{i=1}^n P_{ki}(t) e^{r_i t},$$

where

$$P_{ki}(t) = C_{ki} P_i(t), \quad C_{ki} \text{ constant.}$$

The constant r_i is real or complex, and $P_i(t)$ is a periodic function having a period of τ seconds. The component x_k is the solution corresponding to the k th system state. A development that leads to this conclusion follows.

Theorem 1

A system of equations of the form

$$\dot{\mathbf{X}} = A(t)\mathbf{X}, \quad \mathbf{X} = (x_1, \dots, x_n), \quad -\infty < t < \infty,$$

where

$$A(t + \tau) = A(t)$$

has at least one solution not identically zero (Reference 6) of the form

$$\mathbf{X}(t + \tau) = \lambda \mathbf{X}(t)$$

for all values of t , where $\lambda \neq 0$ is a constant, not necessarily real. The term “at least” has been used in Theorem 1 because even if λ were repeated n times, there would still be at least one solution of the form stated. Further, define a state transition matrix $\phi(t, t_0)$ as an $n \times n$ matrix with the properties that

$$\phi(t_0, t_0) = I,$$

where I is the identity matrix, and

$$\dot{\phi}(t, t_0) = A(t)\phi(t, t_0).$$

Having required that the state transition matrix satisfy the above relationships, it is possible to demonstrate that

$$\mathbf{X}(t) = \phi(t, t_0) \mathbf{X}(t_0),$$

where $\mathbf{X}(t)$ is the state vector at time t , and $\mathbf{X}(t_0)$ is the initial state vector at time t_0 .

Thus, from

$$\dot{\mathbf{X}} = A(t) \mathbf{X},$$

we obtain

$$\frac{d}{dt} (\phi(t, t_0) \mathbf{X}(t_0)) = A(t) [\phi(t, t_0) \mathbf{X}(t_0)],$$

but since $\mathbf{X}(t_0)$ is a constant, it follows that

$$A(t) \phi(t, t_0) \mathbf{X}(t_0) = A(t) [\phi(t, t_0) \mathbf{X}(t_0)]$$

It also follows that

$$\mathbf{X}(t) = \phi(t, t_0) \mathbf{X}(t_0)$$

is indeed a solution of

$$\dot{\mathbf{X}} = A(t) \mathbf{X}.$$

Substituting the time $t + \tau$ for t and setting t_0 equal to t ,

$$\mathbf{X}(t + \tau) = \phi(t + \tau, t) \mathbf{X}(t).$$

From this expression, given the state of the system at time t , the system state can be found at time $t + \tau$, where τ is the periodicity of the periodically varying coefficients.

If this expression for $\mathbf{X}(t + \tau)$ is equated to the one given in Theorem 1,

$$\phi(t + \tau, t) \mathbf{X}(t) = \lambda \mathbf{X}(t),$$

or

$$[\phi(t + \tau, t) - \lambda I] \mathbf{X}(t) = 0.$$

Clearly, if $\mathbf{X}(t)$ is to be nontrivial, then

$$|\phi(t + \tau, t) - \lambda I| = 0,$$

for all values of t , or, specifically

$$|\phi(\tau, 0) - \lambda I| = 0.$$

It is possible to analytically demonstrate that the λ 's are invariant as a function of t (References 6, 7, and 8).

If all λ_i ($i = 1, 2, \dots, n$) are distinct, there will be n independent solutions to the differential equation $\dot{\mathbf{X}} = A(t)\mathbf{X}$, thus verifying Theorem 1 for distinct λ_i . That is,

$$\mathbf{X}(t + \tau) = \lambda \mathbf{X}(t), \text{ for } \lambda = \lambda_i \text{ } (i = 1, 2, \dots, n).$$

If only m values of λ_i are distinct ($1 \leq m \leq n$), then at least m independent solutions of $\dot{\mathbf{X}} = A(t)\mathbf{X}$ exist. Once again, Theorem 1 is proved.

Let

$$\lambda_i = e^{r_i t},$$

where r_i is constant, but not necessarily real. The quantity r_i is defined as the characteristic exponent of the system of first-order differential equations. The λ_i are defined as the characteristic factors or multipliers of $\dot{\mathbf{X}} = A(t)\mathbf{X}$.

Because of the ambiguity associated with the logarithm of a complex number, λ_i , only the real part of r_i is uniquely determined.

Next define the column vector

$$\mathbf{X}_j(t) \equiv \begin{bmatrix} C_{1j}P_j(t)e^{r_j t} \\ C_{2j}P_j(t)e^{r_j t} \\ \vdots \\ C_{mj}P_j(t)e^{r_j t} \end{bmatrix} = P_j(t)e^{r_j t} \begin{bmatrix} C_{1j} \\ C_{2j} \\ \vdots \\ C_{mj} \end{bmatrix},$$

where there is one column vector for each λ_j for $j = 1, 2, \dots, n$, and m corresponds to the number of distinct λ_j 's.

The general solution which satisfies the first-order differential equation set under discussion asserted by Floquet can be written:

$$\mathbf{X}(t) = \begin{bmatrix} \sum_{i=1}^n C_{1i} P_i(t) e^{r_i t} \\ \sum_{i=1}^n C_{2i} P_i(t) e^{r_i t} \\ \vdots \\ \sum_{i=1}^n C_{mi} P_i(t) e^{r_i t} \end{bmatrix} = \sum_{i=1}^n \mathbf{X}_j(t)$$

If the time $(t + \tau)$ is substituted for t into $\mathbf{X}_j(t)$, where τ is the periodicity of the periodically varying coefficients,

$$\mathbf{X}_j(t + \tau) = P_j(t + \tau) e^{r_j(t + \tau)} \begin{bmatrix} C_{1j} \\ C_{2j} \\ \vdots \\ C_{mj} \end{bmatrix}$$

Since $e^{r_j \tau} \equiv \lambda_j$, the column vector can be rewritten as

$$\mathbf{X}_j(t + \tau) = P_j(t + \tau) \lambda_j e^{r_j t} \begin{bmatrix} C_{1j} \\ C_{2j} \\ \vdots \\ C_{mj} \end{bmatrix}$$

From Theorem 1,

$$\mathbf{X}_j(t + \tau) = \lambda_j \mathbf{X}_j(t) = \lambda_j P_j(t) e^{r_j t} \begin{bmatrix} C_{1j} \\ C_{2j} \\ \vdots \\ C_{mj} \end{bmatrix}$$

Accordingly, if $\mathbf{X}(t)$, as asserted by Floquet (Reference 6), is to be the general solution vector for the set of first-order differential equations,

$$\dot{\mathbf{X}} = A(t)\mathbf{X},$$

and also is to satisfy the relationship

$$\mathbf{X}(t + \tau) = \lambda \mathbf{X}(t),$$

then $P_j(t)$ and $P_j(t + \tau)$, as they appear in the two vector expressions for $\mathbf{X}_j(t + \tau)$, must be equal for all values of t . That is, $P_j(t)$ must be periodic with period τ .

To demonstrate that $P_j(t)$ is periodic, write

$$P_j(t) \begin{bmatrix} C_{1j} \\ C_{2j} \\ \vdots \\ C_{mj} \end{bmatrix} = e^{r_j t} \mathbf{X}_j(t).$$

Substituting $t + \tau$ for the time t ,

$$P_j(t + \tau) \begin{bmatrix} C_{1j} \\ C_{2j} \\ \vdots \\ C_{mj} \end{bmatrix} = e^{r_j(t + \tau)} \mathbf{X}_j(t + \tau).$$

From Theorem 1,

$$\mathbf{X}_j(t + \tau) = \lambda_j \mathbf{X}_j(t),$$

and therefore

$$P_j(t + \tau) \begin{bmatrix} C_{1j} \\ C_{2j} \\ \vdots \\ C_{mj} \end{bmatrix} = e^{r_j(t + \tau)} \lambda_j \mathbf{X}_j(t).$$

But

$$e^{r_j \tau} \equiv 1/\lambda_j,$$

So that

$$P_j(t + \tau) \begin{bmatrix} C_{1j} \\ C_{2j} \\ \vdots \\ C_{mj} \end{bmatrix} = \frac{e^{-r_j t}}{\lambda_j} \lambda_j \mathbf{X}_j(t) \equiv P_j(t) \begin{bmatrix} C_{1j} \\ C_{2j} \\ \vdots \\ C_{mj} \end{bmatrix}.$$

We have now deduced that $P_j(t)$ is periodic and that $\dot{\mathbf{X}} = A(t)\mathbf{X}$ has at least m , $1 \leq m \leq n$, independent solutions of the form

$$\begin{bmatrix} x_1 \\ x_2 \\ \vdots \\ x_m \end{bmatrix} = \mathbf{X}(t) = \sum_{j=1}^n \mathbf{X}_j(t).$$

At this point, it should be noted that if the characteristic exponents are not distinct, then $n - m$ of the independent solutions will include functions that, instead of being simply exponential in nature, are products of exponentials and polynomials in time. Indeed, the exponents will still be the characteristic exponents, and these will determine the asymptotic behavior of the solution. System stability will be governed by the exponential portion of the solution and more specifically by the sign associated with the real parts of the r_i 's.

Theorem 2

From the form of the determined solution, the following conclusions can be drawn:

- (1) All solutions $\mathbf{X}(t)$ of $\dot{\mathbf{X}} = A(t)\mathbf{X}$ approach zero as t approaches infinity if and only if $|\lambda_i| < 1$ ($i = 1, \dots, m$) or $\text{Re}(r_i) < 0$.
- (2) All solutions are bounded as t approaches infinity if and only if $|\lambda_i| \leq 1$ ($i = 1, \dots, m$) or $\text{Re}(r_i) \leq 0$. In addition, for those λ_i whose $|\lambda_i| = 1$, it is required that the multiplicity of this characteristic value equal the degeneracy of the matrix $[\phi(\tau, 0) - \lambda_i I]$.
- (3) The solution is periodic of period τ if and only if there is at least one λ_i such that $\lambda_i = +1$, all other $|\lambda_i| < 1$.
- (4) The solution is unstable if any $|\lambda_i| > 1$ or $\text{Re}(r_i) > 0$ ($i = 1, \dots, m$).

5.3 Deriving Physical Meaning From Floquet Theory

The general solution has added physical significance when an element of a typical state solution is detailed in the following manner.

Recall that $\lambda_i = e^{r_i \tau}$, λ_i not necessarily real. Therefore,

$$r_i \tau = \ln \lambda_i = \ln |\lambda_i| + j(\theta + 2\pi k) \text{ for } k = 0, \pm 1, \pm 2, \dots,$$

where θ is the phase angle associated with a complex λ_i :

$$\theta = \tan^{-1} \left[\frac{\text{Im}(\lambda_i)}{\text{Re}(\lambda_i)} \right].$$

Recall further that $P_i(t)$ is periodic of period τ and can therefore be expressed as a Fourier series of the form

$$P_i(t) = \left\{ \frac{a_0}{2} + \sum_{n=1}^{\infty} \left(A_n \cos \frac{2\pi}{\tau} nt + B_n \sin \frac{2\pi}{\tau} nt \right) \right\}.$$

Forming the i th element of the l th system state solution, one can write

$$X_{li}(t) = C_{li} \left[e^{\frac{\ln |\lambda_i|}{\tau} t} e^{j(\frac{\theta}{\tau} + \frac{2\pi k}{\tau})t} \left\{ \frac{a_0}{2} + \sum_{n=1}^{\infty} \left(A_n \cos \frac{2\pi}{\tau} nt + B_n \sin \frac{2\pi}{\tau} nt \right) \right\} \right].$$

Because the infinite series representation of $P_i(t)$ allows for the presence of any or all of the frequency components that are multiples of $2\pi/\tau$, where τ is the period of the time varying coefficient, it is only necessary to consider $k = 0$.

Consider the special case for which $\lambda_i = -a_i$, where a_i is greater than zero and real. One possible form of the solution associated with the λ_i described is

$$r_i \tau = \ln \lambda_i,$$

$$r_i \tau = b_i \pm j\pi,$$

and

$$r_i = \frac{b_i}{\tau} \pm j\frac{\pi}{\tau},$$

where

$$k = 0,$$

$$b_i = \text{real},$$

$$b_i > 0 \text{ for } a_i > 1,$$

$$b_i = 0 \text{ for } a_i = 1,$$

and

$$b_i < 0 \text{ for } a_i < 1.$$

Substituting, we obtain

$$X_{li}(t) = \frac{1}{2} \left[e^{-j\frac{\pi}{\tau} t} + e^{+j\frac{\pi}{\tau} t} \right] C_{li} P_i(t) e^{\frac{b_i}{\tau} t},$$

or

$$X_{li}(t) = \cos \frac{\pi}{\tau} t C_{li} \left\{ \frac{a_0}{2} + \sum_{n=1}^{\infty} A_n \cos \frac{2\pi}{\tau} nt + B_n \sin \frac{2\pi}{\tau} nt \right\} e^{\frac{b_i}{\tau} t}.$$

From this example, it is clear that although the magnitude of a_i determines the stability associated with the i th element of the l th state solution $X_{li}(t)$, it does not affect the frequency content of the solution. Furthermore, if the dominant λ_i has the form $\lambda_i = -a_i$, where a_i is real and positive, then the dominant frequency observed in the solution is likely to be half that associated with the frequency of the periodically varying coefficients rather than $2\pi/\tau$ itself. Specifically, the solution associated with the $\lambda_i = -1$ case will be a periodic function that is expandable into a Fourier series whose basic frequency is half that of the driven coefficients. Only the odd harmonics will be present.

Another λ_i for which the solution is clearly periodic is $\lambda_i = +1$. In this case, the periodicity of the element of the state solution is the same as that of the driven coefficients.

$$X_{li}(t) = C_{li} P_i(t) e^{r_i t},$$

where $r_i = 0 + j0$ for $\lambda_i = +1$, and $P_i(t)$ is of period τ .

Finally, consider the most general case, that of

$$\lambda_i = \alpha + j\beta, \text{ with } \alpha \text{ and } \beta \text{ real.}$$

Clearly, if the solution is to be even possibly periodic, the real part of r_i must be zero.

That is,

$$\sqrt{\alpha^2 + \beta^2} = 1.$$

Also, both the basic frequency associated with the imaginary part of r_i and the frequency associated with the driven coefficients must be rational numbers. Even if these two unlikely requirements are satisfied, it is possible that $P_i(t)$ must be represented by an infinite series whose basic frequency is that of the driven coefficients.

Because of the multiplicative relationship between $P_i(t)$ and $e^{j \text{Im}(r_i)t}$, the associated sum and difference frequencies must be commensurate with one another if the state solution is to be periodic. When $P_i(t)$ must be expressed as an infinite series, it might be necessary to choose a very low basic frequency, one having a very long period, in order that all sum and difference frequencies associated with the infinite series will be commensurate.

As a result, it is evident that at least from a practical engineering point of view, the most common cases whose solutions might be referred to as being periodic in nature are only those that have at least one $\lambda_i = \pm 1$.

In summary, since the λ_i are the eigenvalues of the state transition matrix $\phi(t + \tau, t)$ or of $\phi(\tau, 0)$, the analytic stability problem becomes one of developing this matrix for the state equations that include time-varying coefficients.

In pursuing this problem, it was hoped that the state transition matrix $\phi(\tau, 0)$ could have been determined with some generality (that is without having to resort to numerical techniques). However, after a considerable amount of work, the attempt proved to be fruitless.

In retrospect, one might have expected that since the $\phi(\tau, 0)$ matrix in reality is the solution for all time once given the initial state of the system, finding this matrix in general would mean that it would be possible to find the solution in general for a coupled system with time-varying coefficients.

With this in mind, the problem was pursued numerically in order that the Floquet technique might be applied to a complex set of equations that describe a particular example of a gimbaled-reaction-wheel-scanner class of spacecraft.

5.4 Application of Floquet Theory to Momentum-Bias-Caused Time Variations

A technique both convenient to apply and numerically accurate in spite of the approximations made was one in which the sinusoidally varying H_b and the cosinusoidally varying \dot{H}_b terms were replaced by square waves respectively 90° out of phase. In this manner, the variational equations with periodic coefficients were converted to a set of variational equations having piecewise constant coefficients. This made it possible to define the state transition matrix over one period as the product of four piecewise constant matrices.

$$\phi(\tau, 0) = \phi\left(\frac{2\pi}{\omega}, \frac{3\pi}{2\omega}\right) \phi\left(\frac{3\pi}{2\omega}, \frac{\pi}{\omega}\right) \phi\left(\frac{\pi}{\omega}, \frac{\pi}{2\omega}\right) \phi\left(\frac{\pi}{2\omega}, 0\right),$$

where

$$\tau = \frac{2\pi}{\omega} = \text{the periodicity of the driven coefficients.}$$

Each term in the product can be written:

$$\phi(b, a) = e^{\int_a^b A d\lambda} = e^{A(b-a)},$$

A being a constant matrix.

A digital computer simulation verified that the square-wave approximation introduced no appreciable error as long as use was made of the fact that the magnitude of the equivalent square-wave fundamental component is $4/\pi$ times the amplitude of the sine and cosine waves being approximated.

The linearized equations governing this system might be presented as follows:

$$\begin{cases} \dot{\gamma} = f(H_b, \gamma, \dot{\psi}, \phi) \\ \ddot{\psi} = f(H_b, \dot{H}_b, \gamma, \dot{\gamma}, \dot{\phi}, \psi) \\ \ddot{\phi} = f(H_b, \phi, \dot{\psi}, \gamma, \dot{\gamma}) \end{cases}$$

$$\begin{cases} \ddot{\theta} = f(\ddot{\alpha}, \theta) \\ \dot{\epsilon} = f(\epsilon, \theta, \dot{\theta}) \\ \ddot{\alpha} = f(\ddot{\theta}, \dot{\theta}, \theta, \dot{\epsilon}, \dot{\alpha}) \end{cases}$$

Recall that when the general set of equations was linearized in Chapter 3, the rotor angular velocity was written $\dot{\alpha}_R = H_b + \dot{\alpha}$, where $\dot{\alpha}$, from that point on, was defined to be a variational rotor speed, and H_b was defined to be constant.

If the system were subjected to a sinusoidal pitch disturbance torque such as one that might result from a residual spacecraft magnetic moment, it would be possible to evaluate $\dot{\alpha}$ and $\ddot{\alpha}$ from the pitch, rotor, and error signal set of equations. The resulting instantaneous wheel speed would be a phase-shifted sinusoid and the quantity $I_3(22)\dot{\alpha}$ would represent a variational value of momentum about the heretofore constant momentum bias H_b . As a result, the bias and its derivative as they appear in the roll, yaw, and gimbal equation set can be redefined to reflect the variation resulting from a sinusoidal pitch disturbance torque. If the disturbance were periodic but not sinusoidal, the variation in momentum could be expressed as a Fourier series, and using superposition, the solution would proceed exactly as above.

If the performance of this class of spacecraft is to be acceptable in the presence of pitch axis disturbance torques, the active pitch loop must be tightly controlled. Thus, the disturbance torques must be countered by variations of the reaction wheel speed about its bias rather than by variations of the spacecraft about the pitch axis. This being the case, it is reasonable to consider the variations of all state variables small with the exception of $\dot{\alpha}$. The term H_b can be redefined to account for this variation, and the analysis can be continued using the altered set of variational equations.

Order-of-magnitude experience gained in Chapter 4 allows the roll, yaw, and gimbal equation set to be rewritten in the following form:

$$T_{2x}: -H_b S \beta \dot{\phi} - C \beta H_b \dot{\psi} + B_g \dot{\gamma} - C \beta \Omega_0 H_b \phi + H_b S \beta \Omega_0 \psi + (k_g - H_b \Omega_0) \gamma = 0. \quad (5.1)$$

$$T_{1x}: -\ddot{\phi} + \left\{ \Omega_0 \left[1 + \frac{(1-\rho)}{a} \right] + \frac{H_b}{aI} \right\} \dot{\psi} - \frac{S \beta H_b}{aI} \dot{\gamma} + \left[4\Omega_0^2 \left(\frac{1-\rho}{a} \right) + \frac{\Omega_0 H_b}{aI} \right] \phi + \left[\frac{C \beta \Omega_0 H_b}{aI} - \frac{S \beta \dot{H}_b}{aI} \right] \gamma = 0. \quad (5.2)$$

$$T_{1z}: -\ddot{\psi} + \left[\Omega_0(\rho - 1 - a) - \frac{H_b}{I} \right] \dot{\phi} - \frac{C \beta H_b}{I} \dot{\gamma} + \left[\frac{\Omega_0 H_b}{I} - \Omega_0^2(\rho - a) \right] \psi - \left[\frac{C \beta \dot{H}_b}{I} + \frac{\Omega_0 S \beta H_b}{I} \right] \gamma = 0. \quad (5.3)$$

where

$$I_1(11) = aI,$$

$$I_1(22) = \rho I,$$

and

$$I_1(33) = I.$$

Furthermore, for the purpose of this discussion, it is convenient to define H_b as

$$H_b = H_0 + dHS \frac{2\pi}{\tau} t$$

and

$$H_b = \frac{2\pi}{\tau} dHC \frac{2\pi}{\tau} t, \quad H_0 \text{ and } dH \text{ constant.}$$

τ is the periodicity of the disturbance torque.

The phasing of \dot{a} with respect to the disturbance that produced it is unimportant, since the equation set under investigation is homogeneous. Any roll and/or yaw disturbances will be treated separately in Chapter 6, which deals specifically with the response to disturbance torques. The purpose of the present chapter is only to investigate potential stability problems arising from the time variation of the coefficients H_b and \dot{H}_b . A periodic pitch disturbance produces no steady-state response in the roll, yaw, or gimbal axes.

The details associated with the application of the Floquet criterion to this modified set of variational equations follow.

A convenient starting point for developing a mechanism by which the state transition matrix can numerically be evaluated for the generalized gimballed-reaction-wheel-scanner class of spacecraft was to rewrite the roll, yaw, and gimbal equation set in its state space form.

Define the vector $\mathbf{X} = (x_1, x_2, \dots, x_5)$ as follows.

$$\left. \begin{aligned} x_1 &= \phi \\ x_2 &= \dot{\phi} \\ x_3 &= \gamma \\ x_4 &= \dot{\psi} \\ x_5 &= \psi \end{aligned} \right\}$$

where

$$\dot{\mathbf{X}} = \mathbf{A}\mathbf{X},$$

and \mathbf{A} includes the periodically varying H_b terms.

Substituting these quantities into the roll, yaw, and gimbal equation set, [Equations (5.1), (5.2), and (5.3)], Equation (5.4) can be written directly.

Each of the terms that form the elements of the \mathbf{A} matrix is constant except H_b and \dot{H}_b . Figure 5.1 illustrates the approximation that was used to describe these terms.

In each of the regions over which H_b and \dot{H}_b are simultaneously constant, the state transition matrix for the time-varying coefficient case, $\phi(t + \tau/4, t)$, can be replaced by the state transition matrix for the constant coefficient case, $\phi[(t + \tau/4) - t]$, where τ is the period of the periodically varying coefficients, and the resulting matrix is

$$\phi[(t + \tau/4) - t] = e^{\int_t^{(t + \tau/4)} \mathbf{A} d\lambda}$$

5.5 Numerical Example

For a numerical example utilizing Floquet Theory, consider the stability of the Delta-Packaged Attitude-Control System (Delta-PAC) when acted upon by an external periodic pitch disturbance torque.

$$\dot{\mathbf{X}} = \begin{bmatrix} 0 & 1 & 0 & 0 & 0 \\ \left[4\Omega_0^2 \left(\frac{1-\rho}{\alpha} \right) + \frac{\Omega_0 H_b}{\alpha I} \right. & -\frac{S^2 \beta H_b^2}{\alpha I B_g} & \left[(k_g - H_b \Omega_0) \frac{S \beta H_b}{\alpha I B_g} \right. & \left[\Omega_0 \left(1 + \frac{1-\rho}{\alpha} \right) + \frac{H_b}{\alpha I} \right. & \frac{S^2 \beta \Omega_0 H_b^2}{\alpha I B_g} \\ \left. - \frac{S \beta C \beta \Omega_0 H_b^2}{\alpha I B_g} \right] & & \left. + \left(\frac{C \beta \Omega_0 H_b}{\alpha I} - \frac{S \beta \dot{H}_b}{\alpha I} \right) \right] & \left. - \frac{C \beta S \beta H_b^2}{\alpha I B_g} \right] & \\ \frac{C \beta \Omega_0 H_b}{B_g} & \frac{H_b S \beta}{B_g} & \frac{H_b \Omega_0 - k_g}{B_g} & \frac{C \beta H_b}{B_g} & -\frac{\Omega_0 H_b S \beta}{B_g} \\ -\frac{C^2 \beta \Omega_0 H_b^2}{I B_g} & \left[\Omega_0 (\rho - 1 - \alpha) - \frac{H_b}{I} \right. & \left[(k_g - H_b \Omega_0) \frac{C \beta H_b}{I B_g} \right. & -\frac{C^2 \beta H_b^2}{I B_g} & \left[\frac{\Omega_0 H_b}{I} - \Omega_0^2 (\rho - \alpha) \right. \\ & \left. - \frac{C \beta S \beta H_b^2}{I B_g} \right] & \left. - \left(\frac{C \beta H_b}{I} + \frac{\Omega_0 S \beta H_b}{I} \right) \right] & & \left. + \frac{C \beta S \beta \Omega_0 H_b^2}{I B_g} \right] \\ 0 & 0 & 0 & 1 & 0 \end{bmatrix} \mathbf{X} \quad (5.4)$$

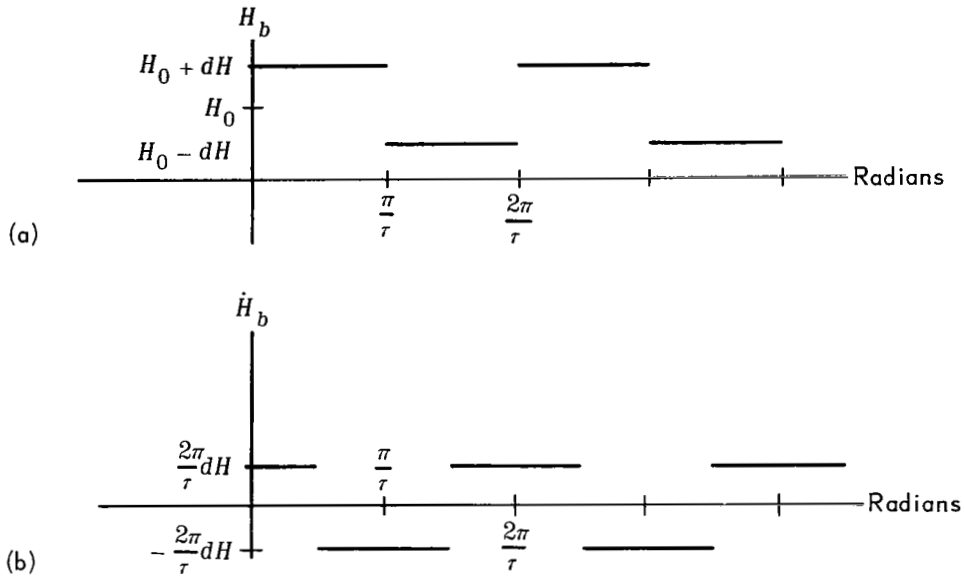


Figure 5.1—Approximation for momentum bias variations, (a) $H_b = H_0 + dH \sin \frac{2\pi}{\tau} t$,
and (b) $\dot{H}_b = \frac{2\pi}{\tau} dH \cos \frac{2\pi}{\tau} t$.

The mission of this Delta-PAC spacecraft was to experimentally test the concept of a gimballed-reaction-wheel-scanner controlled vehicle. The spacecraft was designed and fabricated at Goddard Space Flight Center, Greenbelt, Md., and was launched successfully on August 9, 1969.

The Delta-PAC spacecraft has a gimbal axis angle β of zero (i.e., the gimbal axis is coincident with the spacecraft positive roll axis). In addition, the inertia of the spacecraft roll axis equals that of the pitch axis so that $\alpha = \rho$. These assumptions simplify the system A matrix and the resulting matrix equation is shown below.

$$\dot{\mathbf{X}} = \begin{bmatrix} 0 & 1 & 0 & 0 & 0 \\ 4\Omega_0^2 \left(\frac{1}{\alpha} - 1 \right) + \frac{\Omega_0 H_b}{\alpha I} & 0 & \frac{\Omega_0 H_b}{\alpha I} & \frac{\Omega_0}{\alpha} + \frac{H_b}{\alpha I} & 0 \\ \frac{\Omega_0 H_b}{B_g} & 0 & \frac{H_b \Omega_0 - k_g}{B_g} & \frac{H_b}{B_g} & 0 \\ \frac{-\Omega_0 H_b^2}{IB_g} & -\Omega_0 - \frac{H_b}{I} & \frac{(k_g - \Omega_0 H_b) H_b}{IB_g} - \frac{\dot{H}_b}{I} & -\frac{H_b^2}{IB_g} & \frac{\Omega_0 H_b}{I} \\ 0 & 0 & 0 & 1 & 0 \end{bmatrix} \mathbf{X} \quad (5.5)$$

In order that it be possible to evaluate the state transition matrix for various values of the system parameters as well as for various values of dH and τ , it was convenient to develop a digital computer program. This program, given the system parameters, evaluates the elements of the state transition matrix $\phi(\tau, 0)$ and then evaluates its eigenvalues for various values of dH and τ .

Clearly, for the case of $dH = 0$, the solution obtained by means of Floquet theory must be identical to that obtained if one were to apply classical linear-equation theory to the constant coefficient system A matrix.

Numerical values associated with the nominal set of Delta-PAC parameters follow:

$$B_g = 0.5 \text{ ft-lb/rad-sec}^{-1}$$

$$H_0 = -2 \text{ ft-lb-sec}$$

$$a = 8$$

$$\rho = 8$$

$$I = 200 \text{ ft-lb-sec}^2$$

$$\Omega_0 = 10^{-3} \text{ rad/sec}$$

$$K_g = 0.8 \times 10^{-3} \text{ ft-lb/rad}$$

System characteristic values derived from classical linear theory are shown below. The eigenvalues are denoted by W_i , where W_i may be complex.

$$W = \begin{cases} -4.51636 \times 10^{-2} \\ -0.141329 \times 10^{-3} \pm j 1.9687 \times 10^{-3} \\ -0.768568 \times 10^{-4} \pm j 1.1053 \times 10^{-3} \end{cases}$$

The general solution for the k th system state can be written by partial fraction expansion in the form

$$x_k = C_k e^{-4.51636 \times 10^{-2} t} + e^{-0.141329 \times 10^{-3} t} \left\{ A_{k1} S(1.9687 \times 10^{-3} t) + B_{k1} C(1.9687 \times 10^{-3} t) \right\} \\ + e^{-0.768568 \times 10^{-4} t} \left\{ A_{k2} S(1.1053 \times 10^{-3} t) + B_{k2} C(1.1053 \times 10^{-3} t) \right\}.$$

Solving the equivalent problem by means of Floquet theory requires the assumption of a nonzero periodicity even though dH has been assumed to be zero. This assumption of a nonzero period is required, because for the piecewise constant coefficient case,

$$\phi(\tau - 0) \equiv \phi(\tau, 0) \equiv e^{\int_0^\tau A dt} = e^{A\tau}.$$

The period, in this case, is fictitious and is of no consequence since it is normalized out in the evaluation of the characteristic exponents.

Two arbitrary periods were chosen, and the resulting characteristic multipliers, the eigenvalues of the state transition matrix, are discussed below.

(1) For $dH = 0$,

$$\omega_0 = \frac{2\pi}{\tau} = 1.0 \times 10^{-3} \text{ rad/sec},$$

$$\lambda = \begin{pmatrix} \dots * \\ 0.616988 \angle \pm 37.9^\circ \\ 0.411479 \angle \pm 11.2^\circ \end{pmatrix} = \text{eigenvalues of } \phi(\tau, 0).$$

$$r_i = \frac{\ln \lambda_i}{\tau} = \frac{\text{Re}(\ln \lambda_i)}{\tau} + j \frac{\text{Im}(\ln \lambda_i)}{\tau}$$

$$\text{and } r = \begin{pmatrix} \dots * \\ -0.0768 \times 10^{-3} \pm j \frac{37.9^\circ}{\tau} \\ -0.141329 \times 10^{-3} \pm j \frac{11.2^\circ}{\tau} \end{pmatrix}. \quad \begin{array}{l} \text{Only the primary value of } \text{Im}(\ln \lambda_i) \\ \text{need be considered.} \end{array}$$

$$x_k = \sum_{i=1}^5 e^{r_i t} P_{ki}(t),$$

where $P_{ki}(t)$ is periodic having a period τ .

Before proceeding further with the numerical examples, it is necessary to explain the asterisk as it appears in the λ and the r equations.

As the r_i 's will in fact be identical to the system characteristic values found by classical methods, it is possible to calculate the particular λ_i that would correspond to a given r_i . Taking

$$W_i = -4.51636 \times 10^{-2} = r_i,$$

$$r_i = \frac{\ln \lambda_i}{\tau} = \frac{\text{Re}(\ln \lambda_i)}{\tau} + j \frac{\text{Im}(\ln \lambda_i)}{\tau},$$

or

$$-4.51636 \times 10^{-2} \tau = \ln |\lambda_i|.$$

For

$$\frac{2\pi}{\tau} = 1.0 \times 10^{-3} \text{ rad/sec},$$

$$\ln |\lambda_i| = 2\pi \times 10^3 (-4.51636 \times 10^{-2})$$

or

$$\lambda_i \approx 0.575 \times 10^{-122}.$$

As a result of this exercise, two facts immediately become evident. First, it is not possible to extract accurately a root of this magnitude by numerical methods from a fifth-order polynomial. Second, the accuracy of the remaining roots are essentially unaltered because of the many orders of magnitude that exist between this root and the other four λ_i 's.

Numerical methods have given results in the order of 10^{-10} for the λ_i in question, clearly a great deal smaller than either $\lambda = 0.616988 \angle \pm 37.9^\circ$ or $\lambda = 0.411479 \angle \pm 11.2^\circ$.

Because of the nature of the system under study, one time constant (the one associated with the gimbal itself) will always be very much shorter than the others in the system.

Throughout the presentation that follows, therefore, one of the five roots will be omitted in light of this discussion.

Continuing, then, with

$$x_k = \sum_{i=1}^5 e^{r_i t} P_{ki}(t),$$

which is the general solution for the system state k , and expanding, we obtain

$$x_k = e^{\dots} P_{k1}(t) + e^{-0.141329 \times 10^{-3} t} \left[e^{+j \frac{37.9}{180} \frac{\pi}{\tau} t} P_{k2}(t) + e^{-j \frac{37.9}{180} \frac{\pi}{\tau} t} P_{k3}(t) \right] \\ + e^{-0.768 \times 10^{-4} t} \left[e^{+j \frac{11.2}{180} \frac{\pi}{\tau} t} P_{k4}(t) + e^{-j \frac{11.2}{180} \frac{\pi}{\tau} t} P_{k5}(t) \right].$$

Because x_k must be a real function of time, each of the bracketed terms must also be real. Because the exponentials themselves give rise to complex quantities, the two products that appear within each bracket must be the complex conjugate of one another.

In the numerical example given, the frequency associated with $e^{\pm j(37.9/180)(\pi/\tau)t}$ is 0.1056×10^{-3} rad/sec, whereas that associated with $e^{\pm j(11.2/180)(\pi/\tau)t}$ is 0.0306×10^{-3} rad/sec.

Recalling that $P_{ki}(t)$ is a periodic function with $2\pi/\tau$ as its fundamental frequency of oscillation, then it is possible to represent the bracketed terms as

$$\sum_{m=1}^l \left[C_{mi} S_{\delta_m} t + D_{mi} C_{\delta_m} t \right]$$

where l may or may not be finite. The δ_m 's are the sum and difference frequencies resulting from the product of the periodic exponentials and the various harmonics of the periodic functions $P_{ki}(t)$.

A shortcoming that immediately becomes apparent when this method of comparison is attempted is that without previous knowledge of the solution, it is not possible to determine which of the C_{mi} 's and/or D_{mi} 's will be nonzero. However, Floquet's intent was only to demonstrate asymptotic stability or instability. In the numerical examples that follow, an attempt has been made to extract from the set of characteristic multipliers stability information and information concerning the frequency and damping ratio of each of the solution modes.

In the numerical example under discussion, previous knowledge of the solution permits writing the expansion of x_k as follows:

$$x_k = e^{\dots} P_{k1}(t) + e^{-0.768 \times 10^{-4}t} \left\{ C_{11k} S(\omega_0 + 0.1056 \times 10^{-3}t) + D_{11k} C(\omega_0 + 0.1056 \times 10^{-3}t) \right\} \\ + e^{-0.141329 \times 10^{-3}t} \left\{ C_{12k} S(2\omega_0 - 0.0306 \times 10^{-3}t) + D_{12k} C(2\omega_0 - 0.0306 \times 10^{-3}t) \right\}.$$

for $P_{k1}(t)$ constant.

The constant C_{11k} represents the first nonzero sine coefficient associated with the first bracketed term for the k th system state, and C_{12k} represents the first nonzero sine coefficient associated with the second bracketed term for the k th system state. The D_{mik} 's are defined in a similar manner.

Clearly, the Floquet characteristic multipliers produced both the correct frequencies and their associated damping factors.

(2) Next, for $dH = 0$,

$$\omega_0 = \frac{2\pi}{\tau} = 2.2 \times 10^{-3} \text{ rad/sec},$$

$$\lambda = \begin{cases} \dots \\ 0.66788 \angle \pm 37.8^\circ \\ 0.8029 \angle \pm 179.13^\circ \end{cases}$$

and

$$r = \begin{cases} \dots \\ -0.141329 \times 10^{-3} \pm j \frac{37.8^\circ}{\tau} \\ -0.076856 \times 10^{-3} \pm j \frac{179.13^\circ}{\tau} \end{cases}$$

$$x_k = e^{\dots} P_{k1}(t) + e^{-0.141329 \times 10^{-3} t} \left[e^{+j \frac{37.8}{180} \frac{\pi}{\tau} t} P_{k2}(t) + e^{-j \frac{37.8}{180} \frac{\pi}{\tau} t} P_{k3}(t) \right] \\ + e^{-0.76856 \times 10^{-4} t} \left[e^{+j \frac{179.13}{180} \frac{\pi}{\tau} t} P_{k4}(t) + e^{-j \frac{179.13}{180} \frac{\pi}{\tau} t} P_{k5}(t) \right]$$

The frequency associated with $e^{\pm j (37.8/180) (\pi/\tau) t}$ is 0.23×10^{-3} rad/sec, and that associated with $e^{\pm j (179.13/180) (\pi/\tau) t}$ is 1.105×10^{-3} rad/sec.

Finally,

$$x_k = e^{\dots} P_{k1}(t) + e^{-0.141329 \times 10^{-3} t} \left\{ C_{11k} S(\omega_0 - 0.23 \times 10^{-3}) t + D_{11k} C(\omega_0 - 0.23 \times 10^{-3}) t \right\} \\ + e^{-0.76856 \times 10^{-4} t} \left\{ C_{12k} S(\omega_0 - 1.105 \times 10^{-3}) t + D_{12k} C(\omega_0 - 1.105 \times 10^{-3}) t \right\}$$

for $P_{k1}(t)$ constant.

Once again, previous knowledge was required to determine the specific δ_m 's required.

Since the applicability of the Floquet approach has been demonstrated, numerical establishment of stability thresholds with the following digital computer search routine is now possible.

For a set of parameters representing a stable spacecraft configuration, the variational momentum dH for a given frequency $2\pi/\tau$ is increased from zero until the magnitude of the largest $|\lambda_i|$ equals one. This condition defines the threshold of instability in the Floquet sense. Floquet states that a system whose state transition matrix has at least one root of magnitude one has at least one term in its generalized time solution whose damping factor has been reduced to zero. Whether or not the steady-state time solution that results at this threshold is periodic depends on those conditions discussed in Section (5.3).

To appreciate better the physical interpretations that can be obtained from a Floquet analysis, the numerical example that was begun with $dH = 0$ is continued with $dH > 0$. In exploratory numerical work, the maximum effect of the momentum variation was obtained when the perturbation frequency was twice the frequency of the least damped root of the unperturbed system. For this reason, $2\pi/\tau = 2.2 \times 10^{-3}$ rad/sec was used as a driving frequency in the following example. The state transition matrix eigenvalues and the associated time solution is given for each of the three values of variational momentum dH considered.

(3) For $dH = 0.1$ ft-lb-sec,

$$\lambda = \begin{cases} \dots \\ -0.88 \\ -0.72 \\ 0.527 \pm j0.41 \end{cases}$$

and

$$\tau = \begin{cases} \dots \\ -0.128 \pm j\pi \\ -0.33 \pm j\pi \\ -0.4 \pm j\frac{37.7}{180}\pi \end{cases}$$

Only the principal values of $\ln \lambda_i$ are considered.

$$x_k = e^{\dots} P_{k1}(t) + e^{-0.14 \times 10^{-3}t} \left\{ C_{11k} S(n\omega_0 \pm 0.23 \times 10^{-3})t + D_{11k} C(n\omega_0 \pm 0.23 \times 10^{-3})t \right\} \\ + \left\{ e^{-0.0448 \times 10^{-3}t} + e^{-0.11555 \times 10^{-3}t} \right\} \left\{ C_{12k} S(n\omega_0 \pm \frac{\omega_0}{2})t + D_{12k} C(n\omega_0 \pm \frac{\omega_0}{2})t \right\}.$$

It is reasonable to believe that because dH is small in comparison with H_0 , the frequency content of the perturbed solution should be very close to that of the unperturbed solution.

Therefore, knowledge of the problem indicates that

$$x_k = e^{\dots} P_{k1}(t) + e^{-0.14 \times 10^{-3}t} \left\{ C_{11k} S(\omega_0 - 0.23 \times 10^{-3})t + D_{11k} C(\omega_0 - 0.23 \times 10^{-3})t \right\} \\ + e^{-0.0448 \times 10^{-3}t} \left\{ C_{12k} S(\omega_0 - \frac{\omega_0}{2})t + D_{12k} C(\omega_0 - \frac{\omega_0}{2})t \right\} \\ + e^{-0.11555 \times 10^{-3}t} \left\{ C_{13k} S(\omega_0 - \frac{\omega_0}{2})t + D_{13k} C(\omega_0 - \frac{\omega_0}{2})t \right\}.$$

The general solution of this perturbed case is similar to that of the unperturbed case except that the exponential associated with the least damped resonance has now broken into two parts, one more lightly damped and one more heavily damped than that of the unperturbed solution.

(4) For $dH = 0.2$ ft-lb-sec,

$$\lambda = \begin{cases} \dots \\ -0.9715 \\ -0.657 \\ -0.5283 \pm j0.412 \end{cases}$$

and

$$r_T = \begin{cases} \dots \\ -0.0288 \pm j\pi \\ -0.42 \pm j\pi \\ -0.4 \pm j \frac{37.7}{180} \end{cases}$$

Making use of previous information,

$$\begin{aligned} x_k = & e^{\dots} P_{k1}(t) + e^{-0.14 \times 10^{-3}t} \left\{ C_{11k} S(\omega_0 - 0.23 \times 10^{-3})t + D_{11k} C(\omega_0 - 0.23 \times 10^{-3})t \right\} \\ & + e^{-0.01008 \times 10^{-3}t} \left\{ C_{12k} S(\omega_0 - \frac{\omega_0}{2})t + D_{12k} C(\omega_0 - \frac{\omega_0}{2})t \right\} \\ & + e^{-0.147 \times 10^{-3}t} \left\{ C_{13k} S(\omega_0 - \frac{\omega_0}{2})t + D_{13k} C(\omega_0 - \frac{\omega_0}{2})t \right\}. \end{aligned}$$

As in the previous example, the unperturbed dominant time constant term has been split into two terms. One is even more lightly damped, and the other is even more heavily damped than those in Example 3.

(5) Finally, for $dH = 0.3$ ft-lb-sec,

$$\lambda = \begin{cases} \dots \\ -1.07 \\ -0.5897 \\ -0.5306 \pm j0.4157 \end{cases}$$

and

$$r_T = \begin{cases} \dots \\ +0.0659 \pm j\pi \\ -0.528 \pm j\pi \\ -0.4 \pm j \frac{37.7}{180} \pi \end{cases}$$

The general solution is written,

$$\begin{aligned}
 x_k = & e^{\dots} P_{k1}(t) + e^{-0.14 \times 10^{-3}t} \left\{ C_{11k} S(\omega_0 - 0.23 \times 10^{-3})t + D_{11k} C(\omega_0 - 0.23 \times 10^{-3})t \right\} \\
 & + e^{0.02276 \times 10^{-3}t} \left\{ C_{12k} S(\omega_0 - \frac{\omega_0}{2})t + D_{12k} C(\omega_0 - \frac{\omega_0}{2})t \right\} \\
 & + e^{-0.185 \times 10^{-3}t} \left\{ C_{13k} S(\omega_0 - \frac{\omega_0}{2})t + D_{13k} C(\omega_0 - \frac{\omega_0}{2})t \right\} .
 \end{aligned}$$

Once again, the exponential associated with the dominant unperturbed system root has split. In this case, although one term has become more heavily damped than its counterpart in Example 4, the exponent associated with the other has gone through zero and become positive. As a result, for $\omega_0 = 2.2 \times 10^{-3}$ rad/sec and $dH = 0.3$ ft-lb-sec, x_k for $k = 1, 2, \dots, 5$ is unstable.

Given the proper set of initial conditions, the initial transient of the unstable case exemplified by Case 5 is more heavily damped than any of the stable cases. Also, for $\omega_0 = 2\pi/\tau = 2.2 \times 10^{-3}$ rad/sec, the secondary system resonance is relatively unaffected by the small amplitude time variation of the coefficients. Finally in the neighborhood of the Floquet threshold, either above or below it, the dominant frequency observed in the time solution will be $\omega_0/2$ as long as the threshold eigenvalue remains $\lambda = -1$. In the neighborhood of this threshold, the unperturbed system root associated with this particular eigenvalue is the least damped system root.

A linearized digital computer simulation program was written to illustrate more clearly the phenomena under discussion. The time solutions associated with Cases 1 through 5 generated by this simulation are shown in Figures 5.2 and 5.3.

After the Floquet threshold of instability was established for $\omega_0 = 2\pi/\tau = 2.2 \times 10^{-3}$ rad/sec, where ω_0 is the frequency of the time-varying coefficient, the numeric search was continued by perturbing $\omega_0/2$ both above and below the dominant unperturbed system resonance ω_{n1} . As $|\omega_{n1} - (\omega_0/2)|$ was allowed to increase from zero, it was found that the dH required to cause the system to become unstable was increased from that found when $\omega_0/2 = \omega_{n1}$. Furthermore, as long as $\omega_0/2$ did not approach too closely ω_{n2} , the secondary resonance frequency of the unperturbed system, the eigenvalue associated with the Floquet threshold remained $\lambda = -1$. This factor indicated that the dominant frequency of the time solution, in the neighborhood of the Floquet threshold ($\lambda = -1$), was half that of the driving frequency of the periodic coefficients. Specifically, the time solution corresponding to the

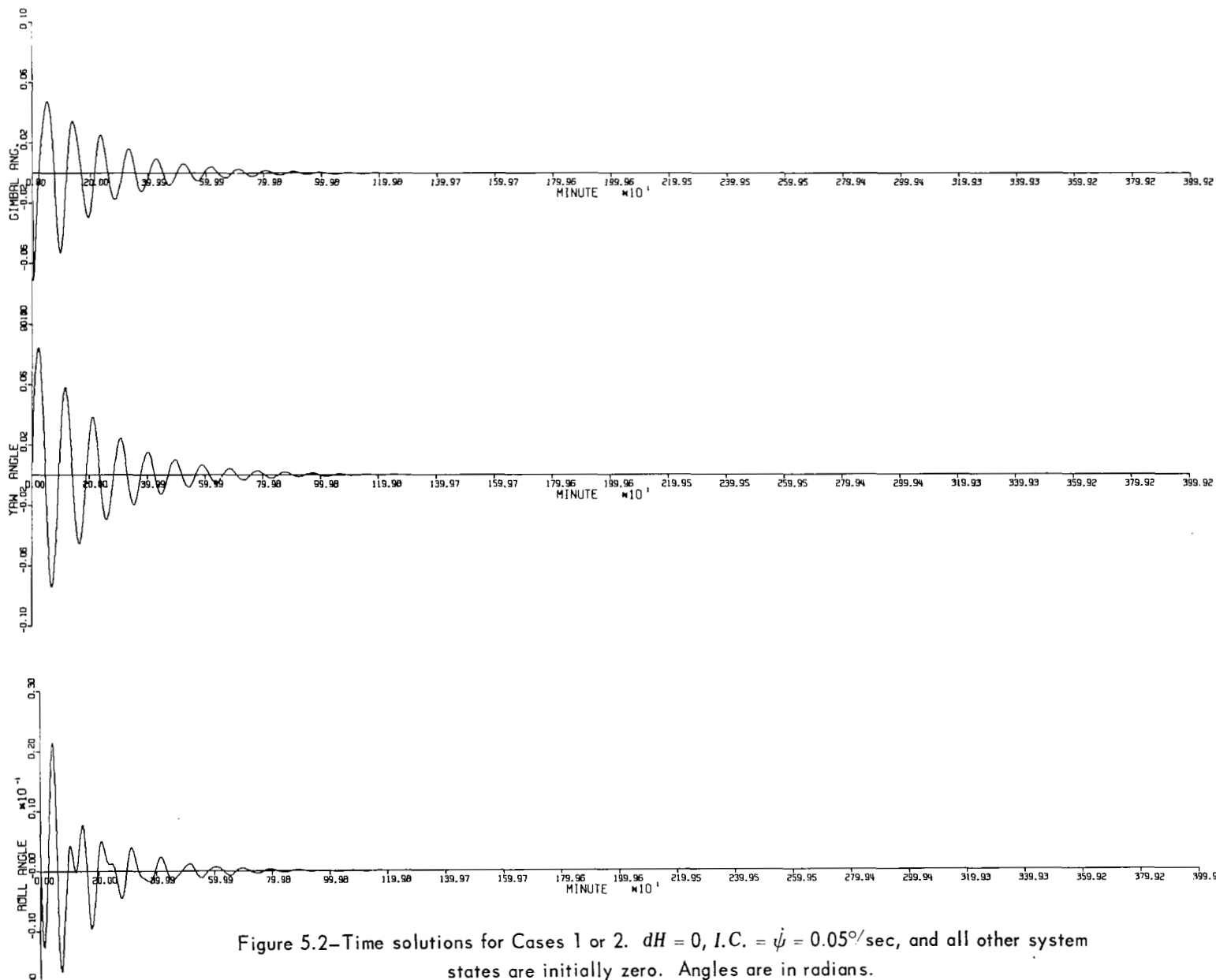


Figure 5.2—Time solutions for Cases 1 or 2. $dH = 0$, $I.C. = \dot{\psi} = 0.05^\circ/\text{sec}$, and all other system states are initially zero. Angles are in radians.

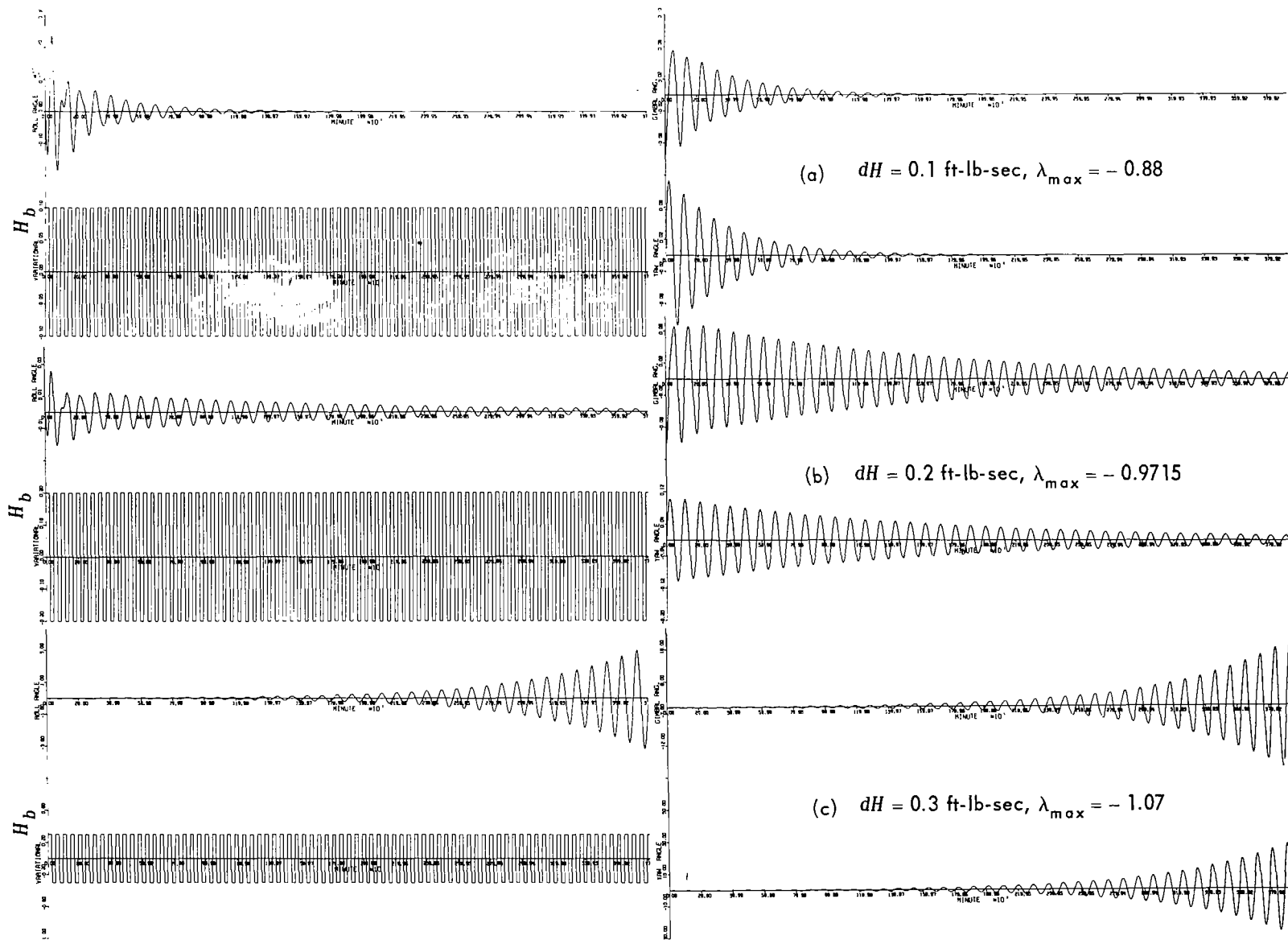


Figure 5.3—Time solutions for Cases 3, 4, and 5. $I.C. = \dot{\psi} = 0.05^\circ/\text{sec}$, and all other system states are initially zero. $\omega_0 = 2.21\Omega_0$. Angles are in radians, variational H_b is in ft-lb-sec.

threshold value of dH was periodic with basic frequency $\omega_0/2$. This phenomena can be observed in Figure 5.4.

As $\omega_0/2$ approached ω_{n2} , the eigenvalue corresponding to the Floquet threshold was now complex and the corresponding time solution was no longer periodic. Corresponding time solutions are shown in Figure 5.5.

Finally, in the vicinity of $\omega_0/2 = \omega_{n2}$, if dH is increased past the first Floquet threshold, a second threshold is found for which one of the $\lambda_i = -1$. This detail will be discussed in Section (5.7).

The results of the numerical study under discussion are presented in Figure 5.6. In this graph, the value of dH necessary to exceed the Floquet stability threshold has been plotted as a function of $\omega_0/2$, one half the applied torque disturbance frequency. The points denoted with a "Δ" correspond to eigenvalues of minus one, and those marked with a "o" correspond to complex eigenvalues whose magnitude is equal to one.

It is clear that dH has its minimum value at $\omega_0/2 = \omega_{n1}$ and that the secondary minimum associated with the complex eigenvalues occurs in the interval between $\omega_0/2 = \omega_{n1}$ and $\omega_0/2 = \omega_{n2}$.

A linearized simulation was used to validate the results obtained through the use of Floquet theory so that the mathematics of Floquet would not be obscured by the nonlinearities of the system.

If an instability were observed for a particular set of spacecraft parameters in using the linearized system of equations, then the nonlinear equations would also exhibit this instability, at least for small angle spacecraft variations.

5.6 Summary of Results

As a result of the numerical study, it was possible to deduce certain general conclusions concerning the effect of a periodic pitch disturbance torque upon the stability of this class of system. From the general discussion that preceded the numerical example, one can recall that when the threshold eigenvalue was $\lambda = -1$, the dominant frequency of the time solution will be half the driving frequency of the periodic coefficients. Accordingly, if the threshold eigenvalues for driving frequencies in the vicinity of twice the dominant resonant peak of the unperturbed system are in fact $\lambda = -1$, it should not be surprising that the most critical frequency, that frequency associated with the smallest value of dH that will drive the system unstable, was exactly twice that of the dominant damped frequency of the unperturbed system.

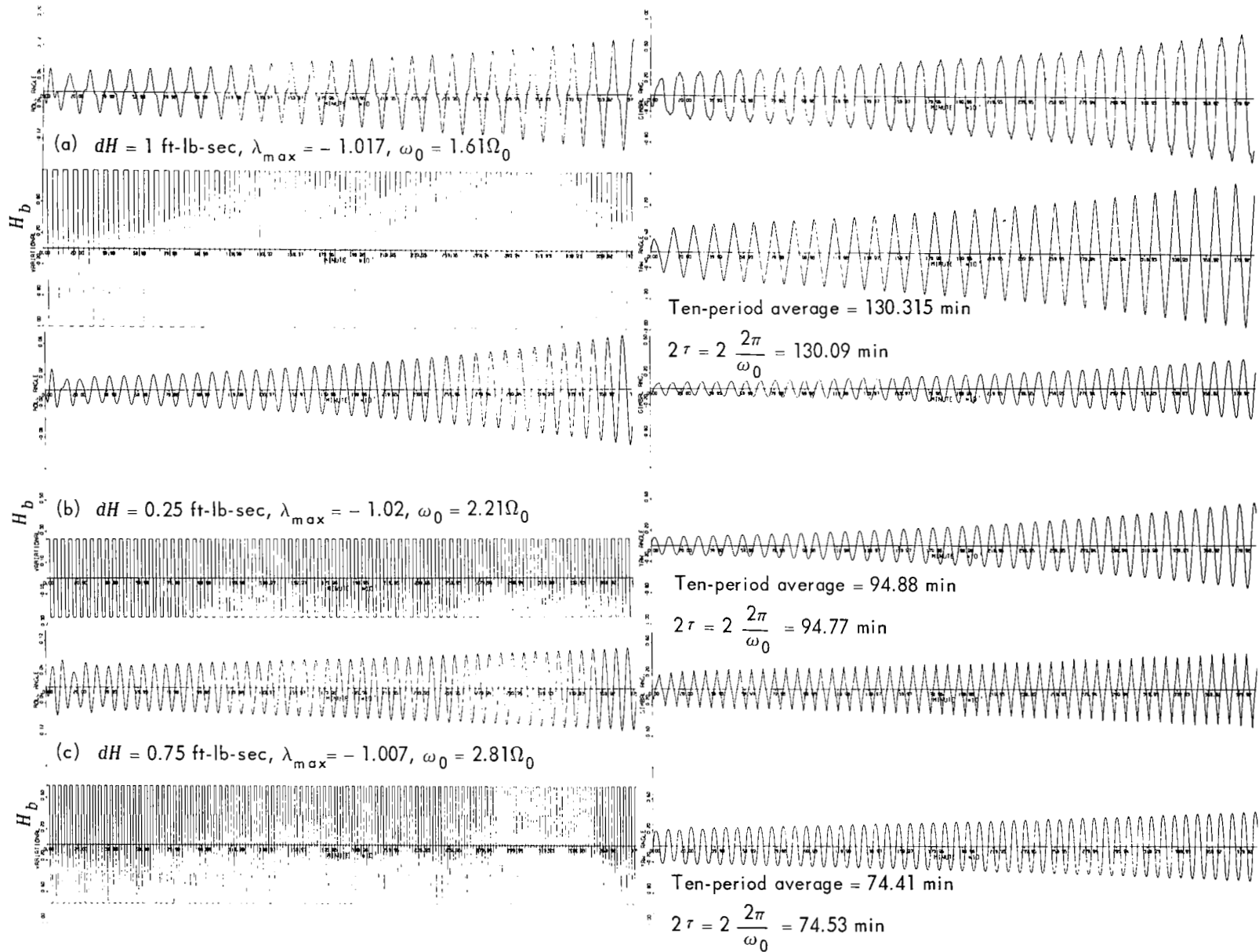


Figure 5.4—Time solutions illustrating frequency tracking characteristics. Each case is run for dH near the Floquet stability threshold. I.C. = $\dot{\psi} = 0.05^\circ/\text{sec}$, and all other system states are initially zero. Angles are in radians, variational H_b is in ft-lb-sec.

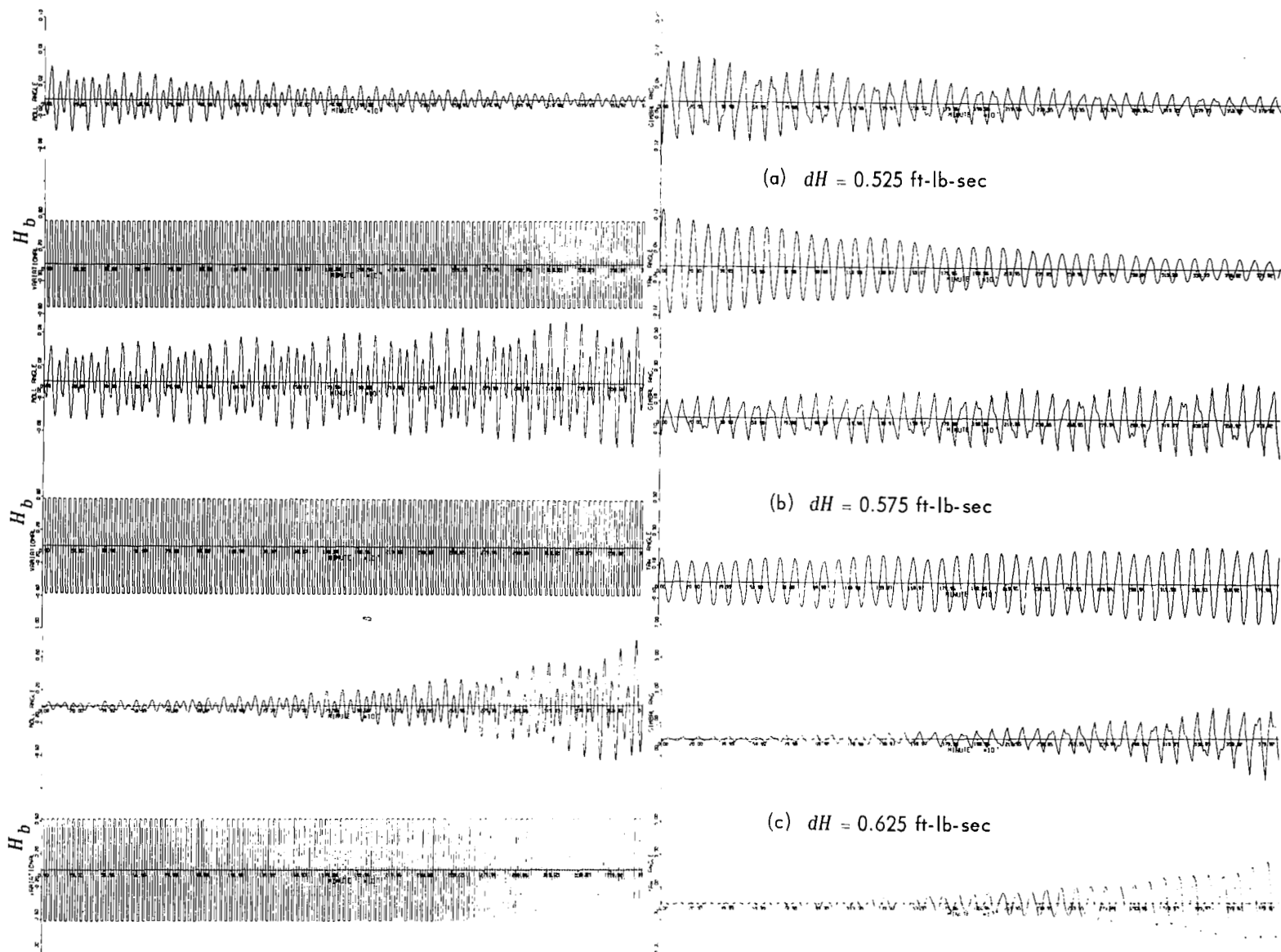


Figure 5.5—Time solutions illustrating nonperiodic instability. I.C. = $\dot{\psi} = 0.05^\circ/\text{sec}$, and all other system states are initially zero. $\omega_0 = 3.2\Omega_0$. For $dH = 0.55$ ft-lb-sec, $\lambda_{\max} = -0.581 \pm j0.808$, $|\lambda_{\max}| = 0.9951$; for $dH = 0.6$ ft-lb-sec, $\lambda_{\max} = -0.596 \pm j0.822$, $|\lambda_{\max}| = 1.015$. Angles are in radians, variational H_b is in ft-lb-sec.

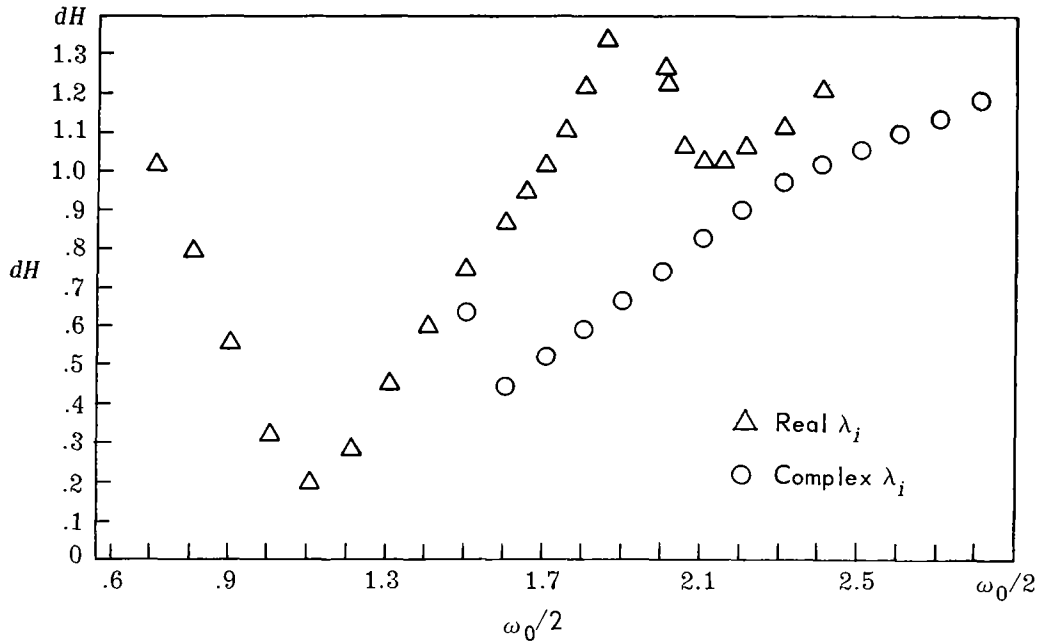


Figure 5.6—Floquet stability thresholds, dH versus $\omega_0/2$. dH is in ft-lb-sec and is the amplitude of a sinusoidal disturbance. ω_0 is in orbit rates (one orbit rate is 10^{-3} rad/sec) and is the frequency of the driven coefficient.

Moreover, the class of systems studied comprises characteristically lightly damped systems. Intuitively, one would expect that if it were possible to make the system unstable by means of a periodic disturbance in pitch, the time solution would show the least damped resonant frequency of the unperturbed system as its dominant frequency component. But this suggests that if the eigenvalue associated with the most easily excitable instability is $\lambda = -1$, the associated driving frequency would be $\omega_0/2 = \omega_{n1}$.

It would be reasonable to assume that the general nature of the dH versus $\omega_0/2$ curve does not change appreciably as the system parameters are perturbed about their nominal values. Thus, the minimum value of dH and its associated $\omega_0/2$ was found for various sets of system parameters.

Let the ordered pair $(dH, \omega_0/2)$ be that pair of values corresponding to the lowest minimum of the dH versus $\omega_0/2$ curve as illustrated by Figure 5.6. Because it was expected that the threshold eigenvalue corresponding to this minimum would be $\lambda_i = -1$, the $\omega_0/2$ in the ordered pair must exactly equal the frequency associated with the most lightly damped root of the unperturbed system. This frequency, ω_{n1} , was found by setting $dH = 0$. The critical value of dH was found numerically by increasing dH from zero until the first $\lambda_i = -1$. It was verified that all other $|\lambda_i| < 1$.

Table 5.1—Parameter variation study.

Case no.	Nominal parameter set except that	dH (ft-lb-sec)	Largest $ \lambda_i $	dH (ft-lb-sec)	Largest $ \lambda_i $
I	$H_0 = -1.575$ ft-lb-sec	0.2	-0.989	0.3	-1.115
II	$H_0 = -2.48$ ft-lb-sec	.2	- .966	.3	-1.04
III	$k_g = .8 \times 10^{-2}$ ft-lb/rad	.025	- .997	.075	-1.017
IV	$k_g = .8 \times 10^{-4}$ ft-lb/rad	.3	- .9498	.4	-1.05
V	$B_g = .25$ ft-lb-sec/rad	.1	- .987	.2	-1.08
VI	$B_g = 1.0$ ft-lb-sec/rad	.4	- .9566	.5	-1.05
VII	$I_z = 190$ ft-lb-sec ² $a = \rho = 9.2$.2	- .969	.3	-1.066
VIII	$I_z = 190$ ft-lb-sec ² $a = \rho = 7.6$.2	- .9756	.3	-1.07
IX	$I_z = 230$ ft-lb-sec ² $a = \rho = 7.6$.2	- .97	.3	-1.07
X	$I_z = 230$ ft-lb-sec ² $a = \rho = 9.2$.2	- .967	.3	-1.067

This numerical search was performed for 10 sets of parameters. The parameter sets and the results are shown in Table 5.1. As might have been expected, those cases associated with the highest value of effective damping required the largest dH to make the system unstable, and those associated with the lowest value of effective damping required the smallest dH . The linear simulation was used to substantiate the threshold values corresponding to the two extreme cases, Case III and Case VI, and the resulting time solutions are shown in Figures 5.7 and 5.8.

In the description of the method for creating the state transition matrix $\phi(\tau, 0)$, it had been stated that the sinusoidally varying component of pitch-momentum bias variation and the cosinusoidally varying \dot{H}_b term would be approximated by quadrature square waves. Thus, each of the time solutions considered until now was obtained with square-wave disturbances. To better appreciate the validity of this approximation, the same set of runs shown in Figures 5.7 and 5.8 were repeated using sinusoidal disturbance torques. These time solutions are shown in Figures 5.9 and 5.10. The two sets of runs exhibit very similar solutions.

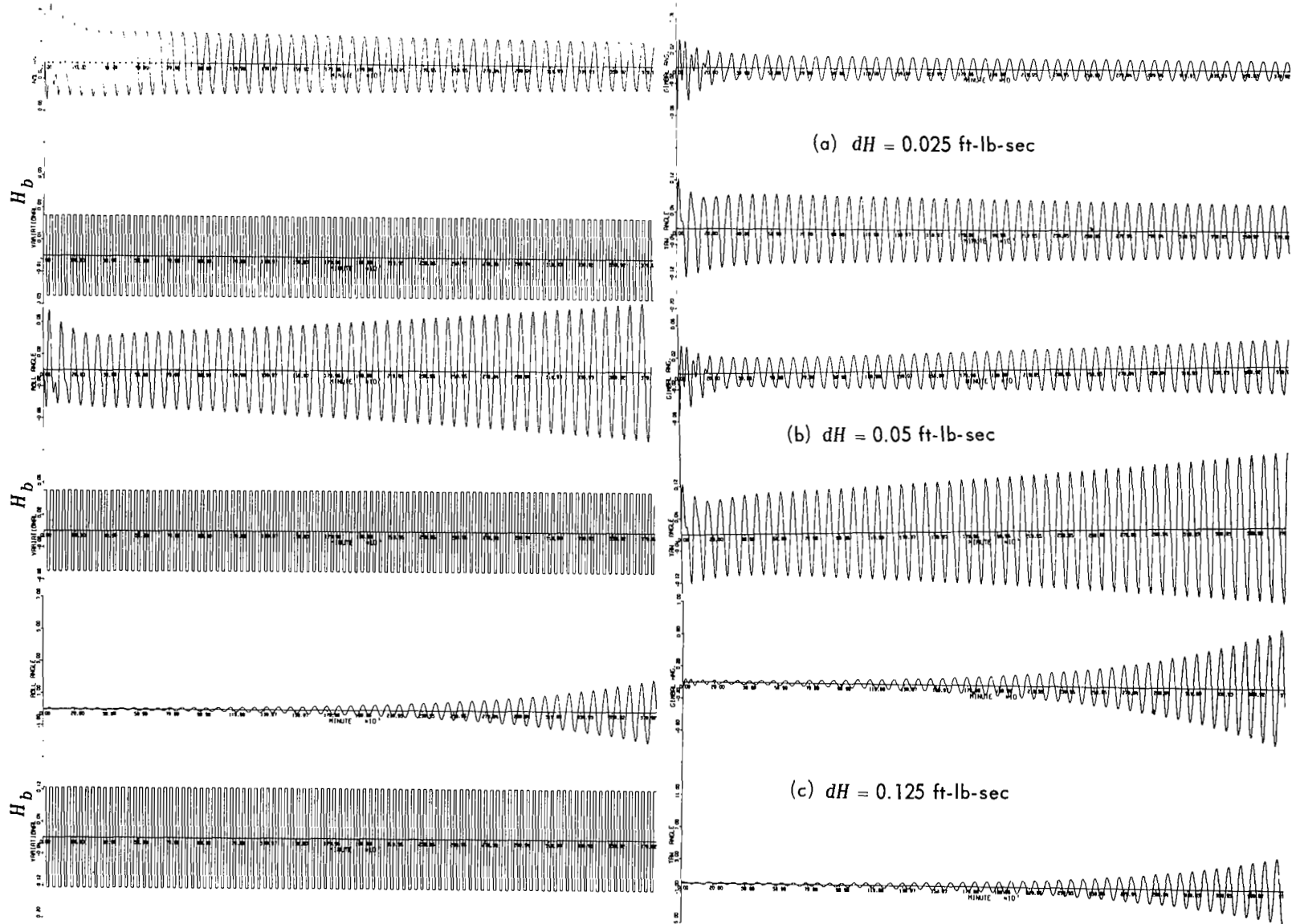


Figure 5.7—Time solutions for parameter variation Case III (square-wave momentum variation). I.C. = $\dot{\psi} = 0.05^\circ/\text{sec}$, and all other system states are initially zero. $\omega_0 = 2.739\Omega_0$. For $dH = 0.025$ ft-lb-sec, $\lambda_{\max} = -0.9968$; for $dH = 0.075$ ft-lb-sec, $\lambda_{\max} = -1.017$. Angles are in radians, variational H_b is in ft-lb-sec.

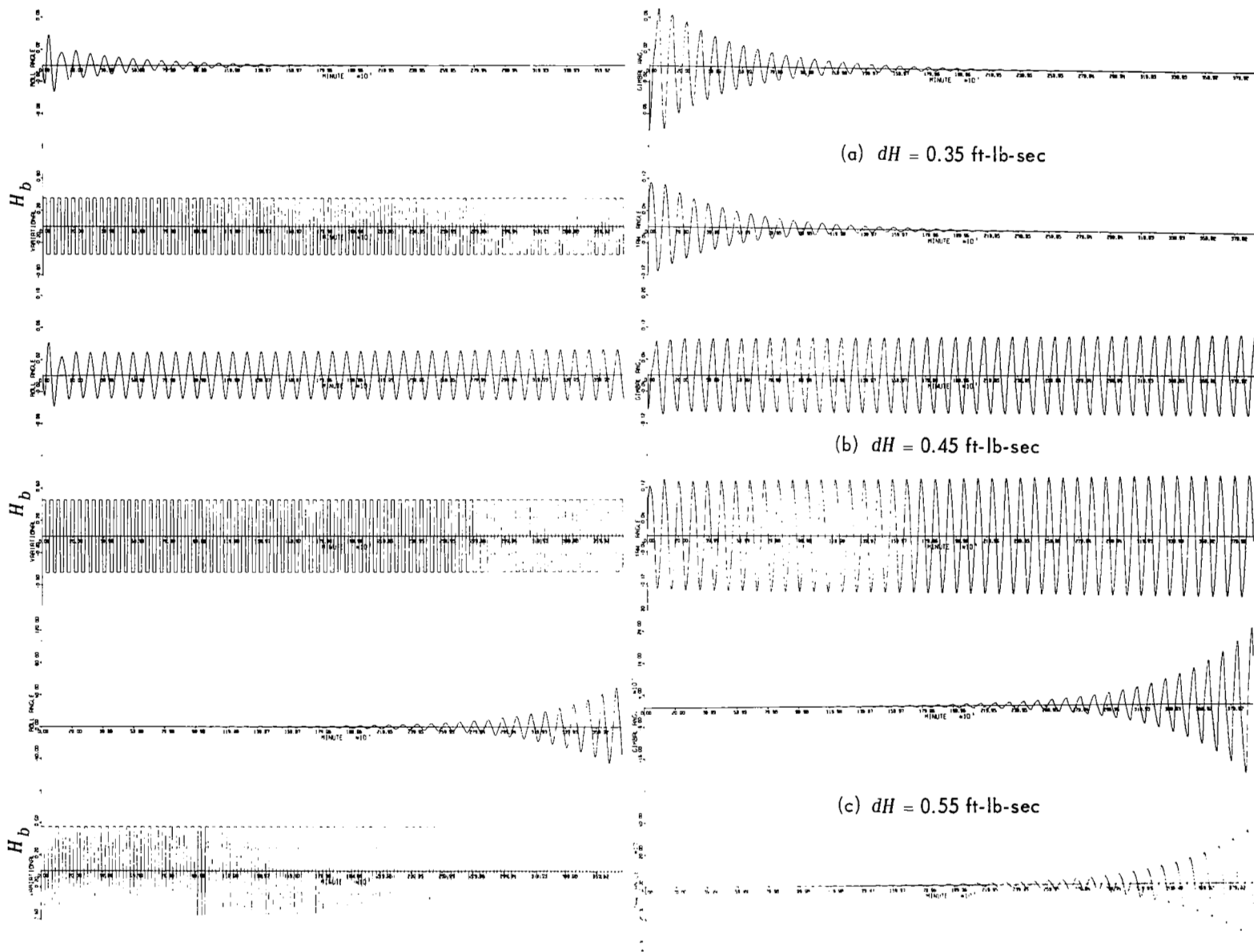


Figure 5.8—Time solutions for parameter variation Case VI (square-wave momentum variation). I.C. = $\dot{\psi} = 0.05^\circ/\text{sec}$, and all other system states are initially zero. $\omega_0 = 2.266\Omega_0$. For $dH = 0.4$ ft-lb-sec, $\lambda_{\max} = -0.9566$; for $dH = 0.5$ ft-lb-sec, $\lambda_{\max} = -1.05$. Angles are in radians, variational H_b is in ft-lb-sec.

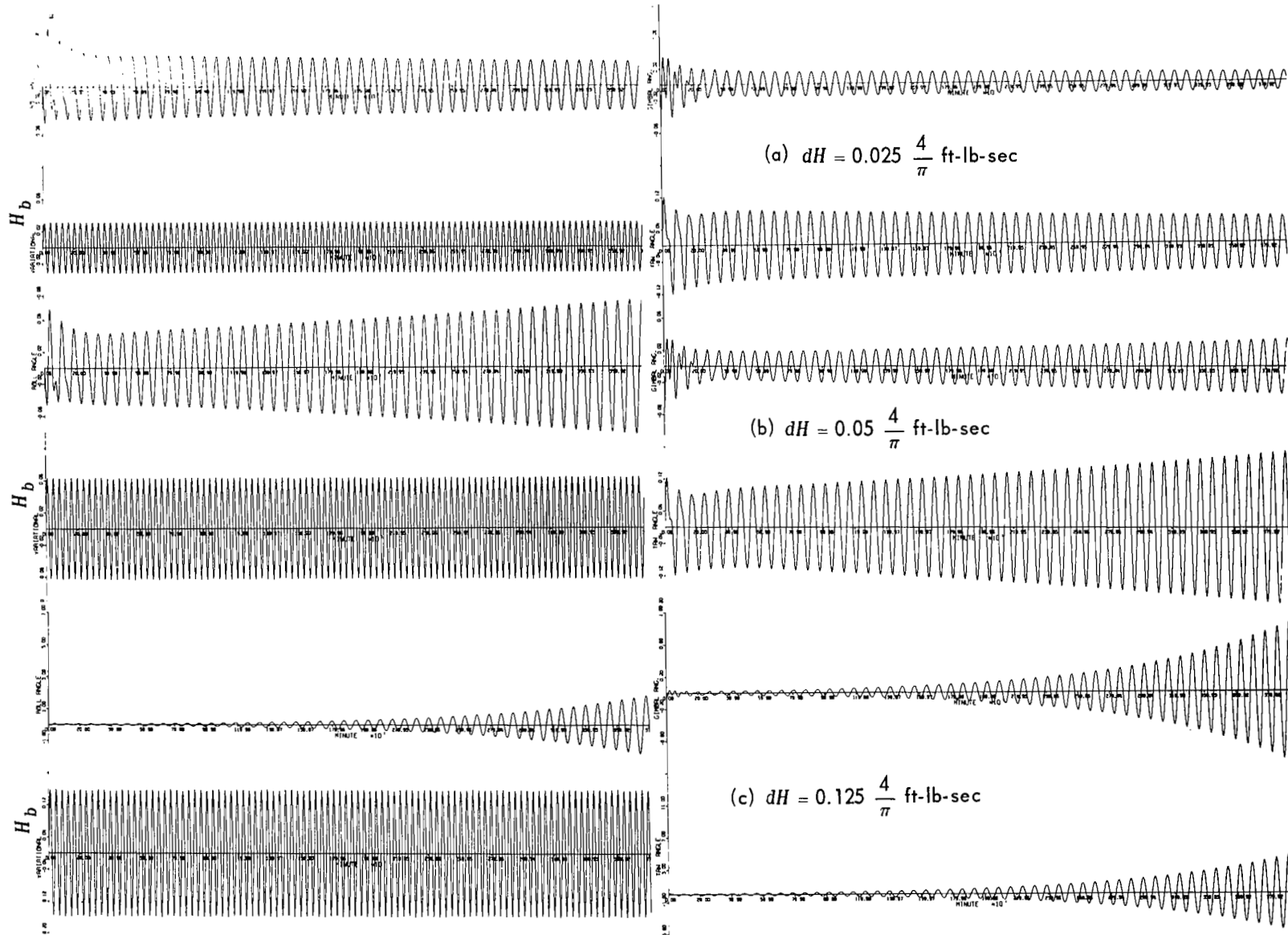


Figure 5.9—Time solutions for parameter variation Case III (sine wave momentum variation). $I.C. = \dot{\psi} = 0.05^\circ/\text{sec}$, and all other system states are initially zero. $\omega_0 = 2.739\Omega_0$. Angles are in radians, variational H_b is in ft-lb-sec.

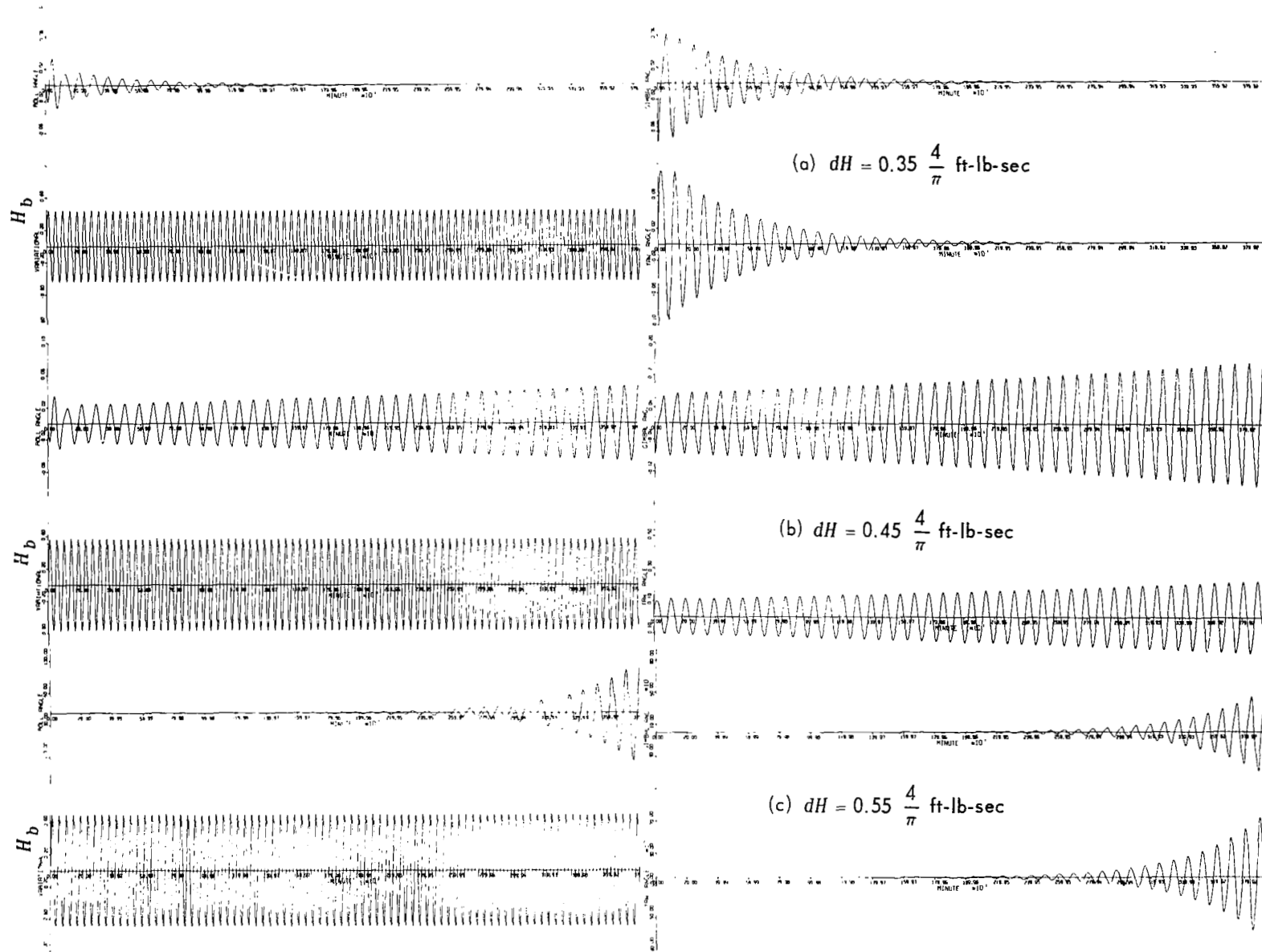


Figure 5.10—Time solutions for parameter variation Case VI (sine wave momentum variation). $I.C. = \dot{\psi} = 0.05^\circ/\text{sec}$, and all other system states are initially zero. $\omega_0 = 2.266\Omega_0$. Angles are in radians, variational H_b is in ft-lb-sec.

5.7 An Attempt at a Generalized Floquet Approach

An attempt to handle the Floquet problem in a more general manner is discussed in this section. Although this approach did not result in the analytic solution sought, it is believed that with some additional work, the general analytic solution of the problem type considered here could be found.

The systems studied rely to a large degree on gravity-gradient torques for control purposes. These systems are lightly damped, and their dominant frequency is close to orbit rate. Because of these characteristics, it would be expected that the general nature of the dH versus $\omega_0/2$ curve shown in Figure 5.6 would be applicable to most practical systems of this type, at least in the neighborhood of $\omega_0/2 = \omega_{n1}$. Practical systems are defined as those systems composed of realizable sets of parameters. In the neighborhood of $\omega_0/2 = \omega_{n1}$, the dH that is required to make the system unstable is small with respect to the bias itself. Hence, once again it would be reasonable to assume that $\lambda = -1$ throughout this neighborhood.

Accordingly, at the stability-instability transition, at least for driving frequencies in the neighborhood of twice the dominant unperturbed system resonance ω_{n1} , the steady-state time solution will be purely periodic and will have as its basic frequency $\omega_0/2$, one-half the frequency of the driven coefficients. If this were true, the solution for this class of system could be assumed to be a Fourier series whose basic frequency is $\omega_0/2$. In this manner, one could determine analytically those constraints imposed upon the general set of parameters for the solution to be periodic. The goal, of course, is to convert the numerical Floquet problem into an analytic one.

The suggested procedure will be demonstrated through the use of a quasi-characteristic equation that will be developed for the time-varying system. The assumed solution was

$$x_k = \sum_{n=1}^{\infty} \left\{ A_{kn} C_{n\omega t} + B_{kn} S_{n\omega t} \right\}$$

where $\omega = \omega_0/2$ and ω_0 is the frequency of driven coefficients. The roots of the unperturbed fifth-order system will be composed of a complex pair associated with the dominant system resonance plus a real negative exponential associated with the gimbal. The complex pair associated with the system resonance will be lightly damped and will have a frequency near orbit rate, whereas the real negative root associated with the gimbal will be a heavily damped root. The remaining two roots will probably be associated with a secondary resonance, more heavily damped than the primary resonance.

If the system parameters are chosen so that a pure oscillation will be sustained in the neighborhood of only the dominant resonance for a given value of dH , then two of the solutions of the yet-to-be-

developed quasi-characteristic polynomial in ω must be real and positive. All other solutions will be either complex or negative. A complex ω indicates that one term in the actual time solution is a damped oscillation, and a purely imaginary root will indicate that one term in the time solution is a sample exponential. In the limit, a pair of repeated positive roots in the ω polynomial for a given set of system parameters and an associated value of dH indicates those constraints dictated by the lowest minimum of the dH versus $\omega_0/2$ curve. This threshold is the one sought analytically. Finally, if the system parameters together with a particular value of dH can sustain pure oscillations in the neighborhood of both the dominant and the secondary system resonances, then ω will have four real positive solutions.

If two of the four real positive roots are repeated, we have found those constraints associated with the secondary minimum. But this threshold is of questionable value because it probably lies outside the neighborhood for which our original assumptions are valid. It should be emphasized that the applied pitch torque disturbance must have a frequency equal to $\omega_0 = 2\omega$ rad/sec and an amplitude equal to dH to realize any of the oscillatory conditions described.

Time solutions not periodic in nature, such as those cases associated with the "o" points of Figure 5.6, do not become evident through the use of this approach. To solve these cases, an infinite set of Fourier series, rather than a single Fourier series must be assumed.

This section discusses a possible approach to reduce these concepts to practice. For reasons of simplicity of presentation, a special spacecraft configuration has been chosen. This configuration was the subclass of gimbaled-reaction-wheel-scanner spacecraft for which $\alpha = \rho$ and $\beta = 0$. These conditions mean that roll inertia is equal to pitch inertia and the gimbal axis is located along the positive roll axis. Clearly, the general case can be treated simply by beginning with the complete system A matrix shown in Equation (5.4) rather than the modified matrix shown in Equation (5.5).

$$\dot{\mathbf{X}} = \mathbf{A}\mathbf{X},$$

where A is defined in Equation (5.5). Replace H_b by $H_0 + dH \sin \omega_0 t$, \dot{H}_b by $\omega_0 dH \cos \omega_0 t$, and H_b^2 by $H_0^2 + 2H_0 dH \sin \omega_0 t + dH^2 \sin^2 \omega_0 t$.

Assume

$$\mathbf{X} = \begin{bmatrix} \sum_{n=1}^{\infty} \begin{Bmatrix} A_{1n} \cos n\omega t + B_{1n} \sin n\omega t \\ \vdots \\ A_{5n} \cos n\omega t + B_{5n} \sin n\omega t \end{Bmatrix} \end{bmatrix}$$

and

$$\dot{\mathbf{X}} = \begin{bmatrix} \sum_{n=1}^{\infty} \left\{ n\omega B_{1n} \text{Cn}\omega t - n\omega A_{1n} \text{Sn}\omega t \right\} \\ \vdots \\ \sum_{n=1}^{\infty} \left\{ n\omega B_{5n} \text{Cn}\omega t - n\omega A_{5n} \text{Sn}\omega t \right\} \end{bmatrix}$$

where $\omega = \omega_0/2$.

After substitution and separation of terms, the resulting matrix representation of the set of first-order differential equations may be expressed as

$$\begin{bmatrix} \sum_{n=1}^{\infty} \left\{ n\omega B_{1n} \text{Cn}\omega t - n\omega A_{1n} \text{Sn}\omega t \right\} \\ \vdots \\ \sum_{n=1}^{\infty} \left\{ n\omega B_{5n} \text{Cn}\omega t - n\omega A_{5n} \text{Sn}\omega t \right\} \end{bmatrix} = \begin{bmatrix} 0 & 1 & 0 & 0 & 0 \\ \left(4\Omega_0^2 \frac{1-\rho}{a} + \frac{\Omega_0 H_0}{aI}\right) & 0 & \left(\frac{\Omega_0 H_0}{aI}\right) & \left(\frac{\Omega_0}{a} + \frac{H_0}{aI}\right) & 0 \\ \left(\frac{\Omega_0 H_0}{B_g}\right) & 0 & \left(\frac{\Omega_0 H_0 - k_g}{B_g}\right) & \left(\frac{H_0}{B_g}\right) & 0 \\ \left(-\frac{\Omega_0 H_0^2}{B_g I}\right) & \left(-\Omega_0 - \frac{H_0}{I}\right) \left(\frac{k_g H_0}{B_g I} - \frac{\Omega_0 H_0^2}{B_g I}\right) & \left(\frac{H_0^2}{B_g I}\right) & \left(\frac{\Omega_0 H_0}{I}\right) & 0 \\ 0 & 0 & 0 & 1 & 0 \end{bmatrix} \begin{bmatrix} \sum_{n=1}^{\infty} \left\{ A_{1n} \text{Cn}\omega t + B_{1n} \text{Sn}\omega t \right\} \\ \vdots \\ \sum_{n=1}^{\infty} \left\{ A_{5n} \text{Cn}\omega t + B_{5n} \text{Sn}\omega t \right\} \end{bmatrix}$$

$$+ dH^2 S^2 \omega_0 t \begin{bmatrix} 0 & 0 & 0 & 0 & 0 \\ 0 & 0 & 0 & 0 & 0 \\ 0 & 0 & 0 & 0 & 0 \\ -\frac{\Omega_0}{B_g I} & 0 & -\frac{\Omega_0}{B_g I} & -\frac{1}{B_g I} & 0 \\ 0 & 0 & 0 & 0 & 0 \end{bmatrix} \begin{bmatrix} \sum_{n=1}^{\infty} \left\{ A_{1n} \text{Cn}\omega t + B_{1n} \text{Sn}\omega t \right\} \\ \vdots \\ \sum_{n=1}^{\infty} \left\{ A_{5n} \text{Cn}\omega t + B_{5n} \text{Sn}\omega t \right\} \end{bmatrix}$$

$$\begin{aligned}
& + dH \sin \omega_0 t \begin{bmatrix} 0 & 0 & 0 & 0 & 0 \\ \frac{\Omega_0}{aI} & 0 & \frac{\Omega_0}{aI} & \frac{1}{aI} & 0 \\ \frac{\Omega_0}{B_g} & 0 & \frac{\Omega_0}{B_g} & \frac{1}{B_g} & 0 \\ -\frac{2\Omega_0 H_0}{B_g I} & -\frac{1}{I} \left(\frac{k_g}{B_g I} - \frac{2\Omega_0 H_0}{B_g I} \right) & -\frac{2H_0}{B_g I} & \frac{\Omega_0}{I} & 0 \\ 0 & 0 & 0 & 0 & 0 \end{bmatrix} \begin{bmatrix} \sum_{n=1}^{\infty} \left\{ A_{1n} \cos n\omega t + B_{1n} \sin n\omega t \right\} \\ \vdots \\ \sum_{n=1}^{\infty} \left\{ A_{5n} \cos n\omega t + B_{5n} \sin n\omega t \right\} \end{bmatrix} \\
& + dH \cos \omega_0 t \begin{bmatrix} 0 & 0 & 0 & 0 & 0 \\ 0 & 0 & 0 & 0 & 0 \\ 0 & 0 & 0 & 0 & 0 \\ 0 & 0 & -\frac{\omega_0}{I} & 0 & 0 \\ 0 & 0 & 0 & 0 & 0 \end{bmatrix} \begin{bmatrix} \sum_{n=1}^{\infty} \left\{ A_{1n} \cos n\omega t + B_{1n} \sin n\omega t \right\} \\ \vdots \\ \sum_{n=1}^{\infty} \left\{ A_{5n} \cos n\omega t + B_{5n} \sin n\omega t \right\} \end{bmatrix} \quad \omega = \omega_0/2 \quad (5.6)
\end{aligned}$$

It is apparent from Section (5.3) that it is necessary to consider only odd values of n when $\lambda = -1$. Furthermore, if the function is to be periodic in $\omega = \omega_0/2$, then the coefficients associated with the $n = 1$ term must be nonzero.

Using common trigonometric identities for expanding products of commensurate sines and cosines it is possible to rewrite the trigonometric products that appear in Equation (5.6) as

$$\begin{aligned}
& S(2\omega t) \left\{ \sum_{\substack{n=1 \\ n \text{ odd}}}^{\infty} \left[A_{kn} \cos(n\omega t) + B_{kn} \sin(n\omega t) \right] \right\} = \frac{1}{2} (A_{k1} - A_{k3}) \sin \omega t + \frac{1}{2} (B_{k1} + B_{k3}) \cos \omega t \\
& + \frac{1}{2} \sum_{\substack{n=3 \\ n \text{ odd}}}^{\infty} \left[(A_{k(n-2)} - A_{k(n+2)}) \sin n\omega t - (B_{k(n-2)} - B_{k(n+2)}) \cos n\omega t \right], \\
& C(2\omega t) \left\{ \sum_{\substack{n=1 \\ n \text{ odd}}}^{\infty} \left[A_{kn} \cos(n\omega t) + B_{kn} \sin(n\omega t) \right] \right\} = \frac{1}{2} (A_{k1} + A_{k3}) \cos \omega t + \frac{1}{2} (B_{k3} - B_{k1}) \sin \omega t
\end{aligned}$$

$$+ \frac{1}{2} \sum_{\substack{n=3 \\ n \text{ odd}}}^{\infty} \left[(A_{k(n-2)} + A_{k(n+2)}) Cn\omega t + (B_{k(n-2)} + B_{k(n+2)}) Sn\omega t \right],$$

and

$$\begin{aligned} S^2(2\omega t) \left\{ \sum_{\substack{n=1 \\ n \text{ odd}}}^{\infty} \left[A_{kn} C(n\omega t) + B_{kn} S(n\omega t) \right] \right\} &= \frac{1}{2} \left\{ \left[A_{k1} - \frac{1}{2} (A_{k3} + A_{k5}) \right] C\omega t \right. \\ &+ \left[B_{k1} - \frac{1}{2} (B_{k5} - B_{k3}) \right] S\omega t + \left[A_{k3} - \frac{1}{2} (A_{k1} + A_{k7}) \right] C3\omega t + \left[B_{k3} - \frac{1}{2} (B_{k7} - B_{k1}) \right] S3\omega t \Big\} \\ &+ \frac{1}{2} \sum_{\substack{n=5 \\ n \text{ odd}}}^{\infty} \left\{ \left[A_{kn} - \frac{1}{2} (A_{k(n-4)} + A_{k(n+4)}) \right] Cn\omega t + \left[B_{kn} - \frac{1}{2} (B_{k(n-4)} + B_{k(n+4)}) \right] Sn\omega t \right\}. \end{aligned}$$

If all odd values of n were to be included, a matrix with an infinite number of rows and columns would have to be dealt with. Therefore, the fact that the system is lightly damped and that it has a dominant resonance near orbit rate must be used. Accordingly, the response of the practical system will fall off rapidly to the right of this resonance so that even the third harmonic will be heavily attenuated.

A Fourier analysis was performed upon one of the cases discussed earlier to illustrate this point. Case III of the parameter variation study was chosen, and the Fourier coefficients associated with the derivatives of each of the five system states are shown in Table 5.2. The computation of these coefficients was performed within the linear digital simulation.

Table 5.2—Fourier coefficients associated with simulation Case III.

	Derivative of system state	Square-wave disturbance $\sqrt{A_n^2 + B_n^2}$		Sine wave disturbance $\sqrt{A_n^2 + B_n^2}$	
		$n = 1$	$n = 3$	$n = 1$	$n = 3$
$\dot{\phi}$	\dot{x}_1	0.139	0.145×10^{-3}	0.132	0.132×10^{-3}
$\ddot{\phi}$	\dot{x}_2	$.191 \times 10^{-3}$	$.593 \times 10^{-6}$	$.18 \times 10^{-3}$	$.524 \times 10^{-6}$
$\dot{\gamma}$	\dot{x}_3	.305	$.244 \times 10^{-2}$.289	$.228 \times 10^{-2}$
$\ddot{\psi}$	\dot{x}_4	$.555 \times 10^{-1}$	$.601 \times 10^{-3}$	$.527 \times 10^{-1}$	$.565 \times 10^{-3}$
$\dot{\psi}$	\dot{x}_5	$.417 \times 10^{-3}$	$.101 \times 10^{-4}$	$.396 \times 10^{-3}$	$.940 \times 10^{-5}$

The numerical accuracy of the coefficients of the fifth harmonic and higher appeared to be questionable. Two reasons for this inaccuracy are the problem of integrating over exactly one cycle and more importantly the problem of adjusting dH so that we are indeed at the threshold.

The Fourier coefficients were computed for both sine wave and square-wave disturbance torques despite the fact that the sine wave disturbance is pertinent in this situation. The computation of the square-wave coefficients was included to illustrate once again the close agreement of the square-wave approximation with that of the sine wave disturbance.

From the above discussion, a fairly good approximation should result if all terms other than $n = 1$ were set to zero and only those terms resulting from $n = 1$ were considered. If this is done, five relatively involved equations can be written by making the appropriate trigonometric substitutions. Moreover, 10 relationships can be written by equating the right- and left-hand-side coefficients of $S\omega t$ and $C\omega t$, respectively, for each of the five equations. Equation (5.6) is rewritten to simplify the development.

$$\begin{aligned}
 & \omega C\omega t \begin{bmatrix} B_{11} \\ B_{21} \\ B_{31} \\ B_{41} \\ B_{51} \end{bmatrix} - \omega S\omega t \begin{bmatrix} A_{11} \\ A_{21} \\ A_{31} \\ A_{41} \\ A_{51} \end{bmatrix} = \begin{bmatrix} 0 & a_{12} & 0 & 0 & 0 \\ a_{21} & 0 & a_{23} & a_{24} & 0 \\ a_{31} & 0 & a_{33} & a_{34} & 0 \\ a_{41} & a_{42} & a_{43} & a_{44} & a_{45} \\ 0 & 0 & 0 & a_{54} & 0 \end{bmatrix} \left\{ C\omega t \begin{bmatrix} A_{11} \\ A_{21} \\ A_{31} \\ A_{41} \\ A_{51} \end{bmatrix} + S\omega t \begin{bmatrix} B_{11} \\ B_{21} \\ B_{31} \\ B_{41} \\ B_{51} \end{bmatrix} \right\} \\
 & + dH^2 \begin{bmatrix} 0 & 0 & 0 & 0 & 0 \\ 0 & 0 & 0 & 0 & 0 \\ 0 & 0 & 0 & 0 & 0 \\ c_{41} & 0 & c_{43} & c_{44} & 0 \\ 0 & 0 & 0 & 0 & 0 \end{bmatrix} \left\{ \frac{1}{2} C\omega t \begin{bmatrix} A_{11} - \frac{1}{2}(A_{13} + A_{15}) \\ A_{21} - \frac{1}{2}(A_{23} + A_{25}) \\ A_{31} - \frac{1}{2}(A_{33} + A_{35}) \\ A_{41} - \frac{1}{2}(A_{43} + A_{45}) \\ A_{51} - \frac{1}{2}(A_{53} + A_{55}) \end{bmatrix} + \frac{1}{2} S\omega t \begin{bmatrix} B_{11} - \frac{1}{2}(B_{15} - B_{13}) \\ B_{21} - \frac{1}{2}(B_{25} - B_{23}) \\ B_{31} - \frac{1}{2}(B_{35} - B_{33}) \\ B_{41} - \frac{1}{2}(B_{45} - B_{43}) \\ B_{51} - \frac{1}{2}(B_{55} - B_{53}) \end{bmatrix} \right\} \\
 & + dH \begin{bmatrix} 0 & 0 & 0 & 0 & 0 \\ b_{21} & 0 & b_{23} & b_{24} & 0 \\ b_{31} & 0 & b_{33} & b_{34} & 0 \\ b_{41} & b_{42} & b_{43} & b_{44} & b_{45} \\ 0 & 0 & 0 & 0 & 0 \end{bmatrix} \left\{ \frac{1}{2} C\omega t \begin{bmatrix} (B_{11} + B_{13}) \\ (B_{21} + B_{23}) \\ (B_{31} + B_{33}) \\ (B_{41} + B_{43}) \\ (B_{51} + B_{53}) \end{bmatrix} + \frac{1}{2} S\omega t \begin{bmatrix} (A_{11} - A_{13}) \\ (A_{21} - A_{23}) \\ (A_{31} - A_{33}) \\ (A_{41} - A_{43}) \\ (A_{51} - A_{53}) \end{bmatrix} \right\}
 \end{aligned}$$

$$+ \omega dH \begin{bmatrix} 0 & 0 & 0 & 0 & 0 \\ 0 & 0 & 0 & 0 & 0 \\ 0 & 0 & 0 & 0 & 0 \\ 0 & 0 & d_{43} & 0 & 0 \\ 0 & 0 & 0 & 0 & 0 \end{bmatrix} \left\{ \frac{1}{2} C\omega t \begin{bmatrix} (A_{11} + A_{13}) \\ (A_{21} + A_{23}) \\ (A_{31} + A_{33}) \\ (A_{41} + A_{43}) \\ (A_{51} + A_{53}) \end{bmatrix} + \frac{1}{2} S\omega t \begin{bmatrix} (B_{13} - B_{11}) \\ (B_{23} - B_{21}) \\ (B_{33} - B_{31}) \\ (B_{43} - B_{41}) \\ (B_{53} - B_{51}) \end{bmatrix} \right\}, \quad (5.7)$$

where $d_{43} = -2/I$ and $\omega = \omega_0/2$.

Finally, it is necessary to make the assumption that $A_{k1} \gg A_{kl}$ and $B_{k1} \gg B_{kl}$, $l \neq 1$. But this assumption is no different from the decision to consider only the $n = 1$ related terms. From Equation (5.7), the ten relationships can be written in matrix form directly as shown in Equation (5.8), and the determinant of the 10×10 matrix yields the quasi-characteristic polynomial in ω .

Clearly, had we retained the $n = 2$ terms as well, our final matrix would have been 20×20 rather than 10×10 , and so on.

Through the use of digital computer manipulations, it was possible to form the required quasi-characteristic equation in ω both numerically and algebraically. As might have been expected, one must now deal with a fifth-order characteristic polynomial in ω^2 . All odd terms of the tenth-order polynomial are identically zero. After transforming the previously defined threshold criterion to the polynomial in ω^2 , the purely imaginary roots of the fifth-order polynomial in ω will be real and negative, and the repeated positive roots of the ω polynomial will remain repeated and positive in the ω^2 polynomial.

To determine the threshold of interest, that threshold corresponding to the detection of the ordered pair $(dH, \omega_0/2)$ that defines the lowest minimum of the dH versus $\omega_0/2$ curve, it is necessary to resolve the set of constraints for which the first pair of real, positive, repeated roots occur.

Although it is possible to solve this problem in a manner similar to that of the Routh technique, the required algebraic manipulation became prohibitive and the attempt to solve for this threshold analytically was abandoned. Additional work in this area, however, should prove to be profitable. To pursue this problem further, the range of system parameters within which the stated approximations are valid must be studied.

The potential usefulness of this approach is demonstrated by presenting the results of a numerical example.

$$\begin{bmatrix}
 -\omega & 0 & 0 & 0 & 0 & 0 & a_{12} & 0 & 0 & 0 \\
 \frac{dHb_{21}}{2} & -\omega & \frac{dHb_{23}}{2} & \frac{dHb_{24}}{2} & 0 & a_{21} & 0 & a_{23} & a_{24} & 0 \\
 \frac{dHb_{31}}{2} & 0 & \left(-\omega + \frac{dHb_{33}}{2}\right) & \frac{dHb_{34}}{2} & 0 & a_{31} & 0 & a_{33} & a_{34} & 0 \\
 \frac{dHb_{41}}{2} & \frac{dHb_{42}}{2} & \frac{dHb_{43}}{2} & \left(-\omega + \frac{dHb_{44}}{2}\right) & \frac{dHb_{45}}{2} & \left(a_{41} + \frac{dH^2c_{41}}{2}\right) & a_{42} & \left(a_{43} + \frac{dH^2c_{43}}{2} + \frac{\omega dHa_{43}}{2}\right) & \left(a_{44} + \frac{dH^2c_{44}}{2}\right) & a_{45} \\
 0 & 0 & 0 & 0 & -\omega & 0 & 0 & 0 & a_{54} & 0 \\
 0 & a_{12} & 0 & 0 & 0 & \omega & 0 & 0 & 0 & 0 \\
 a_{21} & 0 & a_{23} & a_{24} & 0 & \frac{dHb_{21}}{2} & \omega & \frac{dHb_{23}}{2} & \frac{dHb_{24}}{2} & 0 \\
 a_{31} & 0 & a_{33} & a_{34} & 0 & \frac{dHb_{31}}{2} & 0 & \omega + \frac{dHb_{33}}{2} & \frac{dHb_{34}}{2} & 0 \\
 \left(a_{41} + \frac{dH^2c_{41}}{2}\right) & a_{42} & \left(a_{43} + \frac{dH^2c_{43}}{2} - \frac{\omega dHa_{43}}{2}\right) & \left(a_{44} + \frac{dH^2c_{44}}{2}\right) & a_{45} & \frac{dHb_{41}}{2} & \frac{dHb_{42}}{2} & \frac{dHb_{43}}{2} & \left(\omega + \frac{dHb_{44}}{2}\right) & \frac{dHb_{45}}{2} \\
 0 & 0 & 0 & a_{54} & 0 & 0 & 0 & 0 & 0 & \omega
 \end{bmatrix}
 \begin{bmatrix}
 B_{11} \\
 B_{21} \\
 B_{31} \\
 B_{41} \\
 B_{51} \\
 A_{11} \\
 A_{21} \\
 A_{31} \\
 A_{41} \\
 A_{51}
 \end{bmatrix}
 =
 \begin{bmatrix}
 0 \\
 0 \\
 0 \\
 0 \\
 0 \\
 0 \\
 0 \\
 0 \\
 0 \\
 0
 \end{bmatrix}
 \quad (5.8)$$

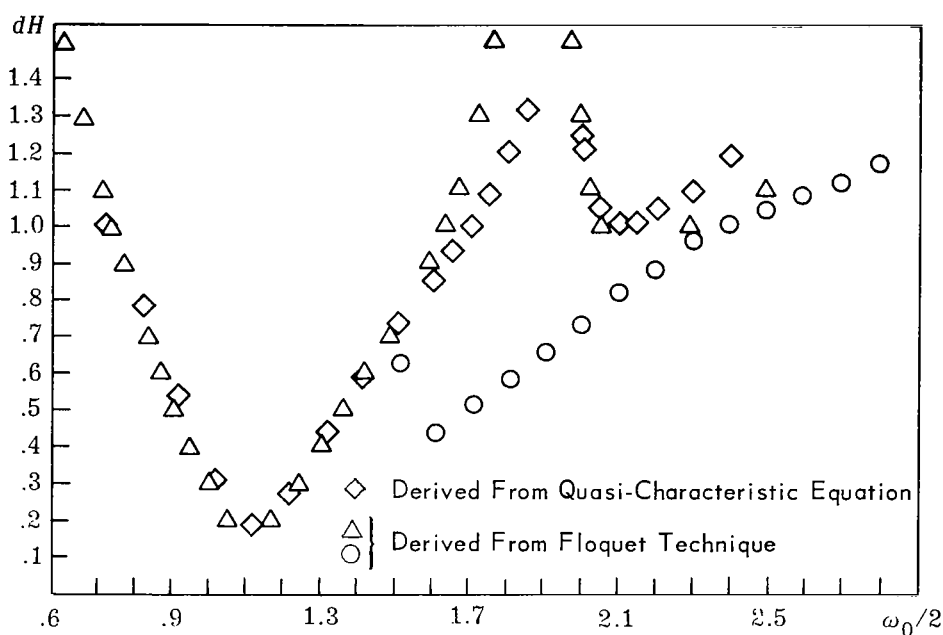


Figure 5.11—Fourier stability thresholds superimposed on Floquet stability thresholds, dH versus $\omega_0/2$. dH is in ft-lb-sec and is the amplitude of a sinusoidal disturbance. ω_0 is in orbit rates (one orbit rate is 10^{-3} rad/sec) and is the frequency of the driven coefficient.

Once again the parameters associated with the Delta-PAC spacecraft were used. These parameters were inserted into the 10×10 matrix leaving dH as the only undefined parameter. A computer was used to form the quasi-characteristic equation, and the resulting polynomial in ω^2 was factored for various values of dH . As stated earlier, only values of dH for which positive real values of ω result are of interest.

The numerical results of this approach have been superimposed upon the dH versus $\omega_0/2$ curve that resulted from the application of the Floquet criterion, and the new plot is shown in Figure 5.11.

Observe that the agreement between those results obtained from Floquet and those obtained from the quasi-characteristic equation is excellent in the neighborhood of ω_{n1} .

CHAPTER 6

PERFORMANCE

6.1 General Discussion

Chapter 5 discussed the effect of a pitch-axis disturbance torque on the stability of the passively controlled spacecraft axes. For that problem, only the homogeneous roll, yaw, and gimbal equation set was of interest, and it was unnecessary to consider the associated roll and yaw disturbance torques. This chapter considers system performance, which relates directly to the determination of a disturbance model and to system steady-state as well as transient response to the derived disturbance torques.

An investigation of system response necessarily uses a linear, time-invariant set of equations, such as Equations (5.1), (5.2), and (5.3), where H_b is constant and $\dot{H}_b = 0$. Once the response characteristics have been established, it must be verified that, within the parameter range of interest, the set of equations used adequately describes the system under study.

Because the linearized, time-invariant, roll-yaw-gimbal equation set is completely decoupled from the pitch, rotor, and error equation set, this chapter considers only the roll and yaw disturbance torque components. It has been shown that in the passively controlled axes the momentum-bias variation resulting from a pitch-axis disturbance causes a reduction of system damping but no steady state response. Furthermore, the extent by which damping was reduced is dependent on both the magnitude and the frequency content of the applied disturbance torque.

The performance criterion for a particular control system must be dependent on its actual input, the uncontrolled disturbances acting on it, and the actual output requirements. It is clearly not sufficient to require that the system step response to a position or a velocity input be well behaved, nor is it necessary or sufficient to require that the system output track a given input signal faithfully.

If, for example, uncontrolled disturbances were present in the input, then perfect following of the input would imply that the output would follow the uncontrolled signal perfectly as well. Consequently, in the presence of the disturbance torques, a compromise must be made between faithfully following the desired input and ignoring the uncontrolled disturbances.

In the classical frequency-domain approach to feedback-control theory, a system is nominally considered to be sufficiently stable, or sufficiently well damped, if its closed-loop gain is less than two at all frequencies (Reference 9). Nevertheless, if certain frequencies are present only to a negligible extent in either the desired input or in the uncontrolled disturbances, it would not be objectionable if the system were underdamped at those frequencies, for they would rarely be excited. The error transfer function should be weighted, therefore, at each frequency according to its probability of occurrence and then the total weighted error function should be minimized. A control system can then be designed to take into account those requirements associated with a particular application.

The gimbaled-reaction-wheel-scanner spacecraft relies, to a large extent, upon gravity-gradient torques for the purpose of control. Consequently, this class of system is lightly damped, and its dominant frequency is near orbit rate. The vehicle in question is expected to maintain a single orientation in space; therefore, its control input signal will be identically zero.

Moreover, the so-called uncontrolled disturbances result from specific environmental phenomena, and their frequency content is well known. Phenomena that give rise to disturbance torques include atmospheric drag, solar radiation pressure, and residual magnetic moments.

Because the magnitudes of these disturbances are heavily dependent on the altitude and inclination of the orbit as well as on the configuration of the vehicle, it is impossible to make any precise statements concerning the magnitudes of these various torques. Qualitative statements regarding the effect of orbit altitude upon these disturbances, however, can be made. Specifically, atmospheric drag can be expected to be the dominant disturbance only at altitudes under a few hundred nautical miles. Only at these low altitudes is the molecular density of space high enough to cause the atmospheric-drag term to be large.

As the orbit altitude increases, the magnitude of this torque decreases sharply. For orbits at altitudes over 400 nautical miles, the residual magnetic disturbance torque clearly dominates over atmospheric drag.

The magnetic disturbance torque is inversely proportional to the cube of the orbital distance from the center of the earth, whereas the solar pressure disturbance is related to the distance of the vehicle from the sun. As a consequence, the magnitude of the magnetic torque falls off as the orbital altitude is increased, until for altitudes over 10 000 nautical miles, solar radiation becomes the dominant disturbance.

Two other forms of disturbances are the internally produced disturbances and orbital eccentricity. The internal spacecraft disturbances must be considered separately because they depend upon the mission of the particular spacecraft under study. The incorporation of an actively controlled pitch loop allows for the inclusion of pitch internal torque-disturbance devices, such as actively driven solar array panels and large data-collecting tape recorders. These devices must be mounted so that their momentum or torque vectors are aligned along the spacecraft pitch axis if disturbance rejection is to be most effective.

The internal torque-disturbance devices cause variations in the speed of the pitch reaction wheel but do not change the total spacecraft momentum along the pitch axis. Because the active pitch loop responds quickly (within a few minutes at most), the effect of high-frequency variations on the passively controlled roll and yaw axes is negligible. Most internal torque-disturbance devices are symmetrical about their rotating axes. If they are not, time-varying inertia terms will result in the roll-yaw plane equations. Driven solar panels fall into this category and are treated separately in Chapter 7.

The major effect of orbital eccentricity is to cause a variation in the orbital velocity of the spacecraft. This variation directly affects only the vehicle pitch rate, which is properly regulated by the actively controlled pitch loop. Here again, the total spacecraft momentum is unchanged, and the effect upon the passively controlled roll-yaw plane is negligible. In addition to the periodic variation in orbital velocity, there is also an orbital period variation in the coefficients of the gravity-gradient restoring torque terms. These variations are negligibly small, but they could be handled by the techniques developed in Chapter 5. Consequently, internal torque disturbances and orbital eccentricity were not given further consideration.

The characteristics of the conical infrared attitude horizon scanner used in vehicles of this class limit the spacecraft orbit altitude to between 400 and 800 nautical miles. Within this range of operation, experience has shown that the residual magnetic disturbance torques, both those resulting from the spacecraft alone and those resulting from current paths on driven solar panels, are the dominant disturbances. It is with this in mind that the discussion is continued. For any practical application, the potential user must demonstrate that for his problem the magnetic disturbance is in fact the dominant disturbance if he is to make use of either the computer program referenced later in this chapter or the conclusions stated in the numerical example presented in Chapter 8.

The dipole model of the earth's magnetic field has been derived by Wheeler (Reference 10). The use of the earth's magnetic field in conjunction with the magnetic moment of the spacecraft and solar panel assembly results in the fact that the dominant frequency components of the residual magnetic disturbance torque are constant, orbit rate, and higher harmonics of orbit rate.

Because the nominal system input is zero, and because of the limited frequency content of the dominant "uncontrolled disturbances," this problem can be treated as discussed earlier. Specifically, a meaningful performance criterion for this class of problem would be one that utilizes the total weighted mean square error, which can be computed by evaluating the error response functions at each of the frequencies resulting from the dominant disturbance torques. This quantity can be used as one element of a factor-of-merit function, and it can be minimized as a function of the system parameters. The second element of a meaningful factor-of-merit function must involve system damping or transient response. This element can be factored into the performance criterion by the consideration of only those sets of parameters for which the time constant associated with the dominant system resonance is less than some predetermined value.

6.2 Development of Error Transfer Functions

Cyclic pitch disturbances that give rise to time-varying coefficients in the roll, yaw, and gimbal equation set are considered in detail in Chapters 5 and 7. For the purposes of a harmonic response study, however, it is necessary to assume that these variations are negligible. Chapter 8 attempts to validate this assumption and to verify that the linearized equation set adequately models the nonlinear system within the neighborhood of interest.

The error transfer functions that must be considered are those that relate the roll, yaw, and gimbal angles to the roll and yaw components of the residual magnetic disturbance torques. The required transfer functions can be derived with the equations developed in Chapter 3, Equations (5.1), (5.2), and (5.3), and Kramer's rule.

$$\begin{bmatrix} G_{11} & G_{12} & G_{13} \\ G_{21} & G_{22} & G_{23} \\ G_{31} & G_{32} & G_{33} \end{bmatrix} \begin{bmatrix} \phi \\ \gamma \\ \psi \end{bmatrix} = \begin{bmatrix} T_{dx} \\ 0 \\ T_{dz} \end{bmatrix},$$

where ϕ = roll angle, γ = gimbal angle, ψ = yaw angle, T_{dx} = roll component of disturbance torque, and T_{dz} = yaw component of disturbance torque.

The G matrix components are

$$G_{11} = \left\{ H_b [\Omega_0 (S^2\beta + C\beta) - s(S\beta C\beta)] - I_{11}s^2 + 4\Omega_0^2(I_{13} - I_{12}) \right\},$$

$$G_{12} = \left\{ H_b [\Omega_0 C\beta - s(S\beta)] \right\},$$

$$G_{13} = \left\{ H_b [s(S^2\beta + C\beta) + \Omega_0 S\beta C\beta] + \Omega_0 s(I_{11} + I_{13} - I_{12}) \right\},$$

$$G_{21} = \left\{ -H_b [s(S\beta) + \Omega_0 C\beta] \right\},$$

$$G_{22} = [k_g + B_g s - \Omega_0 H_b],$$

$$G_{23} = \left\{ H_b [\Omega_0 S\beta - s(C\beta)] \right\},$$

$$G_{31} = \left\{ H_b [\Omega_0 S\beta (C\beta - 1) - s(C^2\beta)] + \Omega_0 s(I_{12} - I_{11} - I_{13}) \right\},$$

$$G_{32} = \left\{ -H_b [s(C\beta) + \Omega_0 S\beta] \right\},$$

and

$$G_{33} = \left\{ H_b [s(S\beta)(C\beta - 1) + \Omega_0 C^2\beta] - I_{13}s^2 - \Omega_0^2(I_{12} - I_{11}) \right\}.$$

By definition

$$\Delta = \begin{vmatrix} G_{11} & G_{12} & G_{13} \\ G_{21} & G_{22} & G_{23} \\ G_{31} & G_{32} & G_{33} \end{vmatrix}.$$

The desired transfer functions can now be written directly.

$$\begin{aligned} R_{1\omega_1} &\equiv \left| \frac{\phi}{T_{dx}}(j\omega) \right|_{\omega=\omega_1} = \left| \frac{G_{22}G_{33} - G_{32}G_{23}}{\Delta} \right|_{s=j\omega_1} \\ R_{2\omega_1} &\equiv \left| \frac{\phi}{T_{dz}}(j\omega) \right|_{\omega=\omega_1} = \left| \frac{G_{12}G_{23} - G_{22}G_{13}}{\Delta} \right|_{s=j\omega_1} \\ R_{3\omega_1} &\equiv \left| \frac{\psi}{T_{dx}}(j\omega) \right|_{\omega=\omega_1} = \left| \frac{G_{21}G_{32} - G_{31}G_{22}}{\Delta} \right|_{s=j\omega_1} \\ R_{4\omega_1} &\equiv \left| \frac{\psi}{T_{dz}}(j\omega) \right|_{\omega=\omega_1} = \left| \frac{G_{11}G_{22} - G_{21}G_{12}}{\Delta} \right|_{s=j\omega_1} \end{aligned} \quad (6.1)$$

$$R_{5\omega_1} \equiv \left| \frac{\gamma}{T_{dx}} (j\omega) \right|_{\omega = \omega_1} = \left| \frac{G_{23} G_{31} - G_{33} G_{21}}{\Delta} \right|_{s = j\omega_1}$$

$$R_{6\omega_1} \equiv \left| \frac{\gamma}{T_{dz}} (j\omega) \right|_{\omega = \omega_1} = \left| \frac{G_{13} G_{21} - G_{23} G_{11}}{\Delta} \right|_{s = j\omega_1}$$

Define R_{i0} as the i th transfer function evaluated at $\omega = 0$, R_{i1} as the i th transfer function evaluated at $\omega = \Omega_0$ (Ω_0 = orbit rate) and R_{i2} as the i th transfer function evaluated at $\omega = 2\Omega_0$.

Algebraic manipulation yields the following results in terms of the normalized parameters defined in Chapter 4 and of the relation $B_g = B\Omega_0 I_3$. The numerators of the six transfer functions are

$$\begin{aligned} \frac{\Delta\phi}{I^2\Omega_0^4 T_{dx}} (j\omega) = & \left[(k-h)(a-\rho+C^2\beta h) + S^2\beta h^2 \right] + \left\{ \beta(a-\rho+C^2\beta h) + (k-h)[S\beta h(C\beta-1)] \right\} j\omega \\ & - \left\{ h[S\beta B(C\beta-1) - C^2\beta h^2] - (k-h) \right\} \omega^2 + [B] j\omega^3, \end{aligned}$$

$$\begin{aligned} \frac{\Delta\phi}{I^2\Omega_0^4 T_{dz}} (j\omega) = & \left[-C\beta S\beta h(k-2h) \right] + \left\{ (k-h)[-1-a+\rho-C\beta h] - S\beta h(S\beta k + C\beta B) - C^2\beta h^2 \right\} j\omega \\ & - [B(\rho-a-1-C\beta h - S^2\beta h) + C\beta S\beta h^2] \omega^2, \end{aligned}$$

$$\begin{aligned} \frac{\Delta\psi}{I^2\Omega_0^4 T_{dx}} (j\omega) = & \left[(k-h)(S\beta h) - C\beta S\beta h(k-2h) \right] + \left\{ (k-h)(1+a-\rho) + h[C^2\beta k + S^2\beta h \right. \\ & \left. + S\beta B[1-C\beta]] \right\} j\omega - [B(1+a-\rho) + C\beta h(C\beta B + S\beta h)] \omega^2, \end{aligned}$$

$$\begin{aligned} \frac{\Delta\psi}{I^2\Omega_0^4 T_{dz}} (j\omega) = & \left[(k-h)(4-4\rho+C\beta h + S^2\beta h) + C^2\beta h^2 \right] + [-S\beta C\beta h(k-h) + hB(C\beta + S^2\beta) \\ & + 4B(1-\rho)] j\omega - [-a(k-h) + S\beta h(-C\beta B - S\beta h)] \omega^2 + [Ba] j\omega^3, \end{aligned}$$

$$\begin{aligned} \frac{\Delta\gamma}{I^2\Omega_0^4 T_{dx}} (j\omega) = & \left[C\beta h(a-\rho+h) - S^2\beta h^2 \right] + [-S\beta h] j\omega - [C\beta h(a-\rho+h) - S^2\beta h^2] \omega^2 \\ & + [S\beta h] j\omega^3, \end{aligned}$$

and

$$\begin{aligned} \frac{\Delta\gamma}{I^2\Omega_0^4 T_{dz}} (j\omega) = & \left[4S\beta h(\rho-1) - S\beta h^2(1+C\beta) \right] + [C\beta h(-a-3\rho+3)] j\omega \\ & - [S\beta h(\rho-1) - S\beta h^2(1+C\beta)] \omega^2 + [C\beta ha] j\omega^3. \end{aligned}$$

If the determinant Δ is evaluated,

$$\begin{aligned} \frac{\Delta}{I^3 \Omega_0^6} (j\omega) = & [(k-h)(-\alpha+\rho-h)(4\rho-4-h) - h^2 C^2 \beta(-\alpha+\rho-h) - h^2 S^2 \beta(4\rho-4-h)] \\ & + [B(-\alpha+\rho-h)(4\rho-4-h)] j\omega \\ & - [(k-h)a_3 + h^2 C^2 \beta(2\alpha+2\rho-3-h) + h^2 S^2 \beta(-\rho+h+2)] \omega^2 \\ & - Ba_3 j\omega^3 + [\alpha(k-h) + h^2(\alpha C^2 \beta + S^2 \beta)] \omega^4 + aBj\omega^5, \end{aligned}$$

where

$$a_3 = \alpha(-\rho+2+h) + \rho^2 + 2(1-h)\rho - 3 + h + h^2.$$

6.3 Factor-of-Merit Function

Unfortunately, it is not possible to arrive at a unique factor-of-merit function by which one could accurately measure overall system performance. However, a reasonable choice for such a function can be made on the basis of the special characteristics of this class of problem. This section defines a function chosen on the basis of the discussion in the first section of this chapter.

$$\begin{aligned} R = & C_\phi \left\{ \overline{\phi^2(\text{const})} + \overline{\phi^2(\Omega_0)} + \dots + \overline{\phi^2(n\Omega_0)} \right\} \\ & + C_\psi \left\{ \overline{\psi^2(\text{const})} + \overline{\psi^2(\Omega_0)} + \dots + \overline{\psi^2(n\Omega_0)} \right\} \\ & + C_\gamma \left\{ \overline{\gamma^2(\text{const})} + \overline{\gamma^2(\Omega_0)} + \dots + \overline{\gamma^2(n\Omega_0)} \right\} \end{aligned} \quad (6.2)$$

where $\overline{\phi^2(\text{const})}$ is the mean square of the roll angle resulting from constant (i.e., not time-varying) components of the disturbance torques and the other mean square quantities are defined in an analogous manner. C_ϕ , C_ψ , and C_γ are weighting factors assigned to each of the three components of R .

In addition to the consideration of the mean square steady-state response function R , for transient response to be factored into this performance criterion, one can require that the real exponential associated with the dominant system resonance have a time constant less than some preassigned maximum T_m . Define $T = 1/\sigma$ where σ is the real part of the complex root in question.

The formulation of this factor-of-merit function affords a potential user the tools by which he might choose a best set of system parameters for a particular problem, given the physically realizable range of these parameters along with some knowledge of spacecraft configuration, system damping requirements, and certain orbit parameters.

Although the optimization of the R function as well as the factorization of the characteristic polynomial are far too complex to be handled analytically, this type of problem is well suited for programmed digital computation. Given an array of possible system parameters and certain orbital information, the user can choose the best set of parameters suited to his particular needs by allowing the computer to search all combinations of parameter sets. Restricting the search to only those cases that meet the constraint placed upon the overall system transient response, the computer will single out that set associated with the minimum value of R .

It is shown in the development that follows that for the spacecraft alone, one with no driven solar panels, the only orbit parameter with which the user must be concerned is the orbit plane inclination. This quantity remains essentially fixed throughout the life of a spacecraft.

In general, the spacecraft magnetic moment has no preferred orientation. This orientation is difficult and expensive to establish before launch and, furthermore, is often affected by the launch operation itself. For this class of spacecraft, it was possible to maximize the response function R analytically as a function of the physical orientation of the residual spacecraft magnetic moment in terms of the system parameters. The maximization of R assures the user that he has accounted for the orientation that would give rise to the worst-case mean square steady-state response. If the actual location of the magnetic moment is different from the worst-case location, the actual response to disturbances will be less than that predicted by the digital computer program.

A spacecraft with driven solar panels requires the definition of certain additional quantities. For these spacecraft, the user must define certain information concerning his proposed orbital parameters according to the needs of his particular problem. Specifically, he must concern himself with the time of year of launch, the projected spacecraft lifetime, and the angle between the ascending node and the vernal equinox at various intervals throughout the spacecraft projected lifetime.

Here, the complexity of the steady-state response function R precludes maximizing it analytically for the worst-case orientation of the spacecraft magnetic moment; however, this maximization has been accomplished by incorporating a search routine within the structure of the optimization program. Furthermore, if the user is unable to arrive at meaningful values for the required orbital parameters, those other than orbital inclination, or if the projected lifetime and/or the precession rate of the orbit were such that it would be desirable to maximize R as a function of these parameters as well, an alternate search routine has been incorporated into the program to eliminate the requirement of defining these parameters. These parameters will be discussed in detail in Appendix C.

Finally, the user is free to assign the values to T_m , the settling time constraint, and the weighting factors C_ϕ , C_ψ , and C_γ that would be commensurate with his particular mission. For example, the weighting factors might be selected to emphasize the importance of a roll error while downgrading the importance of yaw and gimbal angles if the spacecraft mission were to point a sensor or a spacecraft-mounted communications parabolic antenna toward the spacecraft subsatellite point. On the other hand, if the mission were to relay radio signals to a second satellite in the same earth orbit by means of a parabolic dish antenna, the user might wish to downgrade the importance of roll and gimbal angles while emphasizing that of the yaw angle.

A detailed derivation of the residual magnetic disturbance torque model and the associated derivation of the sun angle, solar panel reference angle, umbra half angle, and umbra-associated Fourier coefficients are presented in Appendix C. In addition, a numerical example will be presented in Chapter 8 for the purpose of clarification.

6.4 Formulation of the Weighted Performance Function

The response function R was defined by Equation (6.2).

$$\begin{aligned} R \equiv & C_\phi \left\{ \overline{\phi^2(\text{const})} + \overline{\phi^2(\Omega_0)} + \dots + \overline{\phi^2(n\Omega_0)} \right\} \\ & + C_\psi \left\{ \overline{\psi^2(\text{const})} + \overline{\psi^2(\Omega_0)} + \dots + \overline{\psi^2(n\Omega_0)} \right\} \\ & + C_\gamma \left\{ \overline{\gamma^2(\text{const})} + \overline{\gamma^2(\Omega_0)} + \dots + \overline{\gamma^2(n\Omega_0)} \right\} \end{aligned}$$

where $\overline{\phi^2(\text{const})}$ is the mean square roll angle resulting from the composite constant components of the disturbance torques, and the other mean square factors are analogously defined. C_ϕ , C_ψ , and C_γ are weighting factors assigned to each of the three components of R .

The six required transfer functions were defined by Equation (6.1) as

$$\begin{aligned} R_{1\omega_1} &\equiv \left| \frac{\phi}{T_{dx}}(j\omega) \right|_{\omega=\omega_1} & R_{2\omega_1} &\equiv \left| \frac{\phi}{T_{dz}}(j\omega) \right|_{\omega=\omega_1} \\ R_{3\omega_1} &\equiv \left| \frac{\psi}{T_{dx}}(j\omega) \right|_{\omega=\omega_1} & R_{4\omega_1} &\equiv \left| \frac{\psi}{T_{dz}}(j\omega) \right|_{\omega=\omega_1} \\ R_{5\omega_1} &\equiv \left| \frac{\gamma}{T_{dx}}(j\omega) \right|_{\omega=\omega_1} & \text{and } R_{6\omega_1} &\equiv \left| \frac{\gamma}{T_{dz}}(j\omega) \right|_{\omega=\omega_1} \end{aligned}$$

But the equations have been normalized to orbit rate so that for $\omega = \Omega_0$, $\omega_1 = 1$; for $\omega = 2\Omega_0$, $\omega_1 = 2$; and so on.

For the class of spacecraft without driven solar panels, it is shown in Appendix C, Equation (C.1) that

$$T_{dx} = \frac{m_e}{r_0^3} \left[(m_{z0} C \sigma) + (2m_{y0} S \sigma) S \Omega_0 t \right]$$

and

$$T_{dz} = \frac{m_e}{r_0^3} \left[(-m_{x0} C \sigma) + (-m_{y0} S \sigma) C \Omega_0 t \right],$$

where m_{x0} , m_{y0} , and m_{z0} are the components of the spacecraft magnetic moment vector.

Substituting T_d [Equations (C.1)] and the transfer functions [Equations (6.1)] into R results in the following expression:

$$\begin{aligned} R = \frac{m_e^2}{r_0^6} \left\{ C^2 \sigma \left[m_{z0}^2 (C_\phi R_{10}^2 + C_\psi R_{30}^2 + C_\gamma R_{50}^2) + m_{x0}^2 (C_\phi R_{20}^2 + C_\psi R_{40}^2 + C_\gamma R_{60}^2) \right. \right. \\ \left. \left. - 2m_{x0} m_{z0} (C_\phi R_{10} R_{20} + C_\psi R_{30} R_{40} + C_\gamma R_{50} R_{60}) \right] + \frac{S^2 \sigma m_{y0}^2}{2} \left[4(C_\phi R_{11}^2 + C_\psi R_{31}^2 + C_\gamma R_{51}^2) \right. \right. \\ \left. \left. + (C_\phi R_{21}^2 + C_\psi R_{41}^2 + C_\gamma R_{61}^2) \right] \right\} \end{aligned}$$

It can be demonstrated that the mean square error function $R = C_0^2/4 + 1/2 \sum_{n=1}^{\infty} C_n^2$

where

$$C_n = \sqrt{a_n^2 + b_n^2},$$

$$C_0 = \alpha_0/2,$$

$\alpha_0/2$ = amplitude of constant component,

a_n = amplitude of cosine component of n th harmonic,

and

b_n = amplitude of sine component of n th harmonic.

To maximize out the orientation of the spacecraft magnetic moment as discussed earlier, it was found convenient to define the spacecraft magnetic moment \mathbf{m}_0 in terms of the spherical coordinates shown in Figure 6.1, where $m_{x0} = m_0 S \xi C \tau$, $m_{y0} = m_0 S \xi S \tau$, $m_{z0} = m_0 C \xi$, and $m_0 = |\mathbf{m}_0|$.

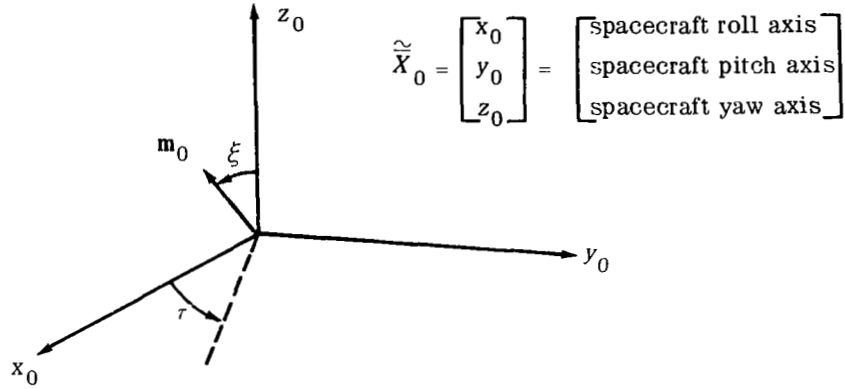


Figure 6.1—Spacecraft magnetic moment in spherical coordinates.

For ease of manipulation, it was convenient to rewrite the response equation as

$$R = \frac{m_c^2}{r_0^6} (m_{z0}^2 A + m_{x0}^2 B + m_{x0} m_{z0} C + m_{y0}^2 D)$$

where

$$A = C^2 \sigma (C_\phi R_{10}^2 + C_\psi R_{30}^2 + C_\gamma R_{50}^2),$$

$$B = C^2 \sigma (C_\phi R_{20}^2 + C_\psi R_{40}^2 + C_\gamma R_{60}^2),$$

$$C = -2C^2 \sigma (C_\phi R_{10} R_{20} + C_\psi R_{30} R_{40} + C_\gamma R_{50} R_{60}),$$

and

$$D = \frac{S^2 \sigma}{2} [4(C_\phi R_{11}^2 + C_\psi R_{31}^2 + C_\gamma R_{51}^2) + (C_\phi R_{21}^2 + C_\psi R_{41}^2 + C_\gamma R_{61}^2)].$$

If substitutions are made for m_{x0} , m_{y0} , and m_{z0} in the expanded expression for R , R is differentiated with respect to ξ and τ , and the resulting expressions are set equal to zero, then

$$\frac{\partial R}{2m_0^2 \partial \xi} = C\xi S\xi [-A + BC^2\tau + DS^2\tau] + C\tau [C^2\xi - S^2\xi] \frac{C}{2} = 0$$

$$\frac{\partial R}{2m_0^2 \partial \tau} = S\xi S\tau \left[C\tau S\xi (D - B) - C\xi \frac{C}{2} \right] = 0.$$

Three possible maxima result from these expressions:

$$(1) \quad \xi = 90^\circ, \tau = 90^\circ$$

$$R = \left(\frac{m_e^2}{r_0^6} \right) m_0^2 D$$

$$(2) \quad \xi = 0^\circ, \tau = 90^\circ$$

$$R = \left(\frac{m_e^2}{r_0^6} \right) m_0^2 A$$

$$(3) \quad \text{Let } \tau = 0^\circ,$$

$$(-A + B)C\xi S\xi + [C^2\xi - S^2\xi] \frac{C}{2} = 0,$$

$$(-A + B) \frac{1}{2} S^2\xi + \frac{C}{2} C^2\xi = 0,$$

$$\tan 2\xi = \frac{C}{A - B}$$

$$R = R \text{ evaluated at } \xi = \frac{1}{2} \tan^{-1} \left(\frac{C}{A - B} \right) \text{ and } \tau = 0^\circ$$

$$(4) \quad \text{Let } C\tau = \frac{1}{2} \frac{C}{D - B} \left(\frac{C\xi}{S\xi} \right)$$

$$C\xi S\xi \left[-A + B \frac{C^2}{4(D - B)^2} \frac{C^2\xi}{S^2\xi} + D - D \frac{C^2}{4(D - B)^2} \frac{C^2\xi}{S^2\xi} \right] + \frac{C^2}{4(D - B)} \frac{C\xi}{S\xi} [C^2\xi - S^2\xi] = 0$$

$$C\xi \left[D - A - \frac{C^2/4}{(D - B)} \right] S^2\xi = 0$$

The only valid solution for Case 4 is the solution already covered by Case 1.

For a given set of parameters that define A , B , C , and D , the resulting R 's must be checked to establish which of the three has the maximum value. In this manner, the user need not concern himself with the location of the spacecraft magnetic dipole. Furthermore, he must only estimate its magnitude if he is interested in relating his normalized response values to actual steady angular errors.

Having maximized out the location of the spacecraft magnetic dipole, the user need only put into the optimization computer program the array of possible system parameters, the proposed orbit inclination angle, the weighting factor values for each of the three components of the steady-state response function R , and the value chosen for T_m , the maximum system settling time. The computer program then selects the best set of parameters commensurate with the factor of merit discussed earlier.

Of course, if a preferred orientation of spacecraft magnetic moment happens to exist for a particular problem, the potential user can override this maximization routine by actually defining ξ and τ .

For spacecraft with driven solar panels, the procedure of choosing a best set of parameters makes use of superposition. The magnetic disturbance torques due to the spacecraft alone must be summed with those due to the incidence of solar energy on the rotating solar panels before the mean square error function R can be formed. The solar panel associated torques are expressed as Fourier series.

For practical systems with which the potential user would be concerned, the six response functions fall off rapidly above $\omega_1 = 2$. With this in mind, the only Fourier expansion terms that are considered to be important are those at $\omega_1 = 0$ (const), $\omega_1 = 1$ (Ω_0), and $\omega_1 = 2$ ($2\Omega_0$).

The total steady-state response function for this more complex problem can be formed as shown in the following development.

Let

$$A_0 = \frac{m_e}{r_0^3} (m_0 C \xi C \sigma),$$

$$A_1 = \frac{m_e}{r_0^3} (2m_0 S \xi S \tau S \sigma),$$

$$B_0 = \frac{m_e}{r_0^3} (-m_0 S \xi C \tau C \sigma),$$

and

$$B_1 = \frac{m_e}{r_0^3} (-m_0 S \xi S \tau S \sigma),$$

where

$$m_{x_0} = S\xi C\tau m_0,$$

$$m_{y_0} = S\xi S\tau m_0,$$

and

$$m_{z_0} = C\xi m_0.$$

Let

$$T_{dx} = A_0 + A_1 S\Omega_0 t + T_{fxp}$$

and

$$T_{dz} = B_0 + B_1 C\Omega_0 t + T_{fzp}$$

where

$$T_{dx} = \text{total } x \text{ component of magnetic torque,}$$

$$T_{dz} = \text{total } z \text{ component of magnetic torque,}$$

and T_{fxp} and T_{fzp} represent Fourier expansions and are defined by Equations (C.12) and (C.13) in Appendix C.

Then,

$$\begin{aligned} R = & C_\phi \left[\overline{\phi^2(\text{const})} + \overline{\phi^2(\Omega_0)} + \overline{\phi^2(2\Omega_0)} \right] + C_\psi \left[\overline{\psi^2(\text{const})} + \overline{\psi^2(\Omega_0)} + \overline{\psi^2(2\Omega_0)} \right] \\ & + C_\gamma \left[\overline{\gamma^2(\text{const})} + \overline{\gamma^2(\Omega_0)} + \overline{\gamma^2(2\Omega_0)} \right] \end{aligned}$$

where

$$\overline{\phi^2(\text{const})} = \left[\left(A_0 + \frac{a_{0x}}{2} \right) R_{10} + \left(B_0 + \frac{a_{0z}}{2} \right) R_{20} \right]^2,$$

$$\overline{\psi^2(\text{const})} = \left[\left(A_0 + \frac{a_{0x}}{2} \right) R_{30} + \left(B_0 + \frac{a_{0z}}{2} \right) R_{40} \right]^2,$$

$$\overline{\gamma^2(\text{const})} = \left[\left(A_0 + \frac{a_{0x}}{2} \right) R_{50} + \left(B_0 + \frac{a_{0z}}{2} \right) R_{60} \right]^2,$$

$$\overline{\phi^2(\Omega_0)} = \frac{1}{2} \left\{ \left[\left(A_1 + b_{1x} \right) R_{11} + b_{1z} R_{21} \right]^2 + \left[\left(B_1 + a_{1z} \right) R_{21} + a_{1x} R_{11} \right]^2 \right\},$$

$$\overline{\psi^2(\Omega_0)} = \frac{1}{2} \left\{ \left[\left(A_1 + b_{1x} \right) R_{31} + b_{1z} R_{41} \right]^2 + \left[\left(B_1 + a_{1z} \right) R_{41} + a_{1x} R_{31} \right]^2 \right\},$$

$$\begin{aligned}
\overline{\gamma^2(\Omega_0)} &= \frac{1}{2} \left\{ \left[(A_1 + b_{1x}) R_{51} + b_{1z} R_{61} \right]^2 + \left[(B_1 + a_{1z}) R_{61} + a_{1x} R_{51} \right]^2 \right\}, \\
\overline{\phi^2(2\Omega_0)} &= \frac{1}{2} \left[(b_{2x} R_{1z} + b_{2z} R_{22})^2 + (a_{2x} R_{12} + a_{2z} R_{22})^2 \right], \\
\overline{\psi^2(2\Omega_0)} &= \frac{1}{2} \left[(b_{2x} R_{32} + b_{2z} R_{42})^2 + (a_{2x} R_{32} + a_{2z} R_{42})^2 \right], \\
\overline{\gamma^2(2\Omega_0)} &= \frac{1}{2} \left[(b_{2x} R_{52} + b_{2z} R_{62})^2 + (a_{2x} R_{52} + a_{2z} R_{62})^2 \right].
\end{aligned}$$

The terms α_{ij} and b_{lj} , for $i = 0, 1, 2$; $l = 1, 2$; and $j = x, z$, are defined in Equation (C.11).

The complexity of the resulting equation makes it impractical to maximize out the location of the spacecraft residual magnetic moment analytically for this more general class of spacecraft.

In addition to being dependent upon ξ and τ , the angles associated with the orientation of the spacecraft magnetic moment, the expression for R is dependent upon λ and ϵ , two of the orbital parameters defined in Appendix C and shown in Figures C.1 and C.2. The angle ϵ defines the position of the sun within the ecliptic plane, and λ defines the angle between the ascending node and the vernal equinox.

These angles might be established as a result of given mission requirements in which case the user would simply put them into the optimization program along with the array of possible system parameters, the proposed orbit plane angle of inclination, the weighting factors for each of the three components of R , and the value chosen for T_m . A search routine was incorporated into the program that establishes the worst-case orientation of the spacecraft moment, and both ξ and τ were eliminated from the R equation.

Although it is conceivable that both ϵ and λ would be defined by mission requirements and the projected time of launch, these quantities, except under very special circumstances, vary with time. The angle ϵ increases at the rate of $1^\circ/\text{day}$, so that unless the proposed lifetime of the spacecraft is very short, ϵ must not be considered constant. In addition, except for purely polar or purely equatorial orbits, the orbit plane will precess at some finite rate and λ will increase or decrease accordingly. For these reasons, an alternate search routine has been incorporated into the optimization program. This routine maximizes R as a function of ξ , τ , ϵ , and λ simultaneously. In this manner it is possible for

the user to consider the worst-case set of conditions that might result throughout the entire lifetime of the spacecraft. Any of these angles can be removed from this four-dimensional search routine by simply defining it equal to some constant value.

Admittedly, the four-dimensional search routine is somewhat time consuming even on a large digital computer, but this is understandable when the complexity of the problem is considered. If the user wishes to make use of the full maximization search routine, it is necessary that the number of parameter sets to be surveyed be limited to a few thousand so computer run time can be kept below 30 minutes. On the other hand, hundreds of thousands of parameter sets can be examined in an equivalent computer run time if the four-dimensional search can be deleted entirely. If a spacecraft without driven solar panels were to be considered, such would be the case.

If the user felt too restricted because of the time limitations imposed by the four-dimensional search, the problem could be broken into two parts. A coarse parameter array could first be considered, and then a fine search about the initial optimum chosen could be performed.

As in the case of the spacecraft alone, the result of the optimization computer survey is the best set of system parameters commensurate with the factor of merit defined in Section (6.3). The set of parameters that minimizes R does so for the worst-case orientation of the spacecraft moment as well as simultaneously for the worst-case combination of ϵ and λ at the option of the user.

6.5 Digital Computer Optimization Program

The program listing appears in Appendix D and was written to accept an array of input parameters and to survey and choose the best set.

These parameters include the normalized roll inertia α , the normalized pitch inertia ρ (note that normalization is with respect to yaw inertia), the angle of gimbal axis with respect to spacecraft roll axis β , the pitch-momentum bias H_b , the gimbal damping B_g , the gimbal spring constant k_g , the weighting factor for mean square roll error C_ϕ , the weighting factor for mean square yaw error C_ψ , the weighting factor for mean square gimbal error C_γ , and the maximum allowable settling time T_m .

The program begins by making use of the stability criterion established in Chapter 4. Any parameter set that would cause an instability in a linear sense is detected and eliminated in this manner. Next, the program eliminates the spherical coordinates ξ and τ associated with the orientation of the spacecraft magnetic moment, analytically for the spacecraft alone and by means of a numerical search for the spacecraft with driven solar panels. In the more complex case, the spacecraft with driven solar

panels, the additional orbit-associated angular parameters ϵ and λ may be eliminated at the user's option by means of an alternate numerical search routine. The maximization routines associated with any of the angles ξ , τ , ϵ , or λ can be bypassed simply by defining the angle in question.

Each of six transfer functions are evaluated at the frequencies of interest. The response is properly weighted by applying the appropriate input torques to each transfer function at each frequency considered, and the R function is formed.

The characteristic polynomial is formed and factored, and the dominant complex pair is singled out by the computer. The real part of this complex root is examined and compared to $1/T_m$. Cases whose real part is less than $1/T_m$ are discarded; those with real parts greater than $1/T_m$ are stored at this point for further consideration.

For the optimum chosen, the normal printout associated with this program includes the parameter set itself, R , the real part of the dominant complex pair, the damped natural frequency of the system, the components of the mean square error from which R was composed, and the worst-case angles ξ , τ , ϵ , and λ when appropriate.

If the number of parameter sets is not prohibitively large, all or some of these quantities may be printed out for each of the parameter sets considered. In this manner tradeoffs between the convenience of achieving a particular parameter set and the poorer performance obtained for a closely associated parameter set that is more easily available might be made. Alternately, a parameter set that corresponds to a more heavily damped system at the expense of a slightly larger weighted mean square error might be chosen.

CHAPTER 7

SOLAR PANELS AND ASSOCIATED SPACECRAFT STABILITY

7.1 General Discussion

It has been pointed out in earlier discussions that the actively controlled pitch loop affords the spacecraft the ability to accomodate pitch axis momentum disturbances. The most severe of these disturbances would probably be the result of a driven solar panel assembly.

The consideration of driven solar panels with regard to the residual magnetic disturbance torques, however, brought to light an area that had been ignored until now. If the treatment of the driven solar panel assembly is to be complete, the effect on vehicle stability of the variation in spacecraft inertia caused by the rotation of this assembly at orbit rate must be considered.

If the performance of the total system is to be acceptable, these periodic variations must have a negligible effect upon the system. This chapter, however, deals only with the effect upon system stability of the time variation of inertias. The method of analysis is identical to that in Chapter 5, and for this reason, the discussion will be kept brief.

7.2 Equations of Motion With Inertia Variation

For the purpose of this discussion, it is assumed that the spacecraft is under perfect control and that the solar panel assembly rotates at exactly orbit rate.

The panel assembly coordinates and the coordinate transformation matrix from panel assembly to spacecraft coordinates are defined in Appendix C.

From Equation (C.2),

$$A_{p0} = \begin{bmatrix} C\theta_p C\mu & -C\theta_p S\mu & S\theta_p \\ S\mu & C\mu & 0 \\ -S\theta_p C\mu & S\theta_p S\mu & C\theta_p \end{bmatrix},$$

where A_{p0} is the transformation matrix from solar panel assembly coordinates to spacecraft coordinates. The angles θ_p and μ are defined in Appendix C.

Φ_{p0} is defined as the inertia tensor of the solar panel assembly in spacecraft coordinates.

$$\Phi_{p0} = A_{p0} \Phi_p A_{p0}^T,$$

where Φ_p is the panel assembly inertia tensor in panel assembly coordinates, and A_{p0}^T is the transpose of the coordinate transformation matrix A_{p0} .

The computation of the solar panel assembly inertia tensor in panel assembly coordinates is summarized in the following calculations. Let $\frac{1}{2}I_{xp}$ be the inertia of each panel about the panel face normal through the panel center of gravity; $\frac{1}{2}I_{yp}$, the inertia of each panel about the panel shaft axis through the panel center of gravity; $\frac{1}{2}I_{zp}$, the inertia of each panel about the axis parallel to the panel hinge line through the panel center of gravity; $\frac{1}{2}m$, the mass of each panel; a , the distance from spacecraft center of gravity to either hinge line; and b , the distance from each hinge line to each panel center of gravity. Figure C.3a shows a and b .

Assume that each solar panel is flat so that $I_{xp} = I_{yp} + I_{zp}$ and that only the panels themselves have mass.

The inertia tensor for each panel referenced to its own center of gravity may be written as

$$\Phi_{pcg} = \begin{bmatrix} \frac{1}{2}I_{xp} & 0 & 0 \\ 0 & \frac{1}{2}I_{yp} & 0 \\ 0 & 0 & \frac{1}{2}I_{zp} \end{bmatrix}. \quad (7.1)$$

When the tensor associated with each panel is translated to the spacecraft center of gravity and the resulting two tensors are summed, the resulting inertia tensor can be written in panel assembly coordinates.

$$\Phi_p = \begin{bmatrix} \{ I_{xp} + m(b + a C\mu)^2 \} & \{ -m(b + a C\mu)(a S\mu) \} & \{ 0 \} \\ \{ -m(b + a C\mu)(a S\mu) \} & \{ I_{xp} + m(a S\mu)^2 \} & \{ 0 \} \\ \{ 0 \} & \{ 0 \} & \{ I_{zp} + m[(a + b C\mu)^2 + (b S\mu)^2] \} \end{bmatrix} \quad (7.2)$$

This tensor was next transformed to spacecraft coordinates, and the result is expressed in the notation

$$\Phi_{p0} = \begin{bmatrix} I_{p0} (11) & I_{p0} (12) & I_{p0} (13) \\ I_{p0} (21) & I_{p0} (22) & I_{p0} (23) \\ I_{p0} (31) & I_{p0} (32) & I_{p0} (33) \end{bmatrix}, \quad (7.3)$$

where

$$\begin{aligned} I_{p0} (11) &= [I_{yp} - I_{zp} S^2 \mu - m (b S \mu)^2] C^2 \theta_p + m [(a + b C \mu)^2 + (b S \mu)^2] + I_{zp}, \\ I_{p0} (12) &= [I_{zp} S \mu C \mu + m (a + b C \mu) (b S \mu)] C \theta_p, \\ I_{p0} (13) &= [I_{yp} - I_{zp} S^2 \mu - m (b S \mu)^2] S \theta_p C \theta_p, \\ I_{p0} (21) &= I_{p0} (12), \\ I_{p0} (22) &= I_{yp} + I_{zp} S^2 \mu + m (b S \mu)^2, \\ I_{p0} (23) &= -[I_{zp} S \mu C \mu + m (a + b C \mu) (b S \mu)] S \theta_p, \\ I_{p0} (31) &= I_{p0} (13), \\ I_{p0} (32) &= I_{p0} (23), \end{aligned} \quad (7.4)$$

and

$$I_{p0} (33) = [I_{yp} - I_{zp} S^2 \mu - m (b S \mu)^2] S^2 \theta_p + m [(a + b C \mu)^2 + (b S \mu)^2] + I_{zp},$$

where

$$\theta_p = \theta_{p0} + \Omega_0 t,$$

$$S^2 \theta_p = [1 - C (2\theta_p)] / 2,$$

$$C^2 \theta_p = [1 + C (2\theta_p)] / 2,$$

and

$$C \theta_p S \theta_p = S (2\theta_p) / 2.$$

The system equations of motion were developed in Chapter 2, and the gimbal, roll, and yaw equations are restated here.

$$\dot{H}_{2x} + \omega_{2y} H_{2z} - \omega_{2z} H_{2y} = T_{21x} + T_{22x} + T_{23x}$$

$$\begin{aligned}\dot{H}_{1x} + \omega_{1y} H_{1z} - \omega_{1z} H_{1y} &= T_{11x} + T_{12x} + T_{13x} + \left\{ A_{12} \begin{bmatrix} 0 \\ -T_{24y} \\ -T_{24z} \end{bmatrix} \right\} \text{ x component} \\ \dot{H}_{1z} + \omega_{1x} H_{1y} - \omega_{1y} H_{1x} &= T_{11z} + T_{12z} + T_{13z} + \left\{ A_{12} \begin{bmatrix} 0 \\ -T_{24y} \\ -T_{24z} \end{bmatrix} \right\} \text{ z component}\end{aligned}$$

The gimbal equation is unaltered by the solar panel assembly inertia terms; however, the terms in the body 1 x and z axes equations are modified to

$$\begin{aligned}\dot{H}_{1x} &= [I_1 + I_{p0} (11)] \dot{\omega}_{1x} + [I_{p0} (12)] \dot{\omega}_{1y} + [I_{p0} (13)] \dot{\omega}_{1z} \\ &\quad + \dot{I}_{p0} (11) \omega_{1x} + \dot{I}_{p0} (12) \omega_{1y} + \dot{I}_{p0} (13) \omega_{1z}, \\ \dot{H}_{1z} &= [I_{p0} (31)] \dot{\omega}_{1x} + [I_{p0} (32)] \dot{\omega}_{1y} + [I_{p0} (33) + I_3] \dot{\omega}_{1z} \\ &\quad + \dot{I}_{p0} (31) \omega_{1x} + \dot{I}_{p0} (32) \omega_{1y} + \dot{I}_{p0} (33) \omega_{1z},\end{aligned}$$

$$H_{1x} = [I_1 + I_{p0} (11)] \omega_{1x} + I_{p0} (12) \omega_{1y} + I_{p0} (13) \omega_{1z},$$

$$H_{1y} = I_{p0} (21) \omega_{1x} + [I_2 + I_{p0} (22)] \omega_{1y} + I_{p0} (23) \omega_{1z},$$

and

$$H_{1z} = I_{p0} (31) \omega_{1x} + I_{p0} (32) \omega_{1y} + [I_3 + I_{p0} (33)] \omega_{1z}.$$

The right-hand torque terms must also be altered to include the solar panel inertia components.

The resulting equation set is

$$\begin{aligned}T_{2x}: & -H_b S\beta \dot{\phi} - C\beta H_b \dot{\psi} + B_g \dot{\gamma} - C\beta \Omega_0 H_b \phi + H_b S\beta \Omega_0 \psi + (k_g - H_b \Omega_0) \gamma = 0 \\ T_{1x}: & I_{p0} (12) \ddot{\theta} - (I_1') \ddot{\phi} + I_{p0} (13) \ddot{\psi} + [-2\Omega_0 I_{p0} (32)] \dot{\theta} \\ & + (\Omega_0 I_{p0} (13) - \Omega_0 I_{p0} (31) - S\beta C\beta H_b) \dot{\phi} + (\Omega_0 I_1' + \Omega_0 I_3' - \Omega_0 I_2' + S^2\beta H_b) \dot{\psi} \\ & + (C\beta B_g - S\beta H_b) \dot{\gamma} + (-3\Omega_0^2 I_{p0} (12)) \theta + (4\Omega_0^2 (I_3' - I_2') + S^2\beta \Omega_0 H_b) \phi \\ & + (\Omega_0^2 I_{p0} (31) + \Omega_0 S\beta C\beta H_b) \psi + (C\beta k_g - S\beta \dot{H}_b) \gamma \\ & + \dot{I}_{p0} (11) [\dot{\phi} - \Omega_0 \psi] + \dot{I}_{p0} (12) [\dot{\theta} - \Omega_0] + \dot{I}_{p0} (13) [\dot{\psi} + \Omega_0 \phi] = -[3\Omega_0^2 I_{p0} (23) \\ & + I_{p0} (32) \Omega_0^2]\end{aligned}$$

T_{1z} :

$$\begin{aligned}
& I_{p0}(32)\ddot{\theta} + I_{p0}(31)\ddot{\phi} + (-I_3')\ddot{\psi} + [2\Omega_0 I_{p0}(12)]\dot{\theta} \\
& + (-\Omega_0(I_3' + I_1' - I_2') - C^2\beta H_b)\dot{\phi} \\
& + (\Omega_0 I_{p0}(13) + S\beta C\beta H_b - \Omega_0 I_{p0}(31))\dot{\psi} + (-S\beta B_g - C\beta H_b)\dot{\gamma} \\
& + [3\Omega_0^2 I_{p0}(23)]\dot{\theta} + [4\Omega_0^2 I_{p0}(13) + S\beta C\beta H_b \Omega_0]\dot{\phi} \\
& + (\Omega_0 C^2\beta H_b - \Omega_0^2(I_2' - I_1'))\dot{\psi} - (C\beta \dot{H}_b + k_g S\beta)\gamma \\
& + \dot{I}_{p0}(31)[\dot{\phi} - \Omega_0\psi] + \dot{I}_{p0}(32)[\dot{\theta} - \Omega_0] \\
& + \dot{I}_{p0}(33)[\dot{\psi} + \Omega_0\phi] = I_{p0}(12)\Omega_0^2
\end{aligned}$$

where

$$I_1' = I_1 + I_{p0}(11)$$

$$I_2' = I_2 + I_{p0}(22)$$

$$I_3' = I_3 + I_{p0}(33)$$

The practical usefulness of this system requires that the active pitch loop be tightly controlled so that it may accurately be assumed that $\ddot{\theta} = \dot{\theta} = \theta = 0$ in the roll and yaw equations. This assumption allows the T_{2x} , T_{1x} , and T_{1z} equations to remain decoupled from the T_{1y} , T_{3y} , and the error equations. After substitution,

T_{2x} :

$$-H_b S\beta \dot{\phi} - C\beta H_b \dot{\psi} + B_g \dot{\gamma} - C\beta \Omega_0 H_b \phi + H_b S\beta \Omega_0 \psi + (k_g - H_b \Omega_0)\gamma = 0 \quad (7.5)$$

T_{1x} :

$$\begin{aligned}
& -I_1'\ddot{\phi} + I_{p0}(13)\ddot{\psi} + \left\{ \Omega_0 [I_{p0}(13) - I_{p0}(31)] - S\beta C\beta H_b + \dot{I}_{p0}(11) \right\} \dot{\phi} \\
& + [\Omega_0(I_1' + I_3' - I_2') + S^2\beta H_b + \dot{I}_{p0}(13)]\dot{\psi} \\
& + (C\beta B_g - S\beta H_b)\dot{\gamma} + [4\Omega_0^2(I_3' - I_2') + S^2\beta \Omega_0 H_b + \Omega_0 \dot{I}_{p0}(13)]\dot{\phi} \\
& + [\Omega_0^2 I_{p0}(31) + \Omega_0 S\beta C\beta H_b - \Omega_0 \dot{I}_{p0}(11)]\dot{\psi} + (-S\beta \dot{H}_b + C\beta k_g)\gamma = \\
& - [3\Omega_0^2 I_{p0}(23) + I_{p0}(32)\Omega_0^2 - \Omega_0 \dot{I}_{p0}(12)]
\end{aligned} \quad (7.6)$$

T_{1z} :

$$\begin{aligned}
& I_{p0}(31)\ddot{\phi} - I_3'\ddot{\psi} + \left[-\Omega_0(I_3' + I_1' - I_2') - C^2\beta H_b + i_{p0}(31) \right] \dot{\phi} \\
& + \left\{ \Omega_0 \left[I_{p0}(13) - I_{p0}(31) \right] + S\beta C\beta H_b + i_{p0}(33) \right\} \dot{\psi} \\
& + (-S\beta B_g - C\beta H_b)\dot{\gamma} + \left[4\Omega_0^2 I_{p0}(13) + S\beta C\beta H_b \Omega_0 + \Omega_0 i_{p0}(33) \right] \phi \\
& + \left[\Omega_0 C^2\beta H_b - \Omega_0^2(I_2' - I_1') - \Omega_0 i_{p0}(31) \right] \psi \\
& - (C\beta H_b + k_g S\beta)\gamma = \Omega_0 \left[I_{p0}(12)\Omega_0 + i_{p0}(32) \right]
\end{aligned} \tag{7.7}$$

The resulting set of coupled linear equations with periodic coefficients is nonhomogeneous. However, as with any set of linear equations, superposition applies and the equation set can be made homogeneous for the purpose of investigating system stability. The details associated with applying the Floquet criterion to this set of equations follow exactly as presented in Chapter 5.

7.3 Floquet Problem

The algebraic manipulation of Equations (7.5), (7.6), and (7.7) that results in the system state matrix A , where $\dot{\mathbf{X}} = A\mathbf{X}$, is detailed in Appendix E. The elements of this state matrix are

$$\begin{aligned}
a(11) &= 0, \\
a(12) &= 1, \\
a(13) &= 0, \\
a(14) &= 0, \\
a(15) &= 0, \\
a(21) &= C_k \left[I_3' d + I_{p0}(13) q + \frac{s}{B_g} C\beta \Omega_0 H_b \right], \\
a(22) &= C_k \left[I_3' a + I_{p0}(13) g + \frac{s}{B_g} S\beta H_b \right], \\
a(23) &= C_k \left[I_3' C\beta k_g - I_{p0}(13) k_g S\beta - \frac{s}{B_g} i \right], \\
a(24) &= C_k \left[I_3' b + I_{p0}(13) h + \frac{s}{B_g} C\beta H_b \right], \\
a(25) &= C_k \left[I_3' e + I_{p0}(13) r - \frac{s}{B_g} H_b S\beta \Omega_0 \right],
\end{aligned}$$

$$a(31) = \frac{1}{B_g} (C\beta\Omega_0 H_b) ,$$

$$a(32) = \frac{1}{B_g} (H_b S\beta) ,$$

$$a(33) = \frac{1}{B_g} (-f) ,$$

$$a(34) = \frac{1}{B_g} (C\beta H_b) ,$$

$$a(35) = \frac{1}{B_g} (-H_b S\beta\Omega_0) ,$$

$$a(41) = C_k \left[I_{p0}(13)d + I_1' q + \frac{t}{B_g} C\beta\Omega_0 H_b \right] ,$$

$$a(42) = C_k \left[I_{p0}(13)a + I_1' g + \frac{t}{B_g} H_b S\beta \right] ,$$

$$a(43) = C_k \left[I_{p0}(13)C\beta k_g - I_1' k_g S\beta - \frac{t}{B_g} f \right] ,$$

$$a(44) = C_k \left[I_{p0}(13)b + I_1' h + \frac{t}{B_g} C\beta H_b \right] ,$$

$$a(45) = C_k \left[I_{p0}(13)e + I_1' r - \frac{t}{B_g} H_b S\beta\Omega_0 \right] ,$$

$$a(51) = 0 ,$$

$$a(52) = 0 ,$$

$$a(53) = 0 ,$$

$$a(54) = 1 ,$$

and

$$a(55) = 0 ,$$

where

$$a = -S\beta C\beta H_b + i_{p0}(11) ,$$

$$b = \Omega_0(I_1' + I_3' - I_2') + S^2\beta H_b + i_{p0}(13) ,$$

$$c = C\beta B_g - S\beta H_b ,$$

$$d = 4\Omega_0^2(I_3' - I_2') + S^2\beta\Omega_0 H_b + \Omega_0 i_{p0}(13) ,$$

$$\begin{aligned}
e &= \Omega_0^2 I_{p0}(13) + \Omega_0 S\beta C\beta H_b - \Omega_0 \dot{I}_p(11) , \\
f &= k_g - H_b \Omega_0 , \\
g &= -\Omega_0(I_1' + I_3' - I_2') - C^2\beta H_b + \dot{I}_{p0}(13) , \\
h &= S\beta C\beta H_b + \dot{I}_{p0}(33) , \\
p &= -S\beta B_g - C\beta H_b , \\
q &= 4\Omega_0^2 I_{p0}(13) + S\beta C\beta H_b \Omega_0 + \Omega_0 \dot{I}_{p0}(33) , \\
r &= \Omega_0 C^2\beta H_b - \Omega_0^2(I_2' - I_1') - \Omega_0 \dot{I}_{p0}(13) , \\
s &= I_3' c + I_{p0}(13)p , \\
t &= I_1' p + I_{p0}(13)c ,
\end{aligned}$$

and

$$C_k = \frac{-1}{I_{p0}^2(13) - I_3' I_1'}$$

The system state vector is defined as

$$\mathbf{X} = \begin{bmatrix} x_1 = \phi \\ x_2 = \dot{\phi} \\ x_3 = \gamma \\ x_4 = \dot{\psi} \\ x_5 = \psi \end{bmatrix}$$

Each of the terms that make up the elements of the A matrix is constant with the exception of the elements of Φ_{p0} and those of $\dot{\Phi}_{p0}$. The approximations used for the purpose of computing the associated state transition matrix are listed below.

$$\begin{aligned}
S^2\theta_p &= \{1 - \text{sgn}[C(2\theta_p)]\}/2 \\
C^2\theta_p &= \{1 + \text{sgn}[C(2\theta_p)]\}/2 \\
S\theta_p C\theta_p &= \text{sgn}[S(2\theta_p)]/2 \\
S\dot{\theta}_p &= \text{sgn}[S(2\theta_p)] \Omega_0
\end{aligned}$$

$$C \dot{\theta}_p = - \operatorname{sgn} [S(2\theta_p)] \Omega_0$$

$$S \theta_p \dot{C} \theta_p = \operatorname{sgn} [C(2\theta_p)] \Omega_0$$

At this point, it is possible to substitute the elements of this piecewise constant A matrix into the computer program listed in Appendix B. A potential user thus could solve for the set of state transition matrix eigenvalues associated with any parameter set he might choose, or he could do an entire Floquet study exactly as was performed in Chapter 5. Since no new technology would be gained by detailing this problem as was done in the case of the variational pitch-momentum bias, this particular program will be used only to verify those results obtained from the optimization program discussed in Chapter 6. That is, the Floquet criterion will be applied to the equation set that includes the time-varying inertias to verify for a given set or sets of system parameters, whether or not system stability is appreciably impaired by the inclusion of variational inertia terms associated with a particular problem and a particular solar panel configuration.

CHAPTER 8

VALIDATION OF THE USE OF A LINEARIZED TIME-INVARIANT EQUATION SET

8.1 General Discussion

The complete equation set that mathematically models the gimbaled-reaction-wheel-scanner spacecraft is very nonlinear. Moreover, the equation set is complicated by the inclusion of large variational momentum bias terms that may result from a pitch axis disturbance torque and the inclusion of the time-dependent inertia terms that would result if a driven solar panel were part of the spacecraft configuration. Lyapunov methods are sometimes used to study the stability of both nonlinear and time-varying systems. However, it is highly unlikely that these methods would yield any useful information if they were applied to a system as complex as the one under study. Clearly, to establish generalized stability thresholds and/or to find a meaningful performance or factor-of-merit criterion, it was necessary to work with a linearized time-invariant equation set. Accordingly, a user must justify the use of this fabricated equation set by validating the results obtained.

The knowledge of stability thresholds alone is of limited usefulness, even when these thresholds are known in general. More important is the ability to choose, from an array of available parameters, those parameter sets that not only cause a particular spacecraft configuration to be stable but also allow the spacecraft to meet certain mission requirements in a favorable manner. For this reason, in the final analysis, the number of parameter sets that a user must numerically validate will be limited. Accordingly, he should not find the given numerical methods too restrictive.

The optimization routine of Chapter 6 singles out parameter sets in their normalized form. At this point, the user must scale his problem by assigning numerical values to the spacecraft and solar panel magnetic moments. The particular values must be chosen to make the roll, yaw, and gimbal components of rms error an acceptable level.

8.2 Method of Validation

When a linearized set of equations is used to determine general thresholds of system stability, validating the results is a two-sided problem.

Certainly the linearized time-invariant equation set will adequately describe the system within some limited neighborhood of \mathbf{X}_0 , the system equilibrium state. When trying to determine whether the neighborhood is sufficiently large to be of practical interest, the general analytic stability problem must be reduced to one that can be handled by numerical methods. A useful method of validation was comparing the output of two digital computer simulations by means of overlay. One simulation contained the linearized equation set; the other, the nonlinear equation set. By choosing initial condition sets arbitrarily large in magnitude, the size of the neighborhood within which the linearized equation set is valid could be approximated. Certainly, this neighborhood must be well in excess of the rms error components associated with the particular parameter set under investigation if the equation set is to be at all valid.

Alternately, the other part of the problem concerns itself with what happens once we cross into the so-called unstable region. Suppose, for example, that the small angle mathematical instability manifests itself in a very small amplitude limit cycle about \mathbf{X}_0 . Moreover, suppose that aside from this limit cycle, the system is well damped and well behaved. Although this parameter set would have been ruled out by the linearized stability study, it might have produced a perfectly acceptable system.

However, because of the method of presentation discussed in Chapter 4, it was possible not only to establish the small angle stability thresholds, but also to determine the type of instability encountered once a threshold was crossed. The type of instability in all but one particular case was found to be a loss in null reference, which would clearly be unacceptable. The particular case excluded above occurs when $\rho = 1$ within an otherwise stable region. The type of instability here would be an undamped oscillation; however, the condition described results from the absence of roll axis gravity-gradient restoring torque. This case is also unacceptable because the instability would be manifested in an uncontrolled coning of the roll-yaw plane about the pitch axis.

Accordingly, it is only necessary to consider the stability of those parameter sets that lie within the linearly predicted stable regions.

Once it has been shown that the system is accurately described by the linearized equation set within the neighborhood of interest, it follows that the response and performance information derived from these equations are valid as well. The validity of neglecting the time-varying coefficients must be considered next.

Because both system stability and harmonic response are directly related to the set of system eigenvalues, the desired validation would be accomplished if it can be shown that the effect of the time-varying terms upon these eigenvalues is small.

The most complex situation is spacecraft with driven solar panels. As a result of the performance study detailed in Chapter 6 and the scaling procedure discussed in the introduction of this chapter, all the necessary information is available to completely define the system, its magnetic disturbance parameters, and its associated orbital parameters. If this information, along with information describing the solar panel assembly, is put into the computer program discussed in Chapter 7, the Floquet characteristic factors result. From these, one can find the associated system characteristic exponents for the time-varying inertia problem, and the exponents may be directly compared with the unperturbed system eigenvalues. If the two sets of system roots compare favorably, it can be assumed that the validity of the results was not impaired by neglecting the time-varying solar panel inertia components.

The validity of neglecting the variational component of the pitch-momentum bias term should be the next consideration. The main body pitch equation is

$$I_y \ddot{\theta} - \dot{H}_b + 3\Omega_0^2(I_z - I_x) \theta = T_{dy}.$$

It is assumed that the pitch axis is under perfect control for the worst-case variational amplitude to be considered.

$\dot{H}_b = T_{dy}$ = pitch component of magnetic disturbance due to both the spacecraft alone and the solar panel assembly.

Substituting the required information into the computer program described in Chapter 5 results in the Floquet characteristic factors associated with this problem. As in the previous case, the system characteristic exponents are evaluated and compared with the eigenvalues of the unperturbed system.

If each of the three proposed comparisons produce favorable results, validation has been completed. However, if the neighborhood within which the linearized equation set was found to be valid was not sufficiently large, or if either set of the Floquet-derived system eigenvalues showed an appreciable change from those of the unperturbed system, further consideration is necessary. For example, the user might require that the chosen system or systems be more tightly damped by redoing the search with a smaller value of T_m . If a favorable validation is still not possible, altering the solar panel

assembly configuration or raising the nominal value of H_b might be tried when either of the respective Floquet validations appears to be the problem area.

If these remedies fail, the user probably must resort to a computer simulation of the full set of nonlinear equations, a clearly undesirable situation.

Two numerical examples are presented to clarify the discussion of this section as well as topics discussed throughout the text of this dissertation.

8.3 Numerical Examples

The design requirement for a spacecraft without driven solar panels is to choose a set of system parameters for a gimballed-reaction-wheel-scanner attitude-control system that would minimize the steady-state spacecraft response to the worst-case magnetic disturbance torques that might act upon the vehicle. Transient settling time* must be constrained to six orbits or less, and the parameters must be chosen from values currently available using present technology. A tabulation of parameters to be considered appears in Table 8.1. It is assumed that the residual spacecraft magnetic moment is 3.96×10^3 pole-cm. This corresponds to 2.5×10^3 pole-cm on each of the three spacecraft axes. The mission requires an orbit plane inclination angle of 30° .

The parameter array of Table 8.1 is inserted into the computer program listed in Appendix D. The total number of combinations of parameter sets considered is: $(3_{I_z})(6_\Delta)(3_{\text{ratio}})(5_\beta)(12_{H_b})(5_{k_g})(3_{B_g}) = 48600$. The output quantities chosen to be printed for each value of $(I_y - I_z)$ considered were the parameter set itself, the square root of the weighted mean square error function R , the real and imaginary parts of the least damped system root normalized by $\Omega_0 = 10^{-3}$ rad/sec, the rms roll, yaw, and gimbal attitude errors, and the worst-case spherical coordinate angles of the spacecraft magnetic moment. These results are tabulated in Table 8.2, and the computer-chosen optimum is marked. The computer time required on an IBM 360-91 was 124 seconds.

The optimum parameter set was inserted into both linear and nonlinear computer simulations, and initial conditions were chosen well in excess of the computer-found steady-state rms errors. The resulting time responses are shown in Figure 8.1. Computation time for each simulation was 75 seconds. Listings of these programs appear in Appendices F and G, respectively.

*Transient settling time is $T_s = 1/(2\pi\sigma)$ (Reference 11), where σ is the real part of the least damped root and T_s is in orbits when σ is normalized by $\Omega_0 = 10^{-3}$ rad/sec.

Table 8.1—Parameter array for use in optimization program.*

I_z (slug-ft ²)	$I_y - I_z$ (slug-ft ²)	Ratio of I_x/I_y	β , gimbal axis angle, (degrees)	H_b , pitch momentum bias (ft-lb-sec)	k_g , gimbal spring constant (ft-lb/rad)	B_g , gimbal damping constant (ft-lb-sec/rad)
$I_z(1) = 10$	$\Delta(1) = 50$	Ratio (1) = 0.75	$\beta(1) = 0$	$H_b(1) = -10.$	$k_g(1) = 10^{-4}$	$B_g(1) = 0.25$
$I_z(2) = 100$	$\Delta(2) = 100$	Ratio (2) = 1.0	$\beta(2) = 22.5$	$H_b(2) = -5.$	$k_g(2) = .33 \times 10^{-3}$	$B_g(2) = .5$
$I_z(3) = 200$	$\Delta(3) = 250$	Ratio (3) = 1.33	$\beta(3) = 45.$	$H_b(3) = -2.5$	$k_g(3) = 10^{-3}$	$B_g(3) = .75$
	$\Delta(4) = 500$		$\beta(4) = 67.5$	$H_b(4) = -1.$	$k_g(4) = .33 \times 10^{-2}$	
	$\Delta(5) = 1000$		$\beta(5) = 90.$	$H_b(5) = -.5$	$k_g(5) = 10^{-2}$	
	$\Delta(6) = 2000$			$H_b(6) = -.1$		
				$H_b(7) = +.1$		
				$H_b(8) = +.5$		
				$H_b(9) = +1.$		
				$H_b(10) = +2.5$		
				$H_b(11) = +5.$		
				$H_b(12) = +10.$		

* $I_y - I_z = \Delta(m_1)$, $I_x/I_y = \text{ratio}(m_2)$, $\beta = \beta(m_3)$, $H_b = H_b(m_4)$, $B_g = B_g(m_5)$, $k_g = k_g(m_6)$, and $I_z = I_z(m_7)$.

Table 8.2—Results of optimization for Example 1.*

m_1	m_2	m_3	m_4	m_5	m_6	m_7	\sqrt{R}	$\dagger(\sigma \pm j \omega_{n1})/\Omega_0$	$\sqrt{\phi^2}$ (deg)	$\sqrt{\psi^2}$ (deg)	$\sqrt{\gamma^2}$ (deg)	ξ (deg)	τ (deg)
1	1	2	5	1	1	1	3.726	$-0.031 \pm j 1.10$	12.98	16.43	4.16	-70	0
2	1	2	4	3	1	2	1.841	$-.027 \pm j 1.11$	6.78	7.91	1.59	90	90
3	1	2	3	3	2	1	.8071	$-.038 \pm j 1.09$	2.55	3.63	1.32	90	90
4	1	2	3	3	3	1	.4786	$-.038 \pm j 1.14$	1.33	2.25	.810	90	90
5	1	2	2	3	3	1	.3095	$-.036 \pm j 1.10$.679	1.45	.75	-84	0
[‡] 6	1	1	3	3	4	1	.1738	$-.034 \pm j 1.36$.424	.865	.251	90	90

*Refer to Table 8.1 for actual parameter values.

[†] $\sigma = -0.0265$ ~ settling time of six orbits.

[‡]Optimum for entire row.

Finally, the parameter set, the orbit plane inclination angle, the magnitude of the spacecraft magnetic moment and its associated worst-case spherical coordinate angles were inserted into the varia-

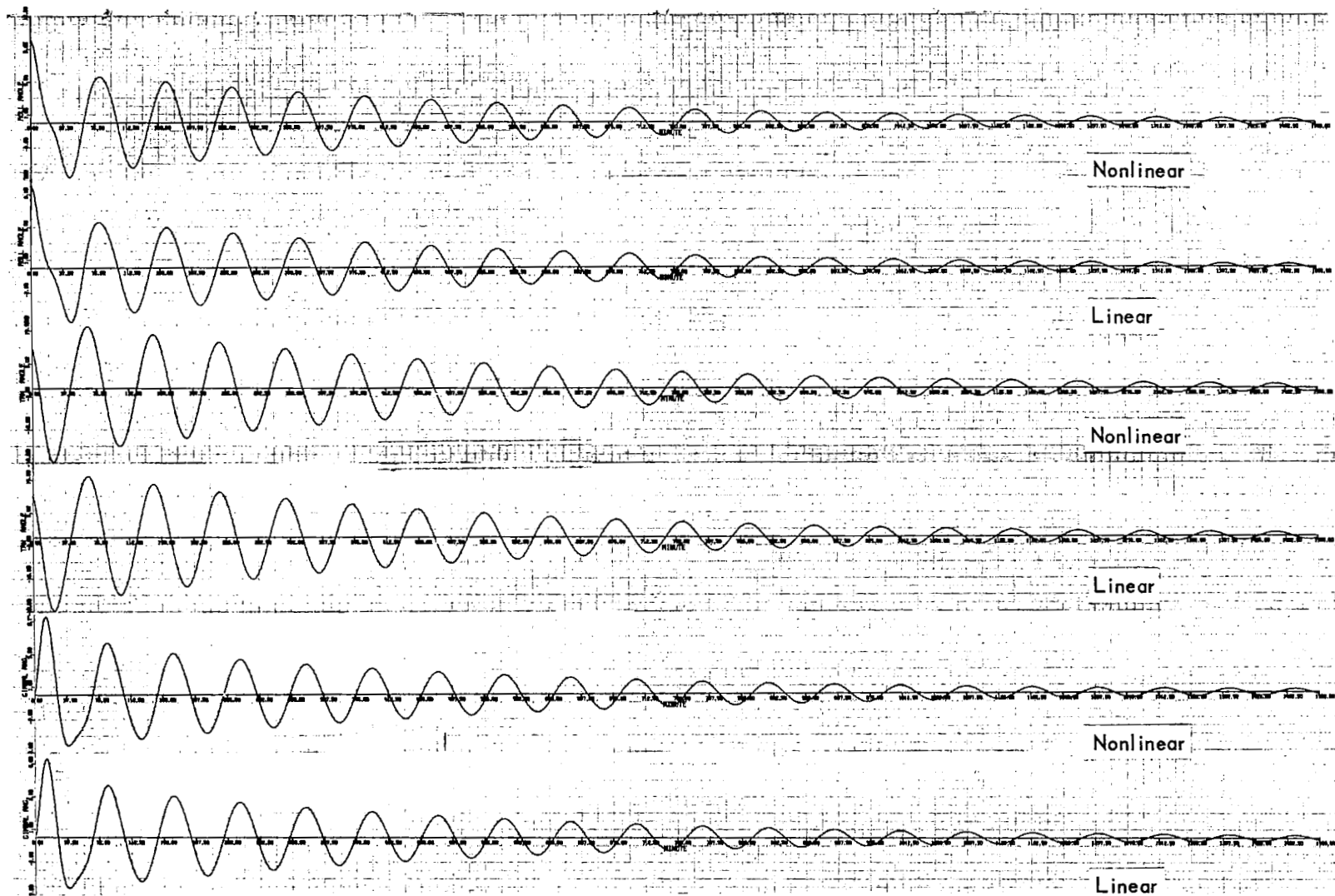


Figure 8.1—Time responses for optimum spacecraft for Example 1. $I.C. = \phi = \psi = 10^\circ$, and all other system states are initially zero. Angles are in degrees.

tional momentum bias Floquet program listed in Appendix B. The Floquet eigenvalues for the unperturbed and the perturbed system can be compared in Table 8.3. Computation time was 5 seconds.

Table 8.3—Results of variational momentum bias Floquet study Example 1.*

Magnetic moments (10^3 pole-cm)	Floquet eigenvalues λ_i	Magnitude of eigenvalues $ \lambda_i $	$\ln \lambda_i /\tau\Omega_0$
$ \mathbf{m}_0 = 0.$	$-0.5128 \pm j .62388$	0.8076063	-0.034008329
$m_{xp} = 0.$	$.0441 \pm j .00445$.044384198	$-.49574734$
	
$ \mathbf{m}_0 = 3.96$	$-.5128 \pm j .6238$.80760601	$-.034008387$
$m_{xp} = 0.$	$.0441 \pm j .00445$.044383999	$-.49574806$
	

* $m_1 = 6$, $m_2 = 1$, $m_3 = 1$, $m_4 = 3$, $m_5 = 3$, $m_6 = 4$, and $m_7 = 1$.

The mission requirement for a spacecraft with two driven solar panels is that each panel have an area of approximately 50 ft^2 . For this second case, a parameter set must be chosen that minimizes the steady-state spacecraft response to the worst-case magnetic disturbance torques that might act upon the vehicle because of the residual spacecraft moment and the magnetic moment due to the current paths on the faces of the solar panels. Transient settling time must be less than six orbits. The set of possible parameters is the set shown in Table 8.1 except $I_z(1)$, $I_z(2)$, $\Delta(1)$, $\Delta(3)$, $\Delta(5)$, $\beta(2)$, $\beta(4)$, $k_g(2)$, and $k_g(4)$. Also, the expression $\alpha = (I_x/I_y)\rho$ was replaced by the relationship $\alpha = (\rho + 125/I_z)$ to account for the pitch-roll inertia differential resulting from the large solar panels chosen. It was assumed for this example that $I_x = I_y$ in the absence of the solar panels. ($\alpha = I_x/I_z$, and $\rho = I_y/I_z$.) The chosen residual spacecraft magnetic moment is 3.96×10^3 pole-cm, and the magnetic moment due to each solar panel is 2.5×10^3 pole-cm. The mission requires an orbit inclination angle of 30° , and neither the location of the sun in the ecliptic plane nor the location of the ascending node with respect to the vernal equinox is known.

The abbreviated parameter array is inserted into the optimization program, and the number of parameter sets considered is $(1_{I_z})(3_\Delta)(3_\beta)(12_{H_b})(3_{k_g})(3_{B_g}) = 972$.

The output quantities printed were the same as in the first example considered, with the addition of the worst-case sun location angle and angle between the ascending node and the vernal equinox. The results of this computer run are tabulated in Table 8.4. Computation time was 18 minutes.

Table 8.4—Results of optimization for Example 2.*

m_1	m_2	m_3	m_4	m_5	m_6	\sqrt{R} (radians)	$(\sigma \pm j \omega_{ni})/\Omega_0$	$\sqrt{\phi^2}$ (deg)	$\sqrt{\psi^2}$ (deg)	$\sqrt{\gamma^2}$ (deg)	ξ (deg)	τ (deg)	ϵ (deg)	λ (deg)
2	1	1	2	1	1	5.45	$0.0354 \pm j 1.03$	22.3	20.6	7.4	270	270	270	270
4	1	1	1	3	1	1.44	$.0395 \pm j 1.01$	4.35	6.07	3.5	270	270	240	240
† 6	1	1	1	3	3	.875	$.0288 \pm j 1.03$	1.07	3.99	2.8	270	270	240	210

* $m_7 = 3$, refer to Table 8.1 for definition of m_i 's, $i = 1 \dots 7$.

† $\sigma = -0.0265$ - settling time of six orbits.

‡Optimum for entire row.

The resulting time responses associated with the optimum parameter set are shown in Figure 8.2.

Next, the parameter set and the required solar panel configuration information was inserted into the variational inertia Floquet program listed in Appendix B. The sun angle μ was spanned from 0° to 90° to consider the effect of the worst-case hinge angle. The program was run assuming each of the panels to be flat plates of dimensions 10 ft \times 5 ft, 7 ft \times 7 ft, or 5 ft \times 10 ft. The Floquet eigenvalues for the perturbed and unperturbed systems are shown in Table 8.5. Computation time was 50 seconds.

For the sake of comparison, only the variational panel-associated inertia terms are considered in the Floquet program. The spacecraft inertias must be altered accordingly to account for any panel-associated constant inertia terms.

Finally, the output data of the optimization program, the magnitude of the magnetic moments of the spacecraft and solar panels, and the orbit plane inclination angle are inserted into the variational momentum bias Floquet program and the resulting eigenvalue sets are shown in Table 8.6. Computation time was 5 seconds.

Clearly, for the examples shown above, all of the comparisons were favorable.

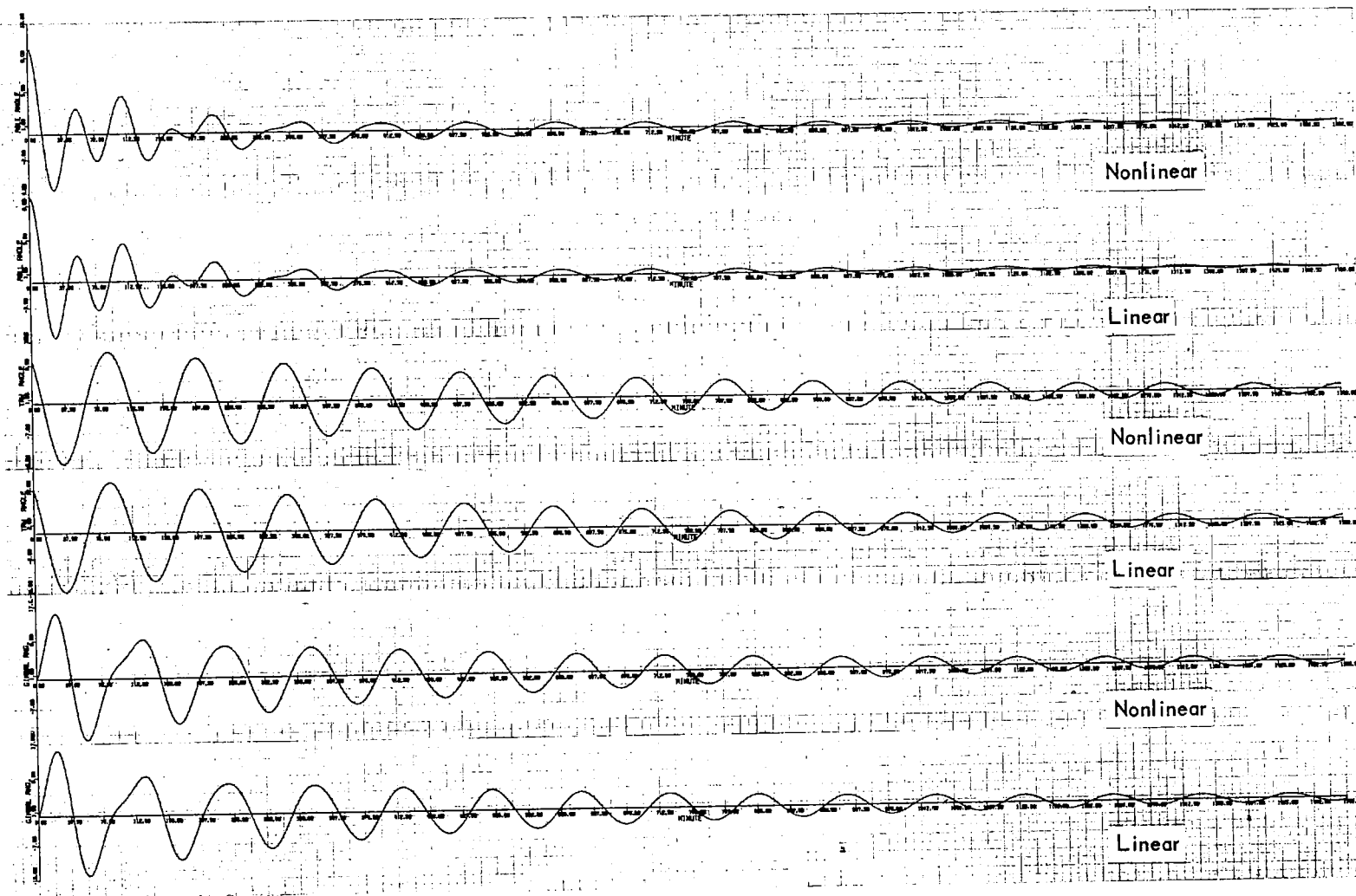
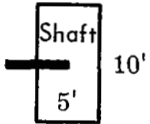
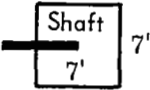
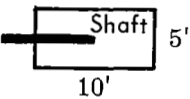


Figure 8.2—Time responses for optimum spacecraft for Example 2. I.C. = $\phi = \psi = 10^\circ$, and all other system states are initially zero. Angles are in degrees.

Table 8.5—Results of variational inertia Floquet study Example 2.*

Floquet eigenvalues λ_i	Magnitude of eigenvalues $ \lambda_i $	$\ln \lambda_i /\tau\Omega_0$	[†] Worst-case sun angle μ (deg)	Panel configuration
$-0.909 \pm j .0889$ $.6027 \pm j .0939$. . .	0.91350131 .60997733 . . .	-0.028797652 $-.15735127$. . .	—	no panels
$-.909 \pm j .0881$ $.6027 \pm j .0994$91341377 .61089151 . . .	$-.028828155$ $-.15687457$. . .	0	
$-.909 \pm j .0935$ $.601 \pm j .0610$91393573 .60454804 . . .	$-.028646314$ $-.16019717$. . .	90	
$-.909 \pm j .0982$ $.5976 \pm j .0226$91452856 .59804089 . . .	$-.028439907$ $-.16364192$. . .	90	

* $m_1 = 6$, $m_2 = 1$, $m_3 = 1$, $m_4 = 1$, $m_5 = 3$, $m_6 = 3$, and $m_7 = 3$.

[†]Largest deviation of $\ln |\lambda_i|/\tau\Omega_0$ from no-panel case.

↑ Hinge Line

Table 8.6—Results of variational momentum bias Floquet study Example 2.*

Magnetic moments (10^3 pole-cm)	Floquet eigenvalues λ_i	Magnitude of eigenvalues $ \lambda_i $	$\ln \lambda_i /\tau\Omega_0$
$ \mathbf{m}_0 = 0$ $m_{xp} = 0$	$0.8167 \pm j .16166$ $.3445 \pm j .1149$. . .	0.83448030 .37266113 . . .	-0.028798479 $-.15709961$. . .
$ \mathbf{m}_0 = 3.96$ $m_{xp} = 5.0$	$.8187 \pm j .16163$ $.3544 \pm j .1152$83450912 .37271575 . . .	$-.028792983$ $-.15707629$. . .

* $m_1 = 6$, $m_2 = 1$, $m_3 = 1$, $m_4 = 1$, $m_5 = 3$, $m_6 = 3$, and $m_7 = 3$.

ACKNOWLEDGMENT

The author wishes to express appreciation to his colleague Seymour Kant for his guidance. He is indebted to Mr. Kant for the hours of technical discussion and for the many constructive recommendations that he offered throughout the evolution of this report.

Goddard Space Flight Center
National Aeronautics and Space Administration
Greenbelt, Maryland, March 7, 1970
630-22-01-01-51

SELECTED BIBLIOGRAPHY

1. "Semi-Active Gravity Gradient System," TRW Systems, Contract NAS 5-9640, February 1966.
2. Goldstein, H., "Classical Mechanics," Reading, Mass.: Addison-Wesley Publishing Co., Inc., 1950.
3. Sabroff, A. E., "A Summary of Gravity Gradient Stabilization of Earth Satellites," TRW Systems Report 9990-6715-RU001, July 27, 1964.
4. Schultheiss, P. M., and Bower, J. L., "Introduction to the Design of Servomechanisms," New York: John Wiley & Sons, Inc., 1958.
5. Floquet, G., "Équations différentielles linéaires à coefficients périodiques," *École Normale Supérieure Annales* 12: 47-88, 1883.
6. Cesari, L., "Asymptotic Behavior and Stability Problems in Ordinary Differential Equations," Berlin: Springer-Verlag, 1959.
7. Minorsky, N., "Nonlinear Oscillations," Princeton: Van Nostrand, 1962.
8. Coddington, E., and Levinson, N., "Theory of Ordinary Differential Equations," New York: McGraw-Hill Book Company, Inc., 1947.
9. James, H. M., Nichols, N.B., and Phillips, R. S., "Theory of Servomechanisms," New York: McGraw-Hill Book Company, Inc., 1947.
10. Wheeler, P. C., "Magnetic Attitude Control of Rigid Axially Symmetric Spinning Satellites in Circular Earth Orbits," Stanford University SUDAER Report No. 224, April 1965.
11. Lewis, J. A., and Zajac, E. E., "A Two-Gyro, Gravity-Gradient Satellite Attitude Control System," *Bell Syst. Tech. J.* 43(6): 2742, November 1964.

APPENDIX A

DEVELOPMENT OF FULLY EXPANDED EXPRESSIONS

The following section includes the expansion details of the development presented in Chapter 2.

$$\bar{\omega}_2 = A_{21}\bar{\omega}_1 + \begin{bmatrix} \dot{\gamma} \\ 0 \\ 0 \end{bmatrix}$$

$$\omega_{2x} = a_{21}(11)\omega_{1x} + a_{21}(12)\omega_{1y} + a_{21}(13)\omega_{1z} + \dot{\gamma}$$

$$\omega_{2y} = a_{21}(21)\omega_{1x} + a_{21}(22)\omega_{1y} + a_{21}(23)\omega_{1z}$$

$$\omega_{2z} = a_{21}(31)\omega_{1x} + a_{21}(32)\omega_{1y} + a_{21}(33)\omega_{1z}$$

$$\bar{\omega}_3 = A_{31}\bar{\omega}_1 + A_{32} \begin{bmatrix} \dot{\gamma} \\ 0 \\ 0 \end{bmatrix} + \begin{bmatrix} 0 \\ \dot{\alpha} \\ 0 \end{bmatrix}$$

$$\omega_{3x} = a_{31}(11)\omega_{1x} + a_{31}(12)\omega_{1y} + a_{31}(13)\omega_{1z} + a_{32}(11)\dot{\gamma}$$

$$\omega_{3y} = a_{31}(21)\omega_{1x} + a_{31}(22)\omega_{1y} + a_{31}(23)\omega_{1z} + a_{32}(21)\dot{\gamma} + \dot{\alpha}$$

$$\omega_{3z} = a_{31}(31)\omega_{1x} + a_{31}(32)\omega_{1y} + a_{31}(33)\omega_{1z} + a_{32}(31)\dot{\gamma}$$

$$\bar{\dot{\omega}}_2 = \dot{A}_{21}\bar{\omega}_1 + A_{21}\bar{\dot{\omega}}_1 + \begin{bmatrix} \ddot{\gamma} \\ 0 \\ 0 \end{bmatrix}$$

$$\dot{\omega}_{2x} = \dot{a}_{21}(11)\omega_{1x} + \dot{a}_{21}(12)\omega_{1y} + \dot{a}_{21}(13)\omega_{1z} + a_{21}(11)\dot{\omega}_{1x} + a_{21}(12)\dot{\omega}_{1y} + a_{21}(13)\dot{\omega}_{1z} + \ddot{\gamma}$$

$$\dot{\omega}_{2y} = \dot{a}_{21}(21)\omega_{1x} + \dot{a}_{21}(22)\omega_{1y} + \dot{a}_{21}(23)\omega_{1z} + a_{21}(21)\dot{\omega}_{1x} + a_{21}(22)\dot{\omega}_{1y} + a_{21}(23)\dot{\omega}_{1z}$$

$$\dot{\omega}_{2z} = \dot{a}_{21}(31)\omega_{1x} + \dot{a}_{21}(32)\omega_{1y} + \dot{a}_{21}(33)\omega_{1z} + a_{21}(31)\dot{\omega}_{1x} + a_{21}(32)\dot{\omega}_{1y} + a_{21}(33)\dot{\omega}_{1z}$$

$$\bar{\omega}_3 = \dot{A}_{31}\bar{\omega}_1 + A_{31}\bar{\omega}_1 + \dot{A}_{32}\begin{bmatrix} \dot{\gamma} \\ 0 \\ 0 \end{bmatrix} + A_{32}\begin{bmatrix} \ddot{\gamma} \\ 0 \\ 0 \end{bmatrix} + \begin{bmatrix} 0 \\ \ddot{a} \\ 0 \end{bmatrix}$$

$$\begin{aligned} \dot{\omega}_{3x} = & \dot{a}_{31}(11)\omega_{1x} + \dot{a}_{31}(12)\omega_{1y} + \dot{a}_{31}(13)\omega_{1z} + a_{31}(11)\dot{\omega}_{1x} + a_{31}(12)\dot{\omega}_{1y} + a_{31}(13)\dot{\omega}_{1z} \\ & + \dot{a}_{32}(11)\dot{\gamma} + a_{32}(11)\ddot{\gamma} \end{aligned}$$

$$\begin{aligned} \dot{\omega}_{3y} = & \dot{a}_{31}(21)\omega_{1x} + \dot{a}_{31}(22)\omega_{1y} + \dot{a}_{31}(23)\omega_{1z} + a_{31}(21)\dot{\omega}_{1x} + a_{31}(22)\dot{\omega}_{1y} + a_{31}(23)\dot{\omega}_{1z} \\ & + \dot{a}_{32}(21)\dot{\gamma} + a_{32}(21)\ddot{\gamma} + \ddot{a} \end{aligned}$$

$$\begin{aligned} \dot{\omega}_{3z} = & \dot{a}_{31}(31)\omega_{1x} + \dot{a}_{31}(32)\omega_{1y} + \dot{a}_{31}(33)\omega_{1z} + a_{31}(31)\dot{\omega}_{1x} + a_{31}(32)\dot{\omega}_{1y} + a_{31}(33)\dot{\omega}_{1z} \\ & + \dot{a}_{32}(31)\dot{\gamma} + a_{32}(31)\ddot{\gamma} \end{aligned}$$

$$\mathbf{H}_1 = \Phi_1 \bar{\omega}_1$$

$$H_{1x} = I_1(11)\omega_{1x} - I_1(12)\omega_{1y} - I_1(13)\omega_{1z}$$

$$H_{1y} = -I_1(21)\omega_{1x} + I_1(22)\omega_{1y} - I_1(23)\omega_{1z}$$

$$H_{1z} = -I_1(31)\omega_{1x} - I_1(32)\omega_{1y} + I_1(33)\omega_{1z}$$

$$\dot{\mathbf{H}}_1 = \Phi_1 \bar{\dot{\omega}}_1$$

$$\dot{H}_{1x} = I_1(11)\dot{\omega}_{1x} - I_1(12)\dot{\omega}_{1y} - I_1(13)\dot{\omega}_{1z}$$

$$\dot{H}_{1y} = -I_1(21)\dot{\omega}_{1x} + I_1(22)\dot{\omega}_{1y} - I_1(23)\dot{\omega}_{1z}$$

$$\dot{H}_{1z} = -I_1(31)\dot{\omega}_{1x} - I_1(32)\dot{\omega}_{1y} + I_1(33)\dot{\omega}_{1z}$$

$$\mathbf{H}_2 = A_{23}\mathbf{H}_3 + \Phi_2\bar{\omega}_2$$

$$H_{2x} = a_{23}(11)H_{3x} + a_{23}(12)H_{3y} + a_{23}(13)H_{3z} + I_2(11)[a_{21}(11)\omega_{1x} + a_{21}(12)\omega_{1y} + a_{21}(13)\omega_{1z} + \dot{\gamma}]$$

$$H_{2y} = a_{23}(21)H_{3x} + a_{23}(22)H_{3y} + a_{23}(23)H_{3z} + I_2(22)[a_{21}(21)\omega_{1x} + a_{21}(22)\omega_{1y} + a_{21}(23)\omega_{1z}]$$

$$H_{2z} = a_{23}(31)H_{3x} + a_{23}(32)H_{3y} + a_{23}(33)H_{3z} + I_2(33)[a_{21}(31)\omega_{1x} + a_{21}(32)\omega_{1y} + a_{21}(33)\omega_{1z}]$$

$$\dot{\mathbf{H}}_2 = \dot{A}_{23}\mathbf{H}_3 + A_{23}\dot{\mathbf{H}}_3 + \Phi_2\bar{\dot{\omega}}_2$$

$$\begin{aligned} \dot{H}_{2x} = & \dot{a}_{23}(11)H_{3x} + \dot{a}_{23}(12)H_{3y} + \dot{a}_{23}(13)H_{3z} + a_{23}(11)\dot{H}_{3x} + a_{23}(12)\dot{H}_{3y} + a_{23}(13)\dot{H}_{3z} \\ & + I_2(11)[\dot{a}_{21}(11)\omega_{1x} + \dot{a}_{21}(12)\omega_{1y} + \dot{a}_{21}(13)\omega_{1z} + \ddot{\gamma} + a_{21}(11)\dot{\omega}_{1x} + a_{21}(12)\dot{\omega}_{1y} + a_{21}(13)\dot{\omega}_{1z}] \end{aligned}$$

$$\begin{aligned} \dot{H}_{2y} = & \dot{a}_{23}(21)H_{3x} + \dot{a}_{23}(22)H_{3y} + \dot{a}_{23}(23)H_{3z} + a_{23}(21)\dot{H}_{3x} + a_{23}(22)\dot{H}_{3y} + a_{23}(23)\dot{H}_{3z} \\ & + I_2(22)[\dot{a}_{21}(21)\omega_{1x} + \dot{a}_{21}(22)\omega_{1y} + \dot{a}_{21}(23)\omega_{1z} + a_{21}(21)\dot{\omega}_{1x} + a_{21}(22)\dot{\omega}_{1y} + a_{21}(23)\dot{\omega}_{1z}] \end{aligned}$$

$$\begin{aligned} \dot{H}_{2z} = & \dot{a}_{23}(31)H_{3x} + \dot{a}_{23}(32)H_{3y} + \dot{a}_{23}(33)H_{3z} + a_{23}(31)\dot{H}_{3x} + a_{23}(32)\dot{H}_{3y} + a_{23}(33)\dot{H}_{3z} \\ & + I_2(33)[\dot{a}_{21}(31)\omega_{1x} + \dot{a}_{21}(32)\omega_{1y} + \dot{a}_{21}(33)\omega_{1z} + a_{21}(31)\dot{\omega}_{1x} + a_{21}(32)\dot{\omega}_{1y} + a_{21}(33)\dot{\omega}_{1z}] \end{aligned}$$

$$\mathbf{H}_3 = \Phi_3\bar{\omega}_3$$

$$H_{3x} = I_3(11)[a_{32}(11)\dot{\gamma} + a_{31}(11)\omega_{1x} + a_{31}(12)\omega_{1y} + a_{31}(13)\omega_{1z}]$$

$$H_{3y} = I_3(22)[\dot{\alpha} + a_{32}(21)\dot{\gamma} + a_{31}(21)\omega_{1x} + a_{31}(22)\omega_{1y} + a_{31}(23)\omega_{1z}]$$

$$H_{3z} = I_3(33)[a_{32}(31)\dot{\gamma} + a_{31}(31)\omega_{1x} + a_{31}(32)\omega_{1y} + a_{31}(33)\omega_{1z}]$$

$$\dot{\mathbf{H}}_3 = \Phi_3\bar{\dot{\omega}}_3$$

$$\begin{aligned} \dot{H}_{3x} = & I_3(11)[\dot{a}_{32}(11)\dot{\gamma} + a_{32}(11)\ddot{\gamma} + \dot{a}_{31}(11)\omega_{1x} + \dot{a}_{31}(12)\omega_{1y} + \dot{a}_{31}(13)\omega_{1z} \\ & + a_{31}(11)\dot{\omega}_{1x} + a_{31}(12)\dot{\omega}_{1y} + a_{31}(13)\dot{\omega}_{1z}] \end{aligned}$$

$$\begin{aligned}\dot{H}_{3y} = I_3(22) & \left[\ddot{\alpha} + \dot{a}_{32}(21)\dot{\gamma} + a_{32}(21)\ddot{\gamma} + \dot{a}_{31}(21)\omega_{1x} + \dot{a}_{31}(22)\omega_{1y} + \dot{a}_{31}(23)\omega_{1z} \right. \\ & \left. + a_{31}(21)\dot{\omega}_{1x} + a_{31}(22)\dot{\omega}_{1y} + a_{31}(23)\dot{\omega}_{1z} \right]\end{aligned}$$

$$\begin{aligned}\dot{H}_{3z} = I_3(33) & \left[\dot{a}_{32}(31)\dot{\gamma} + a_{32}(31)\ddot{\gamma} + \dot{a}_{31}(31)\omega_{1x} + \dot{a}_{31}(32)\omega_{1y} + \dot{a}_{31}(33)\omega_{1z} \right. \\ & \left. + a_{31}(31)\dot{\omega}_{1x} + a_{31}(32)\dot{\omega}_{1y} + a_{31}(33)\dot{\omega}_{1z} \right]\end{aligned}$$

The left-hand side of Equations (2.4) is treated in the following development. To simplify the notation used throughout this development, let

$$\omega_{1x} = \omega_{11}$$

$$\omega_{1y} = \omega_{12}$$

$$\omega_{1z} = \omega_{13}$$

$$\Sigma \equiv \sum_{i=1}^3$$

$$T_{3y} = \dot{H}_{3y} + \omega_{3z}H_{3x} - \omega_{3x}H_{3z}$$

$$\begin{aligned}T_{3y} = I_3(22) & \left[\Sigma \dot{a}_{31}(2i)\omega_{1i} + \Sigma a_{31}(2i)\dot{\omega}_{1i} + \dot{a}_{32}(21)\dot{\gamma} + a_{32}(21)\ddot{\gamma} + \ddot{\alpha} \right] \\ & + \cancel{0 \left[I_3(11) - I_3(33) \right] \omega_{3x}\omega_{3z}}\end{aligned}$$

The rotor is assumed to be symmetric. T_{3x} and T_{3z} are degenerate equations.

$$T_{2x} = \dot{H}_{2x} + \omega_{2y}H_{2z} - \omega_{2z}H_{2y}$$

$$\begin{aligned}T_{2x} = I_2(11) & \left[\Sigma \dot{a}_{21}(1i)\omega_{1i} + \Sigma a_{21}(1i)\dot{\omega}_{1i} + \ddot{\gamma} \right] + \dot{a}_{23}(11)I_3(11) \left[a_{32}(11)\dot{\gamma} + \Sigma a_{31}(1i)\omega_{1i} \right] \\ & + \dot{a}_{23}(12)I_3(22) \left[\ddot{\alpha} + a_{32}(21)\dot{\gamma} + \Sigma a_{31}(2i)\omega_{1i} \right] + \dot{a}_{23}(13)I_3(33) \left[a_{32}(31)\dot{\gamma} + \Sigma a_{31}(3i)\omega_{1i} \right] \\ & + a_{23}(11)I_3(11) \left[\dot{a}_{32}(11)\dot{\gamma} + a_{32}(11)\ddot{\gamma} + \Sigma \dot{a}_{31}(1i)\omega_{1i} + \Sigma a_{31}(1i)\dot{\omega}_{1i} \right] \\ & + a_{23}(12)I_3(22) \left[\ddot{\alpha} + \dot{a}_{32}(21)\dot{\gamma} + a_{32}(21)\ddot{\gamma} + \Sigma \dot{a}_{31}(2i)\omega_{1i} + \Sigma a_{31}(2i)\dot{\omega}_{1i} \right]\end{aligned}$$

$$\begin{aligned}
& + a_{23}(13)I_3(33) \left[\dot{a}_{32}(31)\dot{\gamma} + a_{32}(31)\ddot{\gamma} + \Sigma \dot{a}_{31}(3i)\omega_{1i} + \Sigma a_{31}(3i)\dot{\omega}_{1i} \right] \\
& + \left[\Sigma a_{21}(2i)\omega_{1i} \right] \left\{ I_2(33) \left[\Sigma a_{21}(3i)\omega_{1i} \right] + a_{23}(31)I_3(11) \left[a_{32}(11)\dot{\gamma} + \Sigma a_{31}(1i)\omega_{1i} \right] \right. \\
& + a_{23}(32)I_3(22) \left[\dot{a} + a_{32}(21)\dot{\gamma} + \Sigma a_{31}(2i)\omega_{1i} \right] + a_{23}(33)I_3(33) \left[a_{32}(31)\dot{\gamma} + \Sigma a_{31}(3i)\omega_{1i} \right] \Big\} \\
& - \left[\Sigma a_{21}(3i)\omega_{1i} \right] \left\{ I_2(22) \left[\Sigma a_{21}(2i)\omega_{1i} \right] + a_{23}(21)I_3(11) \left[a_{32}\dot{\gamma} + \Sigma a_{31}(1i)\omega_{1i} \right] \right. \\
& + a_{23}(22)I_3(22) \left[\dot{a} + a_{32}(21)\dot{\gamma} + \Sigma a_{31}(2i)\omega_{1i} \right] + a_{23}(23)I_3(33) \left[a_{32}(31)\dot{\gamma} + \Sigma a_{31}(3i)\omega_{1i} \right] \Big\}
\end{aligned}$$

T_{2y} and T_{2z} are degenerate equations. However, they are necessary to evaluate the constraint torques acting on body 1.

$$T_{2y} = \dot{H}_{2y} + \omega_{2z}H_{2x} - \omega_{2x}H_{2z}$$

$$\begin{aligned}
T_{2y} = & I_2(22) \left[\Sigma \dot{a}_{21}(2i)\omega_{1i} + \Sigma a_{21}(2i)\dot{\omega}_{1i} \right] + \dot{a}_{23}(21)I_3(11) \left[a_{32}(11)\dot{\gamma} + \Sigma a_{31}(1i)\omega_{1i} \right] \\
& + \dot{a}_{23}(22)I_3(22) \left[\dot{a} + a_{32}(21)\dot{\gamma} + \Sigma a_{31}(2i)\omega_{1i} \right] + \dot{a}_{23}(23)I_3(33) \left[a_{32}(31)\dot{\gamma} + \Sigma a_{31}(3i)\omega_{1i} \right] \\
& + a_{23}(21)I_3(11) \left[a_{32}(11)\dot{\gamma} + a_{32}(11)\ddot{\gamma} + \Sigma \dot{a}_{31}(1i)\omega_{1i} + \Sigma a_{31}(1i)\dot{\omega}_{1i} \right] \\
& + a_{23}(22)I_3(22) \left[\ddot{a} + \dot{a}_{32}(21)\dot{\gamma} + a_{32}(21)\ddot{\gamma} + \Sigma \dot{a}_{31}(2i)\omega_{1i} + \Sigma a_{31}(2i)\dot{\omega}_{1i} \right] \\
& + a_{23}(23)I_3(33) \left[\dot{a}_{32}(31)\dot{\gamma} + a_{32}(31)\ddot{\gamma} + \Sigma \dot{a}_{31}(3i)\omega_{1i} + \Sigma a_{31}(3i)\dot{\omega}_{1i} \right] \\
& + \left[\Sigma a_{21}(3i)\omega_{1i} \right] \left\{ I_2(11) \left[\dot{\gamma} + \Sigma a_{21}(1i)\omega_{1i} \right] + a_{23}(11)I_3(11) \left[a_{32}(11)\dot{\gamma} + \Sigma a_{31}(1i)\omega_{1i} \right] \right. \\
& + a_{23}(12)I_3(22) \left[\dot{a} + a_{32}(21)\dot{\gamma} + \Sigma a_{31}(2i)\omega_{1i} \right] + a_{23}(13)I_3(33) \left[a_{32}(31)\dot{\gamma} + \Sigma a_{31}(3i)\omega_{1i} \right] \Big\} \\
& - \left[\dot{\gamma} + \Sigma a_{21}(1i)\omega_{1i} \right] \left\{ I_2(33) \left[\Sigma a_{21}(3i)\omega_{1i} \right] + a_{23}(31)I_3(11) \left[a_{32}(11)\dot{\gamma} + \Sigma a_{31}(1i)\omega_{1i} \right] \right. \\
& + a_{23}(32)I_3(22) \left[\dot{a} + a_{32}(21)\dot{\gamma} + \Sigma a_{31}(2i)\omega_{1i} \right] + a_{23}(33)I_3(33) \left[a_{32}(31)\dot{\gamma} + \Sigma a_{31}(3i)\omega_{1i} \right] \Big\}
\end{aligned}$$

$$T_{2z} = \dot{H}_{2z} + \omega_{2x}H_{2y} - \omega_{2y}H_{2x}$$

$$\begin{aligned}
T_{2z} = & I_2(33) \left[\Sigma \dot{a}_{21}(3i)\omega_{1i} + \Sigma a_{21}(3i)\dot{\omega}_{1i} \right] + \dot{a}_{23}(31)I_3(11) \left[a_{32}(11)\dot{\gamma} + \Sigma a_{31}(1i)\omega_{1i} \right] \\
& + \dot{a}_{23}(32)I_3(22) \left[\dot{a} + a_{32}(21)\dot{\gamma} + \Sigma a_{31}(2i)\omega_{1i} \right] + \dot{a}_{23}(33)I_3(33) \left[a_{32}(31)\dot{\gamma} + \Sigma a_{31}(3i)\omega_{1i} \right] \\
& + a_{23}(31)I_3(11) \left[\dot{a}_{32}(11)\dot{\gamma} + a_{32}(11)\ddot{\gamma} + \Sigma \dot{a}_{31}(1i)\omega_{1i} + \Sigma a_{31}(1i)\dot{\omega}_{1i} \right]
\end{aligned}$$

$$\begin{aligned}
& + a_{23}(32)I_3(22)\left[\ddot{a} + \dot{a}_{32}(21)\dot{\gamma} + a_{32}(21)\ddot{\gamma} + \Sigma\dot{a}_{31}(2i)\omega_{1i} + \Sigma a_{31}(2i)\dot{\omega}_{1i}\right] \\
& + a_{23}(33)I_3(33)\left[\dot{a}_{32}(31)\dot{\gamma} + a_{32}(31)\ddot{\gamma} + \Sigma\dot{a}_{31}(3i)\omega_{1i} + \Sigma a_{31}(3i)\dot{\omega}_{1i}\right] \\
& + \left[\dot{\gamma} + \Sigma a_{21}(1i)\omega_{1i}\right]\left\{I_2(22)\left[\Sigma a_{21}(3i)\omega_{1i}\right] + a_{23}(21)I_3(11)\left[a_{32}(11)\dot{\gamma} + \Sigma a_{31}(1i)\omega_{1i}\right]\right. \\
& + a_{23}(22)I_3(22)\left[\dot{a} + a_{32}(21)\dot{\gamma} + \Sigma a_{31}(2i)\omega_{1i}\right] + a_{23}(23)I_3(33)\left[a_{32}(31)\dot{\gamma} + \Sigma a_{31}(3i)\omega_{1i}\right]\left. \right\} \\
& - \left[\Sigma a_{21}(2i)\omega_{1i}\right]\left\{I_2(11)\left[\Sigma a_{21}(1i)\omega_{1i} + \dot{\gamma}\right] + a_{23}(11)I_3(11)\left[a_{32}(11)\dot{\gamma} + \Sigma a_{31}(1i)\omega_{1i}\right]\right. \\
& + a_{23}(12)I_3(22)\left[\dot{a} + a_{32}(21)\dot{\gamma} + \Sigma a_{31}(2i)\omega_{1i}\right] + a_{23}(13)I_3(33)\left[a_{32}(31)\dot{\gamma} + \Sigma a_{31}(3i)\omega_{1i}\right]\left. \right\}
\end{aligned}$$

$$T_{1x} = \dot{H}_{1x} + \omega_{1y}H_{1z} - \omega_{1z}H_{1y}$$

$$\begin{aligned}
T_{1x} = & I_1(11)\dot{\omega}_{1x} - I_1(12)\dot{\omega}_{1y} - I_1(13)\dot{\omega}_{1z} + \omega_{1y}\omega_{1z}\left[I_1(33) - I_1(22)\right] \\
& - \omega_{1y}\left[I_1(31)\omega_{1x} + I_1(32)\omega_{1y}\right] + \omega_{1z}\left[I_1(21)\omega_{1x} + I_1(23)\omega_{1z}\right]
\end{aligned}$$

$$T_{1y} = \dot{H}_{1y} + \omega_{1z}H_{1x} - \omega_{1x}H_{1z}$$

$$\begin{aligned}
T_{1y} = & -I_1(21)\dot{\omega}_{1x} + I_1(22)\dot{\omega}_{1y} - I_1(23)\dot{\omega}_{1z} + \omega_{1z}\omega_{1x}\left[I_1(11) - I_1(33)\right] \\
& - \omega_{1z}\left[I_1(12)\omega_{1y} + I_1(13)\omega_{1z}\right] + \omega_{1x}\left[I_1(31)\omega_{1x} + I_1(32)\omega_{1y}\right]
\end{aligned}$$

$$T_{1z} = \dot{H}_{1z} + \omega_{1x}H_{1y} - \omega_{1y}H_{1x}$$

$$\begin{aligned}
T_{1z} = & -I_1(31)\dot{\omega}_{1x} - I_1(32)\dot{\omega}_{1y} + I_1(33)\dot{\omega}_{1z} + \omega_{1x}\omega_{1y}\left[I_1(22) - I_1(11)\right] \\
& - \omega_{1x}\left[I_1(21)\omega_{1x} + I_1(23)\omega_{1z}\right] + \omega_{1y}\left[I_1(12)\omega_{1y} + I_1(13)\omega_{1z}\right]
\end{aligned}$$

The right-hand side of Equations (2.4) is treated in the following development. For this phase of the study it is assumed that the disturbance torques \mathbf{T}_d equal zero.

$$\mathbf{T}_{33} = \mathbf{0}$$

$$\mathbf{T}_{23} = \mathbf{0}$$

$$\mathbf{T}_{13} = \mathbf{0}$$

This assumption has been made because disturbance torque inputs cannot affect the stability of the linearized model that shall be considered.

The remaining torque equation is

$$\mathbf{T}_k = \mathbf{T}_{k1} + \mathbf{T}_{k2} + \mathbf{T}_{k4}.$$

The gravity-gradient torques for each of the three bodies are

$$\mathbf{T}_{31} = 3\Omega_0^2 \begin{bmatrix} \{I_3(33) - I_3(22)\} a_{3r}(23) a_{3r}(33) \\ 0 \\ \{I_3(22) - I_3(11)\} a_{3r}(13) a_{3r}(23) \end{bmatrix},$$

where

$$I_3 = \Phi_3;$$

$$\mathbf{T}_{21} = 3\Omega_0^2 \begin{bmatrix} \{I'_2(33) + I'_3(11) - I'_2(22) - I'_3(22)\} a_{2r}(23) a_{2r}(33) \\ \{I'_2(11) - I'_2(33)\} a_{2r}(13) a_{2r}(33) \\ \{I'_2(22) + I'_3(22) - I'_2(11) - I'_3(11)\} a_{2r}(13) a_{2r}(23) \end{bmatrix},$$

where

$$I_2 = \Phi_2 + A_{32} \Phi_3 A'_{32},$$

$$I_2 = \begin{bmatrix} I_2(11) & 0 & 0 \\ 0 & I_2(22) & 0 \\ 0 & 0 & I_2(33) \end{bmatrix} + \begin{bmatrix} Ca & 0 & -Sa \\ 0 & 1 & 0 \\ Sa & 0 & Ca \end{bmatrix} \begin{bmatrix} I_3(11) & 0 & 0 \\ 0 & I_3(22) & 0 \\ 0 & 0 & I_3(11) \end{bmatrix} \begin{bmatrix} Ca & 0 & Sa \\ 0 & 1 & 0 \\ -Sa & 0 & Ca \end{bmatrix},$$

and

$$I_2 = \begin{bmatrix} I_2(11) + I_3(11) & 0 & 0 \\ 0 & I_2(22) + I_3(22) & 0 \\ 0 & 0 & I_2(33) + I_3(11) \end{bmatrix};$$

and

$$\mathbf{T}_{11} = 3\Omega_0^2 \begin{bmatrix} \{I_1(33) - I_1(22)\} a_{1r}(23) a_{1r}(33) + I_1(12) a_{1r}(13) a_{1r}(33) \\ - I_1(13) a_{1r}(13) a_{1r}(23) - I_1(23) \{a_{1r}^2(23) - a_{1r}^2(33)\} \\ \{I_1(11) - I_1(33)\} a_{1r}(13) a_{1r}(33) + I_1(13) \{a_{1r}^2(13) - a_{1r}^2(33)\} \\ + I_1(23) a_{1r}(13) a_{1r}(23) - I_1(12) a_{1r}(23) a_{1r}(33) \\ \{I_1(22) - I_1(11)\} a_{1r}(13) a_{1r}(23) + I_1(12) \{a_{1r}^2(23) - a_{1r}^2(13)\} \\ + I_1(13) a_{1r}(23) a_{1r}(33) - I_1(23) a_{1r}(13) a_{1r}(33) \end{bmatrix},$$

where

$$I_1 = \Phi_1.$$

The only constraint torques that must be considered are those acting on body 1. (See page 24.)

$$\mathbf{T}_{14} = A_{12} \begin{bmatrix} 0 \\ -T_{24y} \\ -T_{24z} \end{bmatrix} = \begin{bmatrix} -a_{12}(12)T_{24y} - a_{12}(13)T_{24z} \\ -a_{12}(22)T_{24y} - a_{12}(23)T_{24z} \\ -a_{12}(32)T_{24y} - a_{12}(33)T_{24z} \end{bmatrix},$$

but

$$T_{24y} = T_{2y}(\text{RHS}) - T_{21y} - \cancel{T_{22y}}^0$$

where

$$T_{21y} = T_{2y} \text{ gravity-gradient torque}$$

and

$$T_{22y} = T_{2y} \text{ control torque,}$$

and

$$T_{24z} = T_{2z}(\text{RHS}) - T_{21z} - \cancel{T_{22z}}^0$$

where $T_{2y}(\text{RHS})$ and $T_{2z}(\text{RHS})$ appears on page A-5, T_{21y} and T_{21z} appear on page A-7, and T_{22y} and T_{22z} appear on page 23.



Finally,

$$T_{3y} = T_w = k_T \left[T_1 \dot{\theta}_s + \theta_s - T_2 \dot{\epsilon} - (H_w - H_b) C_t \right] - H_w B_f \quad [\text{See Equation (2.3).}]$$

$$T_{2x} = 3\Omega_0^2 \left[I_2(33) + I_3(11) - I_2(22) - I_3(22) \right] a_{2r}(23) a_{2r}(33) - k_g \gamma - B_g \dot{\gamma}$$

$$T_{1x} = 3\Omega_0^2 \left\{ \left[I_1(33) - I_1(22) \right] a_{1r}(23) a_{1r}(33) + I_1(12) a_{1r}(13) a_{1r}(33) - I_1(13) a_{1r}(13) a_{1r}(23) \right. \\ \left. - I_1(23) \left[a_{1r}^2(23) - a_{1r}^2(33) \right] \right\} + a_{12}(11) (k_g \gamma + B_g \dot{\gamma}) - a_{12}(12) T_{24y} - a_{12}(13) T_{24z}$$

$$T_{1y} = 3\Omega_0^2 \left\{ \left[I_1(11) - I_1(33) \right] a_{1r}(13) a_{1r}(33) + I_1(13) \left[a_{1r}^2(13) - a_{1r}^2(33) \right] + I_1(23) a_{1r}(13) a_{1r}(23) \right. \\ \left. - I_1(12) a_{1r}(23) a_{1r}(33) \right\} + a_{12}(21) (k_g \gamma + B_g \dot{\gamma}) - a_{12}(22) T_{24y} - a_{12}(23) T_{24z}$$

$$T_{1z} = 3\Omega_0^2 \left\{ I_1(22) - I_1(11) \right\} a_{1r}(13) a_{1r}(23) + I_1(12) \left[a_{1r}^2(23) - a_{1r}^2(13) \right] + I_1(13) a_{1r}(23) a_{1r}(33) \\ - I_1(23) a_{1r}(13) a_{1r}(33) \left\} + a_{12}(31) (k_g \gamma + B_g \dot{\gamma}) - a_{12}(32) T_{24y} - a_{12}(33) T_{24z}$$

APPENDIX B

LISTING OF FLOQUET COMPUTER PROGRAMS FOR VARIATIONAL PITCH-MOMENTUM BIAS AND VARIATIONAL INERTIA

The first listing presented is the main program used for both the Floquet search detailed in Chapter 5 and the validation runs associated with the variational pitch-momentum bias and pitch disturbance torque runs referenced in Chapter 8. Appropriate changes noted within this program are used to specify which of the two type of runs is desired. The two applicable subroutines are listed following the main program.

The next listing includes both the main program and subroutine for use in the validation of the variational inertia computer runs referenced in Chapter 8.

The user is free to insert into any of these programs any parameter set of his choosing. The required information will be available from the computer output of the optimization program detailed in Chapter 6. In addition, the user is free to insert solar panel configurations of his choosing into the variational inertia program.

Three subroutines are required for the execution of these programs. They are QREIG, QRT, and HESSEN. These are available through the SHARE Program Catalog, SDA 3006-01, August 1964. Their purpose is to solve for eigenvalues by the QR transform. The author of the program is F. P. Emad.

```

      IMPLICIT REAL *8(A-H,O-Z,$)
      REAL *4QMAT,RR,RI,ROUTR,ROUTI
      DIMENSIONQ(5,5),P(8,8),X(8,8),Y(8,8),Z(8,8),B(8,8),QH(8,8)
      DIMENSION QMAT(10,10),ROUTR(100),ROUTI(100)
      DIMENSION QQ(10,5,5)
C THE CARDS WITH(*) WERE USED IN THE FLOUQUET SEARCH DETAILED IN CHAPTER 5,
C WHILE THE CARD WITH(***) WERE USED FOR THE VALIDATION MOMENTUM BIAS RUNS.
      WRITE(6,5000)
      WRITE(6,5001)
      WRITE(6,5002)
      WRITE(6,5003)
      WRITE(6,5004)
5000 FORMAT(' TWO SETS OF EIGENVALUES RESULT FOR EACH CASE CONSIDERED,P
1ROBABABLY ONE WHICH IS USEFUL AND ONE')
5001 FORMAT(' WHICH IS NOT. IN THE FIRST SET, THE SYSTEM MATRIX IS NORM
1ALIZED BY 2 TO THE MPQ(MPQ=3),AND IN ')
5002 FORMAT(' THE SECOND,MPQ=8.ALSO, THE EXPONENTIAL SERIES EXPANSION I
1S CARRIED OUT TO NSTOP=50 IN (1) AND ')
5003 FORMAT(' NSTOP=100 TERMS IN (2).THESE CONSTANTS CAN BE ALTERED IF
1NEED BE FOR A PARTICULAR PROBLEM')
5004 FORMAT(' COMPUTED UNDERFLOWS ARE EXPECTED ')
      OMEGA=1.D-3
      DO 32 NCASE=1,4
C      DO 32 NCASE=1,1
C      AST=ARBITRARY DISTURBANCE TORQUE AMPLITUDE IN FT LB SEC
C      WIN=ARBITRARY DISTURBANCE TORQUE FREQ IN RAD/SEC.
      DO 6555 MQQ=1,1
C      W=WIN
      W=OMEGA
      DO 6888 MZQ=1,1
C      A=AST
      NSTOP=50
      MPQ=3
      DO 39 LSTP=1,2
9500 CONTINUE
      FMPQ=2.D0**MPQ
C      INTRV=4(IF DISTURBANCE IS OF A SINGLE FREQ)
      INTRV=8
      FINTV=INTRV
      IMUT=INTRV-1
      DT=2.D0*3.141592D0/(FINTV*W*FMPQ)
      ANGLE=.2D0
      FSTOP=NSTOP+1
      N=5
      DO 11 M1=1,INTRV
      DO 10 IP=1,N
      DO 10 JP=1,N
      P(IP,JP)=0.D0
10 Q(IP,JP)=0.D0
      DO 12 IP=1,N
12 P(IP,IP)=1.D0
      5 CONTINUE
C      WA=W*A
C      CALL QCALC (Q,ANGLE,NCASE,A,WA)
      CALL QCALC (Q,ANGLE,NCASE,XMO,XMXP)
      DO 30 NDT1=1,5
      DO 30 NDT2=1,5
      Q(NDT1,NDT2)=Q(NDT1,NDT2)*DT
30 CONTINUE
      DO 14 L5=1,N
      DO 14 L6=1,N

```

```

14 B(L5,L6)=Q(L5,L6)
   DO 103 M=1,NSTOP
   F=M
   DO 8 L1=1,N
   DO 8 L2=1,N
   Q(L1,L2)=Q(L1,L2)/F
8 P(L1,L2)=P(L1,L2)+Q(L1,L2)
   DO 15 L7=1,N
   DO 15 L8=1,N
   QH(L7,L8)=0.00
   DO 15 L9=1,N
15 QH(L7,L8)=Q(L7,L9)*B(L9,L8)+QH(L7,L8)
   DO 150 L7=1,N
   DO 150 L8=1,N
150 Q(L7,L8)=QH(L7,L8)
103 CONTINUE
   DO 9 L1=1,N
   DO 9 L2=1,N
9 Q(L1,L2)=P(L1,L2)+Q(L1,L2)/FSTOP
C   FOR DO 1,8 DIVIDE DT BY 256
   DO 6960 M=1,MPQ
   DO 6969 L1=1,N
   DO 6969 L2=1,N
   QH(L1,L2)=0.00
   DO 6969 L3=1,N
6969 QH(L1,L2)=Q(L1,L3)*Q(L3,L2)+QH(L1,L2)
   DO 6968 L1=1,N
   DO 6968 L2=1,N
6968 Q(L1,L2)=QH(L1,L2)
6960 CONTINUE
   DO 33 L1=1,N
   DO 33 L2=1,N
33 QQ(M1,L1,L2)=Q(L1,L2)
   ANGLE=ANGLE+2.00*3.14159200/FINTV
11 CONTINUE
   DO 23 K=1,IMULT
   DO 22 J1=1,N
   DO 22 J2=1,N
   QH(J1,J2)=0.00
   DO 22 J3=1,N
22 QH(J1,J2)=QQ(INTRV+1-K,J1,J3)*QQ(INTRV-K,J3,J2)+QH(J1,J2)
   DO 120 L7=1,N
   DO 120 L8=1,N
120 QQ(INTRV-K,L7,L8)=QH(L7,L8)
23 CONTINUE
   DO 111 LL=1,N
   DO 111 JJ=1,N
   Q(LL,JJ)=QQ(1,LL,JJ)
111 QMAT(LL,JJ)=Q(LL,JJ)
   IPRNT=0
   CALL HESSEN(QMAT,N)
   CALL GREIG(QMAT,N,ROOTR,ROOTI,IPRNT)
   DO 9999 NMAG=1,5
   XMAG=ROOTR(NMAG)**2+ROOTI(NMAG)**2
   XMAG=DSQRT(XMAG)
   IF(XMAG)41,41,42
42 CONTINUE
   XLMD1=DL0G(XMAG)/(6.28318400/W)
   XLMD2=(180.00/3.14159200)*ATAN2(ROOTI(NMAG),ROOTR(NMAG))
41 CONTINUE

```

```

1000 FORMAT(' MAG. OF LAMDA (RE+IM)LAMDA(FLOQUET EGNVLUES) (RE+T*IM),
          ILN(LAMDA)/T,T*IM IN DEGREES')
          WRITE(6,1000)
9001 FORMAT(5E16.8)
          WRITE(6,9001) XMAG,ROOTR(NMAG),ROOTI(NMAG) ,XLMD 1,XLMD 2
9999 CONTINUE
C9000 FORMAT(' DISTURBANCE DISTURBANCE CASE') (*)
9000 FORMAT(' VEHICLE MAG MOM. MAG MOM OF PANELS CASE') (***)
          WRITE(6,9000)
C9505 FORMAT(' AMPLITUDE FREQUENCY ') (*)
9505 FORMAT(' FT. LB./GAUSS FT. LB./GAUSS ') (***)
          WRITE(6,9505)
1101 FORMAT(2D18.6,I3)
C          WRITE(6,1101)A,W,NCASE (*)
          WRITE(6,1101)XMO,XMXP,NCASE (***)
          CONTINUE
          WRITE(6,2222)
2222 FORMAT(1H1)
          NSTOP=100
          MPQ=8
39 CONTINUE
C          AST=AST+.1D0 (*)
6888 CONTINUE
C          WIN=WIN+.0002D0 (*)
6555 CONTINUE
32 CONTINUE
          RETURN
          END

```

```

SUBROUTINE QCALC (Q,ANGLE,NCASE,A,WA)
  IMPLICIT REAL*8(A-H,U-Z)
  DIMENSION Q(5,5)
  GO TO (1,2,3,4),NCASE
1 CONTINUE
C GAM appears as  $\rho$  in the text.
  GAM=8.D0
  AL_F=8.D0
  HO=-2.D0
  XIZ=200.D0
  BG=.5D0
  XKG=.8D-3
  BETA=0.D0
  GO TO 20
2 CONTINUE
  GO TO 20
3 CONTINUE
  GO TO 20
4 CONTINUE
20 CONTINUE
  SB=DSIN(BETA)
  CB=DCOS(BETA)
  CSB=CB*CB
  SSB=SB*SB
C VARIATIONAL TERMS
  A=DSIGN(A,DSIN(ANGLE))
  WA=DSIGN(WA,DCOS(ANGLE))
C SYSTEM A MATRIX
  Q(1,2)=1.D0
  Q(2,1)=(1.D-3/AL_F)*(4.D-3*(1.D0-GAM)+(HO+A)/XIZ)

```

```

1-(SB*CB*(HO+A)**2)/(ALF*XIZ*BG*1.D3)
Q(2,2)=-SSB*((HO+A)**2)/(ALF*XIZ*BG)
Q(2,3)=((XKG-(HO+A)*1.D-3)*SB*(HO+A)/BG+CB*1.D-3*(HO+A)-SB*WA)/
1(ALF*XIZ)
Q(2,4)=1.D-3*(1.D0+(1.D0-GAM)/ALF)+((HO+A)-CB*SB*((HO+A)**2)/BG)
1/(ALF*XIZ)
Q(2,5)=(SSB*(1.D-3)*(HO+A)**2)/(ALF*XIZ*BG)
Q(3,1)=((1.D-3*(HO+A)/BG)*CB)
Q(3,2)=(HO+A)*SB/BG
Q(3,3)=((-XKG/BG)+(1.D-3*(HO+A))/BG)
Q(3,4)=((HO+A)/BG)*CB
Q(3,5)=-((1.D-3)*(HO+A)*SB/BG)
Q(4,1)=(((HO+A)**2)/(1.D+3*BG*XIZ))*(-CSB)
Q(4,2)=(1.D-3)*(GAM-1.D0-ALF)-((HO+A)+CB*SB*((HO+A)**2)/BG)/XIZ
Q(4,3)=((XKG-(HO+A)*1.D-3)*CB*(HO+A)/BG-(CB*WA+SB*(HO+A)*1.D-3))/
1XIZ
Q(4,4)=((- (HO+A)**2)/(XIZ*BG))*CSB
Q(4,5)=- (GAM-ALF)*1.D-6+((HO+A)*1.D-3+CB*SB*((HO+A)**2)*1.D-3/BG)/
1XIZ
Q(5,4)=1.D0
RETURN
END

```

```

SUBROUTINE QCALC (Q,ANGLE,NCASE,XM0,XMXP)
IMPLICIT REAL *8(A-H,U-Z)
DIMENSION Q(5,5)
C EARTH MAGNETIC MOMENT IN GAUSS FT FT FT
XME=2.845D21
C EARTH RADIUS PLUS ORBIT ALTITUDE IN NAUTICAL MILES
RO=4040.D0
C ORBIT PLANE INCLINATION ANGLE IN RADIANS
SIGMA=3.141592D0/6.D0
PI=3.141592D0
OMEGA=1.D-3
GO TO (1,2,3,4),NCASE
1 CONTINUE
C EXAMPLE 1 , UNPERTURBED
XM0=0.D0
XMXP=0.D0
C PARAMETER SET OF EXAMPLE 1
C GAM appears as  $\rho$  in the text.
GAM=2010.D0/10.D0
ALF=.75D0*GAM
HO=-2.5D0
XIZ=10.D0
BG=.75D0
XKG=.33D-2
BETA=0.D0
C WORST CASE ANGLES
Z=1.571D0
T=1.571D0
GO TO 20
2 CONTINUE
C EXAMPLE 1 , PERTURBED
XM0=3.96D0*7.38D-5
GO TO 20
3 CONTINUE
C EXAMPLE 2 , UNPERTURBED
XM0=0.D0
XMXP=0.D0

```

C PARAMETER SET OF EXAMPLE 2

GAM=2200.D0/200.D0
ALF=2325.D0/200.D0
H0=-10.D0
XKG=1.D-3
BETA=0.D0
BG=.75D0

C WORST CASE ANGLES

T=4.71D0
Z=4.71D0
XLAM=3.67D0
E=4.19D0
GO TO 20

4 CONTINUE

C EXAMPLE 2 , PERTURBED

XMXP=5.0D0*7.38D-5
XMO=3.96D0*7.38D-5

20 CONTINUE

SB=DSIN(BETA)
CH=DCOS(BETA)
CSB=CB*CB
SSB=SB*SB
SLAM=DSIN(XLAM)
CLAM=DCOS(XLAM)
SE=DSIN(E)
CE=DCOS(E)
CZ=DCOS(Z)
SZ=DSIN(Z)
CT=DCOS(T)
SS=DSIN(SIGMA)
CS=DCOS(SIGMA)
XKMP=XME*XMXP/(((R0*6076.D0)**3)*2.D0)
XKMO=XME*XMO/(((R0*6076.D0)**3))
IF(XMXP)1000,1001,1000

1001 CONTINUE

A1Y=0.D0
A2Y=0.D0
B1Y=0.D0
B2Y=0.D0
GO TO 2000

1000 CONTINUE

C23=DCOS(PI*23.5D0/180.D0)
S23=DSQRT(1.D0-C23*C23)
SMU=CE*SS*CLAM-SE*(CS*S23-SS*SLAM*C23)
CMU=DSQRT(1.D0-SMU*SMU)
CRO=DSQRT(1.D0-(3440.D0/(R0)**2)/CMU)
ROZ=DARCOS(CRO)
SRO=DSIN(ROZ)
S2RO=DSIN(2.D0*ROZ)
S3RO=DSIN(3.D0*ROZ)
S4RO=DSIN(4.D0*ROZ)
SA=(CLAM*(SE*C23*CS+SE*S23*SS*SLAM)+SLAM*(SE*C23*SS*CLAM-CE*SS*SLAM))/CMU
CA=DSQRT(1.D0-SA*SA)
AY0=XKMP*CMU*SS*CA
AY=-3.D0*XKMP*CMU*SS*CA
BY=3.D0*XKMP*CMU*SS*SA
AOY=(2.D0*AY0*(PI-ROZ)+AY*(-S2RO))/PI
A1Y=(2.D0*AY0*SRO+AY*(SRO+S3RO/3.D0))/PI


```

A2Y=(-AYO*SRO+AY*(PI-ROZ-S4RO/4.DO))/PI
B1Y=BY*(SRO-S3RO/3.DO)/PI
B2Y=BY*(PI-ROZ+S4RO/4.DO)/PI
2000 CONTINUE
C11=XKMO*CZ*SS
C12=-2.DO*XKMO*SZ*CT*SS
CUM=DSIGN(1.DO,DCUS(ANGLE))
SUM=DSIGN(1.DO,DSIN(ANGLE))
S2OM=DSIGN(1.DO,DSIN(2.DO*ANGLE))
C2OM=DSIGN(1.DO,DCOS(2.DO*ANGLE))
C VARIATIONAL TERMS
A=((A1Y+C11)*SUM-(B1Y+C12)*CUM+A2Y*S2UM/2.DO-B2Y*C2UM/2.DO)/OMEGA
WA=(A1Y+C11)*CUM+(B1Y+C12)*SUM+A2Y*C2OM+B2Y*S2OM
C SYSTEM A MATRIX
Q(1,2)=1.DO
Q(2,1)=(1.D-3/ALF)*(4.D-3*(1.DO-GAM)+(HO+A)/XIZ)
1-(SB*CB*(HO+A)**2)/(ALF*XIZ*BG*1.D3)
Q(2,2)=-SSB*((HO+A)**2)/(ALF*XIZ*BG)
Q(2,3)=((XKG-(HO+A)*1.D-3)*SB*(HO+A)/BG+CB*1.D-3*(HO+A)-SB*WA)/
1(ALF*XIZ)
Q(2,4)=1.D-3*(1.DO+(1.DO-GAM)/ALF)+((HO+A)-CB*SB*((HO+A)**2)/BG)
1/(ALF*XIZ)
Q(2,5)=(SSB*(1.D-3)*(HO+A)**2)/(ALF*XIZ*BG)
Q(3,1)=((1.D-3*(HO+A)/BG)*CB)
Q(3,2)=(HO+A)*SB/BG
Q(3,3)=((-XKG/BG)+(1.D-3*(HO+A))/BG)
Q(3,4)=((HO+A)/BG)*CB
Q(3,5)=-((1.D-3)*(HO+A)*SB/BG)
Q(4,1)=(((HO+A)**2)/(1.D+3*HG*XIZ))*(-CSB)
Q(4,2)=(1.D-3)*(GAM-1.DO-ALF)-((HO+A)+CB*SB*((HO+A)**2)/BG)/XIZ
Q(4,3)=((XKG-(HO+A)*1.D-3)*CB*(HO+A)/BG-(CB*WA+SB*(HO+A)*1.D-3))/
1XIZ
Q(4,4)=((-HO+A)**2)/(XIZ*BG)*CSB
Q(4,5)=-((GAM-ALF)*1.D-6+((HO+A)*1.D-3+CB*SB*((HO+A)**2)*1.D-3/BG)/
1XIZ
Q(5,4)=1.DO
RETURN
END

IMPLICIT REAL*8(A-H,O-Z,$)
REAL*4QMAT,RR,RI,ROUTR,ROUTI
DIMENSIONQ(5,5),P(8,8),X(8,8),Y(8,8),Z(8,8),B(8,8),QH(8,8)
DIMENSION QMAT(10,10),ROUTR(100),ROUTI(100)
DIMENSION QQ(10,5,5)
200 FORMAT(' FOR THE PURPOSE OF COMPARISON, ONLY THE VARIATIONAL PANEL
1-ASSOCIATED INERTIA TERMS ARE CONSIDERED')
WRITE(6,200)
1005 FORMAT(' THE SPACECRAFT MAIN BODY INERTIAS MUST BE ADJUSTED T
20 ACCOUNT FOR THE CONSTANT INERTIA ')
WRITE(6,1005)
1006 FORMAT(' TERMS ASSOCIATED WITH XI11,XI22,XI33 AS THEY APPEAR IN TH
1E SUBPROGRAM QCALC')
WRITE(6,1006)
5000 FORMAT(' TWO SETS OF EIGENVALUES RESULT FOR EACH CASE CONSIDERED,P
1ROBABABLY ONE WHICH IS USEFUL AND ONE')
WRITE(6,5000)
5001 FORMAT(' WHICH IS NOT. IN THE FIRST SET, THE SYSTEM MATRIX IS NORM
1ALIZED BY 2 TO THE MPQ(MPQ=3),AND IN ')
WRITE(6,5001)

```

```

5002 FORMAT(' THE SECOND,MPQ=8.AL SO, THE EXPONENTIAL SERIES EXPANSION I
      IS CARRIED OUT TO NSTOP=50 IN (1) AND ')
      WRITE(6,5002)
5003 FORMAT(' NSTOP=100 TERMS IN (2).THESE CONSTANTS CAN BE ALTERED IF
      I NEED BE FOR A PARTICULAR PROBLEM')
      WRITE(6,5003)
5004 FORMAT(' COMPUTED UNDERFLOWS ARE EXPECTED ')
      WRITE(6,5004)
      OMEGA=1.D-3
C 4 PANEL CONFIGURATIONS HAVE BEEN ALLOWED FOR
      DO 32 NCASE=1,4
C INITIAL IZATION OF SUN ANGLE SCAN, MU=0.
      XMU=0.D0
C SCAN OF MU IN 10. DEGREE INCREMENTS
      DO 6555 MOQQ=1,10
      W=OMEGA*2.D0
      NSTOP=50
      MPQ=3
      DO 39 LSTP=1,2
9500 CONTINUE
      FMPQ=2.D0**MPQ
      INTRV=4
      FINTV=INTRV
      IMUL_T=INTRV-1
      DT=2.D0*3.141592D0/(FINTV*W*FMPQ)
      ANGLE=.7D0
      FSTOP=NSTOP+1
      N=5
      DO 11 M1=1,INTRV
      DO 10 IP=1,N
      DO 10 JP=1,N
      P(IP,JP)=0.D0
10 Q(IP,JP)=0.D0
      DO 12 IP=1,N
12 P(IP,IP)=1.D0
      5 CONTINUE
      CALL QCALC (Q,ANGLE,NCASE,XMU)
      DO 30 NDT1=1,5
      DO 30 NDT2=1,5
      Q(NDT1,NDT2)=Q(NDT1,NDT2)*DT
30 CONTINUE
      DO 14 L5=1,N
      DO 14 L6=1,N
14 B(L5,L6)=Q(L5,L6)
      DO 103 M=1,NSTOP
      F=M
      DO 8 L1=1,N
      DO 8 L2=1,N
      Q(L1,L2)=Q(L1,L2)/F
      8 P(L1,L2)=P(L1,L2)+Q(L1,L2)
      DO 15 L7=1,N
      DO 15 L8=1,N
      QH(L7,L8)=0.D0
      DO 15 L9=1,N
15 QH(L7,L8)=Q(L7,L9)*B(L9,L8)+QH(L7,L8)
      DO 150 L7=1,N
      DO 150 L8=1,N
150 Q(L7,L8)=QH(L7,L8)
103 CONTINUE
      DO 9 L1=1,N
      DO 9 L2=1,N

```

```

9 Q(L1,L2)=P(L1,L2)+Q(L1,L2)/FSTOP
C   FOR DO 1,8 DIVIDE DT BY 256
   DO 6960 M=1,MPQ
   DO 6969 L1=1,N
   DO 6969 L2=1,N
   QH(L1,L2)=0.DO
   DO 6969 L3=1,N
6969 QH(L1,L2)=Q(L1,L3)*Q(L3,L2)+QH(L1,L2)
   DO 6968 L1=1,N
   DO 6968 L2=1,N
6968 Q(L1,L2)=QH(L1,L2)
6960 CONTINUE
   DO 33 L1=1,N
   DO 33 L2=1,N
33 QQ(M1,L1,L2)=Q(L1,L2)
   ANGLE=ANGLE+2.DO*3.141592DO/FINTV
11 CONTINUE
   DO 23 K=1,IMUL T
   DO 22 J1=1,N
   DO 22 J2=1,N
   QH(J1,J2)=0.DO
   DO 22 J3=1,N
22 QH(J1,J2)=QQ(INTRV+1-K,J1,J3)*QQ(INTRV-K,J3,J2)+QH(J1,J2)
   DO 120 L7=1,N
   DO 120 L8=1,N
120 QQ(INTRV-K,L7,L8)=QH(L7,L8)
23 CONTINUE
   DO 111 LL=1,N
   DO 111 JJ=1,N
   Q(LL,JJ)=QQ(1,LL,JJ)
111 QMAT(LL,JJ)=Q(LL,JJ)
   CALL HESSEN(QMAT,N)
   IPRNT=0
   CALL QREIG(QMAT,N,ROOTR,ROOTI,IPRNT)
   DO 9000 NMAG=1,5
   XMAG=ROOTR(NMAG)**2+ROOTI(NMAG)**2
   XMAG=DSQRT(XMAG)
   IF(XMAG)41,41,42
42 CONTINUE
   XLMD1=LOG(XMAG)/(6.283184DO/W)
   XLMD2=(180.DO/3.141592DO)*ATAN2(ROOTI(NMAG),ROOTR(NMAG))
41 CONTINUE
1000 FORMAT(' MAG. OF LAMDA (RE+IM)LAMDA(FLOQUET EGVNLUES) (RE+T*IM),
1LN(LAMDA)/T,T*IM IN DEGREES')
   WRITE(6,1000)
   WRITE(6,9001) XMAG,ROOTR(NMAG),ROOTI(NMAG),XLMD 1,XLMD 2
9001 FORMAT(5E16.8)
9000 CONTINUE
   XMUD=XMU*180.DO/3.141592DO
5101 FORMAT(' SUN ANGLE IN DEGREES NCASE')
   WRITE(6,5101)
   WRITE(6,1101)XMUD,NCASE
1101 FORMAT(2X,D18.6,2X,I7)
   WRITE(6,2222)
2222 FORMAT(1H1)
   NSTOP=100
   MPQ=8
39 CONTINUE
   XMU=XMU+3.141592DO/18.DO

```

```

6555 CONTINUE
32 CONTINUE
RETURN
END

```

```

SUBROUTINE QCALC (Q,ANGLE,NCASE,XMU)
IMPLICIT REAL*8(A-H,U-Z)
DIMENSION Q(5,5)
C PARAMETER SET FOR EXAMPLE 2.
C GAM appears as  $\rho$  in the text.
GAM=2200.DO/200.DO
ALF=2325.DO/200.DO
HB=-10.DO
XIZ=200.DO
BG=.75DO
XKG=1.D-3
BETA=0.DO
GO TO (1,2,3,4),NCASE
C PANEL CONFIGURATION PARAMETERS ARE A,B,XM=M,XIYP=IYP,XIZP=IZP AS
C DEFINED IN CHAPTER 7.
1 CONTINUE
C NO PANEL CASE
A=0.DO
B=0.DO
XM=0.DO
XIYP=0.DO
XIZP=0.DO
GO TO 20
2 CONTINUE
C 2 PANELS, EACH 10' HIGH BY 5' WIDE
A=3.DO
B=2.5DO
XM=3.12DO
XIYP=6.5DO
XIZP=1.36DO
GO TO 20
3 CONTINUE
C 2 PANELS, EACH 7' HIGH BY 7' WIDE
A=3.DO
B=3.5DO
XIYP=1.6DO
XIZP=1.6DO
GO TO 20
4 CONTINUE
C 2 PANELS, EACH 5' HIGH BY 10' WIDE
A=3.DO
B=5.DO
XIYP=1.36DO
XIZP=6.5DO
20 CONTINUE
C2TP=DSIGN(1.DO,DCOS(ANGLE))
S2TP=DSIGN(1.DO,DSIN(ANGLE))
SSTP=(1.DO-C2TP)/2.DO
CSTP=(1.DO+C2TP)/2.DO
STCTP=S2TP/2.DO
OMEGA=1.D-3
SSTPD=S2TP*OMEGA
CSTPD=-S2TP*OMEGA
STCTD=C2TP*OMEGA

```

```

C      W IN MAIN PROGRAM IS 2 OMEGA
C XMU IS TRANSFERED FROM THE MAIN PROGRAM
      SMU=DSIN(XMU)
      CMU=DCOS(XMU)
      SSMU=SMU*SMU
      SB=DSIN(BETA)
      CB=DCOS(BETA)
      CSB=CB*CB
      SSB=SB*SB
C PANEL ASSEMBLY INERTIAS IN SPACECRAFT COORDINATES
C VARIATIONAL EQUATION
      XI11=(XIYP-XIZP*SSMU-XM*(B*SMU)**2)*CSTP
C ACTUAL EQUATION
C      XI11=(XIYP-XIZP*SSMU-XM*(B*SMU)**2)*CSTP+XM*((A+B*CMU)**2+(B*SMU)
C      1**2)+XIZP
      XI13=(XIYP-XIZP*SSMU-XM*(B*SMU)**2)*STCTP
C VARIATIONAL EQUATION
      XI22=0.00
C ACTUAL EQUATION
C      XI22=XIYP+XIZP*SSMU+XM*(B*SMU)**2
C VARIATIONAL EQUATION
      XI33=(XIYP-XIZP*SSMU-XM*(B*SMU)**2)*SSTP
C ACTUAL EQUATION
C      XI33=(XIYP-XIZP*SSMU-XM*(B*SMU)**2)*SSTP+XM*((A+B*CMU)**2+(B*SMU)
C      1**2)+XIZP
C PRIMED INERTIAS OF CHAPTER 7
      XI1P=ALF*XIZ+XI11
      XI2P=GAM*XIZ+XI22
      XI3P=XIZ+XI33
C DERIVATIVES OF PANEL ASSEMBLY INERTIAS
      XIKUN=(XIYP-XIZP*SSMU-XM*(B*SMU)**2)
      XI11D=XIKUN*CSTPD
      XI13D=XIKUN*STCTD
      XI33D=XIKUN*SSTPD
      A=-SB*CB*HB+XI11D
      B=OMEGA*(XI1P+XI3P-XI2P)+SSB*HB+XI13D
      C=CB*BG-SB*HB
      D=4.00*OMEGA*OMEGA*(XI3P-XI2P)+SSB*OMEGA*HB+OMEGA*XI13D
      E=OMEGA*OMEGA*XI13+OMEGA*SB*CB*HB-OMEGA*XI11D
      F=XKG-HB*OMEGA
      G=-OMEGA*(XI1P+XI3P-XI2P)-CSB*HB+XI13D
      H=SB*CB*HB+XI33D
      P=-SB*BG-CB*HB
C Q RATHER THAN V IS IN THE TEXT
      V=4.00*OMEGA*OMEGA*XI13+SB*CB*HB*OMEGA+OMEGA*XI33D
      R=(OMEGA*CSB*HB-OMEGA*OMEGA*(XI2P-XI1P)-OMEGA*XI13D
      S=XI3P*C+XI13*P
      T=XI1P*P+XI13*C
      CK=-1.00/(XI13*XI13-XI3P*XI1P)
C SYSTEM A MATRIX
      Q(1,2)=1.00
      Q(2,1)=CK*(XI3P*D+XI13*V+S*CB*OMEGA*HB/BG)
      Q(2,2)=CK*(XI3P*A+XI13*G+S*SB*HB/BG)
      Q(2,3)=CK*(XI3P*CB*XKG-XI13*XKG*SB-S*F/BG)
      Q(2,4)=CK*(XI3P*B+XI13*H+S*CB*HB/BG)
      Q(2,5)=CK*(XI3P*E+XI13*R-S*HB*SB*OMEGA/BG)
      Q(3,1)=CB*OMEGA*HB/BG
      Q(3,2)=HB*SB/BG
      Q(3,3)=-F/BG
      Q(3,4)=CB*HB/BG
      Q(3,5)=-HB*SB*OMEGA/BG

```

```

Q(4,1)=CK*(XI13*D+XI1P*V+T*CB*OMEGA*HB/BG)
Q(4,2)=CK*(XI13*A+XI1P*G+T*HB*SB/BG)
Q(4,3)=CK*(XI13*CB*XKG-XI1P*XKG*SB-T*F/BG)
Q(4,4)=CK*(XI13*B+XI1P*H+T*CB*HB/BG)
Q(4,5)=CK*(XI13*E+XI1P*R-T*HB*SB*OMEGA/BG)
Q(5,4)=1.00
RETURN
END

```

APPENDIX C

DERIVATION OF THE RESIDUAL MAGNETIC DISTURBANCE TORQUE MODEL

Before proceeding with the development of the magnetic disturbance torque model, it is necessary to define the coordinate frames pertinent to this discussion.

First, consider the coordinate frame shown in Figure C.1. This figure defines the orientation of the ecliptic plane with respect to the equatorial plane. The line of intersection of the planes defines the vernal and autumnal equinoxes. The angle between the planes remains constant and is $23^\circ 27'$. The angle ϵ defines the position of the sun with respect to the vernal equinox as the sun travels in the ecliptic plane.

$$\hat{\bar{X}}_R = \begin{bmatrix} x_R \\ y_R \\ z_R \end{bmatrix} \quad \text{defines the ecliptic plane coordinate axes,}$$

and

$$\hat{\bar{X}}_e = \begin{bmatrix} x_e \\ y_e \\ z_e \end{bmatrix} \quad \text{defines the equatorial plane coordinate axes.}$$

The ecliptic plane normal is defined by the positive z_R axis, and the equatorial plane normal is defined by the positive z_e axis.

Second, consider the relationship between the orbital and equatorial planes as shown in Figure C.2. The angle σ defines the angle of orbit inclination and is measured between the orbit plane normal and the north spin pole axis, the positive z_e axis. The angular position of the vehicle relative to the ascending node, the point where the vehicle passes from the southern to the northern hemisphere, is defined as $\Omega_0 t$ where Ω_0 is orbit rate and t is time. The angle λ defines the position of the ascending node relative to the vernal equinox.

$$\hat{\bar{X}}_n = \begin{bmatrix} x_n \\ y_n \\ z_n \end{bmatrix} \quad \text{defines the orbit plane coordinate axes.}$$

The orbit plane normal is defined by the positive z_n axis.

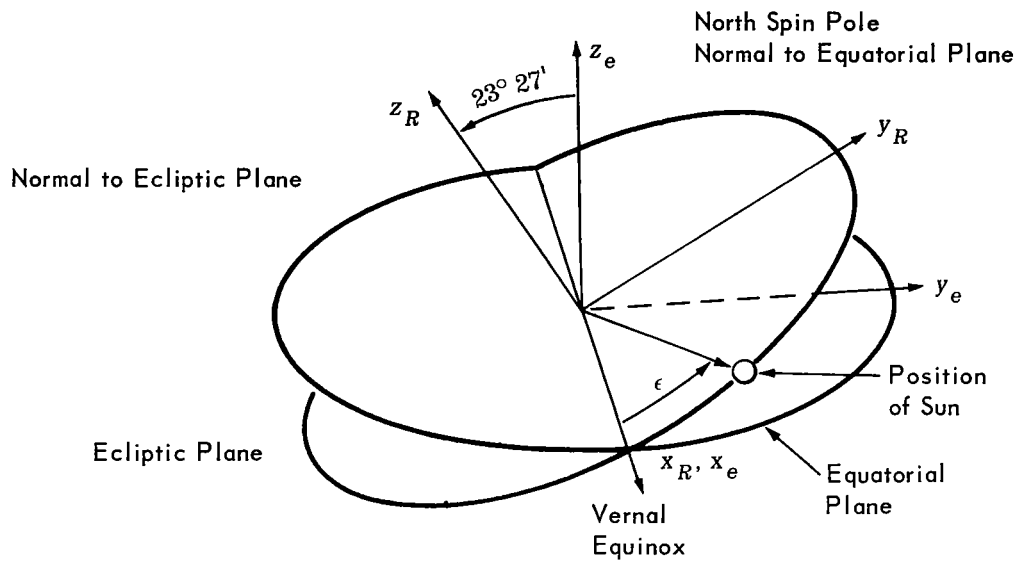


Figure C.1—Orientation of the ecliptic plane relative to the equatorial plane.

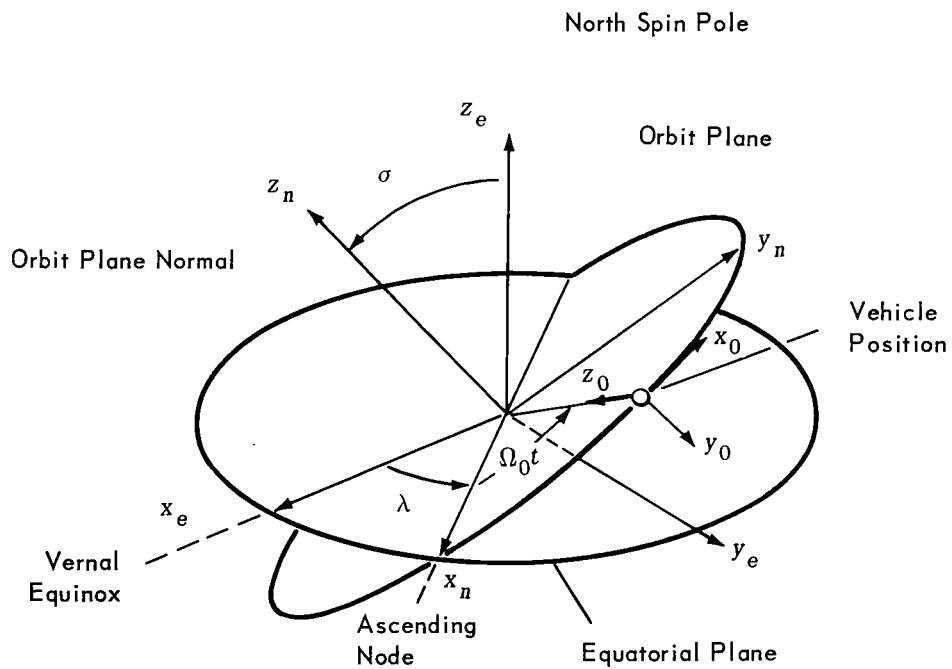


Figure C.2—Orientation of the orbit plane relative to the equatorial plane.



Third, it was assumed that the spacecraft is under perfect control so that the spacecraft coordinate axes are coincident with the orbit reference coordinate axes defined in the beginning of Chapter 2. That is, the spacecraft coordinates

$$\hat{\bar{X}}_0 = \begin{bmatrix} x_0 \\ y_0 \\ z_0 \end{bmatrix} = \begin{bmatrix} \text{spacecraft roll axis} \\ \text{spacecraft pitch axis} \\ \text{spacecraft yaw axis} \end{bmatrix}$$

are coincident with the orbit reference coordinate axes

$$\hat{\bar{X}}_r = \begin{bmatrix} x_r \\ y_r \\ z_r \end{bmatrix}.$$

In general, the torque due to a residual magnetic moment, \mathbf{T}_d , can be written as $\mathbf{T}_d = \mathbf{M} \times \mathbf{B}$, where \mathbf{M} = magnetic moment vector and \mathbf{B} = earth magnetic field vector.

It has been assumed for the purposes of this study that the angle between the geographic and geomagnetic north pole is zero. Accordingly, the components of the earth's magnetic field vector can be expressed in terms of spacecraft coordinates (Reference 10) as

$$\mathbf{B}_0 = \begin{bmatrix} B_{x0} \\ B_{y0} \\ B_{z0} \end{bmatrix}$$

where

$$B_{x0} = \frac{m_e}{r_0^3} (\sin \sigma \cos \Omega_0 t) ,$$

$$B_{y0} = -\frac{m_e}{r_0^3} (\cos \sigma) ,$$

and

$$B_{z0} = \frac{m_e}{r_0^3} (2 \sin \sigma \sin \Omega_0 t) ,$$

where m_e = the magnetic dipole moment of earth in G-ft³ and r_0 = the orbit radius from center of the earth.

Consider the class of spacecraft without driven solar panels. If the magnetic moment vector for the spacecraft alone is defined as

$$\mathbf{m}_0 = \begin{bmatrix} m_{x0} \\ m_{y0} \\ m_{z0} \end{bmatrix},$$

it is a simple matter to express the disturbance torque in terms of its components:

$$\mathbf{T}_{d0} = \mathbf{m}_0 \times \mathbf{B}_0,$$

where

$$\mathbf{T}_{d0} = \begin{bmatrix} T_{dx0} \\ T_{dy0} \\ T_{dz0} \end{bmatrix}$$

or

$$\mathbf{T}_{d0} = \frac{m_e}{r_0^3} \begin{bmatrix} m_{y0}(2S\sigma S\Omega_0 t) + m_{z0}(C\sigma) \\ m_{z0}(S\sigma C\Omega_0 t) - m_{x0}(2S\sigma S\Omega_0 t) \\ -m_{y0}(S\sigma C\Omega_0 t) - m_{x0}(C\sigma) \end{bmatrix}. \quad (\text{C.1})$$

For this case, the disturbance torque $\mathbf{T}_d = \mathbf{T}_{d0}$, and T_{dx} and T_{dz} , the two components of interest, can be written directly in terms of their frequency components:

$$T_{dx} = \frac{m_e}{r_0^3} \left[(m_{z0}C\sigma) + (2m_{y0}S\sigma)S\Omega_0 t \right]$$

$$T_{dz} = \frac{m_e}{r_0^3} \left[(-m_{x0}C\sigma) + (-m_{y0}S\sigma)C\Omega_0 t \right]$$

Next, consider the class of spacecraft with driven solar panels. Since the panels are normally fabricated from nonferrous materials, it is assumed that the only disturbance torque component with which we must concern ourselves is that resulting from a constant current distribution on the panel faces themselves.

The solar panel assembly is detailed in Figure C.3. Where the panel assembly coordinate axes are defined by

$$\tilde{\mathbf{X}}_p = \begin{bmatrix} x_p \\ y_p \\ z_p \end{bmatrix}.$$

The panel face normal is defined by the x_p axis, and the y_p axis lies in the plane of the panel face and is perpendicular to the panel hinge line at its intersection with the panel shaft. z_p is parallel to the panel hinge line and perpendicular to both x_p and y_p . These three axes form a right-handed coordinate system. The $\tilde{\mathbf{X}}_p$ axes originate from the center of the solar panel shaft. The distance between the spacecraft center of gravity and the panel hinge line measured along the y_0 axis is a . The distance between the panel hinge line and the panel center of gravity is b . The smallest angle measured between the panel shaft line and the y_p axis is μ . The angle measured between the z_p and z_0 axes is θ_p . The driven panels are assumed to have two degrees of freedom, one about the panel shaft, which is located along the spacecraft pitch axis, and one perpendicular to this, along the panel hinge line, as shown in Figure C.3. The two degrees of freedom make it possible to align the solar panels so that the solar cell faces are always normal to the spacecraft-sun line, a line drawn between the spacecraft and the sun. The energization of the cells by the sun produces the constant current distribution with which we are concerned.

When the solar panels are normal to the nonocculted spacecraft sunline, the magnetic moment \mathbf{m}_p due to the constant current distribution on the panel face and expressed in solar panel assembly coordinates $\tilde{\mathbf{X}}_p$ is

$$\mathbf{m}_p = \begin{bmatrix} m_{xp} \\ 0 \\ 0 \end{bmatrix}.$$

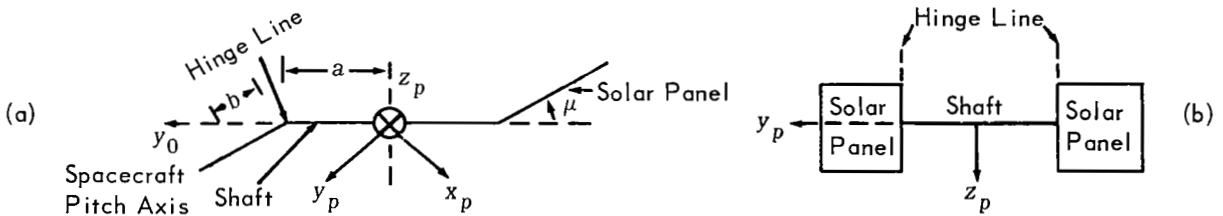


Figure C.3—Solar panel assembly, (a) view looking down panel hinge line, and (b) view normal to shaft and hinge line.

When the earth occults the sun, $\mathbf{m}_p = \mathbf{0}$. The resulting disturbance torque in spacecraft coordinates is $\mathbf{T}_{dp} = \mathbf{m}_{0p} \times \mathbf{B}_0$, where \mathbf{m}_{0p} is the moment expressed in spacecraft coordinates. For this class of spacecraft, the total magnetic disturbance torque is $\mathbf{T}_d = \mathbf{T}_{d0} + \mathbf{T}_{dp}$.

To detail \mathbf{T}_{dp} , it is first necessary to transform \mathbf{m}_p from panel coordinates into \mathbf{m}_{0p} in spacecraft coordinates. For ease of manipulation, it will be assumed that since the vehicle under discussion is in earth orbit, the spacecraft-sun line and earth-sun line are coincident. The problem of occultation will be considered separately.

It can be demonstrated that if the hinge angle μ were adjusted to equal the angle that the earth-sun line makes with the orbit plane and if the proper initial reference angle of the solar panel shaft were chosen, then the sunline will always be kept normal to the panel face if the panel assembly is simply rotated about its shaft at an angular velocity of Ω_0 . The solar panel assembly transformation rotational sequence from panel assembly to spacecraft coordinates, therefore, was chosen to be first a negative μ rotation about the hinge line parallel z_p and second a negative θ_p rotation about y_p , the axis of the shaft. The negative rotations must be performed to negate the effects upon the solar panels of the sun angle and the spacecraft angular position in orbit. The negative θ_p rotation must be performed because the spacecraft rotates once about its pitch axis each orbit.

$$\hat{\mathbf{X}}_0 = \begin{bmatrix} x_0 \\ y_0 \\ z_0 \end{bmatrix} = \begin{bmatrix} C\theta_p & 0 & S\theta_p \\ 0 & 1 & 0 \\ -S\theta_p & 0 & C\theta_p \end{bmatrix} \begin{bmatrix} C\mu & -S\mu & 0 \\ S\mu & C\mu & 0 \\ 0 & 0 & 1 \end{bmatrix} \begin{bmatrix} x_p \\ y_p \\ z_p \end{bmatrix},$$

or

$$\hat{\mathbf{X}}_0 = \begin{bmatrix} x_0 \\ y_0 \\ z_0 \end{bmatrix} = \begin{bmatrix} C\theta_p C\mu & -C\theta_p S\mu & S\theta_p \\ S\mu & C\mu & 0 \\ -S\theta_p C\mu & S\theta_p S\mu & C\theta_p \end{bmatrix} \begin{bmatrix} x_p \\ y_p \\ z_p \end{bmatrix}, \quad (\text{C.2})$$

where

μ = angle between the earth-sun line and the orbit plane,

$\theta_p = \theta_{p0} + \Omega_0 t$ and is the angle between the z_p and z_0 axes,

θ_{p0} = initial solar panel shaft reference angle,

and

Ω_0 = orbital velocity.

It is assumed that μ remains constant during any particular orbit. After transformation,

$$\mathbf{m}_{0p} = \begin{bmatrix} C\theta_p C\mu & -C\theta_p S\mu & S\theta_p \\ S\mu & C\mu & 0 \\ -S\theta_p C\mu & S\theta_p S\mu & C\theta_p \end{bmatrix} \begin{bmatrix} m_{xp} \\ 0 \\ 0 \end{bmatrix},$$

where \mathbf{m}_{0p} is the magnetic moment due to the solar panel assembly in spacecraft coordinates.

$$\mathbf{m}_{0p} = m_{xp} \begin{bmatrix} C\theta_p C\mu \\ S\mu \\ -S\theta_p C\mu \end{bmatrix}$$

Finally

$$\mathbf{T}_{dp} = \mathbf{m}_{0p} \times \mathbf{B}_0,$$

where

$$\mathbf{T}_{dp} = \begin{bmatrix} T_{d xp} \\ T_{d yp} \\ T_{d zp} \end{bmatrix},$$

or

$$\mathbf{T}_{dp} = \frac{m_e m_{xp}}{r_0^3} \begin{bmatrix} (2S\mu S\sigma)S\Omega_0 t + (-C\mu C\sigma)S(\theta_{p0} + \Omega_0 t) \\ [-C\mu S\sigma S(\theta_{p0} + \Omega_0 t)]C\Omega_0 t + [-2C\mu S\sigma C(\theta_{p0} + \Omega_0 t)]S\Omega_0 t \\ (-S\sigma S\mu)C\mu_0 t + (-C\mu C\sigma)C(\theta_{p0} + \Omega_0 t) \end{bmatrix}. \quad (\text{C.3})$$

The components pertinent to this discussion are

$$T_{d xp} = (2S\mu S\sigma)S\Omega_0 t + (-C\mu C\sigma)S(\theta_{p0} + \Omega_0 t)$$

and

$$T_{d zp} = (-S\sigma S\mu)C\Omega_0 t + (-C\mu C\sigma)C(\theta_{p0} + \Omega_0 t).$$

By superposition the total disturbance torque caused by spacecraft alone plus the solar panel assembly

is $\mathbf{T}_d = \mathbf{T}_{d0} + \mathbf{T}_{dp}$.

C.1 Derivation of the Sun Angle

Reference is made to Figures C.1, C.2, and C.3. Define \hat{Z}_n as the orbit plane normal unit vector, \hat{S} as the earth-sun line unit vector, and

$$\hat{\tilde{X}}_e = \begin{bmatrix} \hat{x}_e \\ \hat{y}_e \\ \hat{z}_e \end{bmatrix},$$

where $\hat{\tilde{X}}_e$ is a set of unit vectors coincident with $\hat{\tilde{X}}_e$. Expressing \hat{S} in terms of $\hat{\tilde{X}}_e$ coordinates,

$$\hat{S} = C\epsilon\hat{x}_e + S\epsilon[C(23^\circ 27')\hat{y}_e + S(23^\circ 27')\hat{z}_e].$$

Similarly,

$$\hat{Z}_n = S\sigma(-C\lambda\hat{x}_e - S\lambda\hat{y}_e) + C\sigma\hat{z}_e.$$

The unit vectors \hat{S} and \hat{Z}_n are shown in Figure C.4, and the sun angle μ can be calculated by forming the dot product $\hat{S} \cdot \hat{Z}_n$.

$$\hat{S} \cdot \hat{Z}_n = C(90^\circ + \mu) = -S\mu,$$

or

$$\hat{S} \cdot \hat{Z}_n = -C\epsilon S\sigma C\lambda + S\epsilon[C\sigma S(23^\circ 27') - S\sigma S\lambda C(23^\circ 27')],$$

and

$$S\mu = C\epsilon S\sigma C\lambda - S\epsilon[C\sigma S(23^\circ 27') - S\sigma S\lambda C(23^\circ 27')]. \quad (C.4)$$

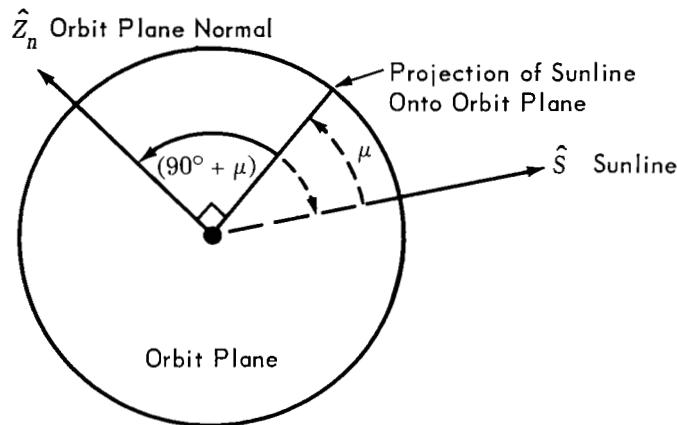


Figure C.4—Definition of sun angle.

C.2 Derivation of the Solar Panel Reference Angle

Reference is made to Figure C.5. The two degrees of freedom associated with the solar panel assembly allow the x_p axis to be adjusted so that it is parallel to the sunline vector \hat{S} . The spacecraft positive roll axis lies along the spacecraft velocity vector.

If the ascending node is expressed in terms of the equatorial plane coordinates,

$$\hat{x}_n = (C\lambda \hat{x}_e + S\lambda \hat{z}_e).$$

Then,

$$C\theta_{p0} = \frac{\hat{S} \times \hat{Z}_n}{|\hat{S} \times \hat{Z}_n|} \cdot (C\lambda \hat{x}_e + S\lambda \hat{z}_e).$$

Algebraic manipulation yields the result

$$|\hat{S} \times \hat{Z}_n|^2 = C^2\mu,$$

and further

$$C\theta_{p0} = \frac{[C\lambda (S\epsilon C(23^\circ 27') C\sigma + S\epsilon S(23^\circ 27') S\sigma S\lambda) + S\lambda (S\epsilon C(23^\circ 27') S\sigma C\lambda - C\epsilon S\sigma S\lambda)]}{C\mu}. \quad (C.5)$$

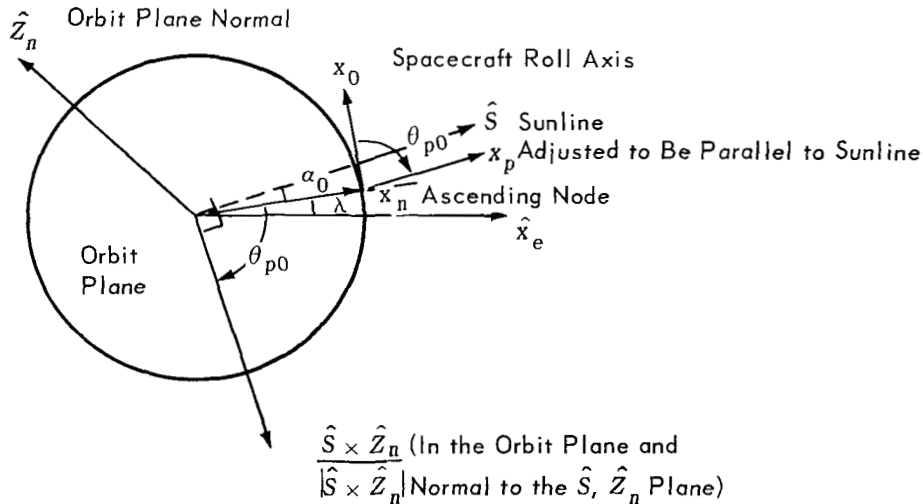


Figure C.5—Definition of initial solar panel reference angle. \hat{S} is not necessarily in the orbit plane.

C.3 Consideration of Umbra Effects

When including the disturbance torque due to driven solar panels, attention must be given to the consideration of the umbra, that portion of the orbit during which the sun is occulted by the earth. This portion of the orbit is defined by the umbra half angle ζ_0 .

In Figure C.6, the x and y axes are orthogonal and fixed in the earth. They are not necessarily coincident with the x_e and y_e axes. The orbit plane is arbitrarily rotated about the x axis through an angle μ' , where $\mu' = 90^\circ - \mu$. R_e is the radius of the earth, and h is the height of the spacecraft path above the earth.

Assume that the sun is located along the z axis and above the x, y plane. For the orientation shown, the sunline is perpendicular to the orbit plane and $\mu = 90^\circ$. If μ' is defined as $90^\circ - \mu$, it is apparent that for $\mu' = 0$, no umbra exists. As μ' is increased from zero by rotating the orbit plane about the x axis, the projected length R_e measured along the y axis on the orbit plane finally reaches $(R_e + h)$ and the earth begins to occult the sun. As μ' is increased past this point, the projected length R_e measured along the y axis on the orbit plane exceeds $(R_e + h)$. It is for this situation that an umbra of finite duration exists. The half umbra angle ζ_0 is measured from the y axis in clockwise direction to that point at which the R_e projected length onto the orbit plane equals $(R_e + h)$. For the minimum value of μ' for which occultation occurs,

$$(R_e + h) \cos \mu'_m = R_e$$

or

$$\mu'_m = \cos^{-1} \frac{R_e}{R_e + h}.$$

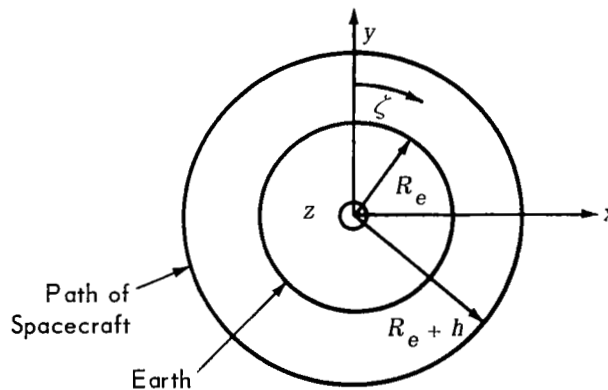


Figure C.6—Definition of half umbra angle.

If corresponding radials are drawn both on the earth cross section and on the orbit plane of Figure C.6 before the rotation of the orbit plane through the angle μ' , then after an x rotation of the orbit plane, the angle between any two of the corresponding radials can be defined by the angle ν as a function of ζ and μ . It can be shown that $C\nu = \sqrt{1 - C^2\zeta S^2\mu'}$, and for $\zeta = 0$, $C\nu = C\mu'$.

For $\mu' > \mu'_m$, the half umbra angle can be computed as

$$(R_e + h) C\nu = R_e$$

or

$$(1 - C^2\zeta S^2\mu') = \left(\frac{R_e}{R_e + h}\right)^2.$$

For $\zeta = 0$, there is a minimum μ' defined by

$$(1 - S^2\mu') = C^2\mu' = \left(\frac{R_e}{R_e + h}\right)^2$$

as before. After rearranging terms,

$$C\zeta_0 = \frac{\sqrt{1 - \left(\frac{R_e}{R_e + h}\right)^2}}{S\mu'},$$

but $S(90^\circ - \mu) = C\mu$, so

$$C\zeta_0 = \frac{\sqrt{1 - \left(\frac{R_e}{R_e + h}\right)^2}}{C\mu},$$

where R_e and h are constant, and μ is the angle between sunline and orbit plane.

Clearly, if orbital precession is neglected during any one orbit, the waveform corresponding to the incident solar energy on the solar panels is periodic at orbit rate. This means that T_{dxp} and T_{dzp} can be expanded into a Fourier series whose basic frequency is orbit rate. Furthermore, the resulting Fourier coefficients can be used to evaluate the previously discussed steady-state response function R with respect to the magnetic disturbances produced by the solar panels.

C.4 Umbra-Associated Disturbance Fourier Coefficients

The nonocculted x and z components of \mathbf{T}_{dp} are rewritten in the following manner.

$$\frac{T_{d xp}}{m_{xp} m_e / r_0^3} = (2 S_\mu S_\sigma) S(\alpha_0 + \Omega_0 t) + (-C_\mu C_\sigma) S(\alpha_0 + \theta_{p0} + \Omega_0 t)$$

$$\frac{T_{d zp}}{m_{xp} m_e / r_0^3} = (-S_\sigma S_\mu) C(\alpha_0 + \Omega_0 t) + (-C_\mu C_\sigma) C(\alpha_0 + \theta_{p0} + \Omega_0 t)$$

The phase angle α_0 was introduced to allow for the convenience of working with an umbra centered at π radians for all ϵ and λ . A plot of incident sun energy on the solar panels versus spacecraft position in orbit is shown in Figure C.7.

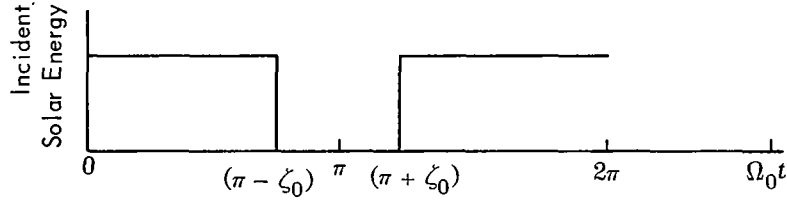


Figure C.7—Plot of incident sun energy versus orbit position.

The angle α_0 is the angle between the ascending node and the projection of the sunline onto the orbit plane. As can be seen in Figure C.5, $(\alpha_0 + \theta_{p0}) = 90^\circ$. For $\alpha_0 = 0$, the projection of the sunline onto the orbit plane is coincident with the radial that defines the ascending node. The angle α_0 can be evaluated simply,

$$C\alpha_0 = C(90^\circ - \theta_{p0}) = S\theta_{p0}$$

and

$$S\alpha_0 = S(90^\circ - \theta_{p0}) = C\theta_{p0}.$$

After expanding $T_{d xp}$ and $T_{d zp}$ and making the required trigonometric substitutions,

$$\frac{T_{d xp}}{m_{xp} m_e / r_0^3} = (2S_\mu S_\sigma S\alpha_0 - C_\mu C_\sigma) C\Omega_0 t + (2S_\mu S_\sigma C\alpha_0) S\Omega_0 t \quad (C.7)$$

and

$$\frac{T_{dzp}}{m_{xp}m_e/r_0^3} = (-S\sigma S\mu C\alpha_0) C\Omega_0 t + (S\sigma S\mu S\alpha_0 + C\mu C\sigma) S\Omega_0 t. \quad (C.8)$$

For simplicity, these equations can be rewritten as

$$T_{dxp} = A_x C\Omega_0 t + B_x S\Omega_0 t \quad (C.9)$$

and

$$T_{dzp} = A_z C\Omega_0 t + B_z S\Omega_0 t. \quad (C.10)$$

The function $f(t)$, used for analytical expression of the effect of the umbra upon these torque equations, is defined as

$$f(t) = \begin{cases} 1 & 0 \leq \Omega_0 t < (\pi - \xi_0) \\ 0 & (\pi - \xi_0) \leq \Omega_0 t < (\pi + \xi_0) \\ 1 & (\pi + \xi_0) \leq \Omega_0 t < 2\pi \end{cases}$$

Then,

$$T_{fip} = f(t) T_{dip} = \frac{a_{0i}}{2} + \sum_{n=1}^{\infty} a_{ni} Cn\Omega_0 t + \sum_{n=1}^{\infty} b_{ni} Sn\Omega_0 t, \text{ for } i = x, z, \quad (C.11)$$

where

$$a_{0i} = \frac{1}{\pi} \int_{-\pi}^{\pi} T_{fip} d\Omega_0 t,$$

$$a_{ni} = \frac{1}{\pi} \int_{-\pi}^{\pi} T_{fip} Cn\Omega_0 t d\Omega_0 t,$$

and

$$b_{ni} = \frac{1}{\pi} \int_{-\pi}^{\pi} T_{fip} Sn\Omega_0 t d\Omega_0 t.$$

The resulting Fourier coefficients are

$$\begin{aligned}
\overline{a_{0i}} &= 2A_i S\xi_0 / \pi, \\
a_{1i} &= \frac{A_i}{\pi} \left[(\pi - \xi_0) - \frac{S(2\xi_0)}{2} \right], \\
a_{2i} &= \frac{A_i}{\pi} \left[S\xi_0 + \frac{S(3\xi_0)}{3} \right], \\
&\vdots \\
a_{ni} &= (-1)^n \frac{A_i}{\pi} \left\{ \frac{S[(1-n)\xi_0]}{(1-n)} + \frac{S[(1+n)\xi_0]}{(1+n)} \right\} \text{ for } n \geq 2, \\
b_{1i} &= \frac{B_i}{\pi} \left[(\pi - \xi_0) + \frac{S(2\xi_0)}{2} \right], \\
b_{2i} &= \frac{B_i}{\pi} \left[S\xi_0 - \frac{S(3\xi_0)}{3} \right], \\
&\vdots \\
b_{ni} &= (-1)^n \frac{B_i}{\pi} \left\{ \frac{S[(1-n)\xi_0]}{(1-n)} - \frac{S[(1+n)\xi_0]}{(1+n)} \right\} \text{ for } n \geq 2.
\end{aligned}$$

The resulting Fourier expansions are

$$\begin{aligned}
T_{fxp} &= \frac{a_{0x}}{2} + a_{1x} C\Omega_0 t + a_{2x} C2\Omega_0 t + \dots + a_{nx} Cn\Omega_0 t \\
&\quad + b_{1x} S\Omega_0 t + b_{2x} S2\Omega_0 t + \dots + b_{nx} Sn\Omega_0 t
\end{aligned} \tag{C.12}$$

and

$$\begin{aligned}
T_{fzp} &= \frac{a_{0z}}{2} + a_{1z} C\Omega_0 t + a_{2z} C2\Omega_0 t + \dots + a_{nz} Cn\Omega_0 t \\
&\quad + b_{1z} S\Omega_0 t + b_{2z} S2\Omega_0 t + \dots + b_{nz} Sn\Omega_0 t.
\end{aligned} \tag{C.13}$$



APPENDIX D

LISTING OF THE OPTIMIZATION COMPUTER PROGRAM

In the computer listing shown, the program has been set up to run the search for the no-solar-panel case described in Chapter 8. The solar panel case, illustrated by Example 2, can be repeated by incorporating the changes noted within the computer program itself. Furthermore, the user is free to incorporate any parameter array of his choosing. This parameter array must include the orbit altitude and orbit inclination angle and may, for the solar panel case, include the location of the sun in the ecliptic plane, and/or the location of the ascending node relative to the vernal equinox. Zero magnetic moment for the solar panel assembly ($XMXP = 0$) tells the program that the user is interested in the no-solar-panel case.

The following four subroutines are required for the execution of the optimization routine:

(1) PRBM. This subroutine is available through the "System/360 Scientific Subroutine Package (360A-CM-03X) Version III Programmers Manual," page 191, IBM H20-0205-3. The subroutine is a polynomial solver.

(2) QREIG.

(3) QRT.

(4) HESSEN. Subroutines 2, 3, and 4 are available through the SHARE Program Catalog, SDA 3006-01, August 1964. Their purpose is to solve for eigenvalues by the QR transform. The author of the SHARE program is F. P. Emad.

```

      IMPLICIT REAL *8(A-H,O-Z)
      REAL *4 COE,X,Y,PUL,DAM,DAMP,DAMM
      DIMENSION CSV(6),CF(6),CCF(6),CSAV(6)
1000 FORMAT(D12.4,2E12.4,7I5,4D12.4)
2000 FORMAT(1H1)
      20 FORMAT(' R IN RADS.-RE AND+IM PARTS OF DUM.          SYSTEM PARAMETE
      1R SETS          TAU          ZETA          EPSILON          LAMDA  ')
      21 FORMAT('          SYST ROOT NRMLZD BY.001  M7  M1  M2  M3
      1M4  M5  M6          ANGLES ARE IN RADIANS  ')
      10 FORMAT('          RMS ROLL          RMS YAW          RMS GIMBAL          ERRO
      1RS IN RADIANS  ')
      C RESIDUAL SPACECRAFT MAGNETIC MUMENT IN FT LB / GAUSS
      XM0=3.96D0*7.38D-5

```

```

C RESIDUAL MAGNETIC MOMENT OF BOTH PANELS IN FT LB /GAUSS
  XMP=0.D0
C USE FOR SOLAR PANEL CASE
  XMP=5.D0*7.380-5
C DAMM=1/TM=MAXIMUM SETTLING TIME IN SECONDS
  DAMM=.0265D0
C IF PROGRAM PRINTS OUT N1=0, NO PARAMETER SET WAS ABLE TO MEET THE DAMPING
C REQUIREMENT
C USE (*) FOR NO SOLAR PANEL CASE, AND (***) FOR SOLAR PANEL CASE
  N1=0
C L1=NO. OF INERTIA DIFFERENTIALS
  L1=6
C      DO 171 M1=2,L1,2                                     (***)
      DO 171 M1=1,L1                                         (*)
      SQ=1.D12
C L7= NO. OF YAW INERTIAS
  L7=3
C      DO 177 M7=3,L7                                     (***)
      DO 177 M7=1,L7                                         (*)
C L2= NO. OF RATIOS
  L2=5
C      DO 172 M2=1,L2                                     (***)
      DO 172 M2=1,L2                                         (*)
C L3= NO. OF GIMBAL AXIS ANGLES
  L3=5
C      DO 173 M3=1,L3,2                                     (***)
      DO 173 M3=1,L3                                         (*)
C L4= NO. OF MOMENTUM BIASES
  L4=12
      DO 174 M4=1,L4
C L5= NO. OF DAMPING RATIOS
  L5=3
      DO 175 M5=1,L5
C L6= NO. OF SPRING CONSTANTS
  L6=5
C      DO 176 M6=1,L6,2                                     (***)
      DO 176 M6=1,L6                                         (*)
      CALL CMPUT(SQR,DAMP,M7,M1,M2,M3,M4,M5,M6,TS,ZS,EPSLS,XLAMS,CSV,
1DAMPF,CF,XIZ,XMP,XM0)
      IF(DAMP -DAMM)176,176,178
178 CONTINUE
C SCALE SQRT(WEIGHTED MEAN SQUARE ERROR FCN) FOR VARIOUS YAW INERTIAS
  SQR=SQR/(XIZ*1.D-6)
  IF( SQR -SQ)179,176,176
C SQRT(WEIGHTED MEAN SQUARE ERROR FCN R )
179 SQ=SQR
C SAVE MINIMUM VALUES ASSOCIATED WITH MINIMUM WEIGHTED MEAN SQUARE ERROR
C NEGATIVE OF REAL PART OF DOMINANT SYSTEM ROOT/ .001
  DAM=DAMP
  N7=M7
  N1=M1
  N2=M2
  N3=M3
  N4=M4
  N5=M5
  N6=M6
C WEIGHTING FACTORS DEFINED IN CMPUT
  CCF(2)=CF(2)
  CCF(4)=CF(4)
  CCF(6)=CF(6)

```

```

C 3 COMPONENTS OF WEIGHTED ERROR
  CSAV(2)=CSV(2)
  CSAV(4)=CSV(4)
  CSAV(6)=CSV(6)
C DAMPED NATURAL FREQ. OF DOMINANT SYSTEM ROOT/.001
  DFREQ=DAMPF
C YAW INERTIA
  XI=XIZ
176 CONTINUE
175 CONTINUE
174 CONTINUE
173 CONTINUE
172 CONTINUE
177 CONTINUE
  WRITE(6,20)
  WRITE(6,21)
  WRITE(6,1000) SQ ,DAM,DFREQ,N7,
    IN1,N2,N3,N4,N5,N6
    2,TS,ZS,EPS,S,XLAMS
CSCALE SQR(TMEAN SQUARE ERROR) COMPONENTS FOR VARIOUS YAW INERTIAS
  DO 4000 KSV=2,6,2
    CSAV(KSV)=(DSQRT(CSAV(KSV)/CF(KSV)))/(XI *1.0-6) )
4000 CONTINUE
3000 FORMAT(3D18.6)
  WRITE(6,10)
  WRITE(6,3000)CSAV(2),CSAV(4),CSAV(6)
  WRITE(6,2000)
  N1=0
171 CONTINUE
C
  RETURN
  END

SUBROUTINE CMPT(SQR,DAMP,M7,M1,M2,M3,M4,M5,M6,TS,ZS,EPSLS,XLAMS,
1CSV,DAMPF,CF,XIZ,XXXP,XM0)
  IMPLICIT REAL*8(A-H,I-Z)
  REAL *4OMAT,RR,RI ,ROUTR,ROUTI
  REAL *4 CUE,X,Y,PUL ,DAM,DAMP
  REAL *4 ZETA
  DIMENSION OMAT(10,10) ,CH1(3,6),SQR2(6)
  DIMENSION E(3),C(6),CF(6),CSV(6),XIZS(5),DIFFR(6)
  DIMENSION A(6,6),U(6),AL(7),BETA(5),RATIO(5),HA(11),BG(6),QG(9)
  DIMENSION CUE(11),X(11),Y(11),POL(11)
  DIMENSION TMX(3),ZMX(3),XMAX(3)
C BYPASS OPTIMIZATION OF LAMDA ,EPSILON, ZETA,AND TAU ACCORDING TO NFG1 THRU 4
C FOR SPACECRAFT WITH SOLAR PANELS. IGNORE FOR NO SOLAR PANEL CASE.
C BYPASS IF 0, DON'T BYPASS IF NOT NFG1=LAMDA,NFG2=EPSILON, NFG3=ZETA,
C NFG4=TAU
C USER MUST DEFINE ANY BYPASSED ANGLES AT THIS POINT (IN RADIANS)
  NFG1=1
  NFG2=1
  NFG3=1
  NFG4=1
C MAGNETIC MOMENT OF EARTH IN GAUSS FT FT FT
  XME=2.845D21
  F=3.141592D0/180.D0
C USER CAN SUPPLY ANY 3 WEIGHTING FACTORS--- CF(2)=CPHI, CF(4)=CPSI, CF(6)=CGAM
  CF(2)=1.00
  CF(4)=1.00
  CF(6)=1.00

```

```

C USER CAN SUPPLY UP TO 5 VALUES OF YAW INERTIA IN FT LB SEC SEC
  XIZS(1)=10.00
  XIZS(2)=100.00
  XIZS(3)=200.00
C USER CAN SUPPLY UP TO 5 VALUES OF GIMBAL AXIS ANGLE IN RADIANS
  BETA(1)=0.00
  BETA(2)=22.500*F
  BETA(3)=45.00*F
  BETA(4)=67.500*F
  BETA(5)=90.00*F
C USER CAN SUPPLY UP TO 6 DIFFERENTIAL INERTIAS IN FT LB SEC SEC
  DIFFR(1)=50.00
  DIFFR(2)=100.00
  DIFFR(3)=250.00
  DIFFR(4)=500.00
  DIFFR(5)=1000.00
  DIFFR(6)=2000.00
C USER CAN SUPPLY UP TO 5 INERTIA RATIOS
  RATIO(1)=.7500
  RATIO(2)=1.00
  RATIO(3)=1.33333300
C USER CAN SUPPLY UP TO 12 MOMENTUM BIAS VALUES IN FT LB SEC(H IN PRGRM=-HA)
  HA(1)=10.00
  HA(2)=5.00
  HA(3)=2.500
  HA(4)=1.00
  HA(5)=.500
  HA(6)=.100
  HA(7)=-.100
  HA(8)=-.500
  HA(9)=-1.00
  HA(10)=-2.500
  HA(11)=-5.00
  HA(12)=-10.00
C USER CAN SUPPLY UP TO 9 SPRING CONSTANTS IN FT LB / RADIAN
  QG(1)=1.0-4
  QG(2)=.33D-3
  QG(3)=1.0-3
  QG(4)=.33D-2
  QG(5)=1.0-2
C USER CAN SUPPLY UP TO 6 DAMPING CONSTANTS IN FT LB SEC/ RADIANS
  BG(1)=.2500
  BG(2)=.500
  BG(3)=.7500
C DEFINITION OF NORMALIZED PARAMETER SET
  H=HA(M4)/(XIZS(M7)*1.0-3)
  H=-H
  Q=QG(M6)/(XIZS(M7)*1.0-6)
C STABILITY CHECK
  IF(Q-H)7,7,8
    7 SQR                                =1.012
      DAMP                                =0.
      GO TO 6
    8 CONTINUE
      B=BG(M5)/(XIZS(M7)*1.0-3)
      SB=DSIN(BETA(M3))
      CB=DCOS(BETA(M3))
      CSB=CB*CB
      SSB=SB*SB

```



```

C GAM appears as  $\rho$  in the text.
  GAM=(DIFFR(M1)+XIZS(M7))/XIZS(M7)
  GAM2=.25D0*(H*H*CSB/(Q-H)+4.D0+H)
  GAM1=H*H*SSB/(Q-H)+ALF+H
C USE (*) FOR NO SOLAR PANEL CASE AND (***) FOR SOLAR PANEL CASE. THE 125.
C FT LB SEC SEC REPRESENTS THE ROLL PITCH INERTIA DIFFERENTIAL DICTATED BY
C A PARTICULAR SET OF PANELS AND MUST BE ALTERED TO MATCH THE PANELS CHOSEN
  ALF=GAM*RATIO(M2)
  ALF=GAM+125.D0/XIZS(M7)
C STABILITY CHECK
  IF(GAM-GAM1)11,11,12
  12 IF(GAM-GAM2)11,11,13
  13 CONTINUE
C STABILITY CHECK
  TSTT=(Q-H)*(-ALF+GAM-H)*(4.D0*GAM-4.D0-H)-H*H*CSB*(-ALF+GAM-H)-H*
  1H*SSB*(4.D0*GAM-4.D0-H)
  IF(TSTT)11,11,9913
  11 CONTINUE
  DAMP =0.
  SQR =1.D12
  GO TO 6
9913 CONTINUE
C COEFFICIENTS OF 6 TRANSFER FUNCTION NUMERATOR POLYNOMIALS IN W
  A(1,1)=(Q-H)*(ALF-GAM+CSB*H)+SSB*H*H
  A(1,2)=B*(ALF-GAM+CSB*H)+(Q-H)*(SB*H*(CB-1.D0))
  A(1,3)=H*(SB*B*(CB-1.D0)-CSB*H) -(Q-H)
  A(1,4)=-B
  A(2,1)=-CB*SB*H*(Q-2.D0*H)
  A(2,2)=(Q-H)*(-1.D0-ALF+GAM-CB*H)-SB*H*(SB*Q+CB*B)-CSB*H*H
  A(2,3)=B*(GAM-ALF-1.D0-CB*H-SSB*H)+CB*SB*H*H
  A(2,4)=0.D0
  A(3,1)=(Q-H)*SB*H-CB*SB*H*(Q-2.D0*H)
  A(3,2)=(Q-H)*(1.D0+ALF-GAM)+H*(CSB*Q+SSB*H+SB*B*(1.D0-CB))
  A(3,3)=B*(1.D0+ALF-GAM)+CB*H*(CB*B+SB*H)
  A(3,4)=0.D0
  A(4,1)=(Q-H)*(4.D0-4.D0*GAM+CB*H+SSB*H)+CSB*H*H
  A(4,2)=-SB*CB*H*(Q-H)+H*B*(CB+SSB)+4.D0*B*(1.D0-GAM)
  A(4,3)=-ALF*(Q-H)+SB*H*(-CB*H-SB*H)
  A(4,4)=-B*ALF
  A(5,1)=CB*H*(ALF-GAM+H)-SSB*H*H
  A(5,2)=-SB*H
  A(5,3)=CB*H*(ALF-GAM+H)-SSB*H*H
  A(5,4)=-SB*H
  A(6,1)=4.D0*SB*H*(GAM-1.D0)-SB*H*H*(1.D0+CB)
  A(6,2)=CB*H*(-ALF-3.D0*GAM+3.D0)
  A(6,3)=SB*H*(GAM-1.D0)-SB*H*H*(1.D0+CB)
  A(6,4)=-CB*H*ALF
C COEFFICIENTS OF CHARACTERISTIC POLYNOMIAL IN W
  D(1)=(Q-H)*(-ALF+GAM-H)*(4.D0*GAM-4.D0-H)-H*H*CSB*(-ALF+GAM-H)-H*
  1H*SSB*(4.D0*GAM-4.D0-H)
  D(2)=(-ALF+GAM-H)*(4.D0*GAM-4.D0-H)*B
  D(4)=ALF*(-GAM+2.D0+H)+GAM*GAM+2.D0*(1.D0-H)*GAM-3.D0+H*H*H
  D(3)=(Q-H)*D(4)+H*H*CSB*(2.D0*ALF+2.D0*GAM-3.D0+H)+H*H*SSB*(-GAM
  1+H+2.D0)
  D(4)=D(4)*B
  D(5)=ALF*(Q-H)+H*H*(ALF*CSB+SSB)
  D(6)=ALF*B
  W=0.D0
  DO 15 N=1,3
  DO 14 M=1,6
  CHID=(A(M,1)-A(M,3)*W*W)**2+(A(M,2)*W-A(M,4)*W**3)**2

```

```

C EVALUATION OF MAGNITUDE OF NUMERATORS OF 6 TRANSFER FUNCTIONS AT W=0,W=1,W=2
  CHID=DSQRT(CHID)
  CHI(N,M)=CHID
14 CONTINUE
C EVALUATION OF MAGNITUDE SQUARED VALUE OF DENOMENATOR OF TRANSFER FUNCTION
C AT W=0,W=1,W=2
  E(N)=(D(1)-D(3)*W*W+D(5)*W**4)**2+(D(2)*W-D(4)*W**3+D(6)*W**5)**2
15 W=W+1.DO
  SQR=0.DO
  C23=DCOS(23.5D0*F)
  S23=DSIN(23.5D0*F)
C USER INPUT ORBIT ALTITUDE IN NAUTICAL MILES
  ALT=600.DO
C USER INPUT SIGMA IN RADIANS , THE ORBIT INCLINATION ANGLE
  SIGMA=1.DO*3.141592D0/6.DO
  PI=3.141592D0
  CMX=XMXP*XME/(((3440.DO+ALT)*6076.DO)**3)
  CMO=XMO *XME/(((3440.DO+ALT)*6076.DO)**3)
  SS=DSIN(SIGMA)
  CS=DCOS(SIGMA)
  UMC=DSQRT(1.DO-(3440.DO/(3440.DO+ALT))**2)
C BYPASS IF NO SOLAR PANELS
  IF(XMXP)1001,1000,1001
1001 CONTINUE
C FINDING WORST CASE LAMDA,EPSILON,ZETA, AND TAU
C ANGLE INCREMENT FOR LAMDA AND EPSILON SEARCH IN RADIANS
  XSEAT=30.DO*F
C ANGLE INCREMENT FOR ZETA AND TAU SEARCH IN RADIANS
  XSEAR=45.DO*F
  IF(NFG1)2000,2001,2000
2000 CONTINUE
  XLAM=0.DO
  DO 100 IS0=1,12
2001 IF(NFG2)2002,2003,2002
2002 CONTINUE
  EPSL=0.DO
  DO 101 IS1=1,12
2003 IF(NFG3)2004,2005,2004
2004 CONTINUE
  Z=0.DO
  DO 102 IS2=1,8
2005 IF(NFG4)2006,2007,2006
2006 CONTINUE
  T=0.DO
  DO 103 IS3=1,8
2007 CONTINUE
  SE=DSIN(EPSL)
  CE=DCOS(EPSL)
  SXL=DSIN(XLAM)
  CXL=DCOS(XLAM)
  ST=DSIN(T)
  CT=DCOS(T)
  SZ=DSIN(Z)
  CZ=DCOS(Z)
  SXMU=CE*SS*CXL-SE*(CS *S23-SS*SXL*C23)
  CXMU=DSQRT(1.DO-SXMU*SXMU)
  IF(DABS(CXMU)-.01D0)105,105,104
105 CONTINUE
  SALZ=1.DO
  CALZ=0.DO

```

```

        CUMB=1.D0
        GO TO 108
104  CONTINUE
        SAL Z =(CXL*(SE*C23*CS+SE*S23*SS*SXL)+SXL*(SE*C23*SS*CXL-CE*SS*SXL)
        1)/CXMU
        CAL Z=DSQRT(1.D0-SAL Z*SAL Z)
        CUMB=UMC/CXMU
        IF(DABS(CUMB)-1.D0)106,106,107
107  CONTINUE
        CUMB=1.D0
106  CONTINUE
108  CONTINUE
        SUMB=DSQRT(1.D0-CUMB*CUMB)
        UMB=DARSIN(SUMB)
C  COMPUTATION OF DISTURBANCE TORQUES
        AX=2.D0*SXMU*SS*SAL Z-CXMU*CS
        AX=AX*CMX
        AZ=-SS*SXMU*CAL Z*CMX
        BX=2.D0*SXMU*SS*CAL Z*CMX
        BZ=SS*SXMU*SAL Z+CXMU*CS
        BZ=BZ*CMX
        AOX=2.D0*AX*SUMB/PI
        AOZ=2.D0*AZ*SUMB/PI
        A1X=AX*(PI-UMB-SUMB*CUMB)/PI
        A1Z=AZ*(PI-UMB-SUMB*CUMB)/PI
        A2X=AX*(SUMB+SUMB-(4.D0/3.D0)*SUMB*SUMB*SUMB)/PI
        A2Z=AZ*(SUMB+SUMB-(4.D0/3.D0)*SUMB*SUMB*SUMB)/PI
        B1X=BX*(PI-UMB+SUMB*CUMB)/PI
        B1Z=BZ*(PI-UMB+SUMB*CUMB)/PI
        B2X=BX*((4.D0/3.D0)*SUMB*SUMB*SUMB)/PI
        B2Z=BZ*((4.D0/3.D0)*SUMB*SUMB*SUMB)/PI
        A0=CZ*CS *CM0
        A1=2.D0*SZ*ST*SS *CM0
        B0=-SZ*CT*CS *CM0
        B1=-SZ*ST*SS *CM0
        CC0=A0+AOX/2.D0
        CC1=B0+AOZ/2.D0
        CC31=A1+B1X
        CC32=B1Z
        CC41=B1+A1Z
        CC42=A1X
        CC61=B2X
        CC62=B2Z
        CC71=A2X
        CC72=A2Z
C  COMPUTATION OF WEIGHTED MEAN SQUARE ERROR
        DO 23 N=2,6,2
        C(N)=CF(N)*(((CC0*CHI(1,N-1)+CC1*CHI(1,N))*2)/E(1)+.5D0*(((
        1CC31*CHI(2,N-1)+CC32*CHI(2,N))*2+(CC41*CHI(2,N)+CC42*CHI(2,N-1))*2
        1*2)
        2/E(2)+((CC61*CHI(3,N-1)+CC62*CHI(3,N))*2+(CC71*CHI(3,N-1)+CC72*
        3CHI(3,N))*2)/E(3)))
        23  CONTINUE
        RH=C(2)+C(4)+C(6)
        RH=DSQRT(RH)
C  FINDING LARGEST SQRT(WEIGHTED MEAN SQUARE ERROR)
        IF(RH-SQR)200,200,201
201  SQR=RH

```

```

C COMPONENTS OF WEIGHTED MEAN SQUARE ERROR
  CSV(2)=C(2)
  CSV(4)=C(4)
  CSV(6)=C(6)
C SAVING WORST CASE ANGLES
  TS=T
  ZS=Z
  EPSL S=EPSL
  XLAMS=XL AM
  200 CONTINUE
    IF(NFG4)2011,2012,2011
  2011 CONTINUE
    103 T=T+XSEAR
  2012 IF(NFG3)2013,2014,2013
  2013 CONTINUE
    102 Z=Z+XSEAR
  2014 IF(NFG2)2015,2016,2015
  2015 CONTINUE
    101 EPSL=EPSL+XSEAT
  2016 IF(NFG1)2017,2018,2017
  2017 CONTINUE
    100 XLAM=XL AM+XSEAT
  2018 CONTINUE
C BYPASS FOR PANEL CASE
  IF(XMXP)1101,1000,1101
C FINDING WORST CASE R (WEIGHTED MEAN SQR ERROR) AS A FUNCTION OF THE
C MAGNETIC MOMENT LOCATION FOR THE CASE OF NO SOLAR PANELS
  1000 CONTINUE
    CAPA=CS*CS*(CF(2)*CHI(1,1)**2+CF(4)*CHI(1,3)**2+CF(6)*CHI(1,5)**2)
    1/E(1)
    CAPB=CS*CS*(CF(2)*CHI(1,2)**2+CF(4)*CHI(1,4)**2+CF(6)*CHI(1,6)**2)
    1/E(1)
    CAPC=-2.00*CS*CS*(CF(2)*CHI(1,1)*CHI(1,2)+CF(4)*CHI(1,3)*CHI(1,4)
    1+CF(6)*CHI(1,5)*CHI(1,6))/E(1)
    CAPD=.50*SS*SS*(4.00*(CF(2)*CHI(2,1)**2+CF(4)*CHI(2,3)**2+CF(6)*
    1CHI(2,5)**2)+(CF(2)*CHI(2,2)**2+CF(4)*CHI(2,4)**2+CF(6)*CHI(2,6)**
    22))/E(2)
    TWOZ=DATAN2(CAPC,CAPA-CAPB)
    XMAX(1)=CAPD
    ZMX(1)=PI/2.00
    TMX(1)=ZMX(1)
    XMAX(2)=CAPA
    ZMX(2)=0.00
    TMX(2)=ZMX(1)
    TMX(3)=0.00
    ZMX(3)=TWOZ/2.00
    CZ=DCOS(ZMX(3))
    SZ=DSIN(ZMX(3))
    XMAX(3)=CAPA*CZ*CZ+CAPB*SZ*SZ+CAPC*CZ*SZ
    RH=0.00
C FINDING LARGEST WEIGHTED NORMALIZED MEAN SQUARE ERROR FUNCTION FOR NO PANEL
C CASE
  DO 1003 MX=1,3
    IF(XMAX(MX)-RH)1003,1002,1002
  1002 RH=XMAX(MX)
    Z=ZMX(MX)
    T=TMX(MX)
    CZ=DCOS(Z)
    SZ=DSIN(Z)
    CT=DCOS(T)
    ST=DSIN(T)

```

```

1003 CONTINUE
  A0=CZ*CS *CM0
  A1=2.00*SZ*ST*SS *CM0
  B0=-SZ*CT*CS *CM0
  B1=-SZ*ST*SS *CM0
  CC0=A0
  CC1=B0
  CC31=A1
  CC32=0.00
  CC41=B1
  CC42=0.00
  CC61=0.00
  CC62=0.00
  CC71=0.00
  CC72=0.00
  DO123 N=2,6,2
  C(N )=CF(N )*((((CC0*CHI(1,N-1)+CC1*CHI(1,N))**2 ) /E(1)+.5D0*((
1CC31*CHI(2,N-1)+CC32*CHI(2,N))**2+(CC41*CHI(2,N)+CC42*CHI(2,N-1))**
1*2)
  2/E(2)+((CC61*CHI(3,N-1)+CC62*CHI(3,N))**2+(CC71*CHI(3,N-1)+CC72*
3CHI(3,N))**2)/E(3)))
123 CONTINUE
C FINDING SQRT(WEIGHTED MEAN SQR ERROR FCN) FOR NO PANEL CASE
  RH=DSQRT(RH) *CM0
  SQR=RH
  RF=RT
C COMPONENTS OF WEIGHTED MEAN SQUARE ERROR FOR NO PANEL CASE
  CSV(2)=C(2)
  CSV(4)=C(4)
  CSV(6)=C(6)
C WORST CASE ANGLES FOR NO PANEL CASE
  TS=T
  ZS=Z
  EPSLS=0.00
  XLAMS=0.00
1101 CONTINUE
  CUE(1)=D(1)
  CUE(2)=D(2)
  CUE(3)=D(3)
  CUE(4)=D(4)
  CUE(5)=D(5)
  CUE(6)=D(6)
  IC=6
C FACTORING NORMALIZED CHARACTERISTIC POLYNOMIAL
  CALL PRBM(CUE,IC,X,Y,POL,IR,IER)
  X(6)=0.
  Y(6)=0.
  IF(IER)20,21,20
C ALTERNATE METHOD OF FACTORING POLYNOMIAL
20 CONTINUE
  H=HA(M4)
  H=-H
  B=BG(M5)
  Q=QG(M6)
  OMG=.001D0
  XI=XIZS(M7)
  QMAT(1,1)=0.00
  QMAT(1,3)=0.00
  QMAT(1,4)=0.00
  QMAT(1,5)=0.00
  QMAT(5,1)=0.00

```

```

      QMAT(5,2)=0.D0
      QMAT(5,3)=0.D0
      QMAT(5,5)=0.D0
      QMAT(1,2)=1.D0
      QMAT(5,4)=1.D0
      QMAT(2,1)=4.D0*UMG*UMG *(1.D0-GAM)/ALF+OMG*H/(ALF*XI)-SB*CB*OMG*H
1)H/(ALF*XI*B)
      QMAT(2,2)=-SSB*H*H/(ALF*XI*B)
      QMAT(2,3)=(Q-H*UMG)*SB*H/(ALF*XI*B)+CB*OMG*H/(ALF*XI)
      QMAT(2,5)=SSB*UMG*H*H/(ALF*XI*B)
      QMAT(3,1)=CB*OMG*H/(B)
      QMAT(3,2)=H*SB/B
      QMAT(3,3)=(H*UMG-Q)/B
      QMAT(3,4)=CB*H/B
      QMAT(3,5)=-OMG*H*SB/B
      QMAT(4,1)=-CSB*UMG*H*H/(XI*B)
      QMAT(4,2)=OMG*(GAM-1.D0-ALF)-H/XI-CB*SB*H*H/(XI*B)
      QMAT(4,3)=(Q-H*OMG)*CB*H/(XI*B)-OMG*SB*H/XI
      QMAT(4,4)=-CSB*H*H/(B*XI)
      QMAT(4,5)=OMG*H/XI-OMG*OMG*(GAM-ALF)+CB*SB*OMG*H*H/(XI*B)
      QMAT(2,4)=OMG*(1.D0+(1.D0-GAM)/ALF)+H/(ALF*XI)-CB*SB*H*H/(ALF*XI*B)
1)
      L=5
      IPRNT=1
      IPRNT=0
      CALL HESSEN(QMAT,L)
      CALL QREIG(QMAT,L,X      ,Y      , IPRNT)
C
C NORMALIZING ROOTS
      DO 9182 NFIN =1,5
      Y(NFIN )=Y(NFIN )*1000.
      X(NFIN )=X(NFIN )*1000.
9182 CONTINUE
      21 CONTINUE
C FINDING LEAST DAMPED ROOT OF CHARACTERISTIC POLYNOMIAL
      DAM=100.
      DO 16 NRT=1,5
      X(NRT)=-X(NRT)
      IF (X(NRT)-DAM)18,16,16
18 DAM=X(NRT)
      DAMF=Y(NRT)
16 CONTINUE
      DAMP                      =DAM
      DAMPF=DAMF
      6 CONTINUE
      XIZ=XIZS(M7)
      RETURN

```

APPENDIX E **DEVELOPMENT OF THE STATE MATRIX FOR THE EQUATION SET** **WITH DRIVEN SOLAR PANELS**

Let

$$x_1 = \phi ,$$

$$x_2 = \dot{\phi} ,$$

$$x_3 = \gamma ,$$

$$x_4 = \dot{\psi} ,$$

$$x_5 = \psi ,$$

$$a = -S\beta C\beta H_b + \dot{I}_{p0}(11) ,$$

$$b = \Omega_0(I_1' + I_3' - I_2') + S^2\beta H_b + \dot{I}_{p0}(13) ,$$

$$c = C\beta B_g - S\beta H_b ,$$

$$d = 4\Omega_0^2(I_3' - I_2') + S^2\beta\Omega_0 H_b + \Omega_0 \dot{I}_{p0}(13) ,$$

$$e = \Omega_0^2 \dot{I}_{p0}(13) + \Omega_0 S\beta C\beta H_b - \Omega_0 \dot{I}_p(11) ,$$

$$f = k_g \cdot H_b \Omega_0 ,$$

$$g = -\Omega_0(I_1' + I_3' - I_2') - C^2\beta H_b + \dot{I}_{p0}(13) ,$$

$$h = S\beta C\beta H_b + \dot{I}_{p0}(33) ,$$

$$p = -S\beta B_g - C\beta H_b ,$$

$$q = 4\Omega_0^2 \dot{I}_{p0}(13) + S\beta C\beta H_b \Omega_0 + \Omega_0 \dot{I}_{p0}(33) ,$$

$$r = \Omega_0 C^2\beta H_b - \Omega_0^2(I_2' - I_1') - \Omega_0 \dot{I}_{p0}(13) ,$$

$$s = I_3' c + \dot{I}_{p0}(13)p ,$$

$$t = I_1' p + \dot{I}_{p0}(13)c ,$$

and

$$C_k = \frac{-1}{I_{p0}^2(13) - I_3' I_1'} .$$

After rewriting Equations (7.5), (7.6), and (7.7) in the notation introduced above,

$$\begin{aligned} & -H_b S \beta x_2 - C \beta H_b x_4 + B_g \dot{x}_3 - C \beta \Omega_0 H_b x_1 + H_b S \beta \Omega_0 x_5 + f x_3 = 0, \\ & -I_1' \dot{x}_2 + I_{p0}(13) \dot{x}_4 + a x_2 + b x_4 + c \dot{x}_3 + d x_1 + e x_5 + C \beta k_g x_3 = 0, \end{aligned}$$

and

$$I_{p0}(31) \dot{x}_2 - I_3' \dot{x}_4 + g x_2 + h x_4 + p \dot{x}_3 + q x_1 + r x_5 - k_g S \beta x_3 = 0.$$

After rearranging terms,

$$\begin{aligned} \dot{x}_3 &= -\frac{1}{B_g} (f x_3 + H_b S \beta \Omega_0 x_5 - C \beta \Omega_0 H_b x_1 - H_b S \beta x_2 - C \beta H_b x_4), \\ I_{p0}(13) \dot{x}_4 - I_1' \dot{x}_2 &= - (a x_2 + b x_4 + c \dot{x}_3 + d x_1 + e x_5 + C \beta k_g x_3), \end{aligned}$$

and

$$-I_3' \dot{x}_4 + I_{p0}(31) \dot{x}_2 = - (g x_2 + h x_4 + p \dot{x}_3 + q x_1 + r x_5 - k_g S \beta x_3),$$

where $I_{p0}(13) = I_{p0}(31)$.

After solving the second two equations simultaneously,

$$\begin{aligned} \dot{x}_2 &= C_k \left\{ x_2 \left[I_3' a + g I_{p0}(13) \right] + x_4 \left[I_3' b + h I_{p0}(13) \right] + \dot{x}_3 \left[I_3' c + p I_{p0}(13) \right] \right. \\ &\quad \left. + x_1 \left[I_3' d + q I_{p0}(13) \right] + x_5 \left[I_3' e + r I_{p0}(13) \right] + x_3 \left[I_3' C \beta k_g - I_{p0}(13) k_g S \beta \right] \right\} \\ \dot{x}_4 &= C_k \left\{ x_2 \left[a I_{p0}(13) + g I_1' \right] + x_4 \left[b I_{p0}(13) + h I_1' \right] + \dot{x}_3 \left[c I_{p0}(13) + p I_1' \right] \right. \\ &\quad \left. + x_1 \left[d I_{p0}(13) + q I_1' \right] + x_5 \left[e I_{p0}(13) + r I_1' \right] + x_3 \left[I_{p0}(13) C \beta k_g - I_1' k_g S \beta \right] \right\}. \end{aligned}$$

After eliminating \dot{x}_3 and rearranging terms, the equation set can be written directly in its state matrix form:

$$\begin{aligned} \dot{x}_1 &= x_1(0) + x_2(1) + x_3(0) + x_4(0) + x_5(0), \\ \dot{x}_2 &= C_k \left\{ x_1 \left[I_3' d + q I_{p0}(13) + \frac{s}{B_g} C \beta \Omega_0 H_b \right] + x_2 \left[I_3' a + g I_{p0}(13) + \frac{s}{B_g} H_b S \beta \right] \right. \\ &\quad \left. + x_3 \left[I_3' C \beta k_g - I_{p0}(13) k_g S \beta - \frac{s}{B_g} f \right] + x_4 \left[I_3' b + h I_{p0}(13) + \frac{s}{B_g} C \beta H_b \right] \right. \\ &\quad \left. + x_5 \left[I_3' e + r I_{p0}(13) - \frac{s}{B_g} H_b S \beta \Omega_0 \right] \right\}, \end{aligned}$$

$$\begin{aligned}\dot{x}_3 &= \frac{-1}{B_g} \left[x_1(-C\beta\Omega_0 H_b) + x_2(-H_b S\beta) + x_3(f) + x_4(-C\beta H_b) + x_5(H_b S\beta\Omega_0) \right], \\ \dot{x}_4 &= C_k \left\{ x_1 \left[dI_{p0}(13) + qI_1' + \frac{t}{B_g} C\beta\Omega_0 H_b \right] + x_2 \left[aI_{p0}(13) + gI_1' + \frac{t}{B_g} H_b S\beta \right] \right. \\ &\quad + x_3 \left[I_{p0}(13)C\beta k_g - I_1' k_g S\beta - \frac{t}{B_g} f \right] + x_4 \left[bI_{p0}(13) + hI_1' + \frac{t}{B_g} C\beta H_b \right] \\ &\quad \left. + x_5 \left[eI_{p0}(13) + rI_1' - \frac{t}{B_g} H_b S\beta\Omega_0 \right] \right\},\end{aligned}$$

and

$$\dot{x}_5 = x_1(0) + x_2(0) + x_3(0) + x_4(1) + x_5(0) .$$

The elements of the system state matrix are

$$a(11) = 0,$$

$$a(12) = 1,$$

$$a(13) = 0,$$

$$a(14) = 0,$$

$$a(15) = 0,$$

$$a(21) = C_k \left[I_3' d + I_{p0}(13)q + \frac{s}{B_g} C\beta\Omega_0 H_b \right],$$

$$a(22) = C_k \left[I_3' a + I_{p0}(13)g + \frac{s}{B_g} S\beta H_b \right],$$

$$a(23) = C_k \left[I_3' C\beta k_g - I_{p0}(13)k_g S\beta - \frac{s}{B_g} f \right],$$

$$a(24) = C_k \left[I_3' b + I_{p0}(13)h + \frac{s}{B_g} C\beta H_b \right],$$

$$a(25) = C_k \left[I_3' e + I_{p0}(13)r - \frac{s}{B_g} H_b S\beta\Omega_0 \right],$$

$$a(31) = \frac{1}{B_g} (C\beta\Omega_0 H_b) ,$$

$$a(32) = \frac{1}{B_g} (H_b S\beta) ,$$

$$a(33) = \frac{1}{B_g} (-f) ,$$

$$a(34) = \frac{1}{B_g} (C\beta H_b) ,$$

$$a(35) = \frac{1}{B_g} (-H_b S\beta\Omega_0) ,$$

$$a(41) = C_k \left[I_{p0}(13)d + I_1' q + \frac{t}{B_g} C\beta\Omega_0 H_b \right] ,$$

$$a(42) = C_k \left[I_{p0}(13)a + I_1' g + \frac{t}{B_g} H_b S\beta \right] .$$

$$a(43) = C_k \left[I_{p0}(13)C\beta k_g - I_1' k_g S\beta - \frac{t}{B_g} f \right] ,$$

$$a(44) = C_k \left[I_{p0}(13)b + I_1' h + \frac{t}{B_g} C\beta H_b \right] ,$$

$$a(45) = C_k \left[I_{p0}(13)e + I_1' r - \frac{t}{B_g} H_b S\beta\Omega_0 \right] ,$$

$$a(51) = 0 ,$$

$$a(52) = 0 ,$$

$$a(53) = 0 ,$$

$$a(54) = 1 ,$$

and

$$a(55) = 0 .$$

:

APPENDIX F

LISTING OF LINEAR DIGITAL COMPUTER SIMULATION PROGRAM

The user may substitute into this computer program any parameter set of his choosing. Similarly, he is free to alter the initial condition set and the length of the computer run by making the appropriate substitutions. In addition, this program can be used to make disturbance torque runs such as those described in Section (5.5) and for finding Fourier coefficients as defined in Section (5.7). With the exception of the Fourier coefficient run, the only computer output is 5-in. by 40-in. Calcomp computer plots that are automatically scaled for each variable.

```

      IMPLICIT REAL *8(A-H,U-Z,$)
      REAL *4 X,Y,TSS ,TTT
      DIMENSION X(6010,4),Y(6010,4),TSS(6010),Q(8),QI(8),QH(8)
      DIMENSION FOUR(8,20),TRIG(18),TRIGL(18) ,B(5,5)
      F=3.141592D0/180.D0
      FI=180.D0/3.141592D0
      CNFOR=0 BYPASSES FOURIER COEFFICIENT ROUTINE REFERRED TO IN SECTION 5.7
      CNFOR=1 ACTIVATES FOURIER COEFFICIENT ROUTINE
      NFOR=0
      CMAYDY IS DO LOOP LIMIT
      MAYDY=2
      CINPUT IN DEGREES
      GAMM=0.D0
      PHI=0.D0
      PSI=0.D0
      PHID=0.D0
      PSID=0.D0
      CW IS FREQUENCY OF TIME VARYING COEFFICIENTS(DON'T SET EQUAL TO ZERO)
      W=1.D-3
      DO 99 N5=1,2
      GO TO (201,202,203),N5
      201 CONTINUE
      CAMPLITUDE OF MOMENTUM BIAS VARIATION
      U=0.D0
      CINTTEGRATION TIME INCREMENT IN SECONDS
      DT=.4D0
      CNSTOP*DT=THE NUMBER OF SECONDS BETWEEN EACH COMPUTED POINT THAT IS PLOTTED
      NSTOP=50
      CTOTAL NUMBER OF PLOT POINTS FOR EACH VARIABLE MUST BE LESS THAN 6000.
      CSIMULATION TIME OFF IN SECONDS
      TMOFF=90000.D0
      COPTIMUM PARAMETER SET FOR EXAMPLE 2
      XIZ=200.D0
      C GAM appears as  $\rho$  in the text.
      GAM=2200.D0/200.D0
      ALF=2325.D0/200.D0
      H0=-10.D0

```

```

      BG=.75D0
      XKG=1.D-3
      BETA=0.D0
      PHI=10.D0
      PSI=10.D0
      GO TO 299
202 CONTINUE
COPTIMUM PARAMETER SET FOR EXAMPLE 1
      GAM=2010.D0/10.D0
      ALF=.75D0*GAM
      H0=-2.5D0
      XIZ=10.D0
      BG=.75D0
      XKG=.33D-2
      BETA=0.D0
      PHI=10.D0
      PSI=10.D0
      GO TO 299
203 CONTINUE
299 CONTINUE
CNSTEP IS INCRIMENTED ONCE EACH TIME STEP
      NSTEF=NSTOP
      SB=DSIN(BETA)
      CB=DCOS(BETA)
      SSB=SB*SB
      CSB=CB*CB
      DO 9959 MAY=1,MAYDY
      C=0.D0
      IF (NFOR)9123,6805,9123
9123 CONTINUE
CPR IS TWICE THE PERIOD OF THE PERIODIC COEFFICIENTS IN SECONDS
      PER=4.D0*3.141592D0/W
      PRD=PER
      WU=W*U
      DO 6805 NT=1,17
      DO 6806 NF=1,8
      FOUR(NF,NT)=0.D0
6806 CONTINUE
6805 CONTINUE
      T=0.D0
CINITIAL CONDITIONS
CQI IS THE INTEGRAL OF Q
      QI(1)=PHI*F
      QI(2)=PHID*F
      QI(3)=GAMM*F
      QI(4)=PSID*F
      QI(5)=PSI*F
CCARDS WITH (***)ARE USED FOR SINUSOIDAL DISTURBANCES, WHILE CARDS WITH
C(*) ARE USED FOR SQUARE WAVE DISTURBANCES
C VARIATIONAL MOMENTUM BIAS
      A=0.D0
C DERIVATIVE OF VARIATIONAL MOMENTUM BIAS
      WA=U*W
C      WA=U*W *4.D0/3.141592D0
      DO 114 L1=1,5
      DO 114 L2=1,5
114 B(L1,L2)=0.D0
CSYSTEM A MATRIX
      B(1,2)=1.D0
      B(2,1)=(1.D-3/ALF)*(4.D-3*(1.D0-GAM)+(H0+A)/XIZ)
      1-(SB*CB*(H0+A)**2)/(ALF*XIZ*BG*1.D3)

```

```

      B(2,2)=-SSB*((H0+A)**2)/(ALF*XIZ*BG)
      B(2,3)= ((XKG-(H0+A)*1.D-3)*SB*(H0+A)/BG+CB*1.D-3*(H0+A)-SB*WA)/
1 (ALF*XIZ)
      B(2,4)=1.D-3*(1.D0+(1.D0-GAM) /ALF)+((H0+A)-CB*SB*((H0+A)**2)/BG)
1/(ALF*XIZ)
      B(2,5)=(SSB*(1.D-3)*(H0+A)**2)/(ALF*XIZ*BG)
      B(3,1)=((1.D-3*(H0+A)/BG)*CB)
      B(3,2)=(H0+A)*SB/BG
      B(3,3)=((-XKG/BG)+(1.D-3*(H0+A))/BG)
      B(3,4)=((H0+A)/BG)*CB
      B(3,5)=-((1.D-3)*(H0+A)*SB/BG)
      B(4,1)=(((H0+A)**2)/(1.D+3*BG*XIZ))*(-CSB)
      B(4,2)=(1.D-3)*(GAM-1.D0-ALF)-((H0+A)+CB*SB*((H0+A)**2)/BG)/XIZ
      B(4,3)=((XKG-(H0+A)*1.D-3)*CB*(H0+A)/BG-(CB*WA+SB*(H0+A)*1.D-3))/
1XIZ
      B(4,4)=((-H0+A)**2)/(XIZ*BG))*CSB
      B(4,5)=-((GAM-ALF)*1.D-6+((H0+A)*1.D-3+CB*SB*((H0+A)**2)*1.D-3/BG)/
1XIZ
      B(5,4)=1.D0
CFORMATION OF 5 SYSTEM STATES
      DO 37 NS1=1,5
      Q(NS1)=0.D0
      DO 37 NS2=1,5
37 Q(NS1)=B(NS1,NS2)*Q(NS2)+Q(NS1)
      NTIM=1
      NXY=1
CTOP OF INTEGRATION SCHEME
      19 CONTINUE
      XTIM=NTIM
      T=DT*1000.D0*C+DT*XTIM
      IF(NSTEP-NSTOP)500,501,501
501 CONTINUE
      X(NXY,1)=A
      X(NXY,2)=Q(5)*FI
      Y(NXY,1)=Q(1)*FI
      Y(NXY,2)=Q(3)*FI
CCAN DEFINE X(NXY,3AND4) AND Y(NXY,3AND4) IF DESIRED
      TSS(NXY)=T/60.
      NXY=NXY+1
      NSTEP=0
500 CONTINUE
      NSTEP=NSTEP+1
CHOLD LAST INTEGRATION STEP
      DO 2001 N1=1,5
      2001 QH(N1)=Q(N1)
CNEXT TIME STEP
CUNITS ARE RADIANs
      A=DSIGN(U,DSIN(W*T)) (*)
C      A=U*DSIN(W*T) *4.D0/3.141592D0 (***)
      WA=DSIGN(WU,DCUS(W*T)) (*)
C      WA=WU*DCUS(W*T) *4.D0/3.141592D0 (***)
CITERATING SYSTEM A MATRIX
      B(2,1)=(1.D-3/ALF)*((4.D-3*(1.D0-GAM)+(H0+A)/XIZ)
1-(SB*CB*(H0+A)**2)/(ALF*XIZ*BG*1.D3)
      B(2,2)=-SSB*((H0+A)**2)/(ALF*XIZ*BG)
      B(2,3)= ((XKG-(H0+A)*1.D-3)*SB*(H0+A)/BG+CB*1.D-3*(H0+A)-SB*WA)/
1(ALF*XIZ)
      B(2,4)=1.D-3*(1.D0+(1.D0-GAM) /ALF)+((H0+A)-CB*SB*((H0+A)**2)/BG)
1/(ALF*XIZ)
      B(2,5)=(SSB*(1.D-3)*(H0+A)**2)/(ALF*XIZ*BG)
      B(3,1)=((1.D-3*(H0+A)/BG)*CB)

```

```

      B(3,2)=(H0+A)*SB/BG
      B(3,3)=((-XKG/BG)+(1.D-3*(H0+A))/BG)
      B(3,4)=((H0+A)/BG)*CB
      B(3,5)=-(1.D-3)*(H0+A)*SB/BG
      B(4,1)=(((H0+A)**2)/(1.D+3*BG*XIZ))*(-CSB)
      B(4,2)=(1.D-3)*(GAM-1.D0-ALF)-((H0+A)+CB*SB*((H0+A)**2)/BG)/XIZ
      B(4,3)=((XKG-(H0+A)*1.D-3)*CB*(H0+A)/BG-(CB*WA+SB*(H0+A)*1.D-3))/
1XIZ
      B(4,4)=((- (H0+A)**2)/(XIZ*BG))*CSB
      B(4,5)=-(GAM-ALF)*1.D-6+((H0+A)*1.D-3+CB*SB*((H0+A)**2)*1.D-3/BG)/
1XIZ
CFORMING 5 SYSTEM STATES
      DO 38 NS1=1,5
      Q(NS1)=0.D0
      DO 38 NS2=1,5
      38 Q(NS1)=B(NS1,NS2)*Q(NS2)+Q(NS1)
CFOURIER COEFFICIENT ROUTINE
CTHIS ROUTINE ONLY WORKS IF (ABS(T-PRD)-.1) IS NEGATIVE AT SOME POINT IN TIME
      IF(NFOR)9500,6910,9500
9500 CONTINUE
      W=W/2.D0
      TRIGL(1)=1.D0
      TRIG(1)=1.D0
      TRIGL(2)=DCOS(W*(T-DT))
      TRIG(2)=DCOS(W*(T))
      TRIGL(3)=DCOS(W*(T-DT)*2.D0)
      TRIG(3)=DCOS(W*(T)*2.D0)
      TRIGL(4)=DCOS(W*(T-DT)*3.D0)
      TRIG(4)=DCOS(W*(T)*3.D0)
      TRIGL(5)=DCOS(W*(T-DT)*4.D0)
      TRIG(5)=DCOS(W*(T)*4.D0)
      TRIGL(6)=DCOS(W*(T-DT)*5.D0)
      TRIG(6)=DCOS(W*(T)*5.D0)
      TRIGL(7)=DCOS(W*(T-DT)*6.D0)
      TRIG(7)=DCOS(W*(T)*6.D0)
      TRIGL(8)=DCOS(W*(T-DT)*7.D0)
      TRIG(8)=DCOS(W*(T)*7.D0)
      TRIGL(9)=DCOS(W*(T-DT)*8.D0)
      TRIG(9)=DCOS(W*(T)*8.D0)
      TRIGL(10)=DSIN(W*(T-DT)*1.D0)
      TRIG(10)=DSIN(W*(T)*1.D0)
      TRIGL(11)=DSIN(W*(T-DT)*2.D0)
      TRIG(11)=DSIN(W*(T)*2.D0)
      TRIGL(12)=DSIN(W*(T-DT)*3.D0)
      TRIG(12)=DSIN(W*(T)*3.D0)
      TRIGL(13)=DSIN(W*(T-DT)*4.D0)
      TRIG(13)=DSIN(W*(T)*4.D0)
      TRIGL(14)=DSIN(W*(T-DT)*5.D0)
      TRIG(14)=DSIN(W*(T)*5.D0)
      TRIGL(15)=DSIN(W*(T-DT)*6.D0)
      TRIG(15)=DSIN(W*(T)*6.D0)
      TRIGL(16)=DSIN(W*(T-DT)*7.D0)
      TRIG(16)=DSIN(W*(T)*7.D0)
      TRIGL(17)=DSIN(W*(T-DT)*8.D0)
      TRIG(17)=DSIN(W*(T)*8.D0)
      W=W*2.D0
      DO 6902 NFOUR=1,5
      DO 6901 NTRIG=1,17
      FOUR(NFOUR,NTRIG)=FOUR(NFOUR,NTRIG)+(3.D0*Q(NFOUR)*TRIG(NTRIG)-
1QH(NFOUR)*TRIGL(NTRIG))*(DT/2.D0)
6901 CONTINUE

```

```

6902 CONTINUE
      IF(DABS(T-PRD)-.1D0)6911,6910,6910
6911 CONTINUE
CINHIBIT TO ALLOW INITIAL TRANSIENT TO DIE DOWN
      IF(T-183480.D0)6711,6712,6712
6712 CONTINUE
      DO 6730 N12=1,5
      DO 6735 N15=2,9
      N20=N15+8
      FOUR(N12,N15)=FOUR(N12,N15)**2+FOUR(N12,N20)**2
      FOUR(N12,N15)=DSQRT(FOUR(N12,N15) )
6735 CONTINUE
6730 CONTINUE
6925 FORMAT(' MAGNITUDE OF FOURIER COEFFICIENTS FOR SYSTEM STATES 1 THR
      IU5, DC THRU EIGHT HARMONIC RESPECTIVELY')
      WRITE(6,6925)
      WRITE(6,6926)((FOUR(NF,NT),NF=1,5 ),NT=1, 9)
6926 FORMAT(5D14.6)
6711 CONTINUE
CINCREMENT PERIOD FOR FOURIER INTEGRATION AND INITIALIZATION OF SAME
      PRD=PRD+PER
      DO 6905 NT=1,17
      DO 6906 NF=1,6
      FOUR(NF,NT)=0.D0
6906 CONTINUE
6905 CONTINUE
6910 CONTINUE
CINTEGRATION OF STATE EQUATION , QI IS INTEGRAL OF Q
      DO 2002 N2=1,5
      2002 QI(N2)=QI(N2)+(3.D0*Q(N2)-QH(N2))*(DT/2.D0)
      NTIM=NTIM+1
      IF(NTIM-1000)31,32,32
      32 C=C+1.D0
      NTIM=0
      31 CONTINUE
      IF(T-TMOFF)19,19,100
      100 CONTINUE
      NXY=NXY-1
CPLOT ROUTINE REQUIRES A CALCOMP 565/570 PLOTTER AND ASSOCIATED SUBPROGRAMS
      CALL PLOTXY (X,Y,TSS,NXY)
      NXY=1
      9123 CONTINUE
CRESET INITIAL CONDITIONS
      PHI=5.D0
      PSI=5.D0
      9959 CONTINUE
      99 CONTINUE
C
      CALL CAL999
      CONTINUE
      RETURN
      END

      SUBROUTINE PLOTXY (X,Y,TSS,NXY)
CFOR LISTING , SEE APPENDIX G

```


APPENDIX G

LISTING OF NONLINEAR DIGITAL COMPUTER SIMULATION PROGRAM

The user may substitute into this computer program any parameter set and any initial condition set of his choosing. He is also free to alter the problem simulation time. Disturbance torque runs can be made by assuming nonzero amplitudes for the disturbance torque coefficients.

The only computer output is 5-in. by 40-in. Calcomp computer plots that are automatically scaled for each variable.

```
      IMPLICIT REAL *8(A-H,U-Z,$)
      REAL *4 X,Y,TSS
      DIMENSION X(6010,4),Y(6010,4),TSS(6010),Q(8),QI(8),QH(8)
      DO 99 N5=1,2
      F=3.14159200/180.00
      FI=180.00/3.14159200
CLIMIT OF DO LOOP 300
      MAYDY=2
CAMP_ITUDE OF DISTURBANCE TORQUES AT DC AND W RAD/SEC RESPECTIVELY
      AMXDC=0.00
      AMYDC=0.00
      AMZDC=0.00
      AMX=0.00
      AMY=0.00
      AMZ=0.00
      W=.00100
      OMEGA=1.0-3
CRESET INITIAL CONDITIONS
      A=0.00
      T=0.00
CSIMULATION TIME OFF IN SECONDS
      TMUFF=90000.00
CINPUT IN DEGREES
      GAMM=0.00
      PHI=10.00
      PSI=10.00
      PSID=0.00
      PHID=0.00
CPITCH RATE
      X15=0.00
CPITCH POSITION
      X16=0.00
      GO TO (201,202,203),N5
201 CONTINUE
COPTIMUM PARAMETER SET FOR EXAMPLE 2
      XISCX=2325.00
      XISCY=2200.00
      XISCZ=200.00
      XKGI=1.0-3
      C=.7500
```

```

        BIAS=-10.00
        BETA=0.00
CINTEGRATION TIME INCREMENT IN SECONDS
        DT=.400
CNSTOP*DT=THE NUMBER OF SECONDS BETWEEN EACH COMPUTED POINT THAT IS PLOTTED
        NSTOP=50
CTOTAL NUMBER OF PLOT POINTS FOR EACH VARIABLE MUST BE LESS THAN 6000.
        GO TO 299
    202 CONTINUE
CUPTIMUM PARAMETER SET FOR EXAMPLE 1
        XISCY=2010.00
        XISCX=XISCY*.7500
        XISCZ=10.00
        XKGI=.330-2
        C=.7500
        BIAS=-2.500
        BETA=0.00
        GO TO 299
    203 CONTINUE
    299 CONTINUE
        DO 300 NCS=1,MAYDY
        CB=DCOS(BETA)
        SB=DSIN(BETA)
CNSTEP IS INCRIMENTED ONCE EACH TIME STEP
        NSTEP=NSTOP
CWHEEL REACTION TORQUE
        X11=0.00
CWHEEL MOMENTUM
        X10=BIAS
        X16=0.00
        X15=0.00
C
CINITIAL CONDITIONS
CQI IS THE INTEGRAL OF Q
        QI(1)=GAMM*F
        SPHI=DSIN(PHI*F)
        CPHI=DCOS(PHI*F)
        SX16=DSIN(X16*F)
        CX16=DCOS(X16*F)
        SPSI=DSIN(PSI*F)
        CPSI=DCOS(PSI*F)
        SG=DSIN(QI(1))
        CG=DCOS(QI(1))
        QI(2)=-PSID*F*SX16*CPHI+PHID*F*CX16-      (CX16*SPSI+SX16*SPHI*CPS
11)*1.0-3
        QI(3)=PSID*F*SPHI+X15*F-      (CPHI*CPSI)*1.0-3
        QI(4)=PSID*F*CX16*CPHI+PHID*F*SX16-(SX16*SPSI-CX16*SPHI*CPSI)*1.0
1-3
        QI(5)=PHI*F
    312 QI(6)=0.00
        QI(7)=PSI*F
CUDIRECTION COSINES
        DC11=CX16*CPSI-SX16*SPHI*SPSI
        DC12=CX16*SPSI+SX16*SPHI*CPSI
        DC13=-SX16*CPHI
        DC21=-SPSI*CPHI
        DC22=CPHI*CPSI
        DC23=SPHI
        DC31=SX16*CPSI+CX16*SPHI*SPSI
        DC32=SX16*SPSI-CX16*SPHI*CPSI
        DC33=CX16*CPHI

```

```

CGIMBAL EQUATION(GAMMA DOT)
  Q(1)=(X10*(SB*CG*QI(2)-SG*QI(3)+CB*CG*QI(4))-XKGI*QI(1))/C
CT1X EQUATION(WX DOT)
  Q(2)=(QI(3)*QI(4)*(XISCY-XISCZ)+3.DO*UMEGA*UMEGA*(XISCZ-XISCY)*DC2
13*DC33
  1 +CB*(XKGI*QI(1)+C *Q(1))+SB*SG*X11-SB*CG*X10*(Q(1)+CB* QI(2)-SB
2*QI(4)))/XISCX
CT1Y EQUATION (WY DOT)
  Q(3)=(QI(4)*QI(2)*(XISCZ-XISCX)+3.DO*UMEGA*UMEGA*(XISCX-XISCZ)*DC
113*DC33+CG*X11+SG*X10*(Q(1)+CB*QI(2)-SB*QI(4)))/XISCY
CT1Z EQUATION (WZ DOT)
  Q(4)=(QI(2)*QI(3)*(XISCX-XISCY)+3.DO*UMEGA*UMEGA*(XISCY-XISCX)*DC
113*DC23-SB*(XKGI*QI(1)+C *Q(1))+CB*SG*X11-CB*CG*X10*(Q(1)+CB*QI(2)
2-SB*QI(4)))/XISCZ
CPHI DOT EQUATION
  Q(5)=CX16*QI(2)+SX16*QI(4)+SPSI*1.D-3
  IF(DABS(CPHI)-.001D0)63,64,64
63 WRITE(6,65)
  CPHI=DSIGN(.001D0,CPHI)
65 FORMAT(///40X,11HGIMBAL LUCK///// )
64 CONTINUE
CPSI DOT EQUATION
  Q(7)=(CX16*QI(4)-SX16*QI(2)-SPHI*CPSI*1.D-3)/CPHI
CTHETA DOT EQUATION
42 Q(6)=0.DO
  NTIM=1
  NXY=1
CTOP OF INTEGRATION SCHEME
19 CONTINUE
  XTIM=NTIM
  T=DT*1000.DO*A+DT*XTIM
CUNITS ARE RADIAN
  SG=DSIN(QI(1))
  CG=DCOS(QI(1))
  SPHI=DSIN(QI(5))
  CPHI=DCOS(QI(5))
  SX16=DSIN(QI(6))
  CX16=DCOS(QI(6))
  SPSI=DSIN(QI(7))
  CPSI=DCOS(QI(7))
  DC11=CX16*CPSI-SX16*SPHI*SPSI
  DC12=CX16*SPSI+SX16*SPHI*CPSI
  DC13=-SX16*CPHI
  DC21=-SPSI*CPHI
  DC22=CPHI*CPSI
  DC23=SPHI
  DC31=SX16*CPSI+CX16*SPHI*SPSI
  DC32=SX16*SPSI-CX16*SPHI*CPSI
  DC33=CX16*CPHI
  IF(NSTEP-NSTOP)500,501,501
501 CONTINUE
  NSTEP=0
  X(NXY,1)=X10
  Y(NXY,1)=QI(5)*FI
  X(NXY,2)=QI(7)*FI
  Y(NXY,2)=QI(1)*FI
CCAN DEFINE X(NXY,3AND4) AND Y(NXY,3AND4) IF DESIRED
  TSS(NXY)=T/60.
  NXY=NXY+1
500 CONTINUE
  NSTEP=NSTEP+1

```

```

CX11 IS WHEEL TORQUE AS IT APPEARS ON VEHICLE
CHOLD LAST INTEGRATION STEP
DO 2001 N1=1,7
  2001 QH(N1)=Q(N1)
CNEXT TIME STEP
CDISTURBANCE TORQUES
  TDY=AMX*DSIN(W*T)+AMXDC
  TDY=AMY*DSIN(W*T)+AMYDC
  TDZ=AMZ*DSIN(W*T)+AMZDC
CSEE ABOVE COMMENTS
  Q(1)=(X10*(SB*CG*QI(2)-SG*QI(3)+CB*CG*QI(4))-XKGI*QI(1))/C
C
  X11 IS MINUS WHEEL TORQUE
  Q(2)=(QI(3)*QI(4)*(XISCY-XISCZ)+3.00*OMEGA*OMEGA*(XISCZ-XISCY)*DC2
13*DC33
1  +CB*(XKGI*QI(1)+C *Q(1))+SB*SG*X11-SB*CG*X10*(Q(1)+CB* QI(2)-SB
2*QI(4)))/XISCX +TDX
  Q(3)=(QI(4)*QI(2)*(XISCZ-XISCX)+3.00*OMEGA*OMEGA*(XISCX-XISCZ)*DC
113*DC33+CG*X11+SG*X10*(Q(1)+CB*QI(2)-SB*QI(4)))/XISCY+TDY
  Q(4)=(QI(2)*QI(3)*(XISCX-XISCY)+3.00*OMEGA*OMEGA*(XISCY-XISCX)*DC
113*DC23-SB*(XKGI*QI(1)+C *Q(1))+CB*SG*X11-CB*CG*X10*(Q(1)+CB*QI(2)
2-SB*QI(4)))/XISCZ+TDZ
  Q(5)=CX16*QI(2)+SX16*QI(4)+SPSI*1.0-3
  IF(DABS(CPHI)-.00100)73,74,74
73 WRITE(6,75)
  CPHI=DSIGN(.00100,CPHI)
75 FORMAT(///40X,11HGIMBAL LUCK///// )
74 CONTINUE
  Q(7)=(CX16*QI(4)-SX16*QI(2)-SPHI*CPSI*1.0-3)/CPHI
67 Q(6)=0.00
CINTEGRATION
DO 2002 N2=1,7
2002 QI(N2)=QI(N2)+(3.00*Q(N2)-QH(N2))*(DT/2.00)
DO 12 N3=5,7
  IF(DABS(QI(N3))-3.1415900)12,12,11
11 QI(N3)=QI(N3)-DSIGN(6.2831800,QI(N3))
12 CONTINUE
  NTIM=NTIM+1
  IF(NTIM-1000)31,32,32
32 A=A+1.00
  NTIM=0
31 CONTINUE
  IF(T-TMOFF)19,19,100
100 CONTINUE
  NXY=NXY-1
CPLT ROUTINE REQUIRES A CALCOMP 565/570 PLOTTER AND ASSOCIATED SUBPROGRAMS
  CALL PLOTXY (X,Y,TSS,NXY)
89 CONTINUE
CRESET INITIAL CONDITIONS
  PHI=5.00
  PSI=5.00
300 CONTINUE
99 CONTINUE
  CALL CAL999
  CONTINUE
  RETURN

END
SUBROUTINE PLOTXY (X,Y,TSS,NXY)
  LOGICAL *1 TITLE1(44),TITLE2(44)
  DATA TITLE1/'VARIATIONAL YAW ANGLE OMEGA Z A33 ' /

```

```

DATA TITLE2/' ROLL ANGLE GIMBAL ANG.      A22      A23      '/
DIMENSION BUFFER(8000),X(6010,4),Y(6010,4),TSS(6010)
INTEGER BUFFER
LOGICAL FIRST/.TRUE./
IF (FIRST) CALL PLUTS (BUFFER,32000)
FIRST=.FALSE.
K=1
CM CAN GO FROM 1 TO 4 IF SO DEFINED IN MAIN PROGRAM
DO 1 M=1,2
CALL SCALE (X(1,M),5.,NXY,1)
XMX=X(NXY+1,M)+5.*X(NXY+2,M)
AYT=0.
IF (XMX*X(NXY+1,M).GE.0.) GO TO 2
AYT=-5.*X(NXY+1,M)/(XMX-X(NXY+1,M))
2 CONTINUE
TSS(NXY+1)=0.
TSS(NXY+2)=(TSS(NXY))/40.
CALL AXIS (0.,0.,TITLE1(K),+11,5.,90.,X(NXY+1,M),X(NXY+2,M))
CALL AXIS (0.,AYT,'MINUTE',-6,40.,0.,0.,TSS(NXY+1),TSS(NXY+2))
CALL LINE(TSS,X(1,M),NXY,1,0,0)
CALL PLUT (0.,5.0,-3)
CALL SCALE (Y(1,M),5.,NXY,1)
YMX=Y(NXY+1,M)+5.*Y(NXY+2,M)
AYT=0.
IF (YMX*Y(NXY+1,M).GE.0.) GO TO 3
AYT=-5.*Y(NXY+1,M)/(YMX-Y(NXY+1,M))
3 CONTINUE
CALL AXIS (0.,0.,TITLE2(K),+11,5.,90.,Y(NXY+1,M),Y(NXY+2,M))
CALL AXIS (0.,AYT,'MINUTE',-6,40.,0.,0.,TSS(NXY)/40.)
CALL LINE(TSS,Y(1,M),NXY,1,0,0)
CALL PLUT (43.,-5.0,-3)
1 K=K+1
CALL PLUT (05.,0.,-3)
RETURN
ENTRY CAL999
CALL PLUT (20.,0.,999)
RETURN
END

```